# *DRUG TRAFFICKING IN MICE: In vivo functions of OATP uptake and ABC efflux transporters*

*Dilek Iusuf*

ISBN: 978-94-6182-323-6

Copyright © 2013 by Dilek Iusuf. All rights reserved.

The research described in this thesis was performed at the Division of Molecular Biology and Molecular Oncology of the Netherlands Cancer Institute, Amsterdam, The Netherlands. This project was partially funded by the Dutch Cancer Society (Grant NKI 2007-3764).

Layout and printing: Off Page, www.offpage.nl, with financial support from the Dutch Cancer Society (www.kwf.nl) and The Netherlands Cancer Institute.

Cover: E.A.J. Reits. The cartoon on the cover depicts an artist's impression of the drug transport processes.

# *DRUG TRAFFICKING IN MICE:*
# *In vivo functions of OATP uptake and ABC efflux transporters*

***Drug transporters in muizen:***
***In vivo functies van OATP opname***
***en ABC efflux transporters***
(met een samenvatting in het Nederlands)

Proefschrift

ter verkrijging van de graad van doctor
aan de Universiteit Utrecht
op gezag van de rector magnificus, prof.dr. G.J. van der Zwaan,
ingevolge het besluit van het college voor promoties
in het openbaar te verdedigen
op woensdag 11 september 2013
des middags te 2.30 uur

door

Dilek Iusuf

geboren op 22 mei 1981 te Constanta, Roemenië

| | |
|---|---|
| **Promotor**: | Prof.dr. J.H. Beijnen |
| **Co-promotor**: | Dr. A.H. Schinkel |

# *Table of contents*

**Chapter 1** **Introduction** 9

Chapter 1.1 Functions of Oatp1a/1b transporters *in vivo*: insights from mouse models 11
*Modified from Trends in Pharmacological Sciences, 2012*

Chapter 1.2 Hepatocyte hopping of OATP1B substrates contributes to efficient hepatic detoxification 31
*Clinical Pharmacology and Therapeutics, 2012*

**Chapter 2** **Mouse and human OATP1A/1B transporters mediate plasma clearance of unconjugated bilirubin and bile acids** 39
*To be submitted*

**Chapter 3** **Role of Oatp1a/1b transporters in the pharmacokinetics of statins** 55

Chapter 3.1 Organic anion-transporting polypeptides 1a/1b control the hepatic uptake of pravastatin in mice 57
*Molecular Pharmaceutics, 2012*

Chapter 3.2 Murine Oatp1a/1b uptake transporters control rosuvastatin systemic exposure without affecting its apparent liver exposure 81
*Molecular Pharmacology, 2013*

**Chapter 4** **Role of Oatp1a/1b transporters in the pharmacokinetics of anticancer drugs** 103

Chapter 4.1 OATP1A/1B transporters affect irinotecan and SN-38 pharmacokinetics and carboxylesterase expression in knockout and humanized transgenic mice 105
*Submitted for publication*

Chapter 4.2 Human OATP1B1, OATP1B3 and OATP1A2 mediate the in vivo uptake of docetaxel 129
*To be submitted*

**Chapter 5** **Role of efflux transporters in the brain accumulation and oral bioavailability of anticancer drugs** 145

Chapter 5.1 Introduction: Single and combined roles of P-gp (ABCB1) and ABCG2 (BCRP) efflux transporters in brain disposition and oral bioavailability of anticancer drugs 147

Chapter 5.2 P-glycoprotein (Abcb1) transports the primary active tamoxifen metabolites endoxifen and 4-hydroxytamoxifen and restricts their brain penetration 153
*Journal of Pharmacology and Experimental Therapeutics, 2011*

Chapter 5.3 Differential impact of P-glycoprotein (ABCB1) and breast cancer resistance protein (ABCG2) on axitinib brain accumulation and oral plasma pharmacokinetics 177
*Drug Metabolism and Disposition, 2011*

**Conclusions and perspectives** 191

**Summary** 197

**Nederlandstalige samenvatting** 205

**Rezumat** 209

**Curriculum Vitae** 211

**List of publications** 213

**Acknowledgements** 217

# Introduction

# 1

# 1.1

# *Functions of Oatp1a/1b transporters in vivo: insights from mouse models*

Dilek Iusuf*[1], Evita van de Steeg*[1] and Alfred H. Schinkel[1],

* contributed equally

[1]Division of Molecular Oncology, The Netherlands Cancer Institute,
Amsterdam, The Netherlands

*Modified from Trends in Pharmacological Sciences, 2012*

# Abstract

Organic anion-transporting polypeptides (OATPs) form a superfamily of uptake transporters that mediate the cellular uptake of a broad range of endogenous and exogenous compounds. Of these OATP transporters, members of the 1A and 1B subfamilies have broad substrate specificities. Because they are mainly expressed in liver, kidney and small intestine, OATP1A/1B transporters can have a major impact on the pharmacokinetics of many drugs. To study their role in physiology and drug disposition, several mouse models lacking functional expression of one or more Oatps and also humanized transgenic mice with liver-specific expression of human OATP1A/1B transporters have been generated. This review discusses recent findings obtained with these models that have led to new insights into the impact of OATP1A/1B transporters on pharmacokinetics and toxicokinetics, and on bilirubin detoxification and bile acid handling in normal liver physiology.

## Organic anion-transporting polypeptides

Organic anion-transporting polypeptides (human: OATP, gene: *SLCO*; rodents: Oatp, gene: *Slco)* represent a superfamily of transmembrane transporters that mediate the sodium-independent cellular uptake of many endogenous and exogenous compounds. OATPs/Oatps are grouped in six families (OATP1-6), each consisting of members with amino acid sequence identities of more than 40%, and several subfamilies (OATP1A, 1B, etc), whose members share more than 60% amino acid identity [1]. The OATP1A and 1B subfamilies and OATP2B1 are believed to have a profound effect on drug absorption, distribution and elimination, because they are mainly expressed in tissues important for pharmacokinetics (e.g. liver, small intestine, and kidney, Figure 1) and exhibit wide substrate specificities encompassing many drugs [2,3].

The OATP1A/1B subfamilies contain 3 human members (OATP1A2, -1B1, and -1B3) but at least 5 mouse members (Oatp1a1, -1a4, -1a5, -1a6, and -1b2). Their subcellular localization can be basolateral or apical depending on tissue, cell type, and species (Figure 1). Based on sequence homology and tissue localization, there are no straightforward one-to-one orthologues between human and mouse Oatp1a/1b proteins. However, considering their shared basolateral (sinusoidal) localization in hepatocytes, it could well be that Oatp1b2 together with Oatp1a1 and Oap1a4 fulfil the same function(s) in mouse liver as OATP1B1 and OATP1B3 in the human liver (Figure 1) [4,5]. Similarly, based on their expression in small intestine, kidney and brain, one or more of the mouse Oatp1a1, -1a4, -1a5, and -1a6 proteins might have mostly analogous functions as the single human OATP1A2 protein (Figure 1).

Human and rodent OATP1A/Oatp1a proteins can transport a wide range of amphipatic compounds, both endogenous (e.g. bile acids, estrogen derivatives, and peptides) as well as exogenous, including many drugs (e.g. fexofenadine, pravastatin, rosuvastatin, D-penicillamine, methotrexate) [6]. In addition to the OATP1A substrates mentioned above, OATP1B1 and OATP1B3 can mediate the hepatic uptake of other endogenous compounds (conjugated, and possibly unconjugated bilirubin, thyroid hormones) as well as digoxin, paclitaxel, rifampicin, enalapril, and SN-38 [6]. Human OATP2B1 does have a single mouse orthologue, Oatp2b1, and is expressed in many tissues including liver, small intestine, kidney, brain, placenta, ovary, and lung (Figure 1) [6]. Studies in individuals with low-activity variants of OATP2B1, together with drug-food and drug-drug interactions studies suggest a role for OATP2B1 in the intestinal absorption of drugs [7-9]. However, further studies will be required to establish the exact *in vivo* role of OATP2B1.

OATP1A/1B uptake transporters can play an important role in drug disposition, drug-drug, and drug-food interactions. This first became apparent with studies reporting wide substrate specificities *in vitro* and the discovery of human polymorphic genetic variants affecting OATP transport capacity [10]. Polymorphisms in the gene encoding OATP1B1 have been extensively characterized. These variants may alter the pharmacokinetics of multiple drugs and thus contribute to interindividual and interethnic variability in drug response and toxicity [11-18]. In addition, drug-drug and drug-food interactions can occur through OATP1A/1B, resulting in potential pharmacodynamic and toxicological risks [19,20].

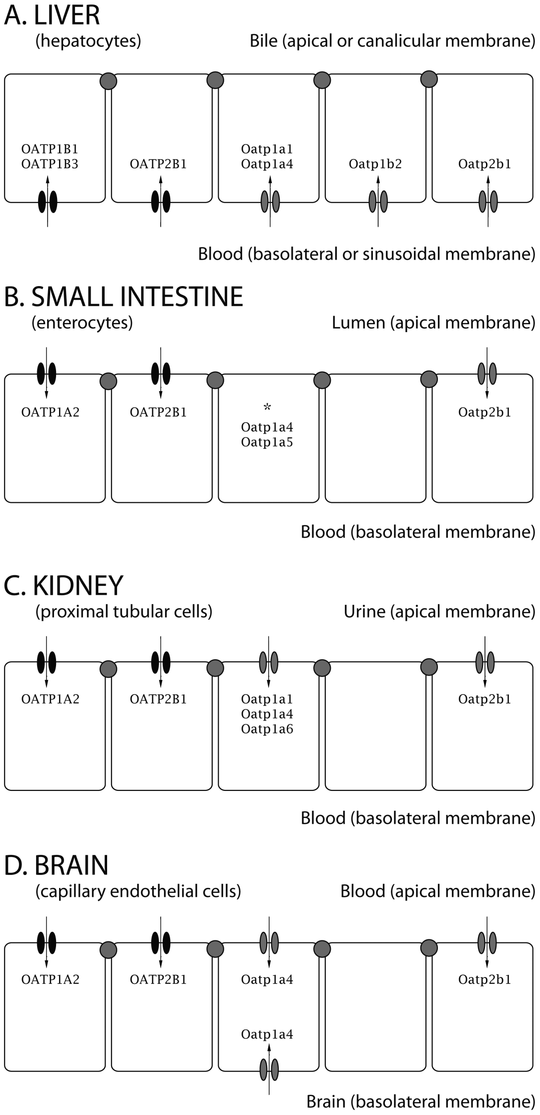
A. LIVER
(hepatocytes)
Bile (apical or canalicular membrane)
OATP1B1
OATP1B3
OATP2B1
Oatp1a1
Oatp1a4
Oatp1b2
Oatp2b1
Blood (basolateral or sinusoidal membrane)
B. SMALL INTESTINE
(enterocytes)
Lumen (apical membrane)
OATP1A2
OATP2B1
*
Oatp1a4
Oatp1a5
Oatp2b1
Blood (basolateral membrane)
C. KIDNEY
(proximal tubular cells)
Urine (apical membrane)
OATP1A2
OATP2B1
Oatp1a1
Oatp1a4
Oatp1a6
Oatp2b1
Blood (basolateral membrane)
D. BRAIN
(capillary endothelial cells)
Blood (apical membrane)
OATP1A2
OATP2B1
Oatp1a4
Oatp2b1
Oatp1a4
Brain (basolateral membrane)

**Figure 1.** Simplified schematic of subcellular localization of human OATP1A/B and OATP2B1 and mouse Oatp1a/1b and Oatp2b1 transporters in polarized cells or epithelia of main organs involved in drug distribution and disposition. (A) Liver. Human OATP1B1, OATP1B3, and OATP2B1 and mouse Oatp1a1, Oatp1a4, Oatp1b2, and Oatp2b1 are present in the sinusoidal (basolateral) membrane of hepatocytes. OATPs take up their substrates from the blood circulation into the liver. Note that in the human liver OATP1A2 is expressed only in cholangiocytes [5]. (B) Small intestine. OATP1A2 and OATP2B1/Oatp2b1 are located at the apical membrane of enterocytes where they can presumably mediate intestinal absorption of compounds [4]. * mRNA expression of mouse Oatp1a4 and Oatp1a5 was also detected in the small intestine, but their protein localization has not been established yet [2, 3]. (C) Kidney. Human OATP1A2 and OATP2B1 and mouse Oatp1a1, Oatp1a4, Oatp1a6 and Oatp2b1 have been described as located in the apical membrane of the proximal tubular cells [3], where they might be involved in reabsorption of substrates. (D) Brain capillary endothelial cells. Human OATP1A2 and mouse Oatp1a4 have high expression in comparison with the other transporters. They might mediate brain uptake or (in case of Oatp1a4) efflux of substrates across the blood-brain barrier [24].

Several knockout mouse models for Oatp1a/1b transporters as wells as humanized transgenic OATP1A/1B strains have been generated recently. Here we discuss the physiological and pharmacological insights obtained with these models and illustrate their usefulness as tools to study the function of OATP1A/1B transporters *in vivo*.

## *Knockout mouse models for studying mouse Oatp1a/1b functions*

The first two single Oatp knockout models, both Oatp1b2(-/-) strains, were independently reported in 2008 [21,22]. Oatp1a4 and Oatp1a1 knockout mice were the next single knockout models to be generated and characterized [23,24]. Because the Oatp1a and Oatp1b transporters display a large overlap in tissue distribution and substrate specificity, mice deficient for all Oatp1a and Oatp1b genes (Oatp1a/1b knockout mouse) were also generated, thus avoiding the risk of compensatory restoration of function by other Oatp1a/1b proteins [25]. All of these strains were fertile, viable and developed normally. Initial characterization of the models revealed comparatively minor changes in the mRNA expression levels of some other transporters, which were unlikely to dramatically affect subsequent functional studies [21-25].

Surprisingly, subsequent pharmacokinetic studies with irinotecan, a pro-drug which gets activated upon hydrolysis by carboxylesterases (Ces), revealed that Oatp1a/1b knockout mice have higher liver, small intestine and kidney mRNA expression of several Ces1 enzymes. This leads to higher plasma esterase activity in these mice and might complicate the interpretation of pharmacokinetic studies with (anticancer) drugs which are substrates of these Ces enzymes (Chapter 4.1).

Studies in both the single and combination knockout strains revealed the physiological importance of these transporters in bilirubin detoxification and bile salt homeostasis, and established their importance in drug disposition.

## *Transgenic humanized mouse models with liver-specific expression of the human OATP1A/1B proteins*

Transgenic mice with liver-specific expression of OATP1B1 have previously been generated and characterized [26], and an analagous approach was used to generate OATP1B3 and OATP1A2 transgenic mice. These mice were crossed back with Oatp1a/1b knockout mice to obtain homozygous mice with predominant liver-specific expression of the three transgenes [27]. Liver-specific expression of human OATP1B1 and OATP1B3 was roughly similar to that in the human liver. Basolateral localization of human OATP1B1 and OATP1B3 throughout the liver lobule was confirmed by immunohistochemistry, with stronger staining of OATP1B1 around the portal vein, while OATP1B3 had more disperse expression throughout the liver lobule [26,27].

Expression of OATP1A2 in the humanized mice as measured by western blot was much higher than in the human liver. This is because in the human liver, expression of OATP1A2 is restricted to cholangiocytes (epithelial cells lining the bile ducts), while in the humanized mice, the ApoE promoter used results in expression in the more abundant hepatocytes in the liver. Localization of OATP1A2 on the basolateral membrane of hepatocytes could be confirmed by functional tests in these mice, as the available OATP1A2 antibodies did not work well in immunohistochemistry [27]. This implies that humanized OATP1A2 mice do not represent a physiological model for the function of OATP1A2 in the human liver, but nevertheless these mice are useful to study the *in vivo* transport capability of OATP1A2, which might be physiologically or pharmacologically relevant in other tissues (kidney, brain, tumors).

Further characterization revealed that these mice had a normal life span, body weight and liver weight. Extensive analysis of expression of other transporters and metabolizing enzymes revealed only one substantial change, namely that Abcc3 (Mrp3) mRNA was down-regulated (2- to 4-fold) in all humanized mouse strains when compared with wild-type and/or Oatp1a/1b knockout mice. However, this was not evident from the protein level expression determined by immunoblotting [27].

## *Physiological functions of OATP1A/1B transporters*

### *Role of OATP1A/1B in bilirubin detoxification*

Bilirubin is the breakdown product of heme, primarily resulting from the degradation of hemoglobin from red blood cells. To limit its high potential toxicity, bilirubin is avidly bound to albumin in the plasma, and is rapidly cleared from the systemic circulation by the liver. Inside hepatocytes, bilirubin glucuronide is formed by (UDP)-glucuronosyltransferase 1A1 (Ugt1a1), followed by efficient elimination into the bile by several efflux transporters (Figure 2, see legend for details).

OATP1B1 and OATP1B3 can transport conjugated, and possibly unconjugated, bilirubin *in vitro* [28,29]. Several studies in humans, including genome-wide association studies, suggested that polymorphisms reducing OATP1B1 activity and/or polymorphisms in *SLCO1B3* (OATP1B3) might be correlated with mildly increased plasma levels of conjugated or unconjugated bilirubin (UCB) [15,30,31]. Rat Oatp1a1, but not Oatp1a4, can transport conjugated bilirubin *in vitro* with high affinity [32], whereas *in vitro* bilirubin transport by the mouse Oatp1a/1b proteins has not been tested.

More clear-cut insights were obtained from *in vivo* studies with the Oatp1a and 1b knockout mice. Firstly, Zaher *et al*. observed in Oatp1b2 knockout mice a modest, 2-fold increase in primarily conjugated plasma bilirubin levels compared with wild-type mice [22]. Independently, Lu *et al*. reported a 2.5-fold elevation in the serum levels of primarily conjugated bilirubin in female Oatp1b2 knockout mice, but not in their male counterparts [21]. Oatp1a1 or Oatp1a4 knockout mice showed no significant changes in bilirubin plasma levels [23]. In contrast to these mild effects, Oatp1a/1b knockout mice lacking all the Oatp1a/1b uptake transporters demonstrated a more than 40-fold increase in total bilirubin plasma levels compared with wild-type mice, with ~95% of this increase attributable to conjugated bilirubin [25]. This high plasma level of conjugated bilirubin initially seemed remarkable. Bilirubin glucuronides are mostly formed in the liver and subsequently eliminated into the bile by the ATP-binding cassette (ABC) transporter Abcc2 and (in mice) Abcg2. However, under pathological conditions such as cholestasis, bilirubin glucuronides can be substantially excreted into the plasma via Abcc3 [33,34] and then eliminated renally. We therefore hypothesized the existence of a seemingly futile cycle of bilirubin glucuronides in normal, healthy liver, in which hepatic bilirubin glucuronide is substantially secreted across the sinusoidal membrane by Abcc3 (Figure 2). Subsequently, in more downstream hepatocytes, sinusoidal Oatp1a/1b proteins can mediate the efficient re-uptake of bilirubin glucuronide into the liver. Ongoing normal Abcc2 excretion would then result in nearly quantitative elimination of bilirubin glucuronide into bile. This so called "hepatocyte-hopping" process might be required to avoid the saturation of detoxifying systems, e.g. canalicular efflux transporters, in upstream hepatocytes. However, in the absence of Oatp1a/1b, this re-uptake is hampered, resulting in much higher residual levels of bilirubin glucuronide in venous blood leaving the liver. Interestingly, in the absence of Oatp1a/1b transporters, the biliary excretion of bilirubin glucuronides was reduced by 50%, indicating that under normal conditions at least half of the bilirubin glucuronide formed in the liver is initially secreted into the plasma, only to be taken up again by downstream hepatocytes via Oatp1a/1b [25].

Importantly, these results could be translated to humans and they aided in elucidating the genetic cause of a rare syndrome, the Rotor syndrome [35]. The main findings are presented later

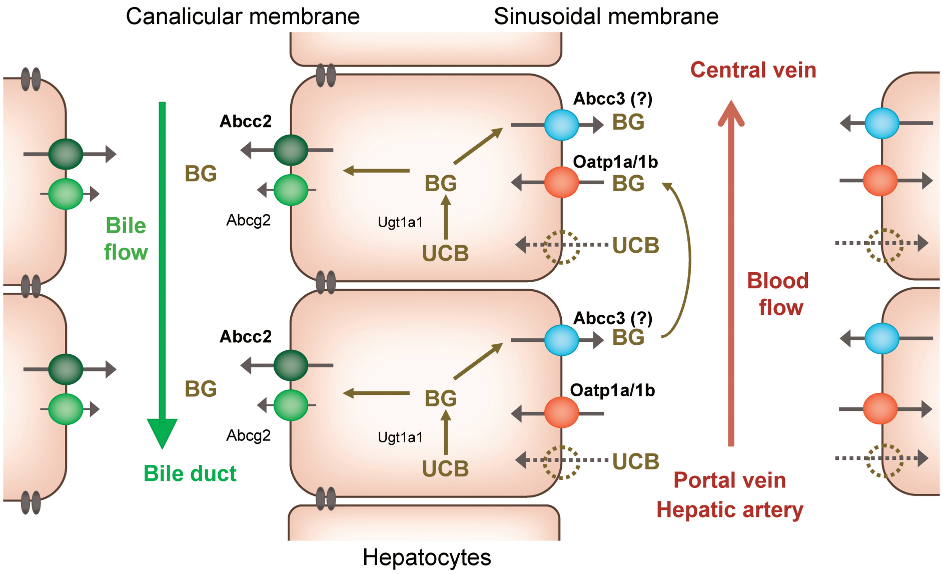

**Figure 2.** Schematic diagram of the hepatic bilirubin detoxification process. Unconjugated bilirubin (UCB) enters the hepatocytes by as yet incompletely defined mechanism(s), possibly transporter–mediated and/or passive diffusion. Inside the hepatocytes, bilirubin is enzymatically conjugated by UDP-glucuronosyltransferase 1A1 (Ugt1a1) to form the more water-soluble bilirubin-glucuronide (BG). BG is subsequently actively secreted into bile, mainly by Abcc2, whereas in mice Abcg2 can also contribute to this process. We hypothesize that, even under physiological conditions, a substantial fraction of the hepatic BG is rerouted to the blood by Abcc3 and/or other sinusoidal efflux transporters, from where it can be taken up again into downstream hepatocytes by Oatp1a/1b transporters. In the absence of Oatp1a/1b-mediated re-uptake, BG will accumulate in the blood.

in chapter 1.2 of this thesis [36]. In short, humanized mice with liver-specific expression of OATP1B1 or OATP1B3 had normal plasma levels of bilirubin glucuronides, indicating that these transporters can mediate efficient liver re-uptake of bilirubin glucuronides *in vivo*. These results together with the findings that Rotor syndrome patients suffer from conjugated hyperbilirubinemia and have a complete deficiency of OATP1B1 and OATP1B3 proteins [35] established an important physiological role of OATP1B transporters in liver-mediated detoxification [36].

In mice, Oatp1b2, -1a1 and -1a4 are the primary hepatic (sinusoidal) Oatp1a/1b proteins (Figure 1). The absence of effects on plasma bilirubin in the single Oatp1a1 and Oatp1a4 knockout mice, and the very modest effects seen in Oatp1b2 knockout mice, suggest that there is substantial redundancy between two or all three of these transporters in mediating sinusoidal re-uptake of conjugated bilirubin.

Sometimes drugs can cause substantial increases in plasma conjugated bilirubin levels in humans, without increases in liver enzyme plasma levels that would signal acute hepatocyte damage [37]. Given the results in Oatp1a/1b(-/-) mice, such effects may be due to inhibition of the sinusoidal OATP-mediated re-uptake of conjugated bilirubin.

Plasma levels of UCB were ~2-fold increased in Oatp1a/1b(-/-) mice compared with wild-type [25]. However, the extensive formation of conjugated bilirubin in these mice, and its biliary and renal excretion indicate that there is no substantial defect in hepatic uptake of UCB. Although Oatp1a/1b proteins might contribute some hepatic UCB uptake, they are clearly not essential for this process. We note that previous *in vitro* studies investigating transport of UCB by human OATP transporters (especially OATP1B1) have yielded conflicting results [28,38]. It may be that UCB enters the liver in part by passive diffusion through the sinusoidal membrane, although the involvement of additional uptake systems seems likely [39]. In a subsequent study (chapter 2 of this thesis), we could demonstrate that the mouse Oatp1a/1b proteins, and human OATP1B1 and OATP1A2 contribute to the plasma clearance of unconjugated bilirubin after intravenous administration *in vivo*, although they have much greater affinity for clearing conjugated bilirubin than for unconjugated bilirubin.

### *Role of OATP1A/1B in bile acid homeostasis*

Bile acids represent one of the major organic solute groups in bile. They are synthesized from cholesterol in the liver, and subsequently conjugated with the amino acids taurine or glycine [40]. Bile acids play an important role in several physiological processes, including facilitating intestinal uptake of dietary lipids, and are therefore subject to strict homeostasis. Bile acids undergo a very efficient enterohepatic circulation which is maintained by several transporters in the liver and small intestine (Figure 3, see legend for details) [40,41].

Historically, the first Oatp uptake protein (rat Oatp1a1) was cloned as a $Na^+$-independent anion transporter that could also transport bile acids [42]. Since then, numerous *in vitro* studies have demonstrated that human OATP1A2, -1B1 and -1B3, rat Oatp1a and Oatp1b2, and mouse Oatp1a1 can transport conjugated and unconjugated bile acids (reviewed in [43,44]). In addition, the independently identified $Na^+$-dependent taurocholate cotransporting polypeptide (NTCP) can facilitate the uptake of (mostly conjugated) bile acids (Figure 3) [17].

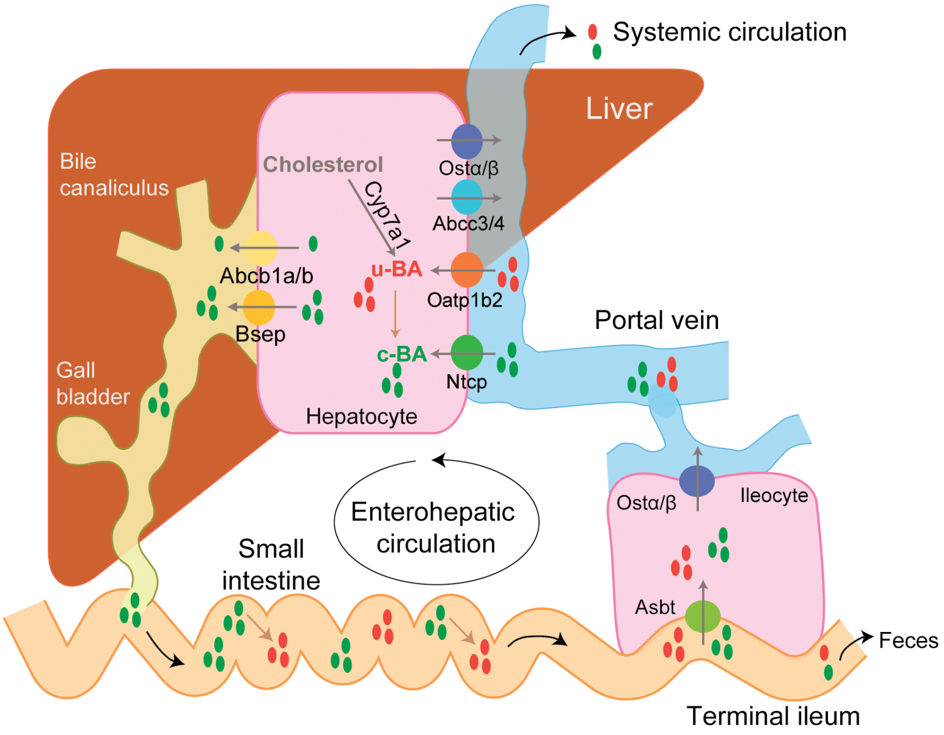
Systemic circulation
Liver
Bile canaliculus
Cholesterol
Cyp7a1
Ostα/β
Abcc3/4
Abcb1a/b
u-BA
Oatp1b2
Bsep
c-BA
Ntcp
Portal vein
Gall bladder
Hepatocyte
Enterohepatic circulation
Small intestine
Ostα/β
Ileocyte
Asbt
Feces
Terminal ileum

**Figure 3.** Enterohepatic circulation of bile acids. Localization of the major transport proteins, Ntcp, Oatp1b2, Bsep, Asbt, and Ostα/β involved in the enterohepatic circulation of bile acids (BA), mediating movement across hepatocytes and ileocytes (ileum enterocytes). In the liver, unconjugated bile acids (u-BA, red) are formed from cholesterol, and subsequently conjugated (c-BA, green). c-BA are secreted across the canalicular membrane into the bile by the bile salt export pump (Bsep), and (in mice) Abcb1a/b. Conjugated bile acids are released from the biliary tract into the small intestine where they are partially deconjugated by bacterial enzymes. In the terminal ileum, both u-BA and c-BA are efficiently absorbed by Asbt and Ostα/β and returned to the liver via the portal circulation. In the liver, Ntcp efficiently extracts most of c-BA, and some u-BA, while Oatp1b2 mediates the uptake of u-BA and some c-BA. A small fraction of BA escapes this enterohepatic cycling, with ~5% lost in the feces and ~5% ending up in the systemic circulation and eliminated via the urine.

It was therefore interesting to find that Oatp1a/1b knockout mice suffered from markedly increased plasma levels of total bile acids (4-fold) compared to wild-type mice. This was primarily caused by 13-fold higher concentrations of unconjugated bile acids, whereas levels of conjugated bile acids remained mostly (albeit not completely) unchanged [25]. Virtually identical results were reported in single Oatp1b2(-/-) mice in an independent study [45], even though Oatp1a1 and Oatp1a4 are still present in the liver of these mice. Collectively, these results point to Oatp1b2 as the main Oatp transporter responsible for hepatic uptake of unconjugated bile acids. Apparently in mice, hepatic Oatp1a1 and Oatp1a4 contribute little to unconjugated bile acid uptake, whereas uptake of most conjugated bile acids is efficiently mediated by Ntcp. Also, humans carrying low-activity OATP1B1 polymorphisms have been reported to have modestly increased blood levels of some unconjugated bile acids [45,46]. This would be consistent with data from Oatp1b2-heterozygous mice, which exhibit intermediate blood concentrations of unconjugated bile acids between wild-type and Oatp1b2-null mice [45,46]. OATP1B3 also mediates uptake of bile acids *in vitro*, so it might also play a role in bile acid homeostasis [47]. Recently, we extended these studies and analyzed endogenous plasma levels of bile acids in humanized mice with liver-specific expression of human OATP1B1, OATP1B3 and OATP1A2. The presence of OATP1B1 or OATP1B3 in the liver provided a partial rescue of the increased plasma concentrations of unconjugated bile acids in the Oatp1a/1b knockout mice, indicating that these transporters can transport unconjugated bile acids *in vivo* (Chapter 2).

In mice, systemic levels of unconjugated bile acid represent only ~5% of the total bile acid pool present in the enterohepatic circulation. This explains why liver and small intestinal concentrations of bile acids, or their biliary excretion were not noticeably changed in the absence of Oatp1b2 or all Oatp1a/1b proteins [25,45]. Nevertheless, the impact on unconjugated and total bile acid levels circulating in the blood is substantial, and we cannot exclude that this might have physiological consequences for some of the exposed organs. Taken together, these results illustrate that conjugated bile acids are primarily taken up into the liver by Ntcp and unconjugated bile acids by Oatp1b2 (Figure 3). The loss of Oatp1b2-mediated uptake of unconjugated bile acids cannot be (completely) compensated by Ntcp. Upon i.p. administration, plasma clearance of cholic acid and chenodeoxycholic acid was impaired in Oatp1a/1b-null mice, confirming that mouse Oatp1b2 mediates the liver uptake of these bile acids (chapter 2). However, transport of bile acids by the human OATP1A/1B transporters was not obvious upon i.p. administration of cholic acid or chenodeoxycholic acid to humanized mice. This was most problably due to very high plasma concentrations of these bile acids, concentrations which are much above the reported Km values *in vitro* (Chapter 2).

### *Additional biological functions of OATP1A/1B proteins*

Numerous *in vitro* studies showed that OATP1A/1B proteins can transport anionic estrogen conjugates, namely estradiol-17β-D-glucuronide (E2-17G) and estrogen-3-sulfate [6]. Uptake of these two compounds was reduced in hepatocytes isolated from Oatp1a1(-/-) mice and Oatp1a4(-/-) mice [23]. Accordingly, upon intravenous administration of E2-17G to Oatp1a1 and Oatp1a4 knockout mice, the plasma levels were clearly increased in the absence of Oatp1a1, although not in Oatp1a4(-/-) mice [23]. Diminished hepatocytic uptake of E2-17G also transiently protected Oatp1b2(-/-) mice from the reduction in bile flow caused by administered E2-17G [21]. These results illustrate the overlapping functions of Oatp1a1 and Oatp1b2, and to some extent Oatp1a4, in mediating liver uptake and plasma clearance of E2-17G, thus modifying its biological effects.

The overlap between Oatp1a1, -1a4 and -1b2 became even clearer in studies with the organic dye dibromosulfophthalein (DBSP) which, due to its rapid uptake in hepatocytes, lack of metabolism, and almost exclusive elimination into the bile, is often used to assess liver excretory function. In Oatp1b2(-/-) mice plasma clearance and biliary clearance of DBSP was decreased, indicating an impaired liver uptake [21]. Similar results, albeit of a lower magnitude, were seen in male and female Oatp1a4(-/-) and male Oatp1a1(-/-) mice [23]. In view of these overlapping functions of Oatp1a1, -1a4, and -1b2 in sinusoidal uptake of a range of compounds, studies in Oatp1a/1b(-/-) mice, which lack all the Oatp1a and -1b transporters, might often yield more clear-cut outcomes. This uncovering of partly redundant functions of the mouse Oatp1a/1b proteins may indirectly also allow better assessment of human OATP1A/1B functions. This is likely especially relevant for the liver, where 3 different mouse Oatp1a and Oatp1b proteins appear to mediate the same sinusoidal uptake functions as the two OATP1B1 and OATP1B3 proteins in human (Figure 1). But also in other organs the simultaneous removal of all Oatp1a and Oatp1b proteins might unmask functional redundancies that could occur between the various mouse Oatp1a proteins when only a single Oatp1a protein gene is knocked out (Figure 1).

Metabolomic profiling of the urine of Oatp1a1(-/-) and Oatp1a4(-/-) mice was performed in order to identify a possible role in urinary excretion of endogenous organic anions [23]. Only a few compounds showed small differences between wild-type and Oatp1a-null mice. The most affected compound was taurine, whose excretion was decreased in both male and female Oatp1a1 and Oatp1a4 knockout mice. This change was accompanied by an increase in the excretion of its deaminated metabolite (isethionic acid). The authors hypothesized that these changes might reflect alterations in the composition of the bacterial intestinal flora in these mice [23]. Comparable metabolomic analyses of Oatp1a/1b(-/-) mice may be of interest.

## *Pharmacological functions of OATP1A/1B transporters*

Many drugs have been described as *in vitro* substrates of human and rat OATP1A/1B proteins (reviewed in [16]), but only for a few *in vitro* transport by mouse Oatp1a and/or Oatp1b2 has been tested [6]. Recently, the role of Oatp1a/1b proteins in drug disposition has been more extensively investigated in the various Oatp1a and Oatp1b knockout and transgenic mouse models. One of the most striking results was observed for methotrexate [48], an anionic anticancer and antirheumatic drug and *in vitro* OATP1B1 and Oatp1a4 substrate [49]. Transgenic overexpression of human OATP1B1 in livers of wild-type mice resulted in modestly increased (~2-fold) liver uptake and decreased (~2-fold) plasma levels of methotrexate upon intravenous administration [26]. In Oatp1a/1b(-/-) mice, absence of Oatp1a/1b transporters resulted in drastically decreased hepatic drug levels (25-fold) and a concomitant high increase in plasma exposure (5-fold) of methotrexate after intravenous (i.v.) administration [25] (Figure 4A, B). Clearly, hepatic Oatp1a/1b transporters dominate the uptake of methotrexate into the liver, and hence the rate of its elimination from plasma. By applying different dose levels (10, 50, or 500 mg/kg), it was further shown that the hepatic Oatp1a/1b transporters have a relatively high capacity to transport methotrexate, because even at the highest dose, no saturation of hepatic uptake was apparent [50]. An impact of OATP1B1 on (i.v.) methotrexate disposition was also observed in a genome-wide analysis of cancer patients: patients carrying low-activity polymorphisms in the OATP1B1 gene displayed increased plasma concentrations concomitant with decreased gastrointestinal toxicities [51]. Most likely, reduced liver uptake in these patients resulted in diminished biliary excretion of methotrexate, thus reducing the direct intestinal exposure and hence the intestinal toxicity of this drug.

Similar pharmacokinetic results as for methotrexate were obtained in Oatp1a/1b knockout mice for fexofenadine, a polar and zwitterionic antihistaminic drug and *in vitro* OATP1A2, -1B1, -1B3 and Oatp1a4 substrate [52]. The anticancer drug paclitaxel, however, is highly lipophilic and lacks anionic groups and is thus not considered a typical OATP substrate. Some paclitaxel transport by OATP1B3 *in vitro* was demonstrated, but not by OATP1B1 or OATP1A2, while mouse Oatp1a/1b transporters have not been tested [53,54]. The lipophilicity aspect made it still rather unexpected that Oatp1a/1b knockout mice displayed clearly increased (>2-fold) plasma concentrations of paclitaxel and decreased (2-fold) liver levels in comparison with wild-type mice after i.v. administration (Figure 4C, D) [50]. These studies show that Oatp1a/1b can strongly affect the pharmacokinetics of a broad range of substrates including charged organic anions (methotrexate), polar zwitterionic drugs (fexofenadine), but also highly hydrophobic drugs (paclitaxel). Recent studies using humanized mice revealed that human OATP1A2, OATP1B1 and OATP1B3 can transport methotrexate *in vivo*, while for paclitaxel only OATP1B3 and OATP1A2, but not OATP1B1, could mediate the liver uptake [27]. An additional anticancer drug which is transported by both mouse and human OATP1A/1B transporters is docetaxel, and the results are presented in chapter 4.2 of this thesis.

Although it has been hypothesized that OATP1A/1B transporters could play a role in the intestinal uptake of several drugs [4], Oatp1a/1b(-/-) mice did not display altered intestinal

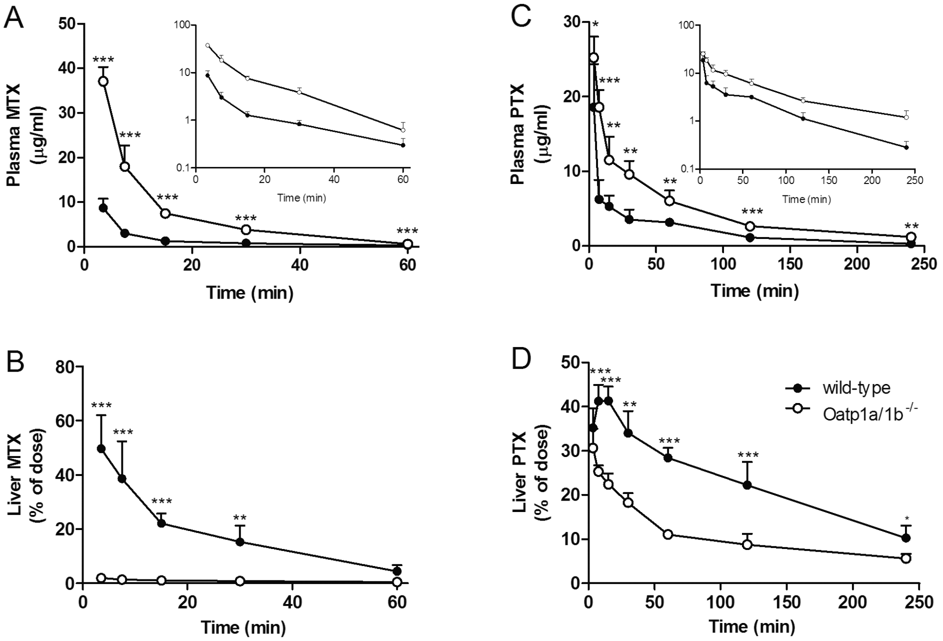

**Figure 4.** Role of Oatp1a/1b proteins in disposition of drugs. Pharmacokinetics of methotrexate (MTX) and paclitaxel (PTX) after intravenous administration of 10 mg/kg to female wild-type and Oatp1a/1b*(-/-)* mice. Plasma concentrations of MTX (A) and PTX (C) versus time curve, with the insert showing a semi-log plot of the data. Liver levels (% of dose) of MTX (B) and PTX (D) versus time curve. All data are presented as means ± S.D. (n = 4-8). * $P < 0.05$; ** $P < 0.01$; *** $P < 0.001$ when compared with wild-type mice. Figures copied with permission from [25, 50].

absorption of methotrexate, fexofenadine, pravastatin, rosuvastatin or docetaxel after oral administration [23,55,56] (Chapter 4.2). Apparently, alternative uptake mechanisms including other apical uptake transporters (e.g., Oatp2b1) or in some cases passive diffusion might dominate the intestinal absorption of these drugs.

Oatp1a/1b uptake transporters are also expressed in the apical membrane of the proximal tubular cells of the kidney [3], where they might in theory be involved in reabsorption of substrates from the tubular fluid, thus reducing their urinary excretion (Figure 1). Indeed, we observed a 15-fold increased renal clearance of rosuvastatin in male Oatp1a/1b knockout mice in comparison with their wild-type conterparts after oral administration (15 mg/kg) [56]. Interestingly, the difference in renal clearance between knockout and wild-type mice was gender-dependent, as it was not observed in female mice. Both wild-type and knockout renal clearance values in female mice were similar to the male Oatp1a/1b knockout values (Table 1). These results could be explained by a differential kidney expression of mouse Oatp1a transporters between male and female mice. Indeed, male wild-type mice (FVB) had 5000-fold higher levels of Oatp1a1 and 2-fold higher levels of Oatp1a6 mRNA in the kidney than the female mice, while Oatp1a4 expression was similar [56]. Collectively, these results indicated that Oatp1a1 is responsible for the renal reabsorption of rosuvastatin, thus reducing its renal clearance. When Oatp1a1 is not present (in male and female Oatp1a/1b knockout mice and female wild-type mice), this process of renal reabsorption is impaired, leading to a significantly higher renal clearance in comparison with male wild-type mice (Table 1) [56]. It should be noted, though, that while the relative shift in renal clearance of rosuvastatin between male wild-type and Oatp1a/1b knockout mice was clear, its contribution to the overall rosuvastatin clearance was small.

The antibiotic rifampicin, a transported substrate of OATP1B1, -1B3 and rat Oatp1b2 [57,58], has been studied in Oatp1b2(-/-) mice. Single dose administration, i.v. or subcutaneous, or continuous subcutaneous infusion led to increased plasma concentrations and decreased liver concentrations, yielding 4- to 8-fold lower liver-to-plasma ratios in Oatp1b2(-/-) mice versus control mice [22,59]. This indicates an important role of Oatp1b2 in the hepatic uptake and

**Table 1.** Renal and non-renal clearance (calculated based on urinary and fecal output) after rosuvastatin administration to wild-type and Oatp1a/1b knockout mice (reproduced from [56]).

| | | **Renal clearance (ml/min/kg)** | **Non-renal clearance (ml/min/kg)** | **Total clearance (ml/min/kg)** |
|---|---|---|---|---|
| 15 mg/kg oral | WT male | 1.3 ± 0.6 | - | - |
| | *Slco1a/1b(-/-)* male | 20.1 ± 9.0 $^{**}$ | - | - |
| | WT female | 20.1 ± 6.4 $^{\#\#}$ | - | - |
| | *Slco1a/1b(-/-)* female | 27.4 ± 4.3 | - | - |
| 5 mg/kg i.v. | WT male | 1.2 ± 0.6 | 11.6 ± 1.3 | 12.8 ± 1.6 |
| | *Slco1a/1b(-/-)* male | 2.4 ± 0.3$^{**}$ | 5.8 ± 0.5$^{**}$ | 8.2 ± 0.3 |

Data presented as mean ± S.E.M. **, *P* < 0.01; ***, *P* < 0.001 when compared with wild-type mice of the same gender, *##, P* < 0.01 when compared with male mice from the same genotype (wild-type or knockout). "-" : non-renal clearance could not be directly calculated for oral administration in the absence of reliable oral bioavailability data.

plasma clearance of rifampicin. Rifampicin was also described as a potent OATP inhibitor [58]. Because Oatp1a/1b knockout mice lack all Oatp1a and Oatp1b proteins, thus minimizing the risk of mutual compensation, they might represent a good model to test the efficacy and specificity of Oatp1a/1b inhibitors by comparing their effects in wild-type and knockout mice. *In vivo* inhibition experiments in these mice showed that rifampicin was indeed an effective and specific Oatp1a/1b inhibitor in modulating methotrexate pharmacokinetics *in vivo* [25]. This confirmed the usefulness of Oatp1a/1b(-/-) mice as a tool to study *in vivo* inhibition properties of OATP inhibitors.

HMG-CoA (3-hydroxy-3-methyl-glutaryl-CoA) reductase inhibitors (statins) act in the liver to reduce cholesterol synthesis, and most have been shown to be human and murine OATP1A/1B substrates *in vitro*. Moreover, many clinical studies have shown a correlation between low-activity polymorphisms in OATP1B1 and increased plasma exposure of these drugs [15]. Theoretically, because the liver represents both the therapeutic target organ of statins and a main clearance organ, OATP1A/1B-mediated liver uptake could have a profound impact on both statin pharmacokinetics and therapeutic efficacy. Increased plasma levels may be of particular relevance for the main side-effect of statins, myopathy, which can sometimes be lethal. Pravastatin, due to its anionic structure and limited metabolism, is regarded as an excellent OATP1A/1B probe drug and has been studied extensively *in vitro*. *In vivo,* however, two independent studies investigating the disposition profile of pravastatin in Oatp1b2(-/-) mice yielded conflicting results. Zaher *et al* found that in Oatp1b2(-/-) mice liver uptake of pravastatin at steady-state concentrations after continuous subcutaneous infusion was up to 2-fold reduced and liver-to-plasma ratios were up to 4-fold decreased in comparison with control mice [22]. Yet, Chen *et al* reported that upon single subcutaneous administration, pravastatin liver-to-plasma ratios two hours after administration were significantly increased (~2-fold) in the same knockout mouse strain [59]. Possible explanations for this discrepancy are differences in dosing regime or age of the mice, and perhaps the small group size used in the latter study. Cerivastatin, simvastatin and lovastatin were also tested. Only for lovastatin the absence of Oatp1b2 resulted in a small, though significant, reduction in liver-to-plasma ratios in comparison with control mice [59]. It could be that Oatp1a1 and/or Oatp1a4, which are still present in the Oatp1b2 knockout mice, might compensate for the loss of function of Oatp1b2 in handling some statins.

Recently we tested the impact of mouse Oatp1a/1b on the disposition of pravastatin and rosuvastatin *in vivo* [55,56]. Absence of mouse Oatp1a/1b transporters resulted in markedly increased plasma exposure of both pravastatin and rosuvastatin, without having a major impact on the liver concentrations. In the case of pravastatin, liver exposure was only 0.5-fold reduced in the Oatp1a/1b knockout mice, while for rosuvastatin liver concentrations were very similar between wild-type and Oatp1a/1b knockout mice after bolus administration. However, the impaired liver uptake is obvious in the markedly decreased liver-to-plasma ratios. These results were qualitatively very different from the previous results with methotrexate, which demonstrated greatly reduced liver concentrations in the Oatp1a/1b knockout mice [25,55,56] (Figure 4). Although counterintuitive, results obtained from the pravastatin and rosuvastatin studies can be easily explained with the help of a physiologically-based pharmacokinetic model [60]. This model predicts that for drugs which are mainly hepatically cleared and have a negligible renal clearance, a diminished liver uptake (like in the case of Oatp1a/1b knockout mice) results in a marked increase in systemic plasma exposure, without affecting the liver concentrations much [60]. Simply put, if there is no alternative clearance pathway for a drug, the markedly increased plasma concentrations which result from the initially reduced hepatic uptake rate (due to absence of Oatp1a/1b transporters) might help to "push" these drugs into the liver via alternative, lower-affinity uptake processes, thus still resulting in an efficient elimination of the drug through the liver [55,56].

Brain penetration and brain clearance of several statins was examined in Oatp1a4(-/-) mice, as it is thought that Oatp1a4, which is present in both the luminal and abluminal membrane of brain capillary endothelial cells (Figure 1D), might mediate bidirectional transport of substrates across the blood-brain barrier [24]. The absence of Oatp1a4 indeed resulted in reduced brain-to-blood transport of various statins and taurocholate after injection into the cerebral cortex, as well as lower blood-to-brain transport after short-term brain *in situ* perfusion of these compounds in a buffer solution [24]. However, after standard i.v. infusion of taurocholate or statins, brain-to-plasma ratios were not significantly different in Oatp1a4(-/-) mice in comparison with wild-type mice [24]. Possibly the short duration of the infusion, low volume of distribution, the presence of active efflux transporters (e.g. P-glycoprotein (Abcb1a/b) or Breast Cancer Resistance Protein (Abcg2)), and/or differences in properties between blood and buffer (e.g., binding to plasma proteins) might explain these discrepancies. For the moment it thus remains an open question whether Oatp1a4 in the blood-brain barrier can contribute significantly to the uptake of drugs into the brain. It is of note, however, that a human counterpart, OATP1A2, is also present in the luminal membrane of brain capillary endothelial cells (Figure 1D), where it might facilitate the uptake of certain drugs into the brain, perhaps resulting in increased neurotoxicity [61].

## *Role of OATP1A/1B in susceptibility to hepatotoxins*

The efficacy of OATP1A/1B transporters in mediating the access of xenobiotics to the liver usually improves overall detoxification, but it may also have negative consequences. This is the case for the mushroom hepatotoxins phalloidin and amantadin, and for microcystin-LR from blue-green algae. These natural compounds can accumulate in the liver, causing severe and sometimes lethal hepatotoxicity in both humans and mice [62,63]. All have been described as OATP1B1 and OATP1B3 substrates *in vitro* [6]. Interestingly, Oatp1b2(-/-) mice were clearly protected (relative to wild-type mice) from the hepatotoxic effects of parenterally administered phalloidin and microcystin-LR, but not of amantadin [21]. Oatp1b2 is apparently the main rodent uptake transporter in the liver for phalloidin and microcystin-LR, and its activity is needed for the hepatotoxicity of these compounds [64,65]. In contrast, based on *in vitro* transport data, Ntcp could also mediate amantadin uptake into the liver. This would explain why Oatp1b2 is not essential for amantadin-induced hepatotoxicity [21].

## Concluding remarks

In recent years many new insights into the physiological and pharmacological functions of OATP transporters have been gained through studies on *in vitro* transport, on the impact of different OATP genetic polymorphisms on clinical pharmacokinetics of drugs, and through analyses of the Oatp1a/1b knockout and humanized transgenic models. We do note that, because there are no straightforward orthologues between the mouse and human OATP1A/1B transporters, results from mouse studies should be extrapolated to the human situation with due caution. Nevertheless, the findings in the Oatp1a and -1b mouse models suggest that one or more hepatic Oatp1a proteins have similar roles as human OATP1B1 and/or OATP1B3 (or mouse Oatp1b2) in mediating the hepatic uptake of compounds. Clearly these studies combined with studies using newly generated humanized mice can completement each other and provide valuable information about the functions of mouse and human OATP1A/1B transporters.

It is clear that the hepatic mouse Oatp1a and Oatp1b2 and human OATP1B transporters have an important role in the dynamic process of bilirubin detoxification. Further elucidation of their interplay with hepatic efflux transporters in this process will be of great interest and may have implications for detoxification of other compounds that are conjugated in the liver as well. Furthermore, Oatp1b2 contributes to the uptake of primarily unconjugated bile acids into the liver, thus having an important role in maintaining their homeostasis and perhaps in their regulatory function elsewhere in the body. We expect that further studies, including metabolomics analyses in single and combination Oatp1a/1b knockout mouse models will reveal additional physiological roles of these transporters.

Pharmacokinetic studies in Oatp knockout and humanized mouse models indicate that the mouse and human Oatp1a/1b transporters have a crucial role in the liver uptake and thereby systemic clearance of anticancer drugs, organic dyes, estrogen derivates, antibiotics, statins and toxins. The fact that Oatp1a/1b transporters can accumulate these drugs in the liver can have profound implications for their pharmacokinetics, pharmacodynamics and toxicity, and hence for their overall therapeutic efficacy. Together with the knowledge of existing polypmorphisms in the OATP1B genes, these findings can contribute to improving the clinical use of drugs. We expect that the Oatp knockout mouse models, together with humanized OATP1B1 and OATP1B3 strains, will provide further insights into the roles of OATP1A/1B transporters, including drug-drug and drug-food interactions, and the possibilities and limitations of various OATP modulation strategies. We hope that these tools and insights will enhance the optimal development of new drugs and drug application regimens.

## Acknowledgements

We thank Seng Chuan Tang, Selvi Durmus and Jeroen Hendrikx for critical reading of the manuscript.

# Reference List

1. Hagenbuch,B. and Meier,P.J. (2004) Organic anion transporting polypeptides of the OATP/ SLC21 family: phylogenetic classification as OATP/ SLCO superfamily, new nomenclature and molecular/functional properties. *Pflügers Arch*. 447, 653-665
2. Cheng,X. *et al*. (2005) Tissue distribution and ontogeny of mouse organic anion transporting polypeptides (Oatps). *Drug Metab. Dispos*. 33, 1062-1073
3. Cheng,X. and Klaassen,C.D. (2009) Tissue distribution, ontogeny, and hormonal regulation of xenobiotic transporters in mouse kidneys. *Drug Metab. Dispos*. 37, 2178-2185
4. Glaeser,H. *et al*. (2007) Intestinal drug transporter expression and the impact of grapefruit juice in humans. *Clin. Pharmacol. Ther*. 81, 362-370
5. Lee,W. *et al*. (2005) Polymorphisms in human organic anion-transporting polypeptide 1A2 (OATP1A2): implications for altered drug disposition and central nervous system drug entry. *J. Biol. Chem*. 280, 9610-9617
6. Klaassen,C.D. and Aleksunes,L.M. (2010) Xenobiotic, bile acid, and cholesterol transporters: function and regulation. *Pharmacol. Rev*. 62, 1-96
7. Bailey,D.G. (2010) Fruit juice inhibition of uptake transport: a new type of food-drug interaction. *Br. J. Clin. Pharmacol*. 70, 645-655
8. Satoh,H. *et al*. (2005) Citrus juices inhibit the function of human organic anion-transporting polypeptide OATP-B. *Drug Metab. Dispos*. 33, 518-523
9. Mougey,E.B. *et al*. (2009) Absorption of montelukast is transporter mediated: a common variant of OATP2B1 is associated with reduced plasma concentrations and poor response. *Pharmacogenet. Genomics* 19, 129-138
10. Kim,R.B. (2003) Organic anion-transporting polypeptide (OATP) transporter family and drug disposition. *Eur. J. Clin. Invest*. 33 Suppl 2, 1-5
11. Marzolini,C. *et al*. (2004) Pharmacogenomics of the OATP and OAT families. *Pharmacogenomics* 5, 273-282
12. Mikkaichi,T. *et al*. (2004) The organic anion transporter (OATP) family. *Drug Metab. Pharmacokinet*. 19, 171-179
13. Nies,A.T. *et al*. (2008) Interplay of conjugating enzymes with OATP uptake transporters and ABCC/MRP efflux pumps in the elimination of drugs. *Expert Opin. Drug Metab. Toxicol*. 4, 545-568
14. Seithel,A. *et al*. (2008) The functional consequences of genetic variations in transporter genes encoding human organic anion-transporting polypeptide family members. *Expert Opin. Drug Metab. Toxicol*. 4, 51-64
15. Ieiri,I. *et al*. (2009) Genetic polymorphisms of uptake (OATP1B1, 1B3) and efflux (MRP2, BCRP) transporters: implications for inter-individual differences in the pharmacokinetics and pharmacodynamics of statins and other clinically relevant drugs. *Expert Opin. Drug Metab. Toxicol*. 5, 703-729
16. Kalliokoski,A. and Niemi,M. (2009) Impact of OATP transporters on pharmacokinetics. *Br. J. Pharmacol*. 158, 693-705
17. Hagenbuch,B. (2010) Drug uptake systems in liver and kidney: a historic perspective. *Clin. Pharmacol. Ther*. 87, 39-47
18. Niemi,M. *et al*. (2011) Organic anion transporting polypeptide 1B1: a genetically polymorphic transporter of major importance for hepatic drug uptake. *Pharmacol. Rev*. 63, 157-181
19. Fahrmayr,C. *et al*. (2010) Hepatic OATP and OCT uptake transporters: their role for drug-drug interactions and pharmacogenetic aspects. *Drug Metab. Rev*. 42, 380-401
20. Farkas,D. and Greenblatt,D.J. (2008) Influence of fruit juices on drug disposition: discrepancies between in vitro and clinical studies. *Expert Opin. Drug Metab. Toxicol*. 4, 381-393
21. Lu,H. *et al*. (2008) Characterization of organic anion transporting polypeptide 1b2-null mice: essential role in hepatic uptake/toxicity of phalloidin and microcystin-LR. *Toxicol. Sci*. 103, 35-45
22. Zaher,H. *et al*. (2008) Targeted disruption of murine organic anion-transporting polypeptide 1b2 (Oatp1b2/Slco1b2) significantly alters disposition of prototypical drug substrates pravastatin and rifampin. *Mol. Pharmacol*. 74, 320-329
23. Gong,L.L. *et al*. (2011) Characterization of Organic Anion Transporting Polypeptide (Oatp) 1a1 and 1a4 Null Mice Reveals Altered Transport Function and Urinary Metabolomic Profiles. *Toxicol. Sci*. 122, 587-597
24. Ose,A. *et al*. (2009) Functional characterization of mouse Oatp1a4 in the uptake and efflux of drugs across the blood-brain barrier. *Drug Metab. Dispos*. 38, 168-176
25. van de Steeg,E. *et al*. (2010) Organic anion transporting polypeptide 1a/1b-knockout

mice provide insights into hepatic handling of bilirubin, bile acids, and drugs. *J Clin Invest* 120, 2942-2952

26. van de Steeg,E. *et al*. (2009) Methotrexate pharmacokinetics in transgenic mice with liver-specific expression of human organic anion-transporting polypeptide 1B1 (SLCO1B1). *Drug Metab. Dispos*. 37, 277-281
27. van de Steeg,E. *et al*. (2013) Influence of human OATP1B1, OATP1B3, and OATP1A2 on the pharmacokinetics of methotrexate and paclitaxel in humanized transgenic mice. *Clin Cancer Res* 19, 821-832
28. Cui,Y. *et al*. (2001) Hepatic uptake of bilirubin and its conjugates by the human organic anion transporter SLC21A6. *J. Biol. Chem*. 276, 9626-9630
29. Briz,O. *et al*. (2003) Role of organic anion-transporting polypeptides, OATP-A, OATP-C and OATP-8, in the human placenta-maternal liver tandem excretory pathway for foetal bilirubin. *Biochem. J*. 371, 897-905
30. Sanna,S. *et al*. (2009) Common variants in the SLCO1B3 locus are associated with bilirubin levels and unconjugated hyperbilirubinemia. *Hum. Mol. Genet*. 18, 2711-2718
31. Zhang,W. *et al*. (2007) OATP1B1 polymorphism is a major determinant of serum bilirubin level but not associated with rifampicin-mediated bilirubin elevation. *Clin. Exp. Pharmacol. Physiol*. 34, 1240-1244
32. Reichel,C. *et al*. (1999) Localization and function of the organic anion-transporting polypeptide Oatp2 in rat liver. *Gastroenterology* 117, 688-695
33. Vlaming,M.L. *et al*. (2008) Impact of Abcc2 (Mrp2) and Abcc3 (Mrp3) on the in vivo elimination of methotrexate and its main toxic metabolite 7-hydroxymethotrexate. *Clin. Cancer Res*. 14, 8152-8160
34. Zelcer,N. *et al*. (2006) Mice lacking Mrp3 (Abcc3) have normal bile salt transport, but altered hepatic transport of endogenous glucuronides. *J. Hepatol*. 44, 768-775
35. van de Steeg,E. *et al*. (2012) Complete OATP1B1 and OATP1B3 deficiency causes human Rotor syndrome by interrupting conjugated bilirubin reuptake into the liver. *J Clin Invest* 122, 519-528
36. Iusuf,D. *et al*. (2012) Hepatocyte hopping of OATP1B substrates contributes to efficient hepatic detoxification. *Clin Pharmacol Ther* 92, 559-562
37. Ah,Y.M. *et al*. (2008) Drug-induced hyperbilirubinemia and the clinical influencing factors. *Drug Metab. Rev*. 40, 511-537
38. Wang,P. *et al*. (2003) The human organic anion transport protein SLC21A6 is not sufficient for bilirubin transport. *J. Biol. Chem*. 278, 20695-20699
39. Zucker,S.D. and Goessling,W. (2000) Mechanism of hepatocellular uptake of albumin-bound bilirubin. *Biochim. Biophys. Acta* 1463, 197-208
40. Dawson,P.A. *et al*. (2009) Bile acid transporters. *J. Lipid Res*. 50, 2340-2357
41. Kosters,A. and Karpen,S.J. (2008) Bile acid transporters in health and disease. *Xenobiotica* 38, 1043-1071
42. Jacquemin,E. *et al*. (1994) Expression cloning of a rat liver Na(+)-independent organic anion transporter. *Proc. Natl. Acad. Sci. U S A* 91, 133-137
43. Kullak-Ublick,G.A. *et al*. (2004) Enterohepatic bile salt transporters in normal physiology and liver disease. *Gastroenterology* 126, 322-342
44. Meier,P.J. and Stieger,B. (2002) Bile salt transporters. *Annu Rev Physiol* 64, 635-661
45. Csanaky,I.L. *et al*. (2011) Organic anion-transporting polypeptide 1b2 (Oatp1b2) is important for the hepatic uptake of unconjugated bile acids: Studies in Oatp1b2-null mice. *Hepatology* 53, 272-281
46. Xiang,X. *et al*. (2009) Effect of SLCO1B1 polymorphism on the plasma concentrations of bile acids and bile acid synthesis marker in humans. *Pharmacogenet. Genomics* 19, 447-457
47. Kullak-Ublick,G.A. *et al*. (2001) Organic anion-transporting polypeptide B (OATP-B) and its functional comparison with three other OATPs of human liver. *Gastroenterology* 120, 525-533
48. Wessels,J.A. *et al*. (2008) Recent insights in the pharmacological actions of methotrexate in the treatment of rheumatoid arthritis. *Rheumatology (Oxford)* 47, 249-255
49. Sasaki,M. *et al*. (2004) Prediction of in vivo biliary clearance from the in vitro transcellular transport of organic anions across a double-transfected Madin-Darby canine kidney II monolayer expressing both rat organic anion transporting polypeptide 4 and multidrug resistance associated protein 2. *Mol Pharmacol* 66, 450-459
50. van de Steeg,E. *et al*. (2011) High impact of Oatp1a/1b transporters on in vivo disposition of the hydrophobic anticancer drug paclitaxel. *Clin. Cancer Res*. 17, 294-301
51. Trevino,L.R. *et al*. (2009) Germline genetic variation in an organic anion transporter polypeptide associated with methotrexate pharmacokinetics and clinical effects. *J. Clin. Oncol*. 27, 5972-5978

52. Shimizu,M. *et al*. (2005) Contribution of OATP (organic anion-transporting polypeptide) family transporters to the hepatic uptake of fexofenadine in humans. *Drug Metab Dispos* 33, 1477-1481
53. Smith,N.F. *et al*. (2005) Identification of OATP1B3 as a high-affinity hepatocellular transporter of paclitaxel. *Cancer Biol Ther* 4, 815-818
54. Smith,N.F. *et al*. (2007) Variants in the SLCO1B3 gene: interethnic distribution and association with paclitaxel pharmacokinetics. *Clin Pharmacol Ther* 81, 76-82
55. Iusuf,D. *et al*. (2012) Organic anion-transporting polypeptides 1a/1b control the hepatic uptake of pravastatin in mice. *Mol Pharm* 9, 2497-2504
56. Iusuf,D. *et al*. (2013) Murine Oatp1a/1b Uptake Transporters Control Rosuvastatin Systemic Exposure without Affecting Its Apparent Liver Exposure. *Mol Pharmacol*
57. Fattinger,K. *et al*. (2000) Rifamycin SV and rifampicin exhibit differential inhibition of the hepatic rat organic anion transporting polypeptides, Oatp1 and Oatp2. *Hepatology* 32, 82-86
58. Vavricka,S.R. *et al*. (2002) Interactions of rifamycin SV and rifampicin with organic anion uptake systems of human liver. *Hepatology* 36, 164-172
59. Chen,C. *et al*. (2008) Utility of a novel Oatp1b2 knockout mouse model for evaluating the role of Oatp1b2 in the hepatic uptake of model compounds. *Drug Metab. Dispos*. 36, 1840-1845
60. Watanabe,T. *et al*. (2009) Physiologically based pharmacokinetic modeling to predict transporter-mediated clearance and distribution of pravastatin in humans. *J Pharmacol Exp Ther* 328, 652-662
61. Urquhart,B.L. and Kim,R.B. (2009) Blood-brain barrier transporters and response to CNS-active drugs. *Eur. J. Clin. Pharmacol*. 65, 1063-1070
62. Pearson,L. *et al*. (2010) On the chemistry, toxicology and genetics of the cyanobacterial toxins, microcystin, nodularin, saxitoxin and cylindrospermopsin. *Mar. Drugs* 8, 1650-1680
63. Wieland,T. (1983) The toxic peptides from Amanita mushrooms. *Int J. Pept. Protein Res*. 22, 257-276
64. Fischer,W.J. *et al*. (2005) Organic anion transporting polypeptides expressed in liver and brain mediate uptake of microcystin. *Toxicol. Appl. Pharmacol*. 203, 257-263
65. Meier-Abt,F. *et al*. (2004) Identification of phalloidin uptake systems of rat and human liver. *Biochim. Biophys. Acta* 1664, 64-69

# 1.2

# *Hepatocyte hopping of OATP1B substrates contributes to efficient hepatic detoxification*

Dilek Iusuf[1], Evita van de Steeg[1] and Alfred H. Schinkel[1]

[1]Division of Molecular Oncology, The Netherlands Cancer Institute,
Amsterdam, The Netherlands

*Clinical Pharmacology and Therapeutics, 2012*

## Introduction

Human organic anion–transporting polypeptides (OATP)1B1 and OATP1B3 are major drug uptake transporters present in the basolateral (sinusoidal) membrane of hepatocytes. Owing to their broad substrate specificity, they have a major impact on the hepatic clearance of numerous anionic drugs and also affect the clearance of hydrophobic and even cationic drugs and drug conjugates. Recent studies have clarified several physiologic and pharmacologic functions of these transporters, as well as their potential contributions to optimal and flexible detoxification in the liver by means of "hepatocyte hopping."

## OATP1B1 and OATP1B3 functions in the liver

The major function of hepatocytes is detoxification. This is achieved by the drug transporters and metabolizing enzymes of the hepatocytes, which work together to eliminate endogenous and exogenous substrates [1]. Organic anion–transporting polypeptides (OATPs, genes: SLCOs) are transmembrane transport proteins that mediate the uptake of compounds into cells [2]. Human OATP1B1 and OATP1B3 mediate the uptake of many compounds from the circulating blood into the liver, including drugs and endogenous compounds such as bile acids and bilirubin. These transporters are of pharmacogenetic importance due to the existence of polymorphic genetic variants that reduce their transport activity [2], leading to higher plasma drug exposure (as a result of impaired liver uptake) and consequently a higher risk of toxicity on exposure to drugs such as statins and irinotecan [2].

OATP1B1 and OATP1B3 substrates are taken up into the liver, are often subsequently conjugated (glucuronidated, sulfated, or glutathionylated), and are mostly eliminated into the bile by effux transporters present in the bile canalicular membrane, especially ATP binding cassette (ABC) effux transporters such as ABCC2 and ABCG2 (Figure 1). The related effux transporter ABCC3, however, is situated in the sinusoidal membrane of hepatocytes, where it can extrude substrates back into the blood. Between the OATPs and ABC effux transporters, there is extensive overlap in substrates, including bilirubin glucuronides (BGs) [1,3]. Here we discuss the physiologic interplay between OATP1B proteins on the one hand and ABCC2 and ABCC3 on the other with respect to BG disposition, and investigate the possible implications for drug detoxification.

## Hepatic OATPS facilitate BG elimination through hepatocyte hopping

Bilirubin is a heme degradation product formed in the spleen from the hemoglobin of spent red blood cells (Figure 1). Because of its high potential toxicity, bilirubin needs to be efficiently cleared by the liver. The classic view of bilirubin disposition is that of a one-way elimination process: unconjugated bilirubin enters the hepatocyte via passive diffusion and/or via uptake transporters and is subsequently conjugated by (UDP)- glucuronosyltransferase 1A1 to more water-soluble bilirubin monoglucuronide (BMG) and bilirubin diglucuronide. These are then efficiently excreted into bile by several efflux transporters, mainly ABCC2 (Figure 1). Until recently, it was thought that it is only under pathological conditions, when biliary excretion is greatly impaired (cholestasis), that ABCC3 will substantially transport BG back from hepatocytes into the blood, thereby allowing their urinary excretion [3].

The results of studies of Oatp1a/1b-null mice, which approximately model the human hepatic OATP1B1 and OATP1B3 functions, challenged this view. Remarkably, Oatp1a/1b-null mice displayed a 40-fold increase in the levels of total bilirubin in plasma, mostly due to increased BMG. In Oatp1a/1b;Abcc3 combination knockout mice, this increase was substantially reversed, indicating that Abcc3 is a prerequisite for most of this increase [4] (Figure 2A). This suggests that mouse

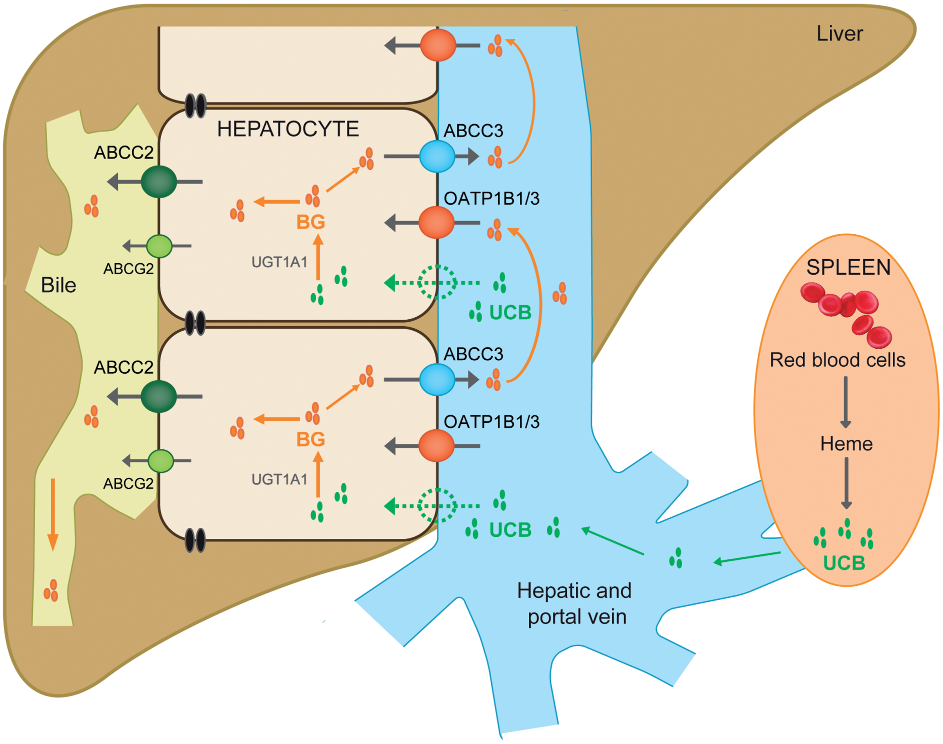

**Figure 1.** Hepatocyte hopping of bilirubin glucuronide. Unconjugated bilirubin (UCB) is formed in the spleen as a degradation product of heme resulting from spent red blood cells, and then travels (tightly bound to albumin) to the liver via the hepatic artery and portal vein. In the liver, UCB enters the hepatocytes via passive diffusion and/or incompletely defined transporters. After conjugation with glucuronic acid by (UDP)-glucuronosyltransferase 1A1 to bilirubin glucuronides (BGs), BGs are secreted into the bile. This secretion is mediated mainly by ATP binding cassette (ABC)C2, although ABCG2 can also contribute to this process. Under physiologic conditions, a substantial fraction of the intracellular BGs is secreted by ABCC3 to the blood, from where it can be taken up again into downstream hepatocytes via organic anion–transporting polypeptides (OATP)1B1 and OATP1B3 (Oatp1a and Oatp1b in mice). This secretion-and-reuptake loop may prevent the saturation of biliary excretion in the upstream hepatocytes, thereby ensuring efficient biliary elimination and hepatocyte detoxification. It is likely that an analogous process applies for many of the drugs conjugated in the liver.

Oatp1a/1b and Abcc3 together form a sinusoidal liver-to-blood shuttling loop. Even under normal physiologic conditions, a substantial portion of the BMG formed in a hepatocyte is not excreted into bile but is transported back to the blood by Abcc3. Oatp1a/1b activity in a downstream hepatocyte allows efficient reuptake of this BMG, again with a possibility of being excreted into bile (Figure 1). In the absence of Oatp1a/1b, this hepatocyte reuptake is impaired, causing greatly increased plasma BMG levels (Figure 2A) and consequent increase in urinary BMG excretion [4].

This arrangement provides an elegant salvage pathway in situations in which the canalicular excretion process in upstream hepatocytes is saturated. This could occur in cases of bilirubin overload (for instance, due to increased hemolysis) or when canalicular ABCC2 activity is compromised (for instance, due to ABCC2-inhibiting drugs, toxins, or endobiotics). Instead of being trapped in upstream hepatocytes, BG can then be easily transferred to downstream hepatocytes via Abcc3 and Oatp1a/1b and then be safely eliminated by excretion into bile (Figure 1). This process allows more flexible and robust detoxification by the liver, potentially distributing the biliary excretion load over all hepatocytes in the liver lobule. In view of the central role of the process involving easy transit of BG from one hepatocyte to the next (and the next), we have dubbed this process "hepatocyte hopping."

Hepatocyte hopping makes biliary excretion of BMG more effcient even under nonpathologic conditions, as is evident from Figure 2B. The removal of either Oatp1a/1b or Abcc3 activity roughly halves the biliary output of BMG as compared with that in wild-type mice. Even the removal of Abcc2, the main canalicular BMG excretion pump, has only limited impact on plasma BMG levels (and a clear but not dramatic effect on biliary excretion of BMG) provided Oatp1a/1b is present (Figure 2A,B). Note that this is a model for greatly reduced (but not obliterated) canalicular BMG excretion, given that Abcg2 is still able to mediate some BMG biliary excretion (Figure 1). However, as soon as Oatp1a/1b is also deleted, a dramatic increase in plasma BG levels and a dramatic reduction in biliary BMG output ensue (Figure 2A,B). Oatp1a/1b activity therefore has the effect of dampening the consequences of compromised canalicular BMG excretion.

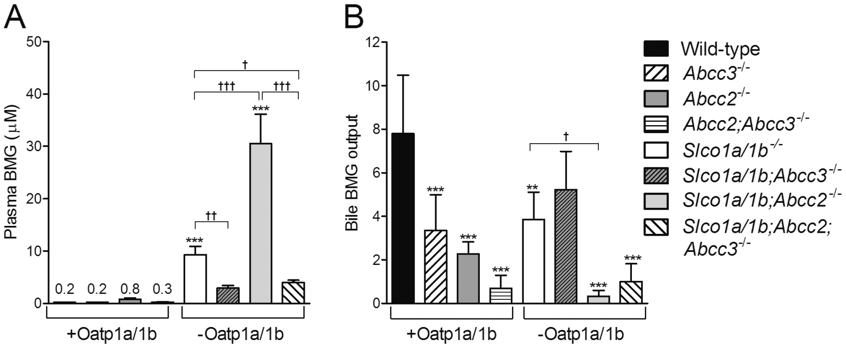

**Figure 2.** The increase in plasma bilirubin monoglucuronide (BMG) in Oatp1a/1b-knockout mice (*Slco1a/1b*(-/-)) is in part dependent on Abcc3. Moreover, Abcc3 can enhance biliary excretion of BMG, but only in the presence of Oatp1a/1b transporters (+Oatp1a/1b), and not in their absence (−Oatp1a/1b). (a) Plasma concentration and (b) bile output levels of BMG in male, wild-type, *Abcc3*(-/-), *Abcc2*(-/-), *Abcc2*(-/-) *Abcc3*(-/-),*Slco1a/1b*(-/-), *Slco1a/1b; Abcc3*(-/-), *Slco1a/1b; Abcc2*(-/-), and *Slco1a/1b; Abcc2; Abcc3*(-/-) mice. Note that BMG represents 95% of the total bilirubin.

## *Full deficiency of OATP1B1 and OATP1B3 underlies human Rotor syndrome*

Studies in humanized Oatp1a/1b-null mice with liver-specific expression of human OATP1B1 or OATP1B3 revealed that these transporters also mediate effcient liver reuptake of BG from plasma [4]. The translation of these findings to humans aided in elucidating the mechanistic and genetic basis of Rotor syndrome (RS) [4]. RS is a rare, benign, hereditary, conjugated hyperbilirubinemia that clinically resembles Dubin–Johnson syndrome (DJS). However, in contrast to DJS, which is caused by mutations in ABCC2 that disrupt the excretion of BG into bile, RS is not associated with ABCC2 mutations. Also, unlike patients with DJS, those with RS have strongly reduced liver uptake of many hepatic diagnostic compounds [4]. The RS pattern of jaundice, with high increases in plasma BG levels and modest increases in the levels of unconjugated bilirubin, was very reminiscent of the Oatp1a/1bknockout phenotype. Sequence analysis of samples from families of patients with RS revealed that all patients with RS had pathogenic mutations that affected both genes encoding OATP1B1 and those encoding OATP1B3, abrogating their protein function. A total deficiency of both OATP1B1 and OATP1B3 thus causes RS in humans by disrupting liver reuptake of conjugated bilirubin [4]. Importantly, the strong similarity in phenotype between human patients with RS and Oatp1a/1b-knockout mice indicates that the same sinusoidal OATP1B-dependent BG efflux/reuptake loop functions in both humans and mice. It is probable that, in humans as well, ABCC3 is an important element of this loop. There is therefore a strong likelihood that hepatocyte hopping occurs in humans just as it does in mice.

## *Pharmacogenetic and clinical–pharmacologic implications*

The RS studies revealed the existence of several different null mutations in OATP1B1 and OATP1B3 in the human population [2]. Three different and independently generated haplotypes associated with total OATP1B1 and OATP1B3 deficiency were found in various RS families. Although the frequency of RS is very low (~1 in 106 ), one individual with a complete homozygous deficiency in OATP1B3 was found in a test group of ~2,300 individuals with no jaundice. Similarly, a single proven null allele of OATP1B1 occurs at a frequency of 0.008 (3 of 354) in a Japanese population, suggesting that the prevalence of total OATP1B1 deficiency is ~1 in 14,000 individuals in this population. Individuals with total deficiency of either OATP1B1 or OATP1B3 alone will therefore be far more numerous than individuals with RS. Given that reduced activity of OATP1B1 (~20% of “wild-type” activity) due to the fairly frequent occurrence of genetic polymorphisms is already a cause of substantially increased toxicity associated with exposure to some drugs, it will be interesting to see what the impact of these dual total deficiencies would be. They could result in idiosyncratic drug hypersensitivities. In contrast to patients with RS, who are easily identifiable from the jaundice present, individuals who are totally deficient in either OATP1B1 or OATP1B3 alone, or who are carriers of low-activity polymorphic variants of OATP1B1/3, can go unidentified. When treated with OATP1B1/3 substrates (such as irinotecan or statins) and/or OATP1B1/3 inhibitors (such as cyclosporine or rifampicin), these individuals might be at risk for severe drug toxicities (e.g., diarrhea, muscular toxicity, or hyperbilirubinemia) [2].

## Broader pharmacologic relevance of hepatocyte hopping

Although not yet proven directly, our findings may have broader pharmacologic implications since hepatocyte hopping allows for more efficient hepatic detoxification. Given the broad substrate specificity for drugs and drug conjugates of these transporters, one can foresee that many drugs and their conjugates will be subject to the same process. Moreover, additional uptake and effux transporters present in the sinusoidal and canalicular membranes (e.g., ABCC4, OATP2B1, NTCP, ABCB11, and ABCB1) will further expand the numbers of substrates affected by hepatocyte hopping. For each of these drugs and drug conjugates accumulating in an upstream hepatocyte, the option to “hop” to downstream hepatocytes reduces the risk of saturating the detoxifying processes in the upstream hepatocyte, including the saturation of hepatobiliary excretion transporters and of the phase I and phase II metabolic conversion steps. For each of these compounds, interference with one or more of the transporters involved (for instance, by drug–drug interactions or due to genetic polymorphisms or mutations) could thus result in altered toxicity. An obvious risk associated with many drug glucuronides and other drug conjugates is that they can give rise to reactive intermediates, leading to protein adduction and subsequent hepatotoxicity [5]. It may therefore be highly beneficial to reduce the likelihood of trapping and accumulating these compounds in upstream hepatocytes due to saturation of canalicular excretion. Clearly, experimental testing of these theoretical predictions is the next priority in this research field.

## Conflict of interest

The research group of A.H.S. receives revenues from commercial distribution of some of the strains described in this study. The other authors declared no conflict of interest.

## Reference list

1. Zamek-Gliszczynski, M.J., Hoffmaster, K.A., Nezasa, K., Tallman, M.N. & Brouwer, K.L. Integration of hepatic drug transporters and phase II metabolizing enzymes: mechanisms of hepatic excretion of sulfate, glucuronide, and glutathione metabolites. Eur. J. Pharm. Sci. 27, 447–486 (2006).
2. Kalliokoski, A. & Niemi, M. Impact of OATP transporters on pharmacokinetics. Br. J. Pharmacol. 158, 693–705 (2009).
3. Iusuf, D., van de Steeg, E. & Schinkel, A.H. Functions of OATP1A and 1B transporters in vivo: insights from mouse models. Trends Pharmacol. Sci. 33, 100–108 (2012).
4. van de Steeg, E. et al. Complete OATP1B1 and OATP1B3 deficiency causes human Rotor syndrome by interrupting conjugated bilirubin reuptake into the liver. J. Clin. Invest. 122, 519–528 (2012).
5. Zhou, S., Chan, E., Duan, W., Huang, M. & Chen, Y.Z. Drug bioactivation, covalent binding to target proteins and toxicity relevance. Drug Metab. Rev. 37, 41–213 (2005).

# 2

# *Mouse and human OATP1A/1B transporters mediate plasma clearance of unconjugated bilirubin and bile acids*

Dilek Iusuf[1], Anita van Esch[1], Dirk R. de Waart[2], Els Wagenaar[1], Evita van de Steeg[1], Ronald P.J. Oude Elferink[2] and Alfred H. Schinkel[1]

[1]Division of Molecular Oncology, The Netherlands Cancer Institute,
[2]Tytgat Institute for Liver and Intestinal Research,
Academic Medical Center, Amsterdam, The Netherlands

*To be submitted*

## Abstract

Organic Anion Transporting Polypeptides (mouse: Oatp, human: OATP) are major uptake transporters with a broad range of endogenous and exogenous substrates. Localized in the basolateral membrane of hepatocytes, the mouse Oatp1a/1b and human OATP1B proteins mediate plasma clearance of compounds by facilitating their uptake into the liver. OATP1A/1B transporters fulfill important physiological functions, aiding in the efficient clearance of bilirubin (by allowing the process of hepatocyte hopping) and in maintaining bile acid homeostasis. Here, we investigated more in depth the role of the mouse and human OATP1A/1B transporters in the plasma clearance of unconjugated bilirubin and unconjugated bile acids *in vivo*, using Oatp1a/1b knockout mice and humanized transgenic mice with liver-specific expression of human OATP1A2, OATP1B1 or OATP1B3. Upon intravenous administration of unconjugated bilirubin (10 mg/kg), the mouse Oatp1a/1b and human OATP1A2 and OATP1B1 transporters clearly contributed to its plasma clearance. Regarding the unconjugated bile acids, Oatp1a/1b knockout mice had significantly increased endogenous plasma levels, while liver-specific expression of OATP1B1 or OATP1B3 provided a partial rescue of this phenotype, indicating that both human proteins contribute to liver uptake of various unconjugated bile acids. In conclusion, we show here that mouse Oatp1a/1b and human OATP1A2 and OATP1B1 transport unconjugated bilirubin, while mouse Oatp1a/1b and human OATP1B1 and OATP1B3 can transport some of the most abundant unconjugated bile acids.

## Introduction

In recent years, there has been great interest in the function of the Organic Anion Transporting Polypeptides (human: OATPs, mouse: Oatps, gene names: *SLCO*, *Slco*). These plasma membrane proteins represent a superfamily of uptake transporters which are localized in various tissues and can mediate the cellular uptake of many endogenous and exogenous compounds [1]. Members of the OATP1A and OATP1B subfamilies are of special interest due to their localization in pharmacokinetically relevant tissues, where they are thought to play an important role in the clearance of endogenous and exogenous compounds [2]. It is important to note that between mouse and human members of the OATP1A/1B subfamilies there are no straightforward orthologues. For example, in the liver, in the basolateral membrane of hepatocytes there are three proteins in the mouse (Oatp1a1, Oatp1a4 and Oatp1b2) and two in humans (OATP1B1 and OATP1B3), while the single human OATP1A member (OATP1A2) is expressed in the liver only in cholangiocytes, the epithelial cells of the bile ducts [3].

The importance of mouse and human OATP1A/1B proteins in the physiological function of the liver became obvious with the discovery of the genetic basis of the Rotor syndrome [4]. This rare, benign, hereditary disorder is characterized by complete deficiency in OATP1B1 and OATP1B3 transporters, leading to conjugated hyperbilirubemia [4]. Previous studies in our group established that mouse and human OATP1A/1B transporters mediate the liver uptake of conjugated bilirubin *in vivo* and *in vitro* [3-5]. Bilirubin is a heme degradation product formed in the spleen from spent red blood cells that, because of its high toxicity, needs to be cleared efficiently by the body [6]. Unconjugated bilirubin (UCB) travels tightly bound to albumin from the spleen to the liver, where it gets glucuronidated to bilirubin mono- and diglucuronide (BMG and BDG). BMG and BDG then get either excreted directly into the bile primarily via ABCC2, or they get secreted back into the blood via an efflux transporter, ABCC3, and then taken up again in downstream hepatocytes by OATP1B transporters [6]. This liver-to-blood shuttling loop, the so-called hepatocyte hopping process, allows for efficient hepatic detoxification of bilirubin [6]. In this process of bilirubin detoxification, a crucial step is the initial liver uptake of UCB, which has been described to occur either via passive diffusion or via transporter-mediated uptake [4, 5, 7-10], although there is no definitive mechanism proven. This is in part because of the great technical difficulty of handling UCB in *in vitro* experiments, whereas OATP substrate-specific functionality, for unknown reasons, also can differ depending on the expression system used. For instance, Cui et al. reported that UCB was taken up by OATP1B1, but not OATP1B3, using expression in mammalian HEK293 cells [9], whereas Wang et al. found that UCB was not transported by OATP1B1 in mammalian HeLa or HEK293 cells [10]. On the other hand, Briz et al. (2003) found, using a *Xenopus laevis* oocyte expression model, that OATP1B1 and OATP1B3 could transport UCB, and OATP1A2 only to a very limited extent [8]. Here, we aimed to better establish the *in vivo* role of mouse and human OATP1A/1B proteins in the plasma clearance of UCB using Oatp1a/1b knockout and liver-specific humanized OATP1A/1B mice.

In addition to bilirubin, bile acids represent one of the first endogenous compounds described as substrates of OATP1A/1B proteins. Bile acids are formed from cholesterol in the liver, and after conjugation [with taurine or glycine], they undergo extensive enterohepatic circulation.

Because bile acids fulfill many biological functions (e.g. facilitation of intestinal uptake of dietary lipids) they are subject to strict homeostasis in the body. This homeostasis is maintained with the help of various transporters in the liver and in the intestine. The Bile acid (or Bile Salt) Export Pump (BSEP/ABCB11) mediates the biliary excretion of conjugated bile acids which end up in the small intestine, where bacterial enzymes partially deconjugate them. In the terminal ileum, both unconjugated and conjugated bile acids are efficiently reabsorbed (by ASBT, (Apical Sodium-dependent Bile acid Transporter) and OST$\alpha/\beta$, (Organic Solute Transporter)) and returned to the liver via the portal vein (reviewed in [3, 11, 12]). In the liver, reuptake of conjugated bile acids from blood is mediated by NTCP, while the unconjugated bile acids are taken up primarily by OATP1B proteins. Several studies *in vitro* and *in vivo* collectively show that, in mice, Oatp1b2 is the main OATP transporter which mediates the liver uptake of unconjugated bile acids [5, 13]. Also human OATP1A2, OATP1B1 and OATP1B3 can transport unconjugated and conjugated bile acids *in vitro* [11, 14], but *in vivo* evidence for a substantial contribution to their hepatic uptake is lacking. In the present study we therefore investigated the role of mouse and human OATP1A/1B proteins in the plasma clearance of unconjugated bile acids *in vivo*.

## Material and methods

### Animals

Animals were housed, when feasible in groups, in a temperature-controlled environment with a 12-hour light/12-hour dark cycle. They received a standard diet (AM-II; Hope Farms) and acidified water *ad libitum*. All mouse experiments were approved by the Animal Experiments Review Board of the Netherlands Cancer Institute (Amsterdam), complying with Dutch legislation and in accordance with European Directive 86/609/EEC. Male or female wild-type, *Slco1a/1b(-/-)* (Oatp1a/1b knockout), *Slco1a/1b(-/-);1B1(tg)*, *Slco1a/1b(-/-);1B3(tg)* and *Slco1a/1b(-/-);1A2(tg)* (liver-specific OATP1B1-, OATP1B3-, and OATP1A2-humanized transgenic) mice of comparable genetic background (>99% FVB) between 8 and 14 weeks of age were used [15].

### Chemicals

UCB was from Sigma-Aldrich (Steinheim, Germany) and unconjugated bile acids (chenodeoxycholic acid and cholic acid) were kindly provided by Dr. Koen van de Wetering (Division of Molecular Oncology, Netherlands Cancer Institute, Amsterdam, The Netherlands). Isoflurane (Forane) was purchased from Abbott Laboratories (Queenborough, Kent, UK) and heparin (5,000 IE/ml) was from Leo Pharma BV (Breda, The Netherlands). Bovine serum albumin (BSA), Fraction V from Roche (Mannheim, Germany) and drug-free lithium-heparinized human plasma was obtained from Bioreclamation LLC (New York, NY, USA).

### Plasma clearance studies

UCB was dissolved in 0.1 M NaOH to a stock of 15 mg/ml, which was further diluted with NaCl (0.9%) to 2 mg/mL and adjusted with HCl (37%) to pH = 8.0. In order to avoid degradation, the solution was shielded from light and samples were collected in amber tubes. Five µL per g of bodyweight of the 2 mg/mL solution was administered i.v. in the tail vein of the mice, in order to achieve a dosage of 10 mg/kg. At different time points (5, 15 and 30 minutes) experiments were terminated by isoflurane anaesthesia and heparin-blood sampling by cardiac puncture followed by cervical dislocation.

Unconjugated bile acids (cholic and chenodeoxycholic acid) were administered intraperitoneally to fasted [for at least 3 hours] female mice in a volume of 5 μL per g of bodyweight, in order to achieve a dosage of 50 μmol/kg. At different time points (7.5, 15 and 30 min) blood was sampled from the tail vein of the mice, and at 60 minutes experiments were terminated by isoflurane anaesthesia and heparin-blood sampling by cardiac puncture followed by cervical dislocation. For determination of endogenous plasma levels of bile acids, male mice were fasted for at least 3 hours and then, under isoflurane anaesthesia, heparin-blood was sampled by cardiac puncture followed by cervical dislocation.

Blood samples were centrifuged at 5,200g for 5 min at 4°C and plasma was collected and stored at -30°C until analysis. Ascorbate (100 mg/ml) was added to bilirubin plasma samples after isolation in order to prevent oxidation of bilirubin.

### *Analysis of bilirubin and bile acids in mouse plasma*

Concentrations of UCB, BMG and BDG and conjugated and unconjugated bile acids were determined by HPLC as described previously [5].

### *Statistical analysis*

The two-sided unpaired Student's *t*-test was used throughout the study to assess the statistical significance of differences between two sets of data. Statistical significance of differences between wild-type and *Slco1a/1b(-/-)*, *Slco1a/1b(-/-);1B1(tg)* or *Slco1a/1b(-/-);1B3(tg) or Slco1a/1b(-/-);1A2(tg)* or between *Slco1a/1b(-/-)* mice and *Slco1a/1b(-/-);1B1(tg)* or *Slco1a/1b(-/-);1B3[tg]* or *Slco1a/1b(-/-);1A2(tg)* mice was assessed by one-way ANOVA followed by Dunett's multiple comparison test. Results are presented as the mean ± S.D. Differences were considered to be statistically significant when $P < 0.05$.

## *Results*

### *Mouse Oatp1a/1b transporters have a clear but non-essential role in the plasma clearance of unconjugated bilirubin*

Initial characterization of the Oatp1a/1b knockout mice revealed that these mice suffered from hyperbilirubinemia, which was mostly due to increased concentrations of conjugated bilirubin in the plasma (Supplemental Figure 1) [5]. However, there was also a consistent 2-fold increase in the levels of unconjugated bilirubin (UCB) in the plasma of these mice [5], which appeared to return to normal levels in the humanized transgenic mice with liver-specific expression of OATP1B1, OATP1B3 or OATP1A2, although this back-shift was only significant for OATP1A2 (Supplemental Figure 1B) [4].

Based on those results, we wanted to obtain additional insight into the role of the mouse and human OATP1A/1B uptake transporters in the plasma clearance of UCB. UCB was therefore administered intravenously (10 mg/kg) to Oatp1a/1b knockout mice and transgenic mice and plasma concentrations of UCB, bilirubin monoglucuronide (BMG) and bilirubin diglucuronide (BDG) were measured by HPLC (Figure 1).

At 15 and 30 minutes, but not at 5 minutes after administration, plasma concentrations of UCB were ~2.5–fold higher in the Oatp1a/1b knockout mice (Figure 1A). These results indicate that the mouse Oatp1a/1b transporters contribute to the plasma clearance of UCB, most likely by mediating its liver uptake. However, they are not essential, given the substantial remaining UCB clearance in the Oatp1a/1b knockout mice (Figure 1A) and the rapid production of BMG seen in these mice already 5 min after UCB administration (Figure 1D). The plasma levels of UCB represented the great majority (>80%) of total bilirubin at 5 min (Figure 1B, C). BMG plasma levels (corrected for endogenous levels) were 7- to 10-fold higher in the Oatp1a/1b knockout mice than in the wild-type mice (Figure 1D), and relative BDG levels were even more increased (Figure 1E). This extends our previous findings that mouse Oatp1a/1b proteins are crucial for the hepatic re-uptake of conjugated bilirubin at steady state endogenous bilirubin levels [4]. Clearly, the relative effect of Oatp1a/1b transporters on conjugated bilirubin clearance was more substantial than that on UCB clearance.

### *Human OATP1B1 and OATP1A2, but not OATP1B3, clear UCB from plasma*

We subsequently measured the plasma levels of bilirubin in the humanized mouse strains after intravenous administration of UCB at 10 mg/kg (Figure 1B-E). Only humanized mice with liver-specific expression of OATP1B1 or OATP1A2 provided a partial rescue from the increased plasma UCB levels in the Oatp1a/1b knockout mice (Figure 1C). In these mice, plasma concentrations of UCB were slightly decreased, albeit mostly not significantly, at 5 and 15 min when compared to Oatp1a/1b knockout mice. At 30 minutes however, plasma UCB levels in the humanized OATP1B1 and OATP1A2 mice were clearly and significantly decreased in comparison with the Oatp1a/1b knockout, and virtually back to wild-type levels (Figure 1C). This suggests that human OATP1B1 and OATP1A2 can transport UCB *in vivo*. In contrast, in the OATP1B3 humanized mice, UCB plasma concentrations were at all time points as high as in the Oatp1a/1b knockout mice (Figure 1C), suggesting that OATP1B3 does not substantially transport UCB *in vivo*. Interestingly, also at endogenous plasma levels of UCB, OATP1A2 could provide a partial rescue of the increased plasma concentrations of UCB in the Oatp1a/1b knockout mice (Supplemental Figure 1B).

### *Human OATP1B1 and OATP1B3, but not OATP1A2, efficiently clear BMG and BDG from plasma*

Extending our previously reported results with steady state endogenous bilirubin levels (Supplemental Figure 1) [4], after intravenous administration of UCB both OATP1B1 and OATP1B3 were able to efficiently clear the produced conjugated bilirubin (BMG and BDG) *in vivo* (Figure 1D, E), albeit that plasma levels were not fully down to wild-type levels. In contrast to its efficiency in clearing UCB, OATP1A2 cleared BMG and BDG only to some extent *in vivo*, as evident from the reduced plasma levels at 5 min compared to the knockout values (Figure 1D and E). However, apparently it can be easily saturated, considering the much higher BMG and BDG plasma concentrations at 15 and 30 minutes compared to those in the other humanized strains, even approaching the Oatp1a/1b knockout levels (Figure 1D and 1E).

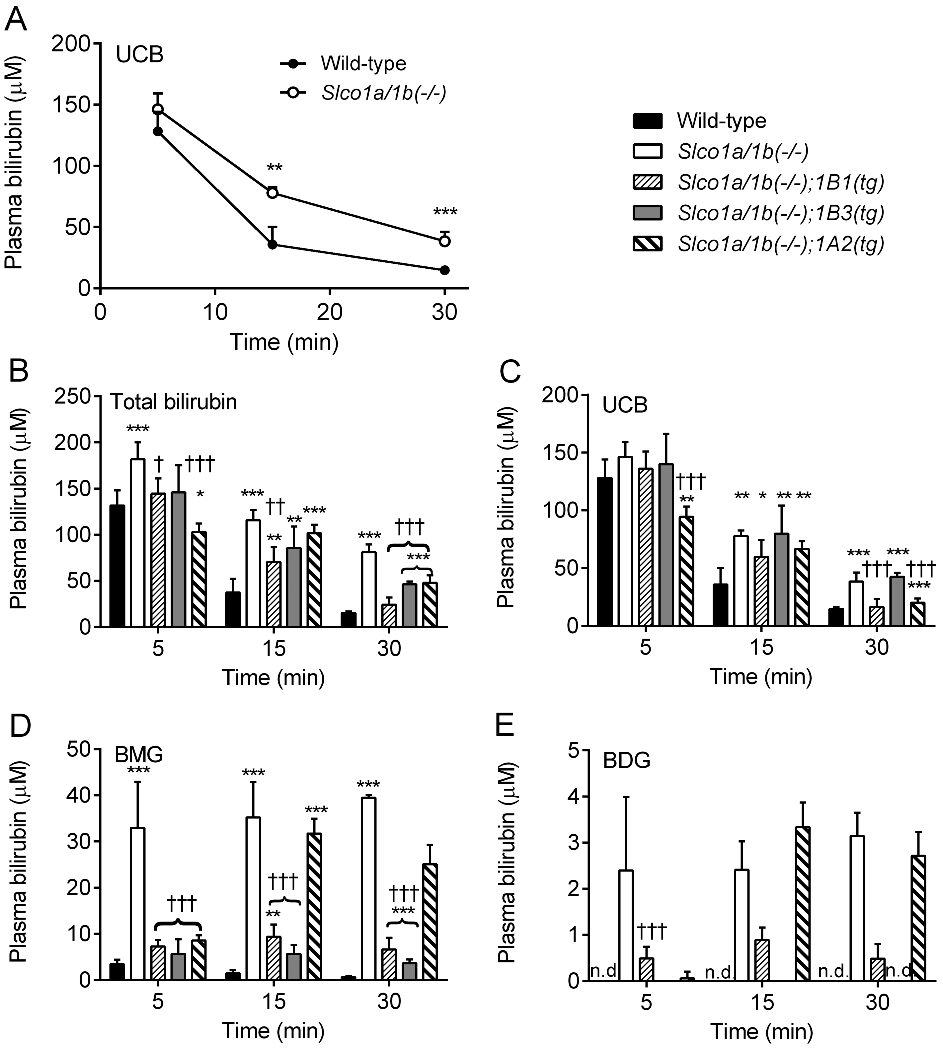

**Figure 1.** Plasma bilirubin levels (minus endogenous levels) after i.v. administration (10 mg/kg) of UCB to male wild-type, Oatp1a/1b knockout and OATP1B1-, 1B3-, and 1A2-humanized transgenic mice. (A) Semi-log plot of UCB plasma concentrations in wild-type and Oatp1a/1b knockout mice at various time points after administration. (B) Total bilirubin, (C) UCB, (D) bilirubin monoglucuronide (BMG) and (E) bilirubin diglucuronide (BDG) plasma concentrations at various time points after administration. Data are presented as mean ± S.D. (n = 5-6, *, $P < 0.05$; **, $P < 0.01$; ***, $P < 0.001$ when compared with wild-type, $^{\dagger}$, $P < 0.05$; $^{\dagger\dagger\dagger}$, $P < 0.001$ when compared with Oatp1a/1b knockout mice).

### *Human OATP1B1 and OATP1B3 clear unconjugated bile acids more efficiently from plasma than OATP1A2*

It was previously reported that mouse Oatp1a/1b proteins, and more specifically Oatp1b2, control the plasma clearance of unconjugated bile acids by facilitating their liver uptake [5, 13]. To study the *in vivo* functionality of the human OATP1A/1B proteins in this process, we measured the endogenous conjugated and unconjugated total bile acid levels in plasma of humanized transgenic mice with liver-specific expression of human OATP1B1, OATP1B3 or OATP1A2 (Figure 2). Note that we presented the results as mean ± SEM, as plasma bile acid levels tend to be highly variable. Most of the bile acids recovered in the plasma of knockout and transgenic strains were unconjugated, and their plasma concentrations were highly significantly increased (~35-fold) in the Oatp1a/1b knockout mice when compared to wild-type. These results obtained in an FVB strain background were similar to those previously obtained in a mixed 129/Ola and FVB genetic background [5]. In the OATP1B1- and OATP1B3-, but not in the OATP1A2-humanized mice, the plasma concentrations of unconjugated bile acids were significantly reduced (~2-fold) compared to those in the Oatp1a/1b knockout mice, although they remained higher than in wild-type mice (Figure 2B). In contrast, conjugated bile acids considered in aggregate [but see below], were not significantly altered in the knockout and transgenic mice (Figure 2C).

Considering specific bile acid species, the most abundant unconjugated bile acids in plasma of the Oatp1a/1b knockout mice were cholic acid, α-muricholic acid and deoxycholic acid, and each was profoundly and highly significantly increased (>30-fold) relative to the wild-type levels (Figure 3A, C, E). Levels of the less abundant chenodeoxycholic acid, ursodeoxycholic acid and

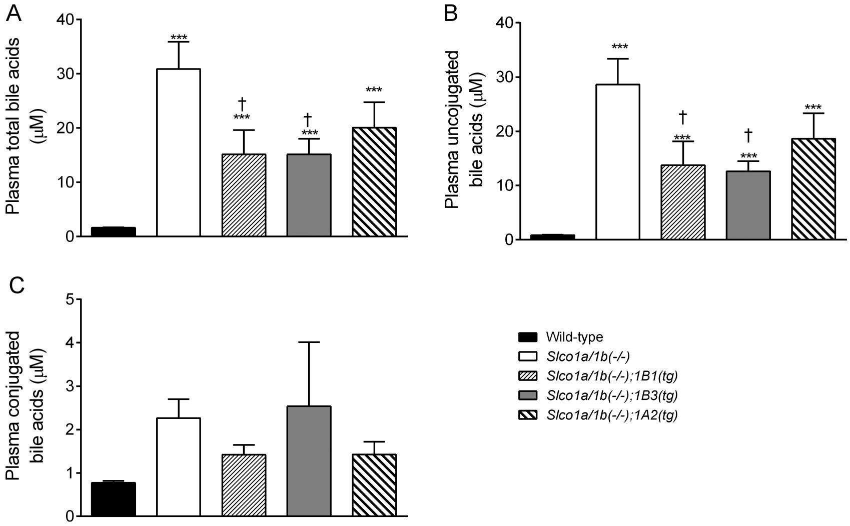

**Figure 2.** Endogenous plasma levels of (A) total, (B) unconjugated and (C) conjugated bile acids in fasted male wild-type, Oatp1a/1b knockout and OATP1B1-, 1B3-, and 1A2-humanized transgenic mice. Data are presented as mean ± S.E.M (n = 6-8, *, $P < 0.05$; **, $P < 0.01$; ***, $P < 0.001$ when compared with wild-type, $^{\dagger}$, $P < 0.05$; $^{\dagger\dagger}$, $P < 0.01$; $^{\dagger\dagger\dagger}$, $P < 0.001$ when compared with Oatp1a/1b knockout mice). Note the difference in Y-axis scale in panel C.

trihydroxy cholestanoic acid were modestly increased (2-3-fold), albeit not significantly for the last compound (Figure 3B, D, F). In the humanized mice OATP1B1 significantly reduced the plasma levels of cholic acid (2.5-fold), chenodeoxycholic acid (2.2-fold) and α-muricholic acid (2-fold) compared to the knockout mice (Figure 3A, B, C). Deoxycholic acid was also reduced (~2-fold), but not significantly (Figure 3E). Transgenic OATP1B3 caused a profound and highly significant decrease (4.4-fold) of α-muricholic acid levels (Figure 3C). Plasma levels of cholic acid (1.5-fold), deoxycholic acid (1.6-fold) and trihydroxy cholestanoic acid (1.9-fold) were also reduced by OATP1B3, but not significantly (Figure 3A, E, F). Finally, OATP1A2-humanized

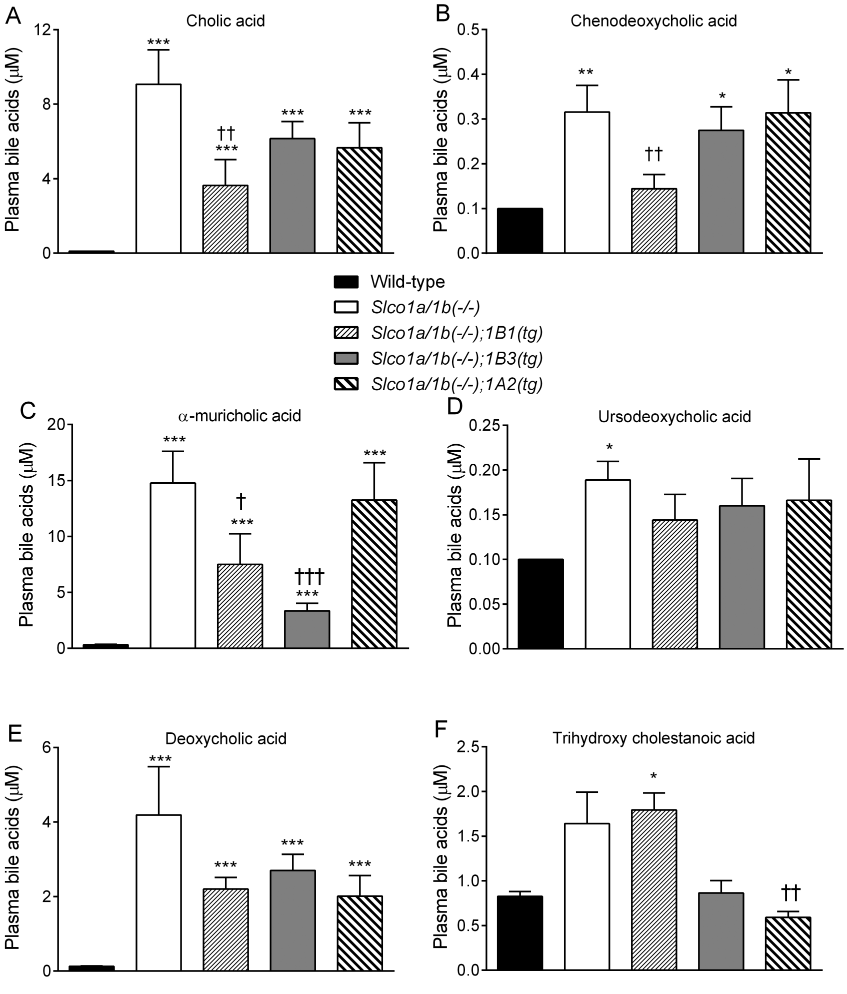

**Figure 3.** Endogenous plasma levels of individual unconjugated bile acids in fasted male wild-type, Oatp1a/1b knockout and OATP1B1-, 1B3-, and 1A2-humanized transgenic mice. Data are presented as mean ± S.E.M (n = 6-8, *, $P < 0.05$; **, $P < 0.01$; ***, $P < 0.001$ when compared with wild-type, $^{\dagger}$, $P < 0.05$; $^{\dagger\dagger}$, $P < 0.01$; $^{\dagger\dagger\dagger}$, $P < 0.001$ when compared with Oatp1a/1b knockout mice). Note the difference in Y-axis scales between the panels.

mice showed reduced plasma levels of cholic acid (1.6-fold), deoxycholic acid (2.1-fold) and trihydroxy cholestanoic acid (2.7-fold) compared to Oatp1a/1b knockout mice, but only the last shift was statistically significant (Figure 3A, E, F). These results suggest that expression of OATP1B1 and OATP1B3, but not OATP1A2, in the liver provides a partial rescue from the increased plasma levels of the most abundant unconjugated bile acids. However, OATP1A2 expression did significantly reduce the plasma levels of trihydroxy cholestanoic acid (Figure 3F). Collectively, the results illustrate partial overlap but also clear differences in *in vivo* substrate preferences between OATP1B1, OATP1B3, and OATP1A2 for liver clearance of unconjugated bile acids.

In plasma of Oatp1a/1b knockout mice the conjugated bile acids were much less abundant than their unconjugated counterparts (Figure 2), but the levels of a few comparatively abundant ones (taurocholic acid and tauro-α-muricholic acid) were significantly increased compared to those in wild-type mice (Figure 4A, C). This indicates a minor role for the mouse Oatp1a/1b proteins in the plasma clearance of some conjugated bile acids. The role of the human OATP1A/1B transporters in conjugated bile acid clearance might be even smaller as there was no statistically significant reversal in the humanized strains of the increased plasma levels in the absence of mouse Oatp1a/1b transporters (Figure 4).

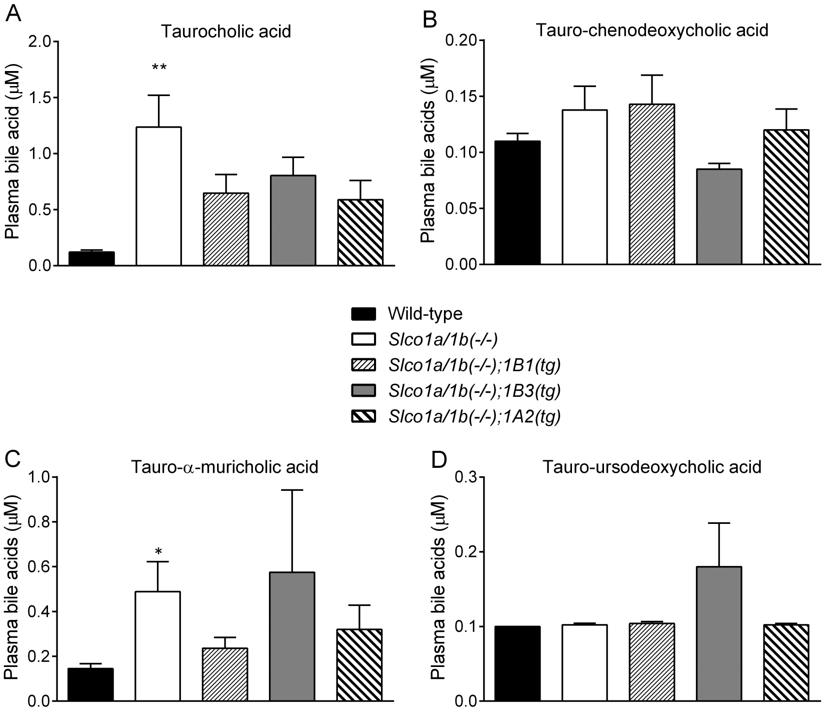

**Figure 4.** Endogenous plasma levels of individual conjugated bile acids in fasted male wild-type, Oatp1a/1b knockout and OATP1B1-, 1B3-, and 1A2-humanized transgenic mice. Data are presented as mean ± S.E.M (n = 6-8, *, $P < 0.05$; **, $P < 0.01$; ***, $P < 0.001$ when compared with wild-type, ††, $P < 0.01$ when compared with Oatp1a/1b knockout mice). Note the difference in Y-axis scales between the panels.

### *Impact of mouse and human OATP1A/1B proteins on plasma clearance of exogenous cholic acid and chenodeoxycholic acid*

To further study the capacity of mouse and human OATP1A/1B proteins to clear unconjugated bile acids, we administered cholic acid or chenodeoxycholic acid (50 µmol/kg) intraperitoneally to wild-type, knockout and transgenic humanized mice and measured the plasma concentrations at various time points. In the absence of Oatp1a/1b transporters, plasma concentrations of both cholic acid and chenodeoxycholic acid were significantly higher at all time points (Figure 5). This further supports that mouse Oatp1a/1b proteins contribute to the plasma clearance of these bile acids also after exogenous administration. However, also considering the higher background plasma levels of especially cholic acid, there was still substantial unconjugated bile acid clearance in the knockout strain. Presumably at these high plasma levels there are other effective clearance mechanisms for unconjugated bile acids, possibly including NTCP [16] and/or renal clearance.

Perhaps not surprisingly in view of this high residual unconjugated bile acid clearance capacity in the knockout strain, and the comparatively modest impact of the OATP1A/1B transgenes on steady-state unconjugated bile acid levels (Figure 3), we did not observe a clear reversal of the impaired plasma clearance of cholic acid or chenodeoxycholic acid in any of the humanized mouse strains compared to the knockout strain (Figure 6).

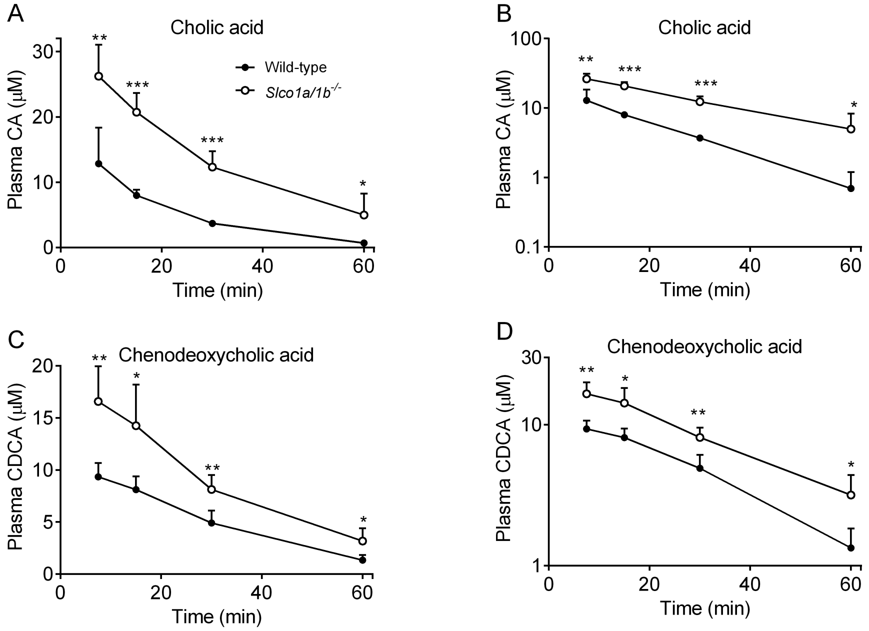

**Figure 5.** Plasma concentrations versus time of (A) cholic acid (CA) or (C) chenodeoxycholic acid (CDCA) after i.p. administration of 50 µmol/kg of cholic acid or chenodeoxycholic acid to fasted female wild-type and Oatp1a/1b knockout mice. (B) and (D) Semi-log plot of plasma concentrations of CA and CDCA, respectively. Values were not corrected for endogenous bile acid levels. Data are presented as mean ± S.D. (n = 6-8, *, $P < 0.05$; **, $P < 0.01$; ***, $P < 0.001$ when compared with wild-type).

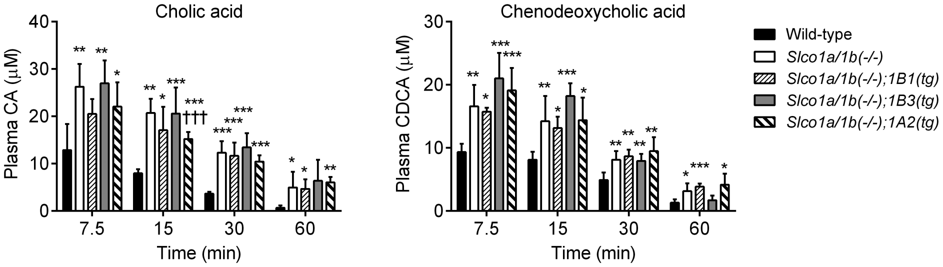

**Figure 6.** Plasma concentrations versus time of (A) cholic acid or (B) chenodeoxycholic acid after i.p. administration of 50 μmol/kg of cholic acid or chenodeoxycholic acid to fasted female wild-type, Oatp1a/1b knockout and OATP1B1-, 1B3-, and 1A2-humanized transgenic mice. Values were not corrected for endogenous bile acid levels. Data are presented as mean ± S.D. (n = 6-8, *, *P* < 0.05; **, *P* < 0.01; ***, *P* < 0.001 when compared with wild-type; †††, *P* < 0.001 when compared with Oatp1a/1b knockout mice).

## Discussion

In this study we gained further insight into how mouse and human OATP1A/1B proteins handle UCB and unconjugated bile acids. We show here that one or more of the mouse hepatic Oatp1a/1b proteins as well as human OATP1B1 and OATP1A2 can contribute to the plasma clearance of UCB after intravenous administration. Regarding the bile acids, at endogenous levels, liver-specific expression of OATP1B1 and OATP1B3 can provide a partial rescue of the increased plasma concentrations of several unconjugated bile acids seen in the Oatp1a/1b knockout mice.

The exact contribution of mouse and human OATP1A/1B transporters to the liver uptake of UCB is not clearly established. As described in the Introduction, *in vitro* experiments suggest that especially the human OATP1B transporters may transport UCB, but results between different research groups are not consistent. The fact that more than 50% of the plasma total bilirubin is represented by conjugated bilirubin in the Oatp1a/1b knockout mice (as well as in Rotor syndrome patients) suggests that the mouse and/or human OATP1A/1B transporters are not strictly essential for the liver uptake of UCB [4, 5]. Indeed, previous studies have reported that UCB can diffuse freely across the membrane of hepatocytes [17], but we cannot exclude that in addition alternative uptake systems (e.g. OATP2B1) can mediate some active transport of UCB into the liver. Accordingly, the clearance defect of UCB we observed in Oatp1a/1b knockout mice was only partial. Our data suggest that, although apparently not essential for the liver uptake of UCB, mouse Oatp1a/1b and human OATP1B1 and OATP1A2 do contribute to its plasma clearance *in vivo*. We observed a 2-fold increase in the plasma UCB levels in Oatp1a/1b knockout mice, while liver-specific expression of OATP1B1 or OATP1A2 could provide a partial rescue of this phenotype. These data are in line with data from Rotor patients (with complete deficiency of OATP1B1 and OATP1B3) which have not only increased plasma levels of conjugated bilirubin, but also of UCB and which also display decreased plasma clearance of intravenously administered UCB [18, 19]. Also, low-activity polymorphic variants in *SLCO1B1* and *SLCO1B3* have been associated with mildly increased plasma levels of UCB [20, 21].

Although UCB was previously described as an *in vitro* substrate of OATP1B3 [8], another study contradicted this [9], and in our study we did not observe a rescue in the OATP1B3-humanized mice upon intravenous administration of UCB. One possible explanation for this discrepancy might perhaps be the relatively high plasma levels of UCB in these mice after intravenous administration, which might lead to saturation of OATP1B3. All in all OATP1B3 is unlikely to be a substantial UCB uptake mechanism in the human liver. In contrast, our data suggest that certainly human OATP1B1 contributes to the uptake of UCB from plasma in the human liver. In the transgenic mice OATP1A2 showed a similar UCB uptake contribution as OATP1B1, but since this protein is not physiologically expressed in hepatocytes in normal human liver (it is only found in cholangiocytes) it won't contribute to hepatic UCB uptake from human plasma.

Interestingly, it appears that OATP1A2 can transport bilirubin glucuronides *in vivo* into the hepatocytes but with much lower efficiency than OATP1B1 or OATP1B3. In contrast, OATP1A2 can mediate quite efficient plasma clearance of UCB *in vivo*, both at endogenous plasma levels and after intravenous administration. Given this efficient UCB transport, it might be that a physiological function of OATP1A2, localized in the apical membrane of cholangiocytes, is to reduce elimination of UCB into the bile by reabsorption before it reaches the gallbladder. Due to its very poor watersolubility UCB might considerably contribute to the risk of forming gallstones. Also, the observation that human OATP1A2 can transport UCB *in vivo* might be relevant for OATP1A2 functions in other tissues, e.g. in kidney or small intestine. Thus, although the OATP1A2-humanized mouse model does not present a true physiological model, it can still be very useful in studying the *in vivo* transport capacity of OATP1A2, which might be relevant for its activity in other healthy tissues [3].

Data from Oatp1b2 and Oatp1a/1b knockout mouse models demonstrated that, in mice, Oatp1b2 is the main Oatp transporter mediating the liver uptake of unconjugated bile acids [3, 5, 13]. We found that human OATP1B1 and OATP1B3 can provide a partial rescue of the increased endogenous plasma levels of unconjugated bile acids, namely cholic acid, $\alpha$-muricholic acid, and chenodeoxycholic acid, observed in the Oatp1a/1b knockout mice. This is in line with *in vitro* data [22] and clinical studies in carriers of low-activity polymorphic variants of *SLCO1B1* which have increased plasma levels of unconjugated bile acids [23]. It should be noted that in the human liver, both OATP1B1 and OATP1B3 are simultaneously expressed, resulting in an additive contribution to the plasma clearance of compounds, whereas in the humanized mice there is only one OATP1B protein present [3]. Also in view of the partial overlap in unconjugated bile acid species transported by OATP1B1 and OATP1B3, our data in the single humanized mice are thus most likely an underestimate of the combined effect of these transporters in the human liver. We note that this will apply not only to bile acids, but also to bilirubin clearance in the human liver.

It would clearly be interesting to investigate the plasma levels of bile acids in Rotor patients (deficient for both OATP1B1 and OATP1B3) and/or the plasma clearance of some of the most abundant bile acids in their plasma. However, given the extremely low frequency with which these patients occur this will be difficult to achieve.

Taken together, our results show that the mouse and human OATP1A/1B transporters play a role in the liver uptake of UCB and unconjugated bile acids *in vivo*, thus providing more insight into their physiological functions.

## *Reference List*

1. Hagenbuch B, Meier PJ. The superfamily of organic anion transporting polypeptides. Biochim Biophys Acta 2003 Jan 10;1609[1]:1-18.
2. Kalliokoski A, Niemi M. Impact of OATP transporters on pharmacokinetics. Br J Pharmacol 2009 Oct;158[3]:693-705.
3. Iusuf D, van de Steeg E, Schinkel AH. Functions of OATP1A and 1B transporters in vivo: insights from mouse models. Trends Pharmacol Sci 2012 Feb;33[2]:100-108.
4. van de Steeg E, Stranecky V, Hartmannova H, Noskova L, Hrebicek M, Wagenaar E, et al. Complete OATP1B1 and OATP1B3 deficiency causes human Rotor syndrome by interrupting conjugated bilirubin reuptake into the liver. J Clin Invest 2012 Feb 1;122[2]:519-528.
5. van de Steeg E, Wagenaar E, van der Kruijssen CM, Burggraaff JE, de Waart DR, Elferink RP, et al. Organic anion transporting polypeptide 1a/1b-knockout mice provide insights into hepatic handling of bilirubin, bile acids, and drugs. J Clin Invest 2010 Aug;120[8]:2942-2952.
6. Iusuf D, van de Steeg E, Schinkel AH. Hepatocyte hopping of OATP1B substrates contributes to efficient hepatic detoxification. Clin Pharmacol Ther 2012 Nov;92[5]:559-562.
7. Zucker SD, Goessling W. Mechanism of hepatocellular uptake of albumin-bound bilirubin. Biochim Biophys Acta 2000 Feb 15;1463[2]:197-208.
8. Briz O, Serrano MA, Macias RI, Gonzalez-Gallego J, Marin JJ. Role of organic anion-transporting polypeptides, OATP-A, OATP-C and OATP-8, in the human placenta-maternal liver tandem excretory pathway for foetal bilirubin. Biochem J 2003 May 1;371[Pt 3]:897-905.
9. Cui Y, Konig J, Leier I, Buchholz U, Keppler D. Hepatic uptake of bilirubin and its conjugates by the human organic anion transporter SLC21A6. J Biol Chem 2001 Mar 30;276[13]:9626-9630.
10. Wang P, Kim RB, Chowdhury JR, Wolkoff AW. The human organic anion transport protein SLC21A6 is not sufficient for bilirubin transport. J Biol Chem 2003 Jun 6;278[23]:20695-20699.
11. Meier PJ. Molecular mechanisms of hepatic bile salt transport from sinusoidal blood into bile. Am J Physiol 1995 Dec;269[6 Pt 1]:G801-G812.
12. Stieger B, Geier A. Genetic variations of bile salt transporters as predisposing factors for drug-induced cholestasis, intrahepatic cholestasis of pregnancy and therapeutic response of viral hepatitis. Expert Opin Drug Metab Toxicol 2011 Apr;7[4]:411-425.
13. Csanaky IL, Lu H, Zhang Y, Ogura K, Choudhuri S, Klaassen CD. Organic anion-transporting polypeptide 1b2 [Oatp1b2] is important for the hepatic uptake of unconjugated bile acids: Studies in Oatp1b2-null mice. Hepatology 2011 Jan;53[1]:272-281.
14. Kullak-Ublick GA, Stieger B, Meier PJ. Enterohepatic bile salt transporters in normal physiology and liver disease. Gastroenterology 2004 Jan;126[1]:322-342.
15. van de Steeg E, van Esch A, Wagenaar E, Kenworthy KE, Schinkel AH. Influence of Human OATP1B1, OATP1B3, and OATP1A2 on the pharmacokinetics of methotrexate and paclitaxel in humanized transgenic mice. Clin Cancer Res 2013 Feb 15;19[4]:821-832.
16. Dawson PA, Oelkers P. Bile acid transporters. Curr Opin Lipidol 1995 Apr;6[2]:109-114.
17. Zucker SD, Goessling W, Hoppin AG. Unconjugated bilirubin exhibits spontaneous diffusion through model lipid bilayers and native hepatocyte membranes. J Biol Chem 1999 Apr 16;274[16]:10852-10862.
18. Fedeli G, Rapaccini GL, Anti M, Miggiano G, Sabelli C, De Vitis I, et al. Impaired clearance of cholephilic anions in Rotor syndrome. Z Gastroenterol 1983 May;21[5]:228-233.
19. Kawasaki H, Kimura N, Irisa T, Hirayama C. Dye clearance studies in Rotor's syndrome. Am J Gastroenterol 1979 Apr;71[4]:380-388.
20. Sanna S, Busonero F, Maschio A, McArdle PF, Usala G, Dei M, et al. Common variants in the SLCO1B3 locus are associated with bilirubin levels and unconjugated hyperbilirubinemia. Hum Mol Genet 2009 Jul 15;18[14]:2711-2718.
21. Zhang W, He YJ, Gan Z, Fan L, Li Q, Wang A, et al. OATP1B1 polymorphism is a major determinant of serum bilirubin level but not associated with rifampicin-mediated bilirubin elevation. Clin Exp Pharmacol Physiol 2007 Dec;34[12]:1240-1244.
22. Yamaguchi H, Okada M, Akitaya S, Ohara H, Mikkaichi T, Ishikawa H, et al. Transport of fluorescent chenodeoxycholic acid via the human organic anion transporters OATP1B1 and OATP1B3. J Lipid Res 2006 Jun;47[6]:1196-1202.
23. Xiang X, Han Y, Neuvonen M, Pasanen MK, Kalliokoski A, Backman JT, et al. Effect of SLCO1B1 polymorphism on the plasma concentrations of bile acids and bile acid synthesis marker in humans. Pharmacogenet Genomics 2009 Jun;19[6]:447-457.

## *Supplemental data*

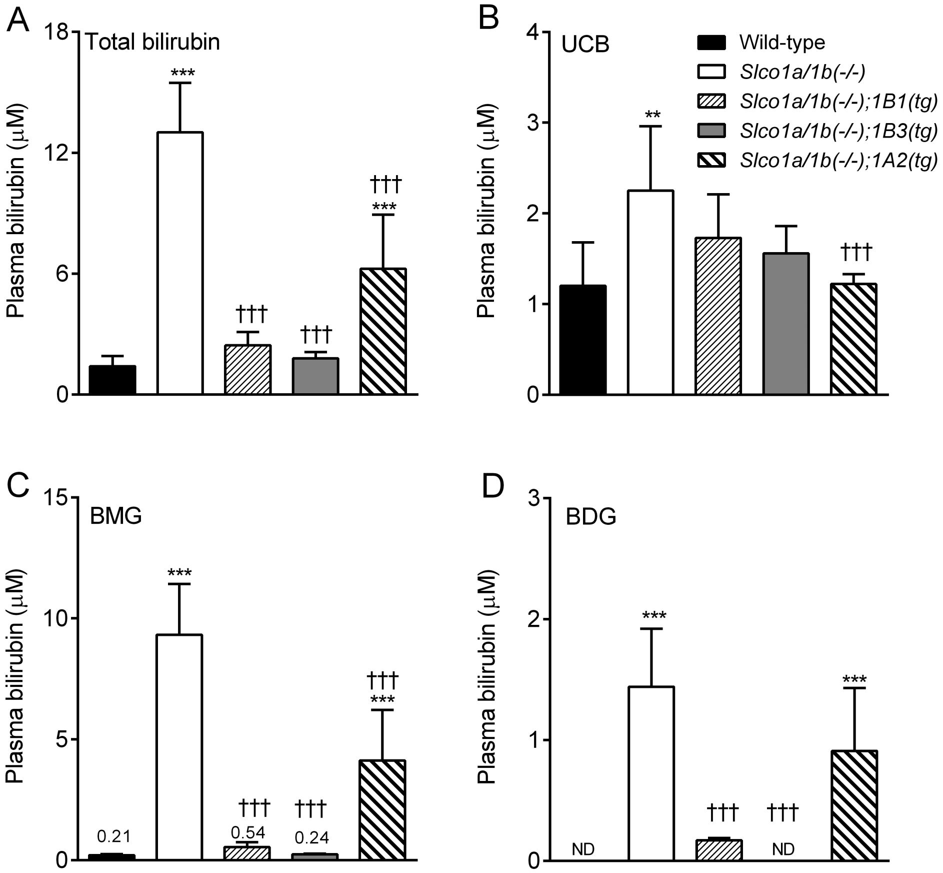

**Supplemental Figure 1.** Endogenous plasma bilirubin levels in male wild-type, Oatp1a/1b knockout and OATP1B1-, 1B3-, and 1A2-humanized transgenic mice. (A) Total bilirubin, (B) UCB, (C) bilirubin monoglucuronide (BMG) and (D) bilirubin diglucuronide (BDG) plasma concentrations. Data are presented as mean ± S.D. (n = 5-6, *, $P < 0.05$; **, $P < 0.01$; ***, $P < 0.001$ when compared with wild-type, †, $P < 0.05$; †††, $P < 0.001$ when compared with Oatp1a/1b knockout mice) (reproduced from [15]).

# Role of Oatp1a/1b transporters in the pharmacokinetics of statins

# 3

# Organic anion-transporting polypeptides 1a/1b control the hepatic uptake of pravastatin in mice

# 3.1

Dilek Iusuf[1], Rolf W. Sparidans[2], Anita van Esch[1], Mike Hobbs[3], Kathryn E Kenworthy[3], Evita van de Steeg[1], Els Wagenaar[1], Jos H. Beijnen[4] and Alfred H. Schinkel[1]

[1]Division of Molecular Oncology,
The Netherlands Cancer Institute, Amsterdam, The Netherlands
[2]Department of Pharmaceutical Sciences,
Utrecht University, Utrecht, The Netherlands,
[3]Department of Drug Metabolism and Pharmacokinetics,
GlaxoSmithkline, Ware, United Kingdom,
[4]Department of Pharmacy & Pharmacology,
Slotervaart Hospital, Amsterdam, the Netherlands

*Molecular Pharmaceutics, 2012*

## *Abstract*

Organic anion-transporting polypeptides (OATPs) mediate the hepatic uptake of many drugs. Hepatic uptake is crucial for the therapeutic effect of pravastatin, a cholesterol-lowering drug and OATP1A/1B substrate. We aimed to gain empirical insight into the relationship between OATPs and pravastatin pharmacokinetics and toxicity. We therefore compared the distribution and toxicity of pravastatin in wild-type and Oatp1a/1b-null mice. Intestinal absorption of pravastatin was not affected by Oatp1a/1b absence, but systemic plasma exposure (AUC) increased up to 30-fold after oral bolus administration. This increased plasma exposure resulted from reduced hepatic uptake, as evident from 10-100-fold lower liver-to-plasma concentration ratios. However, the reductions in liver exposure were far smaller (<2-fold) than the increases in plasma exposure. Reduced pravastatin liver uptake in Oatp1a/1b-null mice was more obvious shortly after intravenous administration, with 8-fold lower biliary pravastatin excretion. Although mice chronically exposed to pravastatin for 60 days evinced little muscular toxicity, Oatp1a/1b-null mice displayed 10-fold higher plasma concentrations and 8-fold lower liver concentrations than wild-type mice. Thus, Oatp1a/1b transporters importantly control the hepatic uptake of pravastatin. Activity-reducing human OATP1B polymorphisms may therefore both reduce pravastatin therapeutic efficacy in the liver and increase systemic toxicity risks, thus compromising its therapeutic index in a two-edged way.

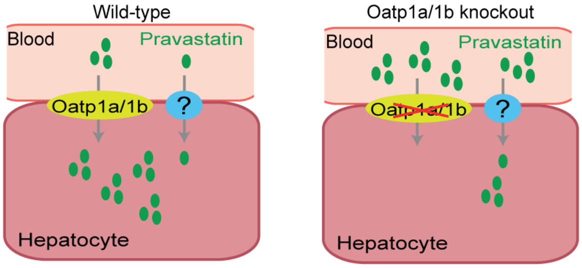

## Introduction

Organic anion-transporting polypeptides (human: OATP, gene: *SLCO*; rodents: Oatp, gene: *Slco)* form a superfamily of transmembrane uptake transporters. The extensively studied OATP1A/1B subfamilies contain three human members (OATP1A2, -1B1, and -1B3), but at least five mouse members (Oatp1a1, -1a4, -1a5, -1a6, and -1b2). Within these subfamilies there are no straightforward orthologs (based on amino acid homology and tissue distribution) between human and mouse Oatps [1]. Because of their primary expression in tissues is important for pharmacokinetics (liver, small intestine, and kidney) and wide substrate specificity including many drugs, OATP1A/1B transporters are believed to profoundly affect drug absorption, distribution, elimination, and toxicity. A recent collaborative study revealed that Rotor syndrome is caused by a complete deficiency of human OATP1B1 and OATP1B3 [2], which are predominantly expressed in the hepatic sinusoidal membrane and thought to play a key role in the hepatic uptake and plasma clearance of drugs. Moreover, treatment with 3- hydroxy-3-methylglutaryl-coenzyme A reductase inhibitors (statins) of carriers of low-activity polymorphisms in *SLCO1B1* has been associated with increased statin plasma exposure and myopathy, the main toxic side effect of statins.

Pravastatin is widely used to treat hypercholesterolemia. Being charged under physiological conditions (log P at pH 7.4 = -0.23), pravastatin requires active transport mechanisms to pass biological membranes. Extensive *in vivo* and *in vitro* studies have suggested that OATP1B1 is a major determinant of pravastatin hepatic uptake [4,5], whereas efflux transporters like ABCC2 (MRP2), ABCG2 (BCRP), and ABCB11 (BSEP) mediate its biliary and renal excretion and may play a role in limiting its oral bioavailability [6-8]. Bioavailability of pravastatin is high, ~30% [9], suggesting the involvement of uptake transporters in its intestinal absorption, perhaps OATP2B1 [10].

The clinically most relevant interaction is with OATP1B1. Patients harboring genetically polymorphic (low-activity) variants of *SLCO1B1* have higher pravastatin plasma exposure and concomitantly increased toxicity, presumably the consequence of impaired OATP1B1-mediated liver uptake [11]. Because the liver harbors the pharmacodynamic target of pravastatin, it was expected that low-activity OATP1B1 variants would also be associated with diminished therapeutic response to pravastatin. Whereas a single large population study showed this association [12], several previous studies were inconclusive because of high variability and limitations in their design number of patients, duration of treatment, time of evaluation) [13].

Pravastatin has been recently investigated *in vivo* using Oatp1b2 knockout mouse models. The involvement of Oatp1b2 in liver uptake of pravastatin appeared inconsistent between two independent studies. One study found that, upon continuous subcutaneous infusion of pravastatin, liver-toplasma ratios were decreased in Oatp1b2 knockout mice [14], whereas the other reported increased liver-to-plasma ratios 2 h after a single subcutaneous administration of pravastatin in these mice [15]. Because mouse Oatp1a and Oatp1b2 can both transport pravastatin and are coexpressed in the sinusoidal membrane, they might compensate for each other's loss of function.

We recently generated an Oatp1a/1b knockout mouse model lacking all Oatp1a/1b transporters, thus avoiding the risk of mutual compensatory restoration of function [16-18]. Employing this mouse model, we aimed to obtain a better understanding of the *in vivo* role of Oatp1a/1b transporters in the oral absorption, hepatic uptake and elimination of pravastatin.

## Materials and methods

### Animals

Animals were housed (grouped) in a temperaturecontrolled environment with a 12-h light/12-h dark cycle. They received a standard diet (AM-II; Hope Farms) and acidified water *ad libitum*. All mouse experiments were approved by the Animal Experiments Review Board of The Netherlands Cancer Institute (Amsterdam), complying with Dutch legislation and in accordance with European Directive 86/609/EEC and the GSK Policy on the Care, Welfare and Treatment of Animals. Male wild-type and *Slco1a/1b(-/-)* (Oatp1a/1b knockout) mice [16] of comparable genetic background (>99% FVB) between 9 and 14 weeks of age, and weights between 25 and 30 g were used.

### Chemicals and reagents

Pravastatin sodium was from Sequoia Research Products (Pangbourne, UK), [3H]pravastatin from Scopus Research (Wageningen, The Netherlands), isoflurane (Forane) from Abbott Laboratories (Queenborough, Kent, UK), and heparin (5000 IE/mL) from Leo Pharma BV Breda, The Netherlands). Other chemicals were from Sigma St. Louis, USA).

### Plasma and tissue pharmacokinetic experiments

Pravastatin was dissolved in saline (0.5 mg/mL or 1 mg/mL, pH ~ 6.2) for administration of 5 mg/kg or 10 mg/kg to mice. 10 µL/g body weight was administered for oral gavage (n = 5-7 for each group) and 5 µL/g body weight for administration in the tail vein. At the various planned sampling time points mice were anesthetized with isoflurane, heparinblood was collected by cardiac puncture, and tissues were isolated after cervical dislocation. After 10 mg/kg oral administration, portal vein blood samples were taken using a Venoflux Microperfuser/Infusion set (Vygon Pharmaceutical Laboratories, France). After collection of approximately 200 µL of heparin blood, the portal vein was clamped with an arterial clamp to ensure high enough blood pressure for a cardiac puncture. This was performed as soon as possible after the portal vein clamping. Blood samples were centrifuged at 5200 g for 5 min at 4 °C, and plasma was collected and stored at -30 °C until analysis.

### Urinary and fecal excretion of pravastatin

A mass balance study was performed with Ruco Type M/1 stainless steel metabolic cages (Valkenswaard, The Netherlands). Male wild-type and *Slco1a/1b(-/-)* mice (n = 5-6) received [3H]pravastatin (10 mg/kg) by oral gavage. Urine and feces were collected in a 0-24 h fraction after drug administration, followed by isolation of blood and tissue samples as described above.

### Biliary excretion of pravastatin

Gall bladder cannulations and collection of bile in wild-type and *Slco1a/1b(-/-)* mice (n = 7) were performed as described [16]. At the end of the experiment, blood and tissue samples were isolated and treated as described above.

### Drug analysis

Concentrations of pravastatin in plasma, liver (homogenized in appropriate volumes of ice-cold 4% (w/ v) BSA), and bile (diluted 100× with human blank plasma) were determined by LC-MS/MS analysis as described [19]. Total levels of radioactivity in urine and feces were determined by liquid scintillation counting (Tri-Carb 2100 Cs Liquid Scintillation Analyzer, Canberra Packard)

### *Toxicity studies after chronic exposure*

Pravastatin was dissolved in drinking water at a concentration of 1.2 g/L (~180 mg/day/kg). Mice were kept on this drinking water for 60 days and checked for body weight changes and signs of toxicity every 2 days. At 15 and 30 days blood was isolated from the tail vein, and creatine kinase levels were determined. On day 60 blood was collected by cardiac puncture, and the liver (part) and several groups of skeletal muscle were isolated for histopathological analysis after hematoxylin-eosin staining. Pravastatin plasma and liver concentrations were determined as described [19].

### *Statistical analysis*

When variances were inhomogeneous, data were log-transformed to obtain normal distribution and equal variances before statistical analysis. The two-tailed unpaired Student's *t*-test was used throughout the study to assess the statistical significance of differences between two sets of data. Differences were considered statistically significant when $P < 0.05$.

### *Pharmacokinetic calculations*

Averaged values (as absolute concentrations or % of dose) for each time point were used to calculate the area under the curve (AUC) from t = 0 to the last sampling time point by the linear trapezoidal rule; SEM was calculated by the law of propagation of errors [16]. Occasionally we represented plasma or liver exposure (analogous to AUC) in [% of dose·min] = amount [% of dose] × time, to better compare absolute exposure levels in plasma and liver between two strains. We estimated the volume of plasma (mL) as follows: body weight of the mouse (in grams) × 0.07 × 0.63, assuming that the blood volume represents ~7% of the body weight, and 63% thereof represents the plasma fraction [20].

### *Pharmacokinetic modeling*

The modeling software Phoenix WinNonlin 6.1 (Phoenix WinNonlin Copyright 1998-2009, Tripos L.P.) was used. Noncompartmental analysis was performed using plasma data from intravenously and orally dosed mice from both strains. As the study design involved composite sampling, the "sparse" sampling function was used to maximize the contribution of the data from each mouse at each sample time. In addition, the following equations were used to calculate additional parameters

F (bioavailability) = $AUC_{po} * Dose_{i.v.} / AUC_{i.v.} * Dose_{po}$;

$E_h$ (Apparent hepatic extraction ratio) = $1 - AUC_{systemic\ oral} / AUC_{portal\ vein}$;

$Cl_r$ (renal clearance) = Amount in urine / AUC systemic plasma/bodyweight (kg)

## Results

### *Oatp1a/1b transporters are not essential for intestinal uptake of pravastatin*

We investigated a possible role of Oatp1a/1b in pravastatin uptake across the intestinal wall at 10 mg/kg oral pravastatin. Pravastatin portal vein concentrations at early time points (7.5, 15 min), which should mainly reflect the amount of drug absorbed from the intestinal lumen, were not significantly different between wild-type and Oatp1a/1b knockout mice (Figure 1A). Oatp1a/1b transporters are thus not essential for the intestinal uptake of pravastatin. Pravastatin portal vein concentrations were highest at the earliest technically feasible sampling time point (7.5 min) in both strains, indicating very rapid absorption of this polar drug. At 30 and 60 min, portal vein concentrations in the Oatp1a/1b knockout mice were higher than in the wild-type mice (Figure 1A), probably reflecting the higher systemic plasma concentrations (Figure 1B and below). Similar results were obtained for 3-α-pravastatin, albeit at much lower concentrations (Supporting Information, Figure 1A,B). 3-a- Pravastatin is a pharmacodynamically active pravastatin isomer, formed under acidic conditions in the stomach or enzymatically in the liver or small intestine [21].

### *Oatp1a/1b transporters control pravastatin systemic plasma levels and liver distribution*

In the same experiment (with an added 3 min time point), pravastatin systemic plasma exposure (AUC) was 7 times higher in Oatp1a/1b-null mice than in wild-type mice (Table 1). The $t_{max}$ of ~7.5 min reconfirmed the rapid oral absorption of pravastatin in both strains (Figure 1B).

We also measured the liver concentrations which were significantly reduced in the Oatp1a/1b-null mice only up to 30 min (Figure 1C,D). The impaired liver uptake was more evident in the profoundly decreased (10-100-fold) liver-toplasma ratios at all time points (Figure 1E). Overall, the reduced liver uptake resulted in a 1.9-fold decreased liver AUC (as % of dose·min) in Oatp1a/1b-null mice (from 86.8 ± 7.2 to 45.1 ± 5.5, Table 1). However, the fold differences

**Table 1.** Pharmacokinetic parameters (calculated from t = 0 to the last sampling time point by the linear trapezoidal rule) after pravastatin administration to wild-type and Oatp1a/1b knockout mice.

| | | | **WT** | ***Slco1a/1b(-/-)*** | **Fold difference (KO / WT)** |
|---|---|---|---|---|---|
| 10 mg/kg oral | Systemic Plasma | $AUC_{(0-2)}$ (μg/mL·min) | 7.2 ± 1.7 | 50.8 ± 6.2** | 7.1 |
| | | $AUC_{(0-2)}$ (% of dose·min) | 3.0 ± 0.7 | 22.3 ± 2.8** | 7.5 |
| | Portal vein plasma | $AUC_{(0-2)}$ (μg/mL·min) | 62.4 ± 3.5 | 105.7 ± 12.8* | 1.7 |
| | Liver | $AUC_{(0-2)}$ (% of dose·min) | 86.8 ± 7.2 | 45.1 ± 5.5* | 0.52 |
| | Apparent hepatic extraction | | 0.88 | 0.52 | 0.59 |
| 5 mg/kg oral | Systemic Plasma | $AUC_{(0-2)}$ (μg/mL·min) | 1.7 ± 0.3 | 51.5 ± 3.4*** | 30.3 |
| | | $AUC_{(0-2)}$ (% of dose·min) | 1.5 ± 0.2 | 45.5 ± 3.0*** | 30.3 |
| | Liver | $AUC_{(0-2)}$ (% of dose·min) | 137.2 ± 9.9 | 85.8 ± 6.5* | 0.63 |
| 5 mg/kg i.v. | Systemic Plasma | $AUC_{(0-1)}$ (μg/mL·min) | 30.3 ± 3.4 | 127.7 ± 6.4** | 4.2 |
| | | $AUC_{(0-1)}$ (% of dose·min) | 21.8 ± 3.0 | 92.9 ± 5.7** | 4.2 |
| | Liver | $AUC_{(0-1)}$ (% of dose·min) | 129.3 ± 12.1 | 72.6 ± 4.2* | 0.56 |

Data presented as mean ± S.E.M.

*, $P < 0.05$; **, $P < 0.01$; ***, $P < 0.001$ when compared with wild-type mice.

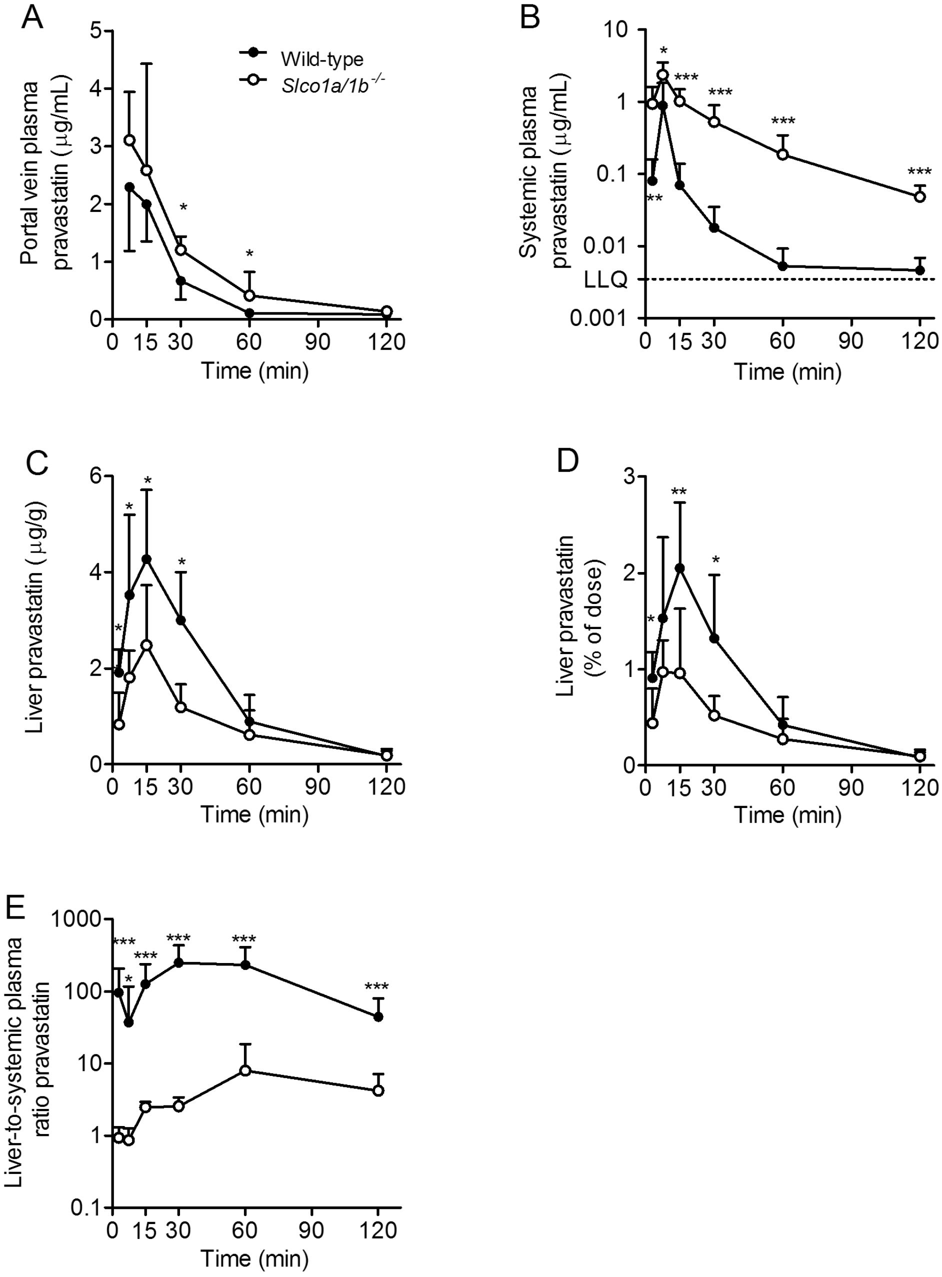

**Figure 1.** Oatp1a/1b transporters control pravastatin hepatic uptake, but not intestinal uptake after oral administration (10 mg/kg) to wildtype and *Slco1a/1b(-/-)* mice. (A) Pravastatin portal vein plasma concentrations (semilog plot). (B) Pravastatin systemic plasma concentration (semilog plot). (C) Pravastatin liver levels as µg/g or (D) % of dose. (E) Liver-to-systemic plasma ratios (semilog plot). Averaged liver-to-systemic plasma ratios were calculated from individual mouse data. Data are presented as mean ± SD (n = 4-7, *, $P < 0.05$; ***, $P < 0.001$ when compared with wild-type).

in pravastatin concentrations between knockout and wild-type mice were much higher for plasma (7.1-fold) than for liver (0.5- fold, Table 1). This apparent discrepancy can be explained using the hepatic extraction ratio, a parameter used to assess liver uptake of a drug [22].

Here we used a modified version of this parameter, which we named the apparent hepatic extraction ratio. Because for pravastatin the hepatobiliary elimination is predominant and the renal clearance (in rats) is negligible [23], we assumed that plasma portal vein concentrations represent the amount of drug before entering the liver and systemic plasma concentrations the amount of drug that escaped liver uptake. Therefore, we calculated the apparent hepatic extraction ratio = $[1 - (AUC_{oral\ systemic}/AUC_{oral\ portal\ vein})]$. Wild-type mice exhibited a high pravastatin hepatic extraction ratio of 0.88, while in Oatp1a/1b-null mice this dropped ~1.7-fold to 0.52 (Table 1). Based on these results, we can understand why the impact (as fold difference) of absence of Oatp1a/1b transporters is apparently higher for the systemic plasma exposure than for the liver exposure. A 1.7-fold decrease in liver uptake (from 0.88 to 0.52) implies a bigger (4-fold) increase in the amount of pravastatin escaping the liver (from 0.12 to 0.48 (1 - apparent hepatic extraction ratio), Table 1)).

At a lower oral pravastatin dosage of 5 mg/kg, we observed an even higher increase (~30-fold) in the systemic plasma exposure of pravastatin in the Oatp1a/1b-null mice (Figure 2A,B, Table 1). The impaired hepatic uptake in Oatp1a/1b-null mice was again evident, with significantly reduced liver levels of pravastatin at 7.5, 30, and 120 min after administration (Figure 2C,D). This led to a 1.6-fold lower liver AUC in Oatp1a/1bnull mice than in wild-type mice. The liver-to-plasma ratios were again at all time points profoundly lower (10-100-fold) in Oatp1a/1b-null mice (Figure 2E). For 3-$\alpha$-pravastatin very similar behaviour was observed at both pravastatin dosages, but with lower concentrations (Supporting Information, Figures 1C-E and 2).

### *Effect of Oatp1a/1b on urinary and fecal excretion of pravastatin*

Increased pravastatin plasma exposure in individuals carrying low-activity variants of OATP1B1 is associated with increased pravastatin urinary output [13]. We therefore performed a mass-balance experiment over 24 h after oral administration of 10 mg/kg [3H]-labeled pravastatin. The urinary output of [3H]-pravastatin was ~10-fold higher in Oatp1a/1b-null mice than in wild-type mice (26.2 ± 9.2 versus 2.4 ± 1.7% of dose, $P < 0.001$). This likely reflected the higher plasma exposure in Oatp1a/1b knockout mice, rather than a direct role for Oatp1a/1b in pravastatin urinary excretion. Fecal excretion was slightly, albeit not significantly, lower in the knockout mice (72.8 ± 10.2 versus 63.8 ± 10.7% of dose). The measurement of unchanged pravastatin in urine yielded a similar increase in Oatp1a/1b-null mice (26.7 ± 1.7 versus 0.22 0.34% of dose, P < 0.001), but fecal unchanged pravastatin measurements were unreliable. Feces represent a difficult matrix for the bioanalytical assay, because of difficulty to achieve sufficient homogenization. Renal clearance (mL/ min·kg) based on the urinary output of pravastatin corrected for bioavailability was 0.17 ± 0.26 in wild-type mice and 6.05 ± 0.5 in knockout mice (Supporting Information, Table 1). The renal clearance (mL/min·kg × F) in the wild-type mice represented a negligible fraction of the total systemic clearance 0.17 versus 85, Supporting Information, Table 1). In Oatp1a/ knockout mice, the renal clearance was much increased,

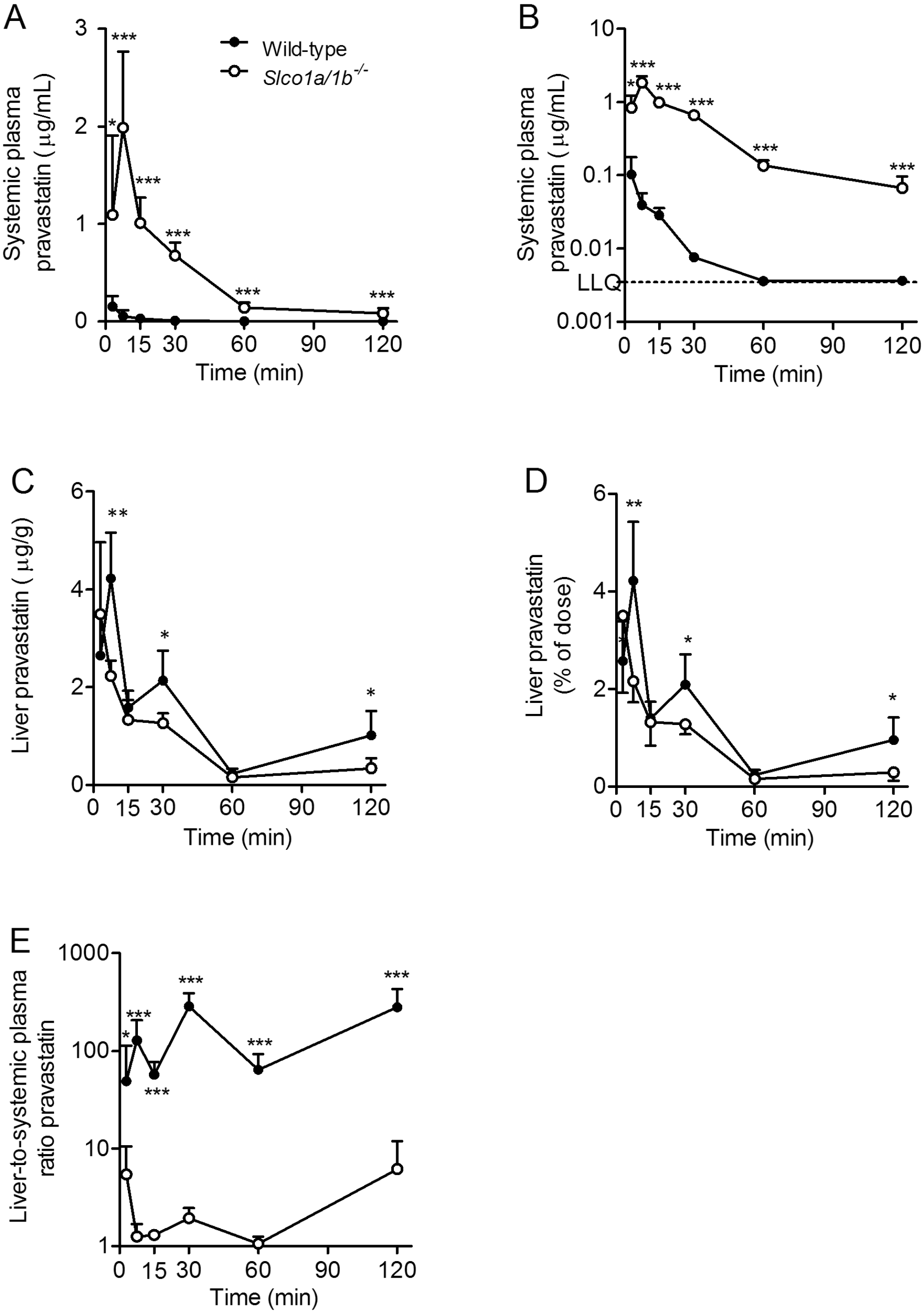

**Figure 2.** Oatp1a/1b transporters control pravastatin hepatic uptake after oral administration (5 mg/kg) to wild-type and *Slco1a/1b(-/-)* mice. (A) Pravastatin systemic plasma concentrations and (B) semilog plot of the data. (C) Pravastatin liver levels as µg/g and (D) as % of dose. (E) Liver-to-systemic plasma ratio versus time curve (semilog plot). Data are presented as mean ± SD (n = 5, *, $P < 0.05$; **, $P < 0.01$; ***, $P < 0.001$ when compared with wild-type).

representing ~25% of total systemic clearance (6.04 versus 24.8, Supporting Information, Table 1). This increased renal clearance is most likely a consequence of the prolonged highly increased plasma levels due to impaired hepatic clearance in these mice.

### *Role of Oatp1a/1b in intravenous pravastatin pharmacokinetics*

We hypothesized that intravenous administration (at 5 mg/kg) might reveal the impact of Oatp1a/1b transporters on hepatic pravastatin uptake more directly, since provides a more equal early plasma exposure. Pravastatin plasma concentrations were (except at 30 min) significantly higher in the Oatp1a/1b-null mice (Figure 3A), yielding a 4- fold increased AUC (Table 1). Liver concentrations were ~2- fold lower in Oatp1a/1b-null than in wild-type mice (Figure 3B,C and Table 1). The decrease in liver exposure represented ~60% of dose·min, correlating well with a plasma AUC increase of ~70% of dose·min (Table 1). Liver-to-plasma ratios were again substantially lower (~10-fold) in Oatp1a/1b-null mice (Figure 3D).

### *Impact of Oatp1a/1b on pravastatin biliary excretion*

We investigated the effect of Oatp1a/1b deficiency on pravastatin elimination in the bile after intravenous administration (5 mg/kg) to mice with a cannulated gall bladder and ligated common bile duct. While bile flow was unchanged (~1.4 μl/min/g liver), pravastatin elimination into the bile over the first 15 minutes was 9-fold lower in Oatp1a/1b-null mice than in wild-type mice (3.9 ± 1.8 versus 34.0 ± 11.7 % of dose, Figure 3E). This indicates a strongly impaired early hepatic uptake, as the rate-limiting step for pravastatin hepatobiliary excretion is most likely the hepatic uptake rate [24]. Note that the canalicular efflux transporters for pravastatin (Abcc2, Abcg2 and Abcb11) are not significantly down-regulated in *Slco1a/1b*(-/-) mice [17].

Beyond 15 min, biliary excretion faded quickly in both mouse strains and became more similar (Figure 3E and F), presumably reflecting differences in plasma clearance and more similar liver concentrations. This resulted in a 4.5-fold decrease in cumulative biliary output between wild-type and knockout mice at 45 min. Indeed, at 45 min, plasma levels were higher in the Oatp1a/1b-null mice (1.2 ± 0.9 versus 0.3 ± 0.5, $P < 0.05$), and whereas liver levels were not significantly different anymore, the liver-to-plasma ratio was 5.5-fold lower (0.6 ± 0.2 versus 3.4 ± 2.5, $P < 0.01$). 3-$\alpha$-pravastatin displayed a very similar pharmacokinetic profile, although liver levels after 15 minutes were too low for reliable measurements (Supplemental Figure 3).

### *Pharmacokinetic modeling*

In view of the somewhat limited set of intravenous data points in this study, which was not originally designed for pharmacokinetic modeling, we used a noncompartmental model and the sparse data function for model fitting. The results are presented in the Supporting Information, Table 1.

After oral administration (of 10 mg/kg or 5 mg/kg), the oral bioavailability (F) was increased in the Oatp1a/1b knockout mice, which most likely reflects the impaired first-pass liver uptake of pravastatin in these mice. Accordingly, because the liver is the main distribution organ for pravastatin, the volume of distribution was markedly decreased (about 4-fold upon oral administration) in the absence of Oatp1a/1b transporters. Closely linked is the total systemic clearance of pravastatin which is predominantly determined by the liver uptake, 23 which was

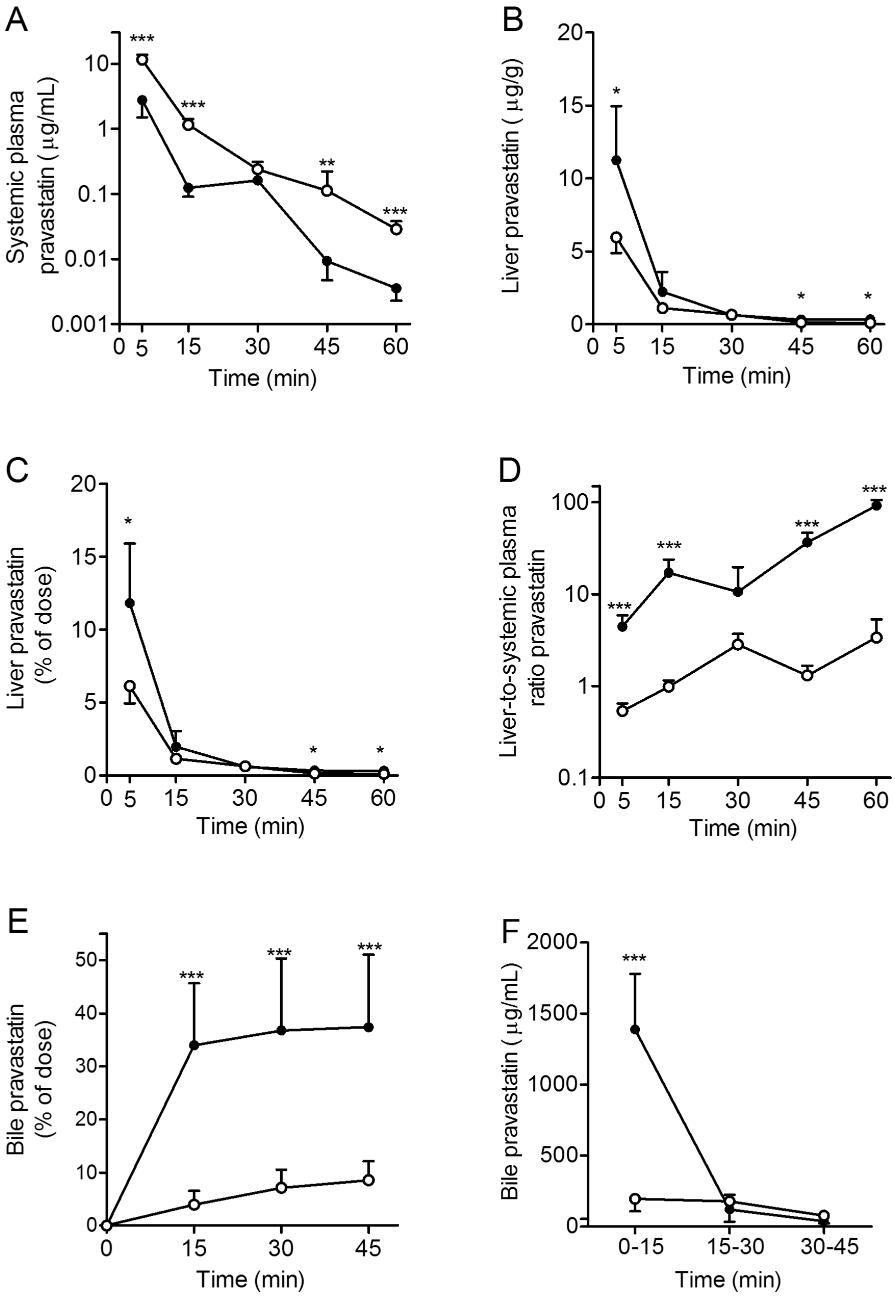

**Figure 3.** Oatp1a/1b transporters control hepatic uptake and biliary excretion of pravastatin after intravenous administration (5 mg/kg) to wild-type and *Slco1a/1b(-/-)* mice. (A) Pravastatin systemic plasma concentrations (semilog plot). (B) Pravastatin liver levels as µg/g and (C) as % of dose and (D) liver-to-systemic plasma ratios (semilog plot). (E) Cumulative biliary excretion of pravastatin (% of dose) and (F) bile concentrations (µg/mL). Data are presented as mean ± SD (n = 4-5, *, $P < 0.05$; **, $P < 0.01$; ***, $P < 0.001$ when compared with wild-type).

also reduced in the Oatp1a/1b knockout mice. After intravenous administration, we observed a similar pattern of reduced clearance and volume of distribution and only minor changes in the pravastatin half-life between the two strains of mice (Supporting Information, Table 1)

### *Toxicity studies upon chronic exposure to pravastatin*

Systemic plasma levels also determine muscle exposure, responsible for pravastatin's most common toxic side effect, myopathy. We therefore investigated whether Oatp1a/1b transporters affect pravastatin-induced myopathy, even though little was known of the susceptibility of mice to pravastatin-induced myotoxicity, as most of these studies are performed in rats. After 60 days of receiving drinking water containing 1.2 g/ L of pravastatin, various skeletal muscles were analyzed for toxicity signs. Despite the highly increased pravastatin plasma concentrations

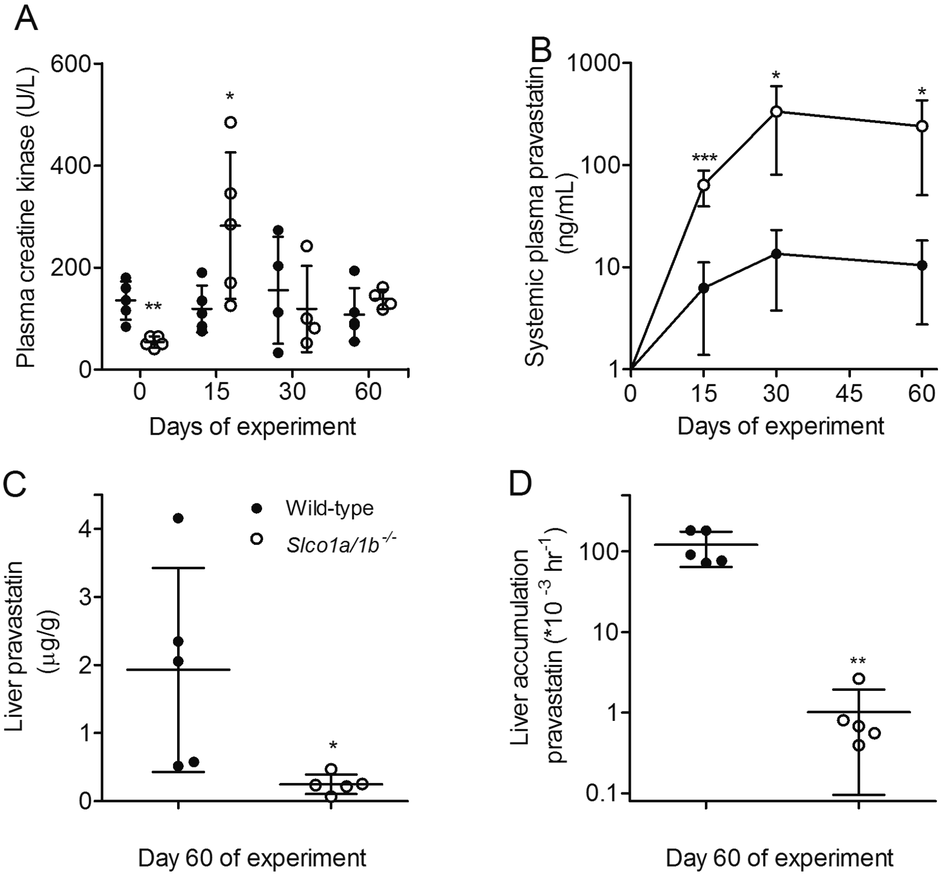

**Figure 4.** Oatp1a/1b transporters control liver and plasma exposure after chronic administration of drinking water containing 1.2 g/L pravastatin. (A) Creatine kinase plasma concentration (U/L) and (B) pravastatin systemic plasma concentrations (semilog plot) at several time points. (C) Pravastatin liver concentrations (µg/g) and (D) liverto-systemic plasma (AUC) ratios (semilog plot) after 60 days of exposure. Data are presented as mean ± SD (n = 4-5, * $P < 0.05$; ** $P < 0.01$; *** $P < 0.001$ when compared with wild-type).

(>10-fold) in Oatp1a/1b-null mice (Figure 4B), only 1/5 knockout mice showed minor, focal lesions in muscles along the vertebral column (data not shown). Also, Oatp1a/1b knockout mice had significantly higher plasma levels of creatine kinase after 15 days, but not after 30 or 60 days of treatment, suggesting only transient and minor muscular lesions in these mice (Figure 4A). The high interindividual variation in pravastatin plasma exposure and liver concentrations may be due to differences in water intake. Strikingly, under these chronic oral exposure conditions, liver concentrations were markedly lower (~8-fold) in the Oatp1a/1b-null mice, as were the liver-to-plasma ratios (~100-fold) (Figure 4C and D). Virtually identical behavior was observed for 3-$\alpha$-pravastatin, albeit at lower concentrations (Supporting Information, Figure 4).

## Discussion

We describe here that Oatp1a/1b transporters are not essential for pravastatin intestinal absorption, but that they do control pravastatin hepatic uptake and clearance in mice. After bolus oral administration, the absence of Oatp1a/1b resulted in higher plasma exposure and lower liver exposure, but the impact on liver exposure was much more limited. Interestingly, after chronic administration of pravastatin, the impact of Oatp1a/1b transporters on plasma and liver exposure was similarly high. The active metabolite of pravastatin, 3-$\alpha$- pravastatin, displayed similar pharmacokinetic behavior as the parent compound, albeit at generally lower concentrations.

It has been proposed that OATP1A/1B transporters could mediate the intestinal uptake of several drugs, including pravastatin [25–27]. However, despite being polar, pravastatin was rapidly and extensively absorbed in Oatp1a/1b-null mice, with 27% oral bioavailability (Supporting Information, Table 1). Although intestinal uptake transporters are therefore almost certainly involved in the oral absorption of pravastatin, their identity remains unknown. Perhaps Oatp2b1 might be involved [10], but also other, as yet unspecified transporters. Given the likely importance of intestinal drug uptake transporters, surprisingly little is still known about this area.

Previously, Oatp1b2-null mice displayed a 1.8-fold increase in pravastatin plasma levels and a similar decrease in liver levels, yielding 4-fold decreased liver-to-plasma ratios upon continuous subcutaneous pravastatin infusion. This suggested a modest impairment of pravastatin hepatic uptake [14]. In contrast, an independent study in the same Oatp1b2-null strain found that upon subcutaneous bolus administration, pravastatin hepatic uptake was not impaired, and 4 h after administration, liver-toplasma ratios were significantly increased, rather than decreased [15]. Differences in dosing regimen, mouse age, and small mouse numbers in the latter study may perhaps explain these contradictory results. The contrast with our findings in full Oatp1a/1b-null mice suggests that, in addition to Oatp1b2, also hepatic Oatp1a proteins affect pravastatin disposition, presumably primarily its liver uptake. Of note, in our study we used the clinically more relevant oral administration route.

Plasma exposure of oral pravastatin in Oatp1a/1b knockout mice was highly increased (7–30-fold). Because mouse Oatp1a1, Oatp1a4, and Oatp1b2 likely mediate the same sinusoidal uptake functions as human OATP1B1 and OATP1B3, our results are consistent with data from patients harboring low-activity SLCO1B1 polymorphisms. SLCO1B1 polymorphism c.521T > C was associated with up to ~100%

higher plasma pravastatin concentrations in carriers than the reference SLCO1B1 gene [12]. Other SLCO1B1 polymorphisms associated with low transport activity, e.g., c.388A > G and g.- 1187G > A, also correlate with altered pravastatin pharmacokinetics [3,11,28]. The impact of SLCO1B3 polymorphisms on pravastatin pharmacokinetics is unknown yet. Co-administration of pravastatin with established OATP1B inhibitors, like cyclosporine, atorvastatin, or gemfibrozil, results in higher plasma pravastatin concentrations [29–31], supporting an important role of OATP1B in pravastatin clearance.

Surprisingly, in Oatp1a/1b-null mice, whereas plasma exposure was 7.5 to 30-fold increased, reduced liver exposure was only ~0.5-fold that in wild-type mice after bolus oral pravastatin administration. In previous studies, Oatp1a/1b absence resulted in more similar increases in plasma and decreases in liver exposure of several xenobiotic substrates (e.g., methotrexate), presumably caused by reduced liver uptake [16,18], Although counterintuitive, this differential impact of Oatp1a/1b transporters on plasma versus liver exposure is supported by a physiologically based pravastatin pharmacokinetic model [23]. This predicts that, for an oral pravastatin bolus, a markedly diminished hepatic uptake clearance (as in Oatp1a/1b-null mice) causes substantial increases in plasma exposure, but only minor decreases in liver exposure (Supporting Information, Figure 1). Simply put, for a hepatically cleared drug, if there is no substantial alternative (renal) elimination route, the reduced hepatic uptake rate is soon offset by the highly increased plasma drug concentrations, driving comparatively more drug into the liver. The liver-to-plasma ratio is therefore strongly reduced, but the overall liver exposure is not so much affected. Accordingly, the absolute liver concentrations were significantly reduced only up to 60 min after oral administration in the knockout mice. The markedly increased plasma concentrations may “push” the pravastatin into the liver via alternative uptake routes. Possibly Oatp2b1 and/or other unknown hepatic uptake transporters with low affinity but high capacity for pravastatin transport might thus partly compensate for the loss of Oatp1a/1b transporters at high plasma concentrations [10]. An additional indication for the presence of these alternative transporters is that, in the Oatp1a/1b knockout mice, there is still substantial hepatic clearance, accounting for ~75% of the total clearance ((24.8 − 6.04)/24.8 × 100, Supporting Information, Table 1).

In wild-type mice, renal clearance is negligible, whereas in the Oatp1a/1b knockout mice the renal clearance represents ~25% of the total systemic clearance, which is no longer negligible. This is in line with the modest decrease in liver exposure that we observed. In humans, urinary excretion accounts for ~8% of the pravastatin dose after oral administration [9,21]. When the pharmacokinetic model of Watanabe et al. takes this modest renal elimination into account, it predicts that hepatic uptake rate changes will result in modest alterations in the liver exposure concomitant with large shifts in plasma exposure [23]. Such results are perfectly compatible with our experimental findings in mice. They therefore mutually support each other’s validity. Conversely, the quantitatively more similar impact of Oatp1a/1b absence on plasma and liver exposure of methotrexate [16] can be explained by the greater extent of renal elimination of this drug, ~50% of the dose in humans and mice. Biliary elimination of methotrexate on the other hand amounted to only ~12% of the dose in wild-type mice (Supporting Information, Figure 2).

Pharmacokinetic modeling of our intravenous data indicated that, whereas plasma AUC was 3.4-fold increased, both clearance and volume of distribution were reduced ~0.3-0.4- fold in the Oatp1a/1b-null mice, resulting in only a modestly changed half-life (1.4-fold, Supporting Information, Table 1). This finding is in line with clinical studies. In carriers of polymorphic variants of SLCO1B1, the half-life of pravastatin is also unchanged despite increased plasma exposure [32]. In another study, coadministration with the OATP inhibitor gemfibrozil increased pravastatin plasma exposure, without affecting its halflife [29]. This suggests that clearance and volume of distribution of pravastatin are closely related and under the control of Oatp1a/ 1b activity. The simplest explanation for these findings is that Oatp1a/1b-mediated hepatic uptake is the main determining process for both clearance and volume of distribution of pravastatin. Most likely the same applies in humans for hepatic OATP1B1.

Clinically, pravastatin is taken chronically. Low-activity OATP1B1 polymorphisms can increase pravastatin plasma exposure and muscular toxicity in patients [33,34]. Our failure to induce significant muscular toxicity after prolonged pravastatin exposure even in Oatp1a/1b-null mice may relate to an intrinsically low susceptibility to this toxicity in mice [35]. Interestingly, however, chronic pravastatin administration revealed a similarly large impact on plasma (~10-fold increased) and liver exposure (~10-fold decreased) in Oatp1a/1b-null mice. A comparatively high renal clearance of pravastatin in Oatp1a/1b-null mice, especially under chronic administration conditions, might explain this observation. A recent study showed that patients with low-activity OATP1B1 polymorphisms had decreased pravastatin therapeutic efficacy after chronic treatment [12]. This is in line with our findings that Oatp1a/1b deficiency reduces pravastatin access to the liver as primary therapeutic target organ.

Taken together, our findings indicate that OATP1B uptake transporters determine the therapeutic index of pravastatin in two ways: first by affecting pravastatin efficacy by controlling its liver concentrations, and second by affecting pravastatin systemic toxicity by controlling its plasma concentrations. Therefore Rotor syndrome patients, who suffer from complete deficiency of OATP1B1 and OATP1B3, as well as the much more frequently occurring individuals with full OATP1B1 deficiency [2] might have little benefit from statin therapy and be at increased risk for developing life-threatening toxicity.

## Acknowledgements

We thank Seng Chuan Tang, Selvi Durmus and Ning Xu for critical reading of the manuscript.

## Reference List

1. Hagenbuch, B.; Meier, P. J. Organic anion transporting polypeptides of the OATP/ SLC21 family: phylogenetic classification as OATP/ SLCO superfamily, new nomenclature and molecular/functional properties. *Pflugers Arch*. 2004, *447* (5), 653-665.
2. van de Steeg, E.; Stranecky, V.; Hartmannova, H.; Noskova, L.; Hrebicek, M.; Wagenaar, E.; van Esch, A.; de Waart, D. R.; Oude Elferink, R. P.; Kenworthy, K. E.; Sticova, E.; Al Edreesi, M.; Knisely, A. S.; Kmoch, S.; Jirsa, M.; Schinkel, A. H. Complete OATP1B1 and OATP1B3 deficiency causes human Rotor syndrome by interrupting conjugated bilirubin reuptake into the liver. *J. Clin. Invest*. 2012, *122* (2), 519-528.
3. Kalliokoski, A.; Niemi, M. Impact of OATP transporters on pharmacokinetics. *Br. J. Pharmacol*. 2009, *158* (3), 693-705.

4. Kameyama, Y.; Yamashita, K.; Kobayashi, K.; Hosokawa, M.; Chiba, K. Functional characterization of SLCO1B1 (OATP-C) variants, SLCO1B1*5, SLCO1B1*15 and SLCO1B1*15+C1007G, by using transient expression systems of HeLa and HEK293 cells. *Pharmacogenet. Genomics* 2005, *15* (7), 513-522.
5. Nakai, D.; Nakagomi, R.; Furuta, Y.; Tokui, T.; Abe, T.; Ikeda, T.; Nishimura, K. Human liver-specific organic anion transporter, LST-1, mediates uptake of pravastatin by human hepatocytes. *J. Pharmacol. Exp. Ther.* 2001, *297* (3), 861-867.
6. Chen, C.; Mireles, R. J.; Campbell, S. D.; Lin, J.; Mills, J. B.; Xu, J. J.; Smolarek, T. A. Differential interaction of 3-hydroxy-3-methylglutaryl-coa reductase inhibitors with ABCB1, ABCC2, and OATP1B1. *Drug Metab. Dispos.* 2005, *33* (4), 537-546.
7. Hirano, M.; Maeda, K.; Hayashi, H.; Kusuhara, H.; Sugiyama, Y. Bile salt export pump (BSEP/ABCB11) can transport a nonbile acid substrate, pravastatin. *J. Pharmacol. Exp. Ther.* 2005, *314* (2), 876-882.
8. Kivisto, K. T.; Grisk, O.; Hofmann, U.; Meissner, K.; Moritz, K. U.; Ritter, C.; Arnold, K. A.; Lutjoohann, D.; von Bergmann, K.; Kloting, I.; Eichelbaum, M.; Kroemer, H. K. Disposition of oral and intravenous pravastatin in MRP2-deficient TR-rats. *Drug Metab. Dispos.* 2005, *33* (11), 1593-1596.
9. Singhvi, S. M.; Pan, H. Y.; Morrison, R. A.; Willard, D. A. Disposition of pravastatin sodium, a tissue-selective HMG-CoA reductase inhibitor, in healthy subjects. *Br. J. Clin. Pharmacol.* 1990, *29* (2), 239-243.
10. Kobayashi, D.; Nozawa, T.; Imai, K.; Nezu, J.; Tsuji, A.; Tamai, I. Involvement of human organic anion transporting polypeptide OATP-B (SLC21A9) in pH-dependent transport across intestinal apical membrane. *J. Pharmacol. Exp. Ther.* 2003, *306* (2), 703-708.
11. Niemi, M.; Pasanen, M. K.; Neuvonen, P. J. Organic anion transporting polypeptide 1B1: a genetically polymorphic transporter of major importance for hepatic drug uptake. *Pharmacol. Rev.* 2011, *63* (1), 157-181.
12. Akao, H.; Polisecki, E.; Kajinami, K.; Trompet, S.; Robertson, M.; Ford, I.; Jukema, J. W.; de Craen, A. J.; Westendorp, R. G.; Shepherd, J.; Packard, C.; Buckley, B. M.; Schaefer, E. J. Genetic variation at the SLCO1B1 gene locus and low density lipoprotein cholesterol lowering response to pravastatin in the elderly. *Atherosclerosis* 2012, *220* (2), 413-417.
13. Romaine, S. P.; Bailey, K. M.; Hall, A. S.; Balmforth, A. J. The influence of SLCO1B1 (OATP1B1) gene polymorphisms on response to statin therapy. *Pharmacogenomics J.* 2010, *10* (1), 1-11.
14. Zaher, H.; zu Schwabedissen, H. E.; Tirona, R. G.; Cox, M. L.; Obert, L. A.; Agrawal, N.; Palandra, J.; Stock, J. L.; Kim, R. B.; Ware, J. A. Targeted disruption of murine organic anion-transporting polypeptide 1b2 (Oatp1b2/Slco1b2) significantly alters disposition of prototypical drug substrates pravastatin and rifampin. *Mol. Pharmacol.* 2008, *74* (2), 320-329.
15. Chen, C.; Stock, J. L.; Liu, X.; Shi, J.; Van Deusen, J. W.; DiMattia, D. A.; Dullea, R. G.; de Morais, S. M. Utility of a novel Oatp1b2 knockout mouse model for evaluating the role of Oatp1b2 in the hepatic uptake of model compounds. *Drug Metab. Dispos.* 2008, *36* (9), 1840-1845.
16. van de Steeg, E.; Wagenaar, E.; van der Kruijssen, C. M.; Burggraaff, J. E.; de Waart, D. R.; Elferink, R. P.; Kenworthy, K. E.; Schinkel, A. H. Organic anion transporting polypeptide 1a/1b-knockout mice provide insights into hepatic handling of bilirubin, bile acids, and drugs. *J. Clin. Invest.* 2010, *120* (8), 2942-2952.
17. van de Steeg, E.; van Esch, A.; Wagenaar, E.; van der Kruijssen, C. M.; van Tellingen, O.; Kenworthy, K. E.; Schinkel, A. H. High impact of Oatp1a/1b transporters on in vivo disposition of the hydrophobic anticancer drug paclitaxel. *Clin. Cancer Res.* 2010.
18. Iusuf, D.; van de Steeg, E.; Schinkel, A. H. Functions of OATP1A and 1B transporters in vivo: insights from mouse models. *Trends Pharmacol. Sci.* 2011.
19. Sparidans, R. W.; Iusuf, D.; Schinkel, A. H.; Schellens, J. H.; Beijnen, J. H. Liquid chromatography-tandem mass spectrometric assay for pravastatin and two isomeric metabolites in mouse plasma and tissue homogenates. *J. Chromatogr. B Analyt Technol. Biomed. Life Sci.* 2010.
20. Van Zutphen, L. F. [Laboratory animals and animal experiments]Proefdieren en dierproeven159. *Tijdschr. Diergeneeskd.* 1986, *111* (3), 121-131.
21. Everett, D. W.; Chando, T. J.; Didonato, G. C.; Singhvi, S. M.; Pan, H. Y.; Weinstein, S. H. Biotransformation of pravastatin sodium in humans. *Drug Metab. Dispos.* 1991, *19* (4), 740-748.
22. Gridelli, B.; Scanlon, L.; Pellicci, R.; LaPointe, R.; DeWolf, A.; Seltman, H.; Diven, W.; Shaw, B.; Starzl, T.; Sanghvi, A. Cyclosporine metabolism and pharmacokinetics following intravenous and oral administration in the dog 2. *Transplantation* 1986, *41* (3), 388-391.
23. Watanabe, T.; Kusuhara, H.; Maeda, K.; Shitara, Y.; Sugiyama, Y. Physiologically

based pharmacokinetic modeling to predict transporter-mediated clearance and distribution of pravastatin in humans. *J. Pharmacol. Exp. Ther.* 2009, *328* (2), 652-662.

24. Yamazaki, M.; Akiyama, S.; Nishigaki, R.; Sugiyama, Y. Uptake is the rate-limiting step in the overall hepatic elimination of pravastatin at steady-state in rats. *Pharm. Res.* 1996, *13* (10), 1559-1564.
25. Glaeser, H.; Bailey, D. G.; Dresser, G. K.; Gregor, J. C.; Schwarz, U. I.; McGrath, J. S.; Jolicoeur, E.; Lee, W.; Leake, B. F.; Tirona, R. G.; Kim, R. B. Intestinal drug transporter expression and the impact of grapefruit juice in humans. *Clin. Pharmacol. Ther.* 2007, *81* (3), 362-370.
26. Shirasaka, Y.; Suzuki, K.; Nakanishi, T.; Tamai, I. Intestinal absorption of HMG-CoA reductase inhibitor pravastatin mediated by organic anion transporting polypeptide. *Pharm. Res.* 2010, *27* (10), 2141-2149.
27. Shirasaka, Y.; Suzuki, K.; Nakanishi, T.; Tamai, I. Differential effect of grapefruit juice on intestinal absorption of statins due to inhibition of organic anion transporting polypeptide and/or P-glycoprotein. *J. Pharm. Sci.* 2011.
28. Seithel, A.; Glaeser, H.; Fromm, M. F.; Konig, J. The functional consequences of genetic variations in transporter genes encoding human organic anion-transporting polypeptide family members. *Expert Opin. Drug Metab. Toxicol.* 2008, *4* (1), 51-64.
29. Kyrklund, C.; Backman, J. T.; Neuvonen, M.; Neuvonen, P. J. Gemfibrozil increases plasma pravastatin concentrations and reduces pravastatin renal clearance. *Clin. Pharmacol. Ther.* 2003, *73* (6), 538-544.
30. Kyrklund, C.; Backman, J. T.; Neuvonen, M.; Neuvonen, P. J. Effect of rifampicin on pravastatin pharmacokinetics in healthy subjects. *Br. J. Clin. Pharmacol.* 2004, *57* (2), 181-187.
31. Regazzi, M. B.; Iacona, I.; Campana, C.; Raddato, V.; Lesi, C.; Perani, G.; Gavazzi, A.; Vigano, M. Altered disposition of pravastatin following concomitant drug therapy with cyclosporin A in transplant recipients. *Transplant Proc.* 1993, *25* (4), 2732-2734.
32. Igel, M.; Arnold, K. A.; Niemi, M.; Hofmann, U.; Schwab, M.; Lutjohann, D.; von Bergmann, K.; Eichelbaum, M.; Kivisto, K. T. Impact of the SLCO1B1 polymorphism on the pharmacokinetics and lipid-lowering efficacy of multiple-dose pravastatin. *Clin. Pharmacol. Ther.* 2006, *79* (5), 419-426.
33. Schindler, C.; Thorns, M.; Matschke, K.; Tugtekin, S. M.; Kirch, W. Asymptomatic statin-induced rhabdomyolysis after long-term therapy with the hydrophilic drug pravastatin. *Clin. Ther.* 2007, 29 (1), 172-176.
34. Voora, D.; Shah, S. H.; Spasojevic, I.; Ali, S.; Reed, C. R.; Salisbury, B. A.; Ginsburg, G. S. The SLCO1B1*5 genetic variant is associated with statin-induced side effects. *J. Am. Coll. Cardiol.* 2009, *54* (17), 1609-1616.
35. Smith, P. F.; Eydelloth, R. S.; Grossman, S. J.; Stubbs, R. J.; Schwartz, M. S.; Germershausen, J. I.; Vyas, K. P.; Kari, P. H.; MacDonald, J. S. HMG-CoA reductase inhibitor-induced myopathy in the rat: cyclosporine A interaction and mechanism studies. *J. Pharmacol. Exp. Ther.* 1991, *257* (3), 1225-1235.

# *Supplemental data*

**Supplemental Table 1.** Non-compartmental pharmacokinetic modeling using sparse data function after pravastatin administration to wild-type and Oatp1a/1b knockout mice.

| | | | **WT** | ***Slco1a/1b(-/-)*** | **Fold difference (KO / WT)** |
|---|---|---|---|---|---|
| 10 mg/kg oral | Systemic plasma | $c_{max}$ (μg/mL) | 0.881 | 2.376 | 2.7 |
| | | $t_{max}$ (min) | 7.5 | 7.5 | |
| | | $AUC_{0-2}$ (min*μg/mL) | 7.2 | 52.4 | 7.3 |
| | | F | 6.3 % | 13.4 % | 2.1 |
| | | Clearance * F (mL/min/kg) | 85.1 | 24.8 | 0.29 |
| | | Volume of distribution * F (mL/kg) | 3857 | 915 | 0.23 |
| | | Half-life (min) | 31.4 | 25.6 | |
| | Portal vein plasma | $AUC_{0-2}$ (min*μg/mL) | 62 | 106 | 1.7 |
| 10 mg/kg oral | Renal clearance * F (mL/min/kg) | | 0.17 ± 0.26 | 6.04 ± 0.5*** | 35 |
| 5 mg/kg oral | Systemic plasma | $c_{max}$ (μg/mL) | 0.15 | 1.98 | 13.2 |
| | | $t_{max}$ (min) | 3 | 7.5 | |
| | | $AUC_{0-2}$ (min*μg/mL) | 1.8 | 52 | 28.9 |
| | | F | 3.2 % | 26.7 % | 8.3 |
| | | Clearance * F (mL/min/kg) | 82 | 24.3 | 0.29 |
| | | Volume of distribution * F (mL/kg) | 3814 | 1009 | 0.26 |
| | | Half-life (min) | 32.2 | 28.9 | |
| 5 mg/kg i.v. | Systemic plasma | $AUC_{0-1}$ (min*μg/mL) | 57 | 195 | 3.4 |
| | | Clearance (mL/min/kg) | 88 | 26 | 0.29 |
| | | Volume of distribution (mL/kg) | 786 | 328 | 0.42 |
| | | Half-life (min) | 6.2 | 8.9 | |

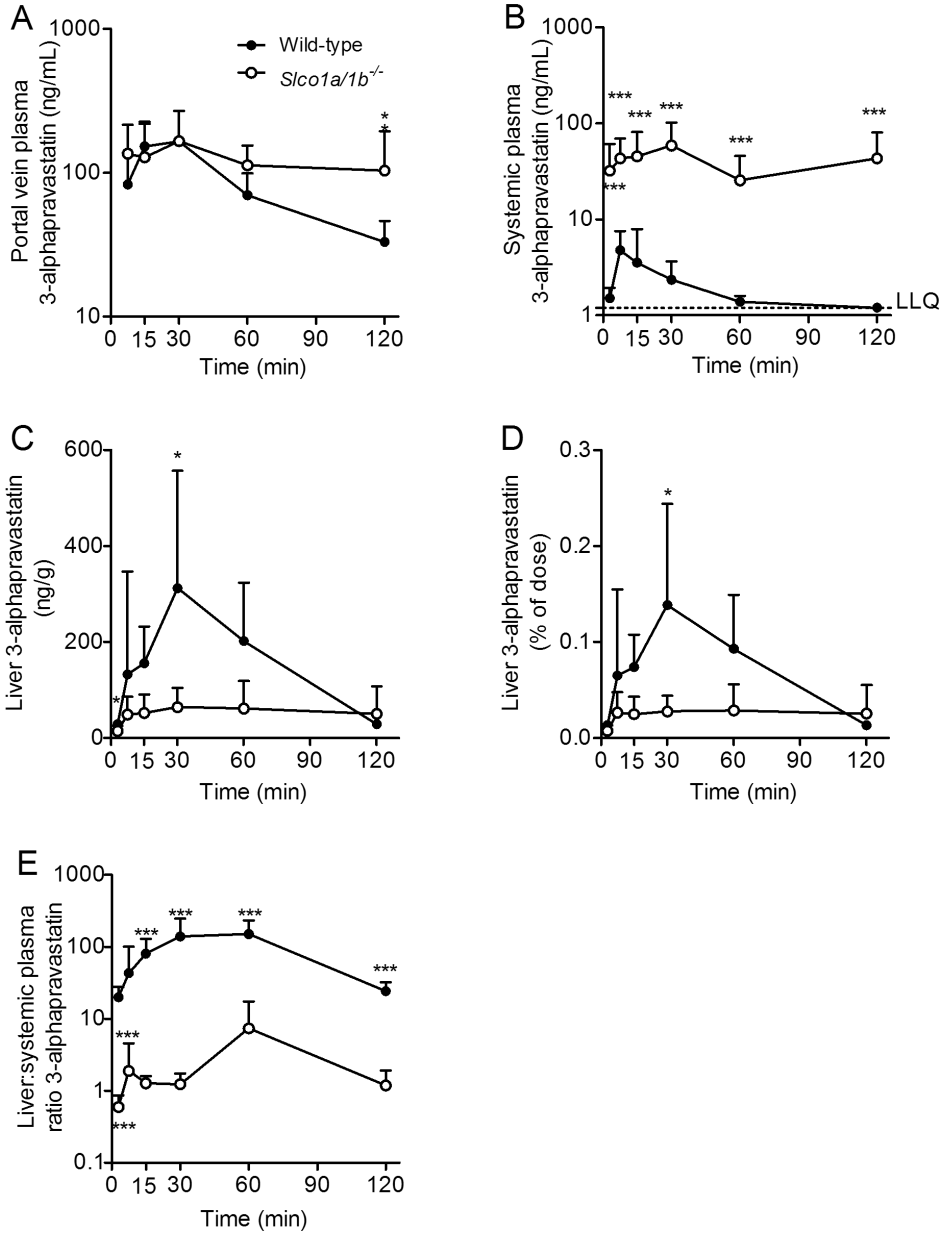

**Supplemental figure 1.** Role of Oatp1a/1b transporters in 3-alphapravastatin disposition after oral administration of 10 mg/kg pravastatin to wild-type and *Slco1a/1b(-/-)* mice. (A) 3-alphapravastatin portal vein plasma concentrations (semi-log plot) versus time curve. (B) 3-alphapravastatin systemic plasma concentrations (semi-log plot) versus time curve. (C) 3-alphapravastatin liver levels as µg/g and (D) as % of dose and (E) liver-to-systemic plasma ratio (semi-log plot) versus time curve. All data are presented as mean ± SD (n = 4-7, *, $P < 0.05$; **, $P < 0.01$ ; ***, $P < 0.001$ when compared with wild-type).

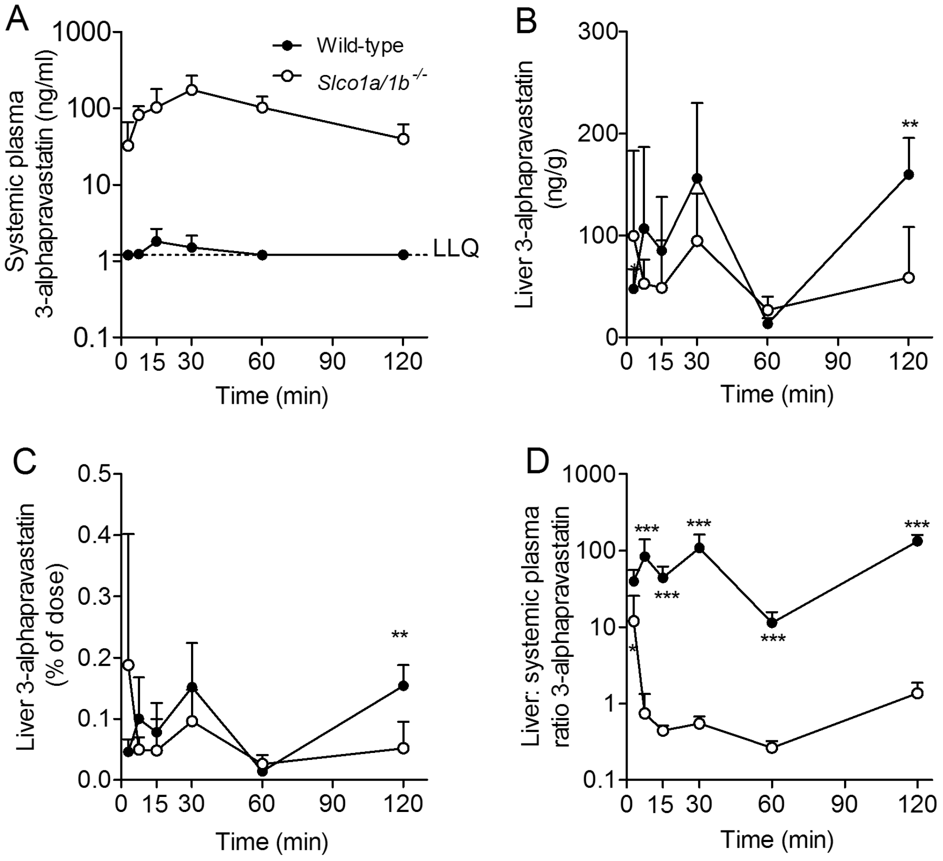

**Supplemental figure 2.** Role of Oatp1a/1b transporters in 3-alphapravastatin disposition after oral administration of 5 mg/kg pravastatin to wild-type and *Slco1a/1b(-/-)* mice. (A) 3-alphapravastatin systemic plasma concentrations (semi-log) versus time curve. (B) 3-alphapravastatin liver levels as ng/g (B), as % of dose (C) and (D) liver-to-systemic plasma ratio (semi-log plot) versus time curve. All data are presented as mean ± SD (n = 4-7, *, $P < 0.05$; **, $P < 0.01$; ***, $P < 0.001$ when compared with wild-type).

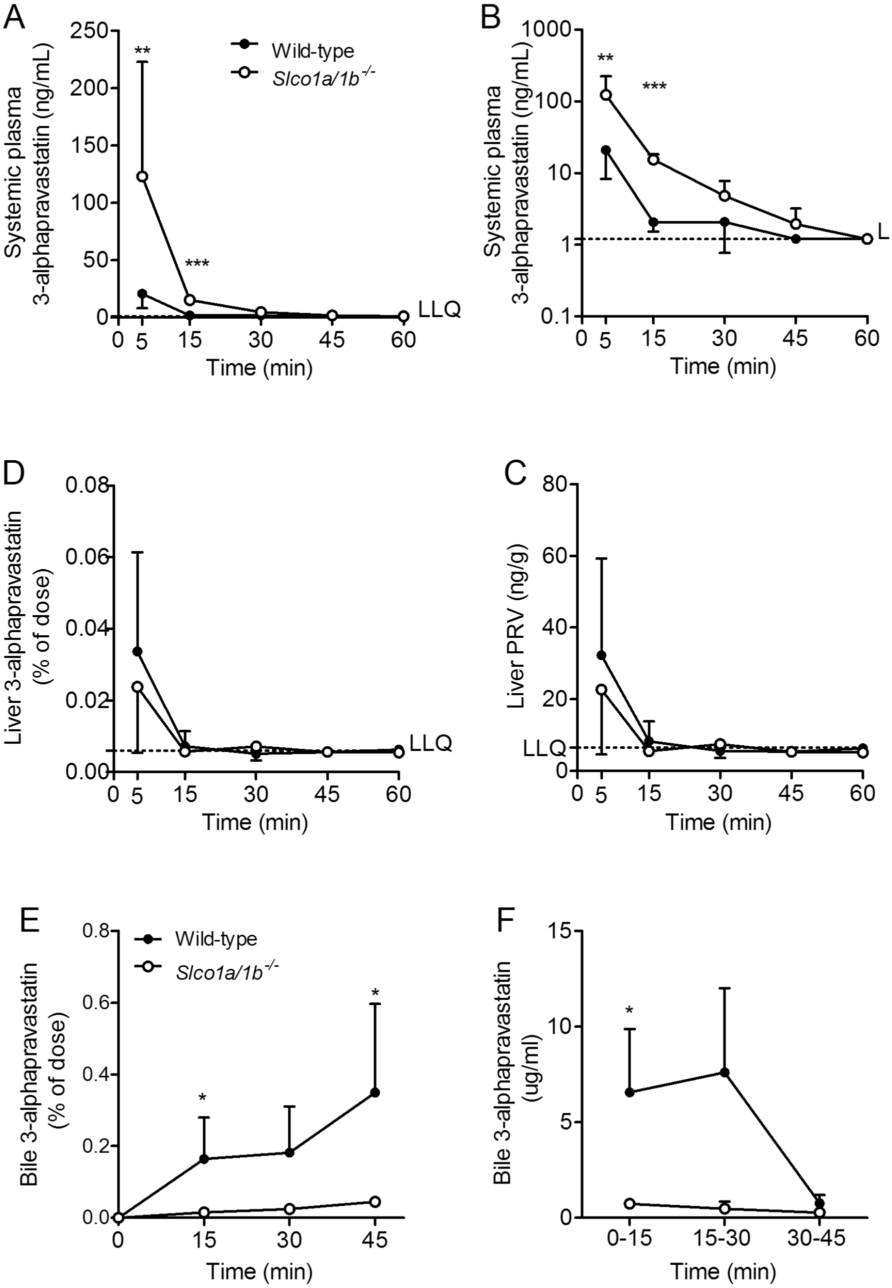

**Supplemental figure 3.** Oatp1a/1b transporters control hepatic uptake and biliary excretion of 3-alphapravastatin after intravenous administration (5 mg/kg pravastatin) to wild-type and *Slco1a/1b(-/-)* mice. (A) 3-alphapravastatin systemic plasma concentrations (semi-log plot). (B) 3-alphapravastatin n liver levels as µg/g and (C) as % of dose and (D) liver-to-systemic plasma ratios (semi-log plot). (E) Cumulative biliary excretion of 3-alphapravastatin (% of dose) and (F) bile concentrations (µg/mL). Data are presented as mean ± SD (n = 4-5, *, $P < 0.05$; **, $P < 0.01$ ; ***, $P < 0.001$ when compared with wild-type).

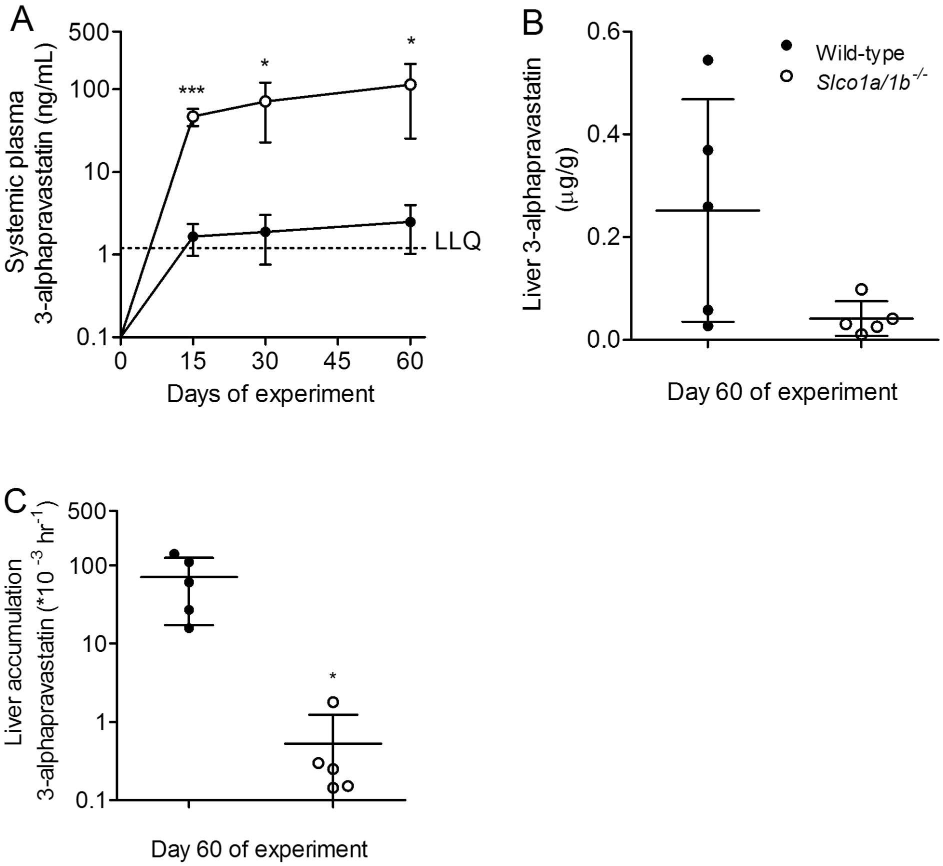

**Supplemental figure 4.** Role of Oatp1a/1b transporters in 3-alphapravastatin distribution after long-term exposure. (A) 3-alphapravastatin systemic plasma concentrations (semi-log plot) at several time points during the exposure to drinking water containing 1.2 g/L pravastatin (~180 mg/kg/day PRV). (B) 3-alphapravastatin liver levels (µg/g) and (C) liver-to-systemic plasma ratio (semi-log plot) after 60 days of exposure. All data are presented as mean ± SD (n = 4-5, *, $P < 0.05$; **, $P < 0.01$ ; ***, $P < 0.001$ when compared with wild-type).

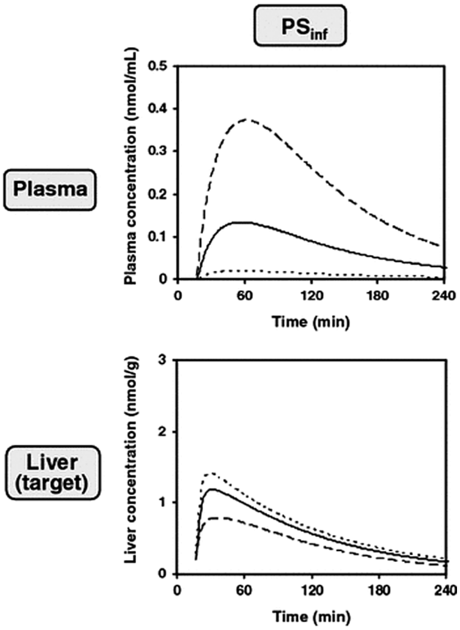

**Supplemental figure 5.** Simulated effects of changes in uptake transporter activity (PSinf) on time profiles of plasma and liver (target organ) concentrations of pravastatin in humans. Plasma and liver concentrations after oral administration (40 mg) were simulated using the PBPK model with varying hepatic transport activities over a 1/3- to 3-fold range of the initial values (———-, initial; – – –, x1/3, ········· ,x3) (modified from Watanabe et al (27)).

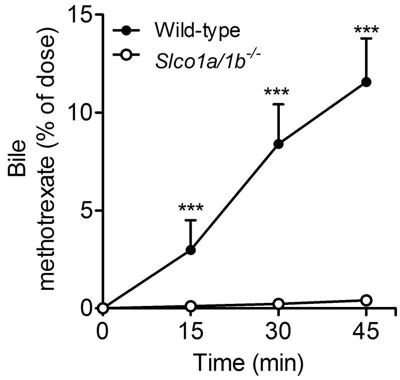

**Supplemental figure 6.** Role of Oatp1a/1b transporters in the cumulative biliary excretion of methotrexate after intravenous administration of 10 mg/kg methotrexate to female wild-type and *Slco1a/1b(-/-)* mice with cannulated gall bladder. (A) Cumulative biliary excretion of methotrexate (% of dose) versus time curve after intravenous administration. All data are presented as mean ± SD (n = 5-8, ***, *P* < 0.001 when compared with wild-type).

# 3.2

# *Murine Oatp1a/1b uptake transporters control rosuvastatin systemic exposure without affecting its apparent liver exposure*

Dilek Iusuf[1], Anita van Esch[1], Michael Hobbs[2],
Maxine Taylor[2], Kathryn E. Kenworthy[2], Evita van de Steeg[1],
Els Wagenaar[1] and Alfred H. Schinkel[1]

[1]Division of Molecular Oncology,
The Netherlands Cancer Institute, Amsterdam, The Netherlands,
[2]Department of Drug Metabolism and Pharmacokinetics,
GlaxoSmithKline, Ware, United Kingdom

*Molecular Pharmacology, 2013*

## Abstract

Organic anion-transporting polypeptides (OATPs) mediate the liver uptake and hence plasma clearance of a broad range of drugs. For rosuvastatin, a cholesterol-lowering drug and OATP1A/1B substrate, the liver represents both its main therapeutic target and its primary clearance organ. Here we studied the impact of Oatp1a/1b uptake transporters on the pharmacokinetics of rosuvastatin using wild-type and Oatp1a/1b-null mice. After oral administration (15 mg/kg), intestinal absorption of rosuvastatin was not impaired in Oatp1a/1b-null mice, but systemic exposure (AUC) was 8-fold higher in these mice compared with wild-type. Although liver exposure was comparable between the two mouse strains (despite the increased blood exposure), the liver-to-blood ratios were markedly decreased (>10-fold) in the absence of Oatp1a/1b transporters. After intravenous administration (5 mg/kg), systemic exposure was 3-fold higher in Oatp1a/1b-null mice than in the wild-type mice. Liver, small intestinal and kidney exposure were slightly, but not significantly, increased in Oatp1a/1b-null mice. The biliary excretion of rosuvastatin was very fast, with 60% of the dose eliminated within 15 minutes after intravenous administration, and also not significantly altered in Oatp1a/1b-null mice. Rosuvastatin renal clearance, although still minor, was ~15-fold increased in Oatp1a/1b-null males, suggesting a role of Oatp1a1 in the renal re-absorption of rosuvastatin.

Conclusion: Absence of Oatp1a/1b uptake transporters increases the systemic exposure of rosuvastatin by reducing its hepatic extraction ratio. However, liver concentrations are not significantly affected, most likely due to the compensatory activity of high-capacity, low-affinity alternative uptake transporters at higher systemic rosuvastatin levels, and the absence of efficient alternative rosuvastatin clearance mechanisms.

## Introduction

Organic anion transporting polypeptides (human: OATP, gene: *SLCO* (solute carrier organic-anion); rodents: Oatp, gene: *Slco)* form a superfamily of transmembrane transporters which mediate the cellular uptake of structurally diverse endogenous and exogenous compounds [1]. With wide and overlapping substrate specificities and expressed in tissues important for pharmacokinetics (liver, small intestine and kidney), the OATP1A/1B subfamilies are thought to have an important role in drug absorption, distribution and elimination. Based on tissue distribution and amino acid sequence, there are no straightforward orthologues between mouse and human members of these subfamilies. OATP1A/1B subfamilies contain 3 human members (OATP1A2, -1B1, and -1B3) but at least 5 mouse members (Oatp1a1, -1a4, -1a5, -1a6 and -1b2) [2]. Human OATP1B1 and OATP1B3 are predominantly expressed in the hepatic sinusoidal membrane and thought to play a key role in the hepatic uptake and plasma clearance of drugs. Several low-activity polymorphic variants of human OATP1B1 have been associated with decreased transport activity and increased plasma levels and hence toxicity of statins (cholesterol-lowering drugs) (reviewed in [3]). In addition, a previous study revealed that Rotor syndrome is caused by a complete simultaneous deficiency in the OATP1B1 and OATP1B3 genes [4]. While Rotor syndrome is very rare (~1 in $10^6$ individuals), individuals with complete deficiencies in either OATP1B1 or OATP1B3 alone likely exist at a much higher frequency in various populations.

Rosuvastatin is one of the most efficacious 3-hydroxy-3-methylglutaryl-coenzyme A reductase inhibitors (statins), and widely used in the treatment of hypercholesterolemia. Its high potency in inhibiting cholesterol synthesis is mainly due to liver-selective distribution of rosuvastatin [5;6]. Rosuvastatin has very low passive membrane permeability and with limited metabolism, its disposition is mediated almost entirely by uptake and efflux transporters. Rosuvastatin can be transported *in vitro* by multiple hepatic uptake transporters, e.g. OATP1B1, OATP1B3 and OATP2B1 and a bile acid-uptake transporter in the liver, the sodium-taurocholate co-transporting polypeptide (NTCP) [7-9]. In human hepatocytes OATP1B1, OATP1B3 and NTCP are the predominant uptake transporters, with OATP1B1 and/or OATP1B3 accounting for ~55% of the rosuvastatin uptake, both having a high affinity and high capacity, while NTCP accounts for ~35%, having high capacity but lower affinity for rosuvastatin [7] The ATP-binding cassette (ABC) efflux transporters ABCG2 and ABCC2 are responsible for the biliary excretion of rosuvastatin in humans, as demonstrated by *in vitro* and *in vivo* studies [8; 10;11].

Patients carrying polymorphic variants of *SLCO1B1* exhibit increased rosuvastatin plasma concentrations (12;15;13;Pasanen et al., 2007a), but evidence regarding a correlation between *SLCO1B1* genotype and therapeutic response is equivocal. Some studies find no correlation between polymorphic variants of *SLCO1B1* and cholesterol lowering efficacy of rosuvastatin [16, 17], while others do observe an association between these factors [18]. These findings raise the question how reduced hepatic uptake by OATP proteins affects systemic and liver concentrations of rosuvastatin.

Several single (Oatp1b2, Oatp1a1, Oatp1a4) and combined knockout mouse models (Oatp1a/1b knockout mice) are available and have proved very useful in elucidating the *in vivo* physiological and pharmacological functions of OATP1A/1B (reviewed in [19]). First, *Ose et al* showed that Oatp1a4 can transport rosuvastatin across the blood brain barrier, but only upon *in situ* injection into the brain [20]. Using Oatp1b2 knockout mice, a small-scale study showed that mouse Oatp1b2 might contribute to the liver uptake of rosuvastatin after intravenous administration, although only the liver-to-plasma ratio was significantly decreased in comparison with wild-type mice, whereas the plasma or liver concentrations were not significantly affected [21].

In the present study, we aimed to obtain an in depth understanding of the *in vivo* role of Oatp1a/1b transporters in the oral absorption and hepatic uptake of rosuvastatin. For this we used the Oatp1a/1b knockout mouse model (*Slco1a/1b*(-/-) mice, lacking all Oatp1a and -1b transporters) [22]. We compared the disposition of rosuvastatin in Oatp1a/1b knockout and wild-type mice after oral and intravenous administration.

## Materials and methods

### Animals

Animals were housed in small groups in a temperature-controlled environment with a 12-hour light/12-hour dark cycle. They received a standard diet (AM-II; Hope Farms) and acidified water *ad libitum*. All mouse experiments were approved by the Animal Experiments Review Board of the Netherlands Cancer Institute (Amsterdam), complying with Dutch legislation and in accordance with European Directive 86/609/EEC and the GSK Policy on the Care, Welfare and Treatment of Animals. Male or female wild-type and *Slco1a/1b*(-/-) (Oatp1a/1b knockout) mice [22] of comparable genetic background (>99% FVB) between 9 and 14 weeks of age were used as indicated.

### Chemicals and reagents

Rosuvastatin calcium salt [(3R,5S,6E)-7-[4-(4-Fluorophenyl)-6-(1-methylethyl)-2-[methyl (methylsulfonyl)amino]-5-pyrimidinyl]-3,5-dihydroxy-6-heptenoic Acid Calcium Salt)] was from Sequoia Research Products (Pangbourne, UK), and other chemicals (dimethyl sulfoxide, bovine serum albumin) were from Sigma (St. Louis, USA), isoflurane (Forane) from Abbott Laboratories (Queenborough, Kent, UK) and disodiumEDTA (Ethylenediaminetetraacetic acid) from LeoPharma BV (Breda, The Netherlands).

### Drug analysis

Concentrations of rosuvastatin in blood, organs (homogenized in 1:10 volumes of ice-cold 4% (w/v) BSA) and bile (diluted 100 times with human blank plasma) were determined by LC-MS/MS analysis as described [23].

### Blood and tissue pharmacokinetic experiments

Rosuvastatin was dissolved in dimethylsulfoxide (DMSO) and diluted with saline (to 1 mg/mL or 1.5 mg/mL) for administration of dose levels of 5 mg/kg i.v. or 15 mg/kg oral to mice. The maximum concentration of DMSO in the final solution was 2%. Ten μL/g body weight were administered via oral gavage (n = 5 - 7 for each group), and 5 μL/g body weight were used for administration in the tail vein of mice. At different time points, EDTA-blood (via cardiac puncture) was sampled under isoflurane anaesthesia. Mice were then sacrificed by cervical dislocation and tissues (liver without gall bladder) were isolated. After 15 mg/kg oral administration to male mice, portal vein blood samples were taken prior to cardiac puncture. Blood samples were diluted 1:1 with water and then stored at -20°C until analysis.

### *Biliary excretion of rosuvastatin*

Gall bladder cannulations and collection of bile in male wild-type and *Slco1a/1b*(-/-) mice (n = 7) were performed as described [24]. At the end of the experiment, blood and tissue samples were isolated and treated as described above.

### *Urinary and fecal excretion of rosuvastatin*

A mass balance study was performed with Rucco Type M/1 stainless steel metabolic cages (Valkenswaard, The Netherlands). Mice (n = 5) received rosuvastatin orally (15 mg/kg) or intravenously (5 mg/kg). Urine and feces were collected in a 0-24 hour fraction after the drug administration, followed by isolation of blood and tissue samples as described above. For female mice, rosuvastatin was only given orally (15 mg/kg) and at different times after administration (7.5, 15, 30, 60 and 120 minutes) blood samples were isolated from the tail vein. After collecting the urine and feces for 24 hours, mice were sacrificed as described above.

### *RNA isolation, cDNA synthesis and RT-PCR*

RNA isolation from mouse kidney and subsequent cDNA synthesis and RT-PCR were performed as described [25]. Specific primers (QIAGEN, Hilden, Germany) were used to detect expression levels of the following mouse Oatp1a genes: *Oatp1a1, Oatp1a4 and Oatp1a6*.

### *Pharmacokinetic calculations and statistical analysis*

When variances were not homogeneous, the data were log-transformed in order to obtain normal distribution and equal variances. The two-sided unpaired Student's *t*-test was used throughout the study to assess the statistical significance of differences between two sets of data. Results are presented as the means ± S.D. Differences were considered to be statistically significant when $P < 0.05$. Averaged blood concentrations for each time point were used to calculate the area under the blood concentration versus time curve (AUC) from t = 0 to the last sampling time point by the linear trapezoidal rule; S.E. was calculated by the law of propagation of errors [26]. Results of the AUC measurements are presented as means ± S.E.M. We calculated the ratio between plasma exposure after i.v. and oral administration, corrected for dose levels $(AUC_{oral}/AUC_{i.v.}) \cdot (Dose_{i.v.}/Dose_{oral})$. The apparent hepatic extraction ratio was calculated as $E = [1-(AUC_{oral\ systemic}/\ AUC_{oral\ portal\ vein})]$ (27).

### *Pharmacokinetic modeling*

The modeling software Phoenix WinNonlin 6.1 (Tripos, L.P., St. Louis, MO.) was used. Non-compartmental analysis was performed using blood data from intravenously and orally dosed mice from both strains. As the study design involved composite sampling, the 'sparse' sampling function was used to maximize the contribution of the data from each mouse at each sample time. After oral administration, we calculated the renal clearance based on the amount of rosuvastatin recovered in the urine over 24 hours after oral administration corrected for $AUC_{systemic}$ extrapolated to infinity ($AUC_{0\text{-}inf}$) and for individual mouse body weight. After intravenous administration, we calculated both renal and non-renal clearance based on the amount of rosuvastatin recovered in the urine or the feces corrected for $AUC_{systemic}$ extrapolated to infinity ($AUC_{0\text{-}inf}$) and for individual mouse body weight.

## *Results*

### *Oatp1a/1b transporters are not essential for the intestinal absorption of rosuvastatin*

Rosuvastatin is administered orally to patients, but not much is known about the transporters which facilitate its intestinal absorption. In wild-type mice, Oatp1a4 and Oatp1a5 are expressed in the small intestine [4], where they might theoretically facilitate the absorption of various drugs. Therefore, we first investigated a possible role of Oatp1a uptake transporters in absorption of rosuvastatin across the intestinal wall using wild-type and Oatp1a/1b knockout mice. We measured rosuvastatin portal vein blood concentrations at various time points after oral administration (15 mg/kg). Oral absorption was very rapid, with the highest blood rosuvastatin concentrations observed at the earliest technically feasible time point, 5 minutes after dosing (Figure 1A). The portal vein blood concentrations were modestly increased in Oatp1a/1b knockout mice (Figure 1A, Table 1), indicating that Oatp1a transporters are not essential for the intestinal absorption of rosuvastatin. The modest increase in the portal vein blood concentrations in Oatp1a/1b knockout mice likely reflects the higher systemic blood concentrations (see below, Figure 1B, C).

### *Increased systemic exposure of rosuvastatin in Oatp1a/1b-null mice after oral administration*

We also determined the systemic blood concentrations after oral administration of 15 mg/kg rosuvastatin to wild-type and Oatp1a/1b knockout mice. Rosuvastatin blood concentrations were markedly increased in Oatp1a/1b knockout mice in comparison with wild-type mice (Figure 1B, C), with an 8.2-fold higher blood $AUC_{(5\text{-}240)}$ (Table 1). Although liver concentrations were not significantly different between the mouse strains (Figure 1D, E), liver-to-blood ratios were at least 10-fold decreased in Oatp1a/1b-null mice at most time points, indicating a partially impaired liver uptake in the absence of Oatp1a/1b transporters (Figure 1F).

The liver represents both the therapeutic target and the main clearance organ for rosuvastatin. Therefore, the extraction capacity of the liver is an important parameter to assess. Assuming that portal vein blood concentrations represent the amount of rosuvastatin before entering the liver, and the systemic blood concentrations represent the amount of drug escaping the uptake in the liver, we calculated the apparent hepatic extraction ratio $E = [1\text{-}(AUC_{oral\ systemic}/\ AUC_{oral\ portal\ vein})]$ (Table 1). This approach assumes there is little alternative clearance (e.g., metabolic or renal) and tissue distribution of rosuvastatin outside of the liver, as was previously described for the rat [5]. In wild-type mice, rosuvastatin distributes almost exclusively to the liver after oral administration, with a very high apparent hepatic extraction ratio (0.93). Interestingly, in the absence of Oatp1a/1b uptake transporters this ratio dropped to 0.72, indicating a diminished efficacy in hepatic uptake in Oatp1a/1b knockout mice (Table 1).

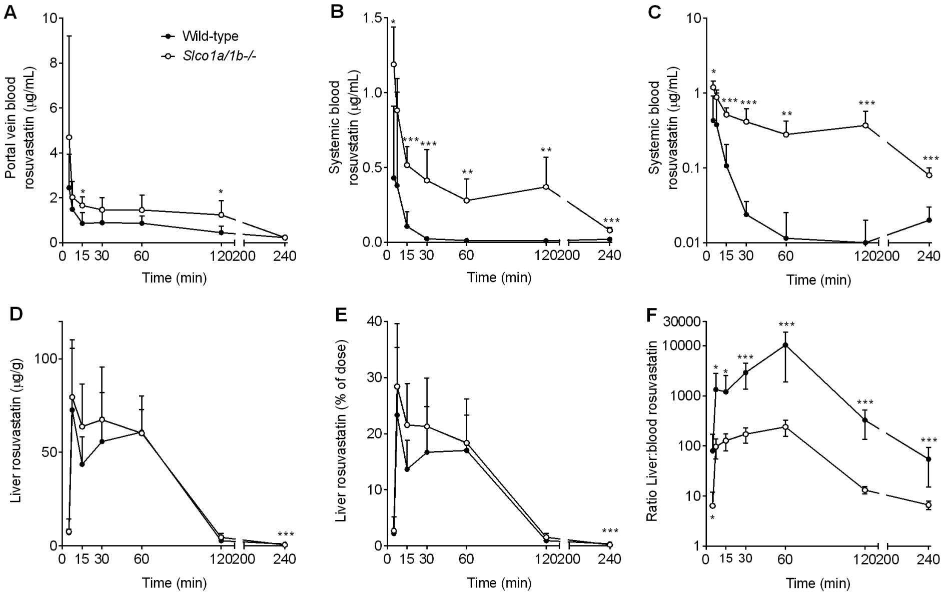

**Figure 1.** Oatp1a/1b uptake transporters control systemic exposure of rosuvastatin, but not intestinal uptake after oral administration (15 mg/kg) to male wild-type and *Slco1a/1b(-/-)* mice. (A) Rosuvastatin portal vein blood concentrations. (B) Rosuvastatin systemic blood concentrations and semi-log plot of data (C). Rosuvastatin liver levels in (D) µg/g and (E) % of dose. (F) Liver-to-systemic blood ratios (semi-log plot). Averaged liver-to-systemic blood ratios were calculated from individual mouse data. Data are presented as mean ± SD (n = 5-6, *, $P < 0.05$; **, $P < 0.01$; ***, $P < 0.001$ when compared with wild-type).

**Table 1.** Pharmacokinetic parameters after rosuvastatin administration to male wild-type (WT) and Oatp1a/1b knockout (KO) mice.

| Dose | Sample Site | Parameter | WT | *Slco1a/1b(-/-)* | Fold Difference (KO/WT) |
|---|---|---|---|---|---|
| 15 mg/kg orally | Blood | $AUC_{5-240}$ (min·µg/ml), portal vein | 169.8 ± 17.9 | 330.9 ± 39.8* | 1.9 |
| | | $AUC_{5-240}$ (min·µg/ml), systemic | 11.3 ± 2.4 | 9.3 ± 11.7** | 8.2 |
| | | Apparent hepatic extraction ratio | 0.93 | 0.72 | 0.77 |
| 5 mg/kg i.v. | Systemic blood | $AUC_{5-240}$ (min·µg/ml) | 13.9 ± 2.5 | 43.2 ± 4.0** | 3.1 |

Data presented as mean ± S.E.M.
* $P < 0.05$; **$P < 0.01$ vs. wild-type mice.

### *Increased systemic exposure of rosuvastatin in Oatp1a/1b-null mice after intravenous administration*

To further increase our understanding of how Oatp1a/1b transporters modulate the liver uptake of rosuvastatin we performed a pharmacokinetic study upon intravenous administration of rosuvastatin (5 mg/kg). Similar to the oral administration experiment, the systemic exposure of rosuvastatin was markedly higher in Oatp1a/1b knockout mice in comparison with wild-type mice (Figure 2A, B), with a 3.1-fold higher blood AUC$_{(5\text{-}240)}$ (Table 1). Again, liver concentrations were not significantly different between the two mouse strains (Figure 2C, D), whereas liver-to-blood ratios were significantly and substantially reduced (5- to 10-fold) at most time points from 15 min on in Oatp1a/1b knockout mice (Figure 2E), indicating a partially impaired hepatic uptake.

For the small intestinal wall (tissue) and small intestinal content concentrations and tissue-to-blood ratios of rosuvastatin we observed very similar results as for the liver (Figure 3A-D). These results would be in line with the liver concentrations and liver-to-blood ratios: The substantial % of dose of rosuvastatin (~15%) found in the small intestinal wall early after administration (Figure 3A), may reflect extensive entero-hepatic circulation of rosuvastatin, assuming rapid hepatobiliary excretion in the intestine (see below). The kidney concentrations of rosuvastatin were also increased in Oatp1a/1b knockout mice, most likely reflecting the increased systemic exposure. There were no significant differences in kidney-to-blood ratios between the strains, suggesting that there is no important role of Oatp1a/1b transporters in the uptake of rosuvastatin into the kidney (Figure 4A-C).

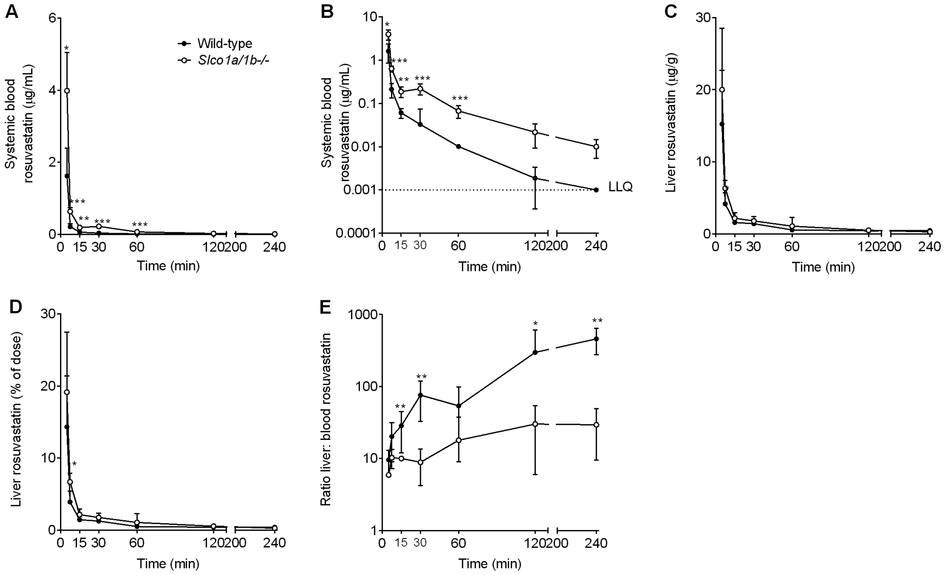

**Figure 2.** Oatp1a/1b transporters control systemic exposure of rosuvastatin after intravenous administration (5 mg/kg) to male wild-type and *Slco1a/1b(-/-)* mice. (A) Rosuvastatin systemic blood concentrations and semi-log plot (B). Rosuvastatin liver levels in (C) µg/g and (D) as % of dose. (E) Liver-to-systemic blood concentrations (semi-log plot). Data are presented as mean ± SD (n = 3-5, *, $P < 0.05$; **, $P < 0.01$; ***, $P < 0.001$ when compared with wild-type).

### *Effect of Oatp1a/1b transporters on the biliary excretion of rosuvastatin*

We investigated the effect of Oatp1a/1b deficiency on biliary elimination of rosuvastatin after intravenous administration (5 mg/kg) to mice with a cannulated gall bladder and ligated common bile duct. The bile flow was not different between the two mouse strains (~1.5 µL/min/g

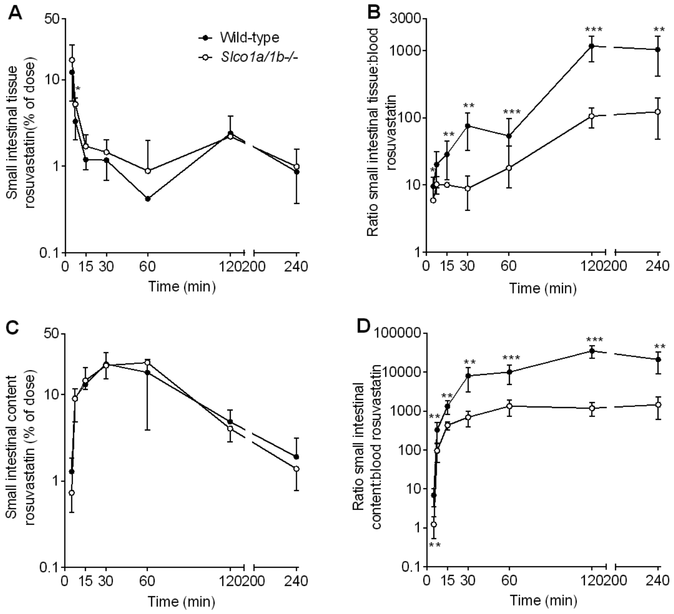

**Figure 3.** Role of Oatp1a/1b in the intestinal disposition of rosuvastatin after intravenous administration (5 mg/kg) to male wild-type and *Slco1a/1b(-/-)* mice. Small intestinal tissue levels as (A) % of dose and (B) small intestinal tissue-to-systemic blood ratios (semi-log plot). (C) Small intestinal content levels as % of dose and (D) small intestinal content-to-systemic blood ratios (semi-log plot). Data are presented as mean ± SD (n = 3-5, *, *P* < 0.05; **, *P* < 0.01; ***, *P* < 0.001 when compared with wild-type).

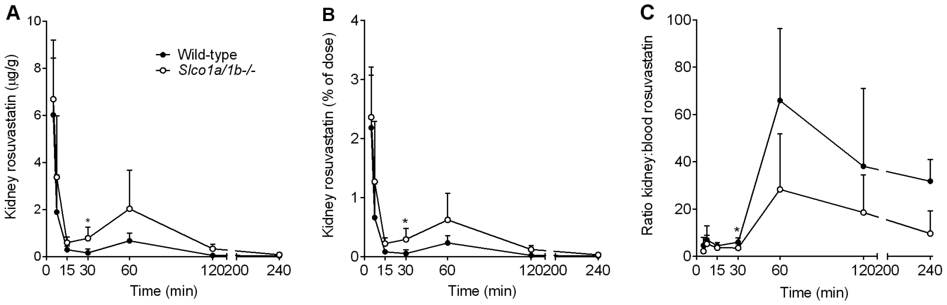

**Figure 4.** Role of Oatp1a/1b in the kidney disposition of rosuvastatin after intravenous administration (5 mg/kg) to male wild-type and *Slco1a/1b(-/-)* mice. Kidney levels in (A) µg/g and (B) % of dose. (C) Kidney-to-systemic blood ratios (semi-log plot). Data are presented as mean ± SD (n = 3-5, *, *P* < 0.05; **, *P* < 0.01; ***, *P* < 0.001 when compared with wild-type).

of liver). Biliary excretion of rosuvastatin was very rapid in both strains, with ~60 % of the dose being excreted in the first 15 minutes (Figure 5A). In the first 30 minutes there was no significant difference between the two strains of mice, and only from 30 minutes on there was a slightly higher biliary output of rosuvastatin in Oatp1a/1b knockout mice (Figure 5A), possibly reflecting

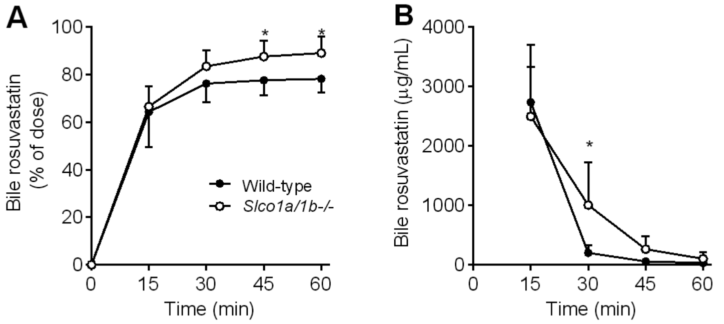

**Figure 5.** Role of Oatp1a/1b in the biliary excretion of rosuvastatin in gall bladder-cannulatedmice after intravenous administration (5 mg/kg) to wild-type and *Slco1a/1b(-/-)* mice. (A) Rosuvastatin cumulative biliary excretion (in % of dose) and (B) rosuvastatin bile concentration (µg/mL). Data are presented as mean ± SD (n = 6-7, *, $P < 0.05$; **, $P < 0.01$; ***, $P < 0.001$ when compared with wild-type).

slightly higher liver concentrations (e.g. Figure 2C). Additionally, from 30 minutes after dosing, biliary excretion of rosuvastatin was much slower in both strains than in the first 15 minutes after intravenous administration (Figure 5B). In this experiment enterohepatic circulation of rosuvastatin is interrupted due to ligation of the common bile duct, blocking possible recharging of the liver with rosuvastatin reabsorbed from the intestinal lumen, and thus continued biliary excretion. Note that the mRNA expression of Abcc2, one of the canalicular efflux transporters responsible for the biliary excretion of rosuvastatin, is somewhat lower in the Oatp1a/1b knockout mice, while expression of Abcg2 is not changed [4].

There were no significant differences in the blood, liver and small intestinal tissue concentrations in gall bladder-cannulated wild-type and Oatp1a/1b knockout mice 60 minutes after dosing (Supplemental Figure 1). In the small intestinal content we observed significantly higher levels of rosuvastatin in Oatp1a/1b knockout mice compared to wild-type (1.1 ± 0.8 versus 0.4 ± 0.2 % of dose, $P < 0.05$, Supplemental Figure 1). It is notable that only a small fraction of rosuvastatin was found back in the small intestinal wall and lumen. In the context of a ligated common bile duct, rosuvastatin can only reach the small intestinal lumen via direct intestinal excretion from the blood possibly mediated by Abcg2 or Abcc2, whose mRNA expression levels in the small intestine are similar in both strains [4]. Note that the amount of rosuvastatin directly excreted from the blood (Supplemental Figure 1B, C) is far lower than that excreted via the bile and probably reabsorbed via the small intestinal wall (Figure 3A). Taken together these data suggest that rosuvastatin undergoes extensive enterohepatic circulation.

### *Effect of Oatp1a/1b transporters on the urinary and fecal excretion of rosuvastatin*

Next, we performed a mass-balance experiment over 24 hours after intravenous (5 mg/kg) or oral (15 mg/kg) administration of rosuvastatin to male wild-type and Oatp1a/1b knockout mice. In line with the similar and high % of dose excreted in the bile after intravenous administration (Figure 5A), the dose recovered in the feces was nearly 60% in the wild-type mice and slightly, albeit significantly, lower in the Oatp1a/1b-null mice (57.3 ± 6.7 versus 49 ± 4.1 % of dose,

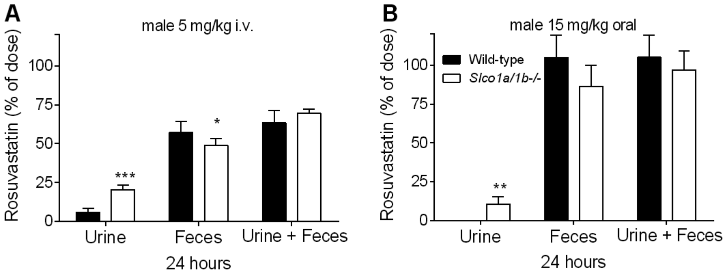

**Figure 6.** Role of Oatp1a/1b transporters in the urinary and fecal excretion of rosuvastatin in male mice. Rosuvastatin (% of dose) recovered in the urine, feces and urine plus feces combined after (A) 15 mg/kg oral and (B) 5 mg/kg intravenous administration of rosuvastatin. Data are presented as mean ± SD (n = 5, *, $P < 0.05$; **, $P < 0.01$; ***, $P < 0.001$ when compared with wild-type).

$P < 0.05$) (Figure 6A). The amount of rosuvastatin recovered in the urine was 3-fold higher in the Oatp1a/1b knockout mice (20.4 ± 3 versus 5.9 ± 2.5 % of dose) (Figure 6A), probably reflecting the 3-fold higher systemic exposure of rosuvastatin after intravenous administration (Table 1) and the diminished renal reabsorption of rosuvastatin in the Oatp1a/1b-null mice (see below and Table 2). The recovery after intravenous administration was ~70%, possibly because upon intravenous administration rosuvastatin can distribute more extensively to other compartments in the body, from which rosuvastatin may be released only after 24 hours after administration.

After oral administration to male mice, the total rosuvastatin recovery was close to 100% of the dose (Figure 6B), indicating very limited metabolism of this drug in mice. In line with the high apparent hepatic extraction ratio after oral administration (Table 1), the % of dose recovered in the feces in wild-type mice was very high (~100%), while it was reduced to ~86% in Oatp1a/1b knockout mice, albeit not significantly (Figure 6B). The amount of rosuvastatin recovered in the urine of wild-type mice was very low (0.10 ± 0.04 % of dose), while in the absence of Oatp1a/1b transporters it was about 100-fold higher (10.7 ± 4.7) (Figure 6B). As a consequence, the renal clearance of rosuvastatin was 15.5-fold increased, from 1.3 ± 0.6 to 20.1 ± 9.0 ml/min/kg ($P < 0.01$) in the male Oatp1a/1b knockout mice (Table 2).

### *Role of Oatp1a/1b transporters in the renal and non-renal clearance of rosuvastatin*

The increased renal clearance of rosuvastatin in the Oatp1a/1b knockout mice might be explained if one or more of the Oatp1a/1b proteins in the kidney played a role in the tubular reabsorption of glomerularly filtrated or otherwise renally secreted rosuvastatin. It has been demonstrated that only Oatp1a1 and Oatp1a6, and to a lesser extent Oatp1a4, are significantly expressed in the male kidney [28]. If Oatp1a1 would be primarily responsible for renal rosuvastatin reabsorption, the renal clearance in female wild-type mice should be higher than in male wild-type mice, and female Oatp1a/1b knockouts should show little increase in clearance. To test whether this was the case, we performed an oral systemic exposure and mass balance study with 15 mg/kg rosuvastatin in female mice (Figure 7). Similar to results obtained in male mice (Figure 1B), systemic blood concentrations were highly increased in female Oatp1a/1b

**Table 2.** Renal and nonrenal clearance (calculated based on urinary and fecal output) after rosuvastatin administration to wildtype (WT) and Oatp1a/1b knockout mice.

| Dose | Experimental Group | Renal Clearance ml/min/kg | Nonrenal Clearance ml/min/kg | Total Clearance ml/min/kg |
|---|---|---|---|---|
| 15 mg/kg orally | WT male | 1.3 ± 0.6 | – | – |
| | *Slco1a/1b(-/-)* | 20.1 ± 9.0$^{**}$ | – | – |
| | WT female | 20.1 ± 6.4$^{\#\#}$ | – | – |
| | *Slco1a/1b(-/-)* female | 27.4 ± 4.3 | – | – |
| 5 mg/kg i.v. | WT male | 1.2 ± 0.6 | 11.6 ± 1.3 | 12.8 ± 1.6 |
| | *Slco1a/1b(-/-)* male | 2.4 ± 0.3$^{**}$ | 5.8 ± 0.5$^{**}$ | 8.2 ± 0.3 |

Data presented as mean ± S.E.M.
–, nonrenal clearance could not be directly calculated for oral administration in the absence of reliable oral bioavailability data.
** $P < 0.01$ vs. wild-type mice of the same gender; $^{\#\#}P < 0.01$ vs. male mice from the same genotype (wild-type or knockout).

knockout mice (Figure 7A). Most of the rosuvastatin was recovered in the feces with similar levels in wild-type and Oatp1a/1b-null mice (~75 % of dose) (Figure 7B), while the amount in the urine was 19-fold higher in the female Oatp1a/1b knockout mice in comparison with wild-type controls (18.9 ± 3 versus 1 ± 0.3 % of dose). Importantly, when comparing the male versus female mice, we observed that the amount of rosuvastatin in the urine of female wild-type mice was 9-fold higher than in the male wild-type mice (Figure 7C), and 1.7-fold higher in the female Oatp1a/1b-null mice than in the male Oatp1a/1b-null mice (Figure 7C).

Subsequent calculation of the renal clearances (Table 2) showed that renal clearance in wild-type females was 15 times higher than that in wild-type males, but not different from that in Oatp1a/1b knockout males. Moreover, the renal clearance was not significantly increased in female Oatp1a/1b knockout compared to wild-type female mice (Table 2). These results are consistent with a renal rosuvastatin reabsorption role of Oatp1a1 in male mice. RT-PCR analysis of Oatp1a1,

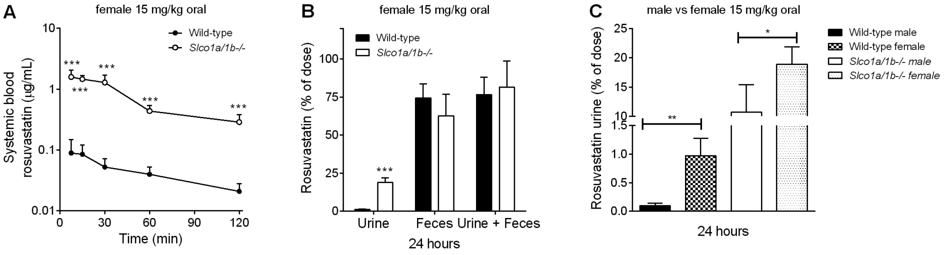

**Figure 7.** Role of Oatp1a/1b transporters in the urinary and fecal excretion of rosuvastatin after 15 mg/kg oral rosuvastatin administration. (A) Blood rosuvastatin concentrations (as µg/mL) versus time (semi-log plot) and (B) rosuvastatin (% of dose) recovered in the urine, feces and urine plus feces combined, in female mice. (C) Comparison between rosuvastatin (% of dose) recovered in urine in male versus female wild-type and Oatp1a/1b knockout mice. Data are presented as mean ± SD (n = 5, *, $P < 0.05$; **, $P < 0.01$; ***, $P < 0.001$ when compared with wild-type).

Oatp1a4, and Oatp1a6 expression in kidney of our FVB strain wild-type mice (Supplemental Figure 2) confirmed that Oatp1a1 was far more highly expressed in male than in female kidney (about 5000-fold), whereas Oatp1a4 was not differentially expressed, and Oatp1a6 only slightly (about 2-fold) more in male mice than in female mice. Collectively, the data suggest that Oatp1a1 plays a role in the renal reabsorption of rosuvastatin, and thus diminishes its renal clearance.

After intravenous administration, the renal clearance was only 2-fold increased in Oatp1a/1b knockout male mice in comparison with wild-type mice and the non-renal clearance was 2-fold decreased (Table 2). This reflects the decreased renal reabsorption of rosuvastatin in the male Oatp1a/1b knockout mice (see above, Table 2). The renal clearance accounted for ~10% of the total clearance in the male wild-type mice and for ~30% in the Oatp1a/1b knockout mice (Table 2).

### *Pharmacokinetic modeling*

We further performed a limited non-compartmental modeling of the pharmacokinetic data using the sparse sampling function. The results are presented in Table 3. It is noteworthy that values for blood AUC after intravenous administration calculated using the pharmacokinetic software are much higher than the AUC values observed from t = 5 until t = 240 min, calculated using the linear trapezoidal rule (Table 1 versus Table 3). This discrepancy is mainly due to the extrapolation of the blood concentration data to t = 0 min. Below we discuss only the data from Table 3.

The ratio between blood exposure after oral versus i.v. administration of rosuvastatin was increased in the Oatp1a/1b knockout mice (from 0.011 to 0.058), most likely as a consequence of the impaired first-pass uptake in the liver of these mice after oral administration (Table 3).

After intravenous administration we observed a decrease, albeit modest, in the total clearance (from 20.3 to 11.8 mL/min/kg). Finally, the half-life of rosuvastatin after intravenous administration was almost 2-fold higher (26.2 in wild-type mice versus 49.9 minutes in Oatp1a/1b knockout mice) (Table 3).

**Table 3.** Noncompartmental pharmacokinetic modeling using sparse data function after rosuvastatin administration to wild-type (WT) and Oatp1a/1b knockout (KO) mice.

| **Dose** | **Sample Site** | **Parameter** | **WT** | ***Slco1a/1b(-/-)*** | **Fold Difference (KO/WT)** |
|---|---|---|---|---|---|
| 15 mg/kg orally (male) | Systemic blood | $c_{max}$ (µg/ml) | 0.4 | 1.2 | 3.0 |
| | | $t_{max}$ (min) | 5 | 5 | |
| | | $AUC_{0-\infty}$ (min·µg/ml) | 11.3 | 80.1 | 7.1 |
| | | $AUC_{oral}/AUC_{i.v.}$ * $Dose_{i.v.}/Dose_{oral}$ | 0.011 | 0.058 | 5.2 |
| | | Half-life (min) | 89 | 74 | |
| | Portal blood | $AUC_{0-\infty}$ (min·µg/ml) | 174 | 296 | 1.7 |
| 15 mg/kg orally (female) | Systemic blood | $AUC_{0-\infty}$ (min·µg/ml) | 7.3 | 103.3 | 14.2 |
| | | Half-life (min) | 67.4 | 42.7 | 0.6 |
| 5 mg/kg i.v. (male) | Systemic blood | $AUC_{0-\infty}$ (min·µg/ml) | 246 | 423 | 1.7 |
| | | Clearance (ml/min/kg) | 20.3 | 11.8 | 0.58 |
| | | Half-life (min) | 26.2 | 49.9 | |

The pharmacokinetic parameters (total clearance and exposure) we obtained after oral and intravenous administration of the wild-type mice were in general agreement with previous studies, although there were some differences in half-life values, probably due to different genetic background of the mice and the dosages used [29].

## Discussion

Here we show that Oatp1a/1b uptake transporters are not essential for the intestinal absorption of rosuvastatin after oral administration, but that they strongly affect rosuvastatin systemic exposure after oral and intravenous administration. Interestingly, the strong increase (8-fold) in systemic exposure in Oatp1a/1b-null mice is not accompanied by a significant decrease in liver exposure, or in biliary excretion of rosuvastatin after intravenous administration, but the hepatic extraction ratio is markedly decreased in the absence of Oatp1a/1b transporters. The major pharmacokinetic impact of Oatp1a/1b transporters on rosuvastatin therefore occurs through their hepatic uptake activity. We also show that renal clearance of rosuvastatin, while small compared to hepatic clearance, is gender-dependent and might be affected by the different expression levels of Oatp1a1 in the kidney of male versus female wild-type mice.

It has been proposed that OATP1A/Oatp1a transporters can mediate the intestinal absorption of many drugs, including statins. Despite being quite polar, rosuvastatin was very rapidly and efficiently absorbed, with both portal vein and systemic blood concentrations highest at the earliest feasible sampling time point (5 minutes) in both wild-type and Oatp1a/1b knockout mice. Although Oatp1a/1b uptake transporters are clearly not essential for the intestinal uptake of rosuvastatin, given its polarity (logP = 1.92) it is almost certain that other uptake transporters must be involved. One candidate could be mouse Oatp2b1, since several studies have shown that its human orthologue OATP2B1 can transport rosuvastatin *in vitro* [7, 8, 30]. The contribution of OATPs in the oral absorption of rosuvastatin was also investigated in an *in vivo* study in pigs, where gemfibrozil (an OATP inhibitor) was co-administered with rosuvastatin [31]. However, despite high concentrations of gemfibrozil, enough to efficiently inhibit OATP1A2 and OATP2B1 in the small intestine, the intestinal absorption of rosuvastatin was not affected [31]. Additional studies are therefore required to establish the transporters responsible for the intestinal uptake of rosuvastatin.

Interestingly, our results suggest that Oatp1a1 in the kidney might play a role in the renal reabsorption of rosuvastatin, although the contribution of renal clearance to the systemic clearance of rosuvastatin is small in wild-type mice. We observed a gender-dependent difference in the renal clearance of rosuvastatin, which has also been described in rats for perfluorooctanoic acid, a potentially toxic chemical and substrate of Oatp1a1, which is mainly eliminated renally [32]. Therefore, besides their predominant role in mediating hepatic clearance of drugs, Oatp1a transporters might affect the renal clearance of drugs as well.

Systemic exposure of rosuvastatin after oral administration was 7- to 14-fold higher in the absence of Oatp1a/1b transporters. Oatp1a1, Oatp1a4 and Oatp1b2, present in the basolateral membrane of hepatocytes in mice, likely mediate the same function(s) as human OATP1B1 and

OATP1B3. Therefore, our results are in line with data from patients carrying low-activity genetic polymorphic variants of OATP1B1. These variants are associated with increased plasma levels of rosuvastatin (reviewed in [15]), but it seems that the magnitude of effects varies between different ethnic groups. For example, Korean individuals with the low activity variant *15/*15 (two copies of the 521T>C allele) had 1.7-fold higher rosuvastatin AUCs than the control group [12]. In a study comparing white and Asian subjects, the variant *15/*15 was associated with higher rosuvastatin AUC only in the white subjects, and not in the Asian ones [13]. Similarly, in a Finnish population, a slightly higher systemic exposure to rosuvastatin was observed in carriers of the OATP1B1 521T>C variant [14]. In addition, documented drug-drug interactions between rosuvastatin and OATP1B inhibitors further support the importance of OATP1B1 in the systemic exposure of rosuvastatin. In humans, it was shown that after repeated administrations of oral gemfibrozil (at plasma concentrations which mainly inhibit OATP1B1) the plasma AUC of rosuvastatin was 1.8-fold higher [33]. Co-administration with cyclosporine led to 7-10-fold higher rosuvastatin AUCs [34]. The net effect of OATP1B inhibition by cyclosporine is difficult to estimate as cyclosporine can also inhibit various other influx and efflux transporters involved in the pharmacokinetics of rosuvastatin, e.g. NTCP and/or ABCC2 and ABCG2. A similar pronounced effect of co-administration of cyclosporine and rosuvastatin was seen in a study with pigs [31].

Despite the markedly increased systemic exposure of rosuvastatin in Oatp1a/1b knockout mice, the liver concentrations were not significantly reduced in these mice. However, the liver-to-blood ratios were markedly decreased, indicating an impaired liver uptake. A recent small-scale study in Oatp1b2-null mice showed that at 30 minutes after intravenous administration, liver-to-plasma ratios of rosuvastatin were 2.7-fold lower than in wild-type mice, while the plasma concentrations were not significantly different between the two mouse strains [21]. We observed 10-fold lower liver-to-blood ratios in Oatp1a/1b-null mice at the same time point, and 7-fold increased blood concentrations. This indicates that, in addition to Oatp1b2, hepatic Oatp1a1 and/or Oatp1a4 also play an important role in liver uptake of rosuvastatin.

As previously mentioned, liver (and bile) concentrations of rosuvastatin were mostly not significantly altered by the absence of Oatp1a/1b transporters, in spite of the strongly increased blood exposure. This surprising finding can be explained by the intrinsic properties of rosuvastatin. While our data show a very high hepatic extraction ratio (0.93) of rosuvastatin in wild-type mice after oral administration, this dropped only to 0.72 in Oatp1a/1b knockout mice (Table 1), indicating that in the knockouts there is still a very substantial hepatic uptake of rosuvastatin. Considering the high and similar amount of rosuvastatin taken up in wild-type and knockout liver (Figure 1E), the modest decrease in hepatic extraction is sufficiently offset by the higher portal vein concentrations. Small differences in liver concentration can be easily lost in the experimental variation and thus not become obvious. However, any small decrease in liver exposure theoretically translates into a much larger (4-fold) increase in the fraction of rosuvastatin that “escapes” theliver [from 0.07 to 0.28 (1 2 apparent hepatic extractionratio)] (Table 1) and thus ends up in the systemic circulation. Note that the estimated total amount of rosuvastatin in the systemic circulation represents less than 0.5% of the dose (at 1 μg/mL, Figure 1B), an amount that is negligible compared to the ~20% of dose found in the liver over the first 15-60 min (Figure 1E). It is therefore not surprising that a relatively big change in systemic blood concentrations can occur with little impact on the liver concentrations. This idea is also supported by a physiologically based pharmacokinetic (PBPK) model described for pravastatin [35]. This model predicts that, for a predominantly hepatically cleared drug, a diminished hepatic uptake (like in the absence of Oatp1a/1b transporters) leads to a substantial increase in the systemic exposure, while the liver exposure is not so much affected, especially for drugs which have a negligible renal clearance. In our study renal clearance of rosuvastatin accounts for maximally 1% of total clearance in the wild-type mice, versus 25% in the Oatp1a/1b-null mice after oral administration (Table 2). This is in line with data from humans [36] and rats [37], which also exhibit a low renal clearance of rosuvastatin.

The still substantial hepatic uptake of rosuvastatin in Oatp1a/1b knockout mice, albeit at higher blood concentrations, indicates that alternative transporters for rosuvastatin can partially compensate for the loss of Oatp1a/1b transporters. We hypothesize that already shortly after administration, reduced liver uptake due to the absence of Oatp1a/1b transporters results in a substantial increase in rosuvastatin blood concentrations. This high blood concentration allows continued substantial uptake of rosuvastatin into the liver via low-affinity, but high-capacity alternative transporters. Nevertheless, the rescue provided by these alternative transporters is partial as the systemic blood concentrations remain markedly increased in the Oatp1a/1b-null mice over at least 4 hours after administration. The most obvious candidate as an alternative transporter in mouse or human, but not rat, would be NTCP/Ntcp, which has been described to facilitate cellular uptake of rosuvastatin *in vitro* [7, 8]. Using double expressing-oocytes of wild-type and/or polymorphic variants of OATP1B1 and NTCP, it was shown that reduced rosuvastatin uptake by OATP1B1*15 can be masked in the presence of NTCP, suggesting that NTCP can rescue OATP1B1 loss of function *in vitro* [9]. Another transporter which might compensate for the loss of Oatp1a/1b function is OATP2B1 (human) or Oatp2b1 (mouse/rat), which is also present in the basolateral membrane of hepatocytes and can mediate rosuvastatin transport *in vitro* [7, 8, 30].

Previously, we showed that mouse Oatp1a/1b uptake transporters control the hepatic uptake of pravastatin [38]. Similar to rosuvastatin, absence of Oatp1a/1b resulted in a substantial increase in systemic exposure of pravastatin both after oral and intravenous administration. However, in contrast to rosuvastatin, pravastatin liver exposure was 2-fold reduced in the Oatp1a/1b-null mice, and the impact of Oatp1a/1b transporters was very obvious in the 8-fold decreased biliary excretion of pravastatin after intravenous administration [38]. Although similar in hydrophilicity, (pravastatin, logP = 1.65 and rosuvastatin, logP = 1.92), rosuvastatin has a higher affinity to distribute to the liver than pravastatin [5, 39]. Indeed, rosuvastatin has a higher apparent hepatic extraction ratio (0.93 in wild-type versus 0.72 in Oatp1a/1b-null mice, Table 1) than pravastatin (0.88 in wild-type versus 0.52 in Oatp1a/1b-null mice) [38]. In addition, rosuvastatin appears to be more substantially transported by alternative transporters such as Ntcp and/or Oatp2b1 when compared to pravastatin, resulting in a somewhat less pronounced increase in the systemic exposure in the Oatp1a/1b knockout model. Nevertheless, hepatic uptake of both compounds is still substantial in the absence of Oatp1a/1b transporters, indicating that the uptake transporters involved have an appreciable redundancy and are capable of relatively efficient clearance even when the main disposition mechanism has been compromised.

In conclusion, Oatp1a/1b uptake transporters determine the systemic exposure of rosuvastatin, without substantially affecting its liver exposure after bolus administration. Whether this is also true after chronic administration of rosuvastatin in patients remains to be seen. Our findings are clinically relevant for individuals with low-activity polymorphic variants of OATP1B1, and heterozygous carriers of the various full-deficiency mutations of OATP1B1 and/or OATP1B3 [4, 40]. These individuals, when treated with rosuvastatin, might be at risk of developing myopathy, the major systemic side effect of statins. On the other hand, the therapeutic effect of rosuvastatin in the liver might be less affected.

## *Acknowledgments*

We thank Marion Ludwig for technical assistance.

## *Reference List*

1. Hagenbuch B, Meier PJ. Organic anion transporting polypeptides of the OATP/ SLC21 family: phylogenetic classification as OATP/ SLCO superfamily, new nomenclature and molecular/functional properties. Pflugers Arch 2004 Feb;447(5):653-665.
2. Hagenbuch B, Meier PJ. The superfamily of organic anion transporting polypeptides. Biochim Biophys Acta 2003 Jan 10;1609(1):1-18.
3. Kalliokoski A, Niemi M. Impact of OATP transporters on pharmacokinetics. Br J Pharmacol 2009 Oct;158(3):693-705.
4. van de Steeg E, Stranecky V, Hartmannova H, Noskova L, Hrebicek M, Wagenaar E, et al. Complete OATP1B1 and OATP1B3 deficiency causes human Rotor syndrome by interrupting conjugated bilirubin reuptake into the liver. J Clin Invest 2012 Feb 1;122(2):519-528.
5. Nezasa K, Higaki K, Matsumura T, Inazawa K, Hasegawa H, Nakano M, et al. Liver-specific distribution of rosuvastatin in rats: comparison with pravastatin and simvastatin. Drug Metab Dispos 2002 Nov;30(11):1158-1163.
6. Olsson AG, McTaggart F, Raza A. Rosuvastatin: a highly effective new HMG-CoA reductase inhibitor. Cardiovasc Drug Rev 2002;20(4):303-328.
7. Ho RH, Tirona RG, Leake BF, Glaeser H, Lee W, Lemke CJ, et al. Drug and bile acid transporters in rosuvastatin hepatic uptake: function, expression, and pharmacogenetics. Gastroenterology 2006 May;130(6):1793-1806.
8. Kitamura S, Maeda K, Wang Y, Sugiyama Y. Involvement of multiple transporters in the hepatobiliary transport of rosuvastatin. Drug Metab Dispos 2008 Oct;36(10):2014-2023.
9. Choi MK, Shin HJ, Choi YL, Deng JW, Shin JG, Song IS. Differential effect of genetic variants of Na(+)-taurocholate co-transporting polypeptide (NTCP) and organic anion-transporting polypeptide 1B1 (OATP1B1) on the uptake of HMG-CoA reductase inhibitors. Xenobiotica 2011 Jan;41(1):24-34.
10. Hu M, Lui SS, Mak VW, Chu TT, Lee VW, Poon EW, et al. Pharmacogenetic analysis of lipid responses to rosuvastatin in Chinese patients. Pharmacogenet Genomics 2010 Oct;20(10):634-637.
11. Jemnitz K, Veres Z, Tugyi R, Vereczkey L. Biliary efflux transporters involved in the clearance of rosuvastatin in sandwich culture of primary rat hepatocytes. Toxicol In Vitro 2010 Mar;24(2):605-610.
12. Choi JH, Lee MG, Cho JY, Lee JE, Kim KH, Park K. Influence of OATP1B1 genotype on the pharmacokinetics of rosuvastatin in Koreans. Clin Pharmacol Ther 2008 Feb;83(2):251-257.
13. Lee E, Ryan S, Birmingham B, Zalikowski J, March R, Ambrose H, et al. Rosuvastatin pharmacokinetics and pharmacogenetics in white and Asian subjects residing in the same environment. Clin Pharmacol Ther 2005 Oct;78(4):330-341.
14. Pasanen MK, Fredrikson H, Neuvonen PJ, Niemi M. Different effects of SLCO1B1 polymorphism on the pharmacokinetics of atorvastatin and rosuvastatin. Clin Pharmacol Ther 2007 Dec;82(6):726-733.

15. Hua WJ, Hua WX, Fang HJ. The Role of OATP1B1 and BCRP in Pharmacokinetics and DDI of Novel Statins. Cardiovasc Ther 2011 May 25.

16. Sirtori CR, Mombelli G, Triolo M, Laaksonen R. Clinical response to statins: Mechanism(s) of variable activity and adverse effects. Ann Med 2011 May 31.

17. Romaine SP, Bailey KM, Hall AS, Balmforth AJ. The influence of SLCO1B1 (OATP1B1) gene polymorphisms on response to statin therapy. Pharmacogenomics J 2010 Feb;10(1):1-11.

18. Chasman DI, Giulianini F, MacFadyen J, Barratt BJ, Nyberg F, Ridker PM. Genetic determinants of statin-induced low-density lipoprotein cholesterol reduction: the Justification for the Use of Statins in Prevention: an Intervention Trial Evaluating Rosuvastatin (JUPITER) trial 2. Circ Cardiovasc Genet 2012 Apr 1;5(2):257-264.

19. Iusuf D, van de Steeg E, Schinkel AH. Functions of OATP1A and 1B transporters in vivo: insights from mouse models. Trends Pharmacol Sci 2012 Feb 1;33(2):100-108.

20. Ose A, Kusuhara H, Endo C, Tohyama K, Miyajima M, Kitamura S, et al. Functional characterization of mouse organic anion transporting peptide 1a4 in the uptake and efflux of drugs across the blood-brain barrier. Drug Metab Dispos 2010 Jan;38(1):168-176.

21. Degorter MK, Urquhart BL, Gradhand U, Tirona RG, Kim RB. Disposition of Atorvastatin, Rosuvastatin, and Simvastatin in Oatp1b2-/- Mice and Intraindividual Variability in Human Subjects. J Clin Pharmacol 2011 Dec 13.

22. van de Steeg E, Wagenaar E, van der Kruijssen CM, Burggraaff JE, de Waart DR, Elferink RP, et al. Organic anion transporting polypeptide 1a/1b-knockout mice provide insights into hepatic handling of bilirubin, bile acids, and drugs. J Clin Invest 2010 Aug;120(8):2942-2952.

23. Hobbs M, Parker C, Birch H, Kenworthy K. Understanding the interplay of drug transporters involved in the disposition of rosuvastatin in the isolated perfused rat liver using a physiologically-based pharmacokinetic model. Xenobiotica 2012 Apr;42(4):327-338.

24. van Herwaarden AE, Jonker JW, Wagenaar E, Brinkhuis RF, Schellens JH, Beijnen JH, et al. The breast cancer resistance protein (Bcrp1/Abcg2) restricts exposure to the dietary carcinogen 2-amino-1-methyl-6-phenylimidazo[4,5-b]pyridine. Cancer Res 2003 Oct 1;63(19):6447-6452.

25. van Waterschoot RA, van Herwaarden AE, Lagas JS, Sparidans RW, Wagenaar E, van der Kruijssen CM, et al. Midazolam metabolism in cytochrome P450 3A knockout mice can be attributed to up-regulated CYP2C enzymes. Mol Pharmacol 2008 Mar;73(3):1029-1036.

26. Bardelmeijer HA, Beijnen JH, Brouwer KR, Rosing H, Nooijen WJ, Schellens JH, et al. Increased oral bioavailability of paclitaxel by GF120918 in mice through selective modulation of P-glycoprotein. Clin Cancer Res 2000 Nov;6(11):4416-4421.

27. Gridelli B, Scanlon L, Pellicci R, LaPointe R, DeWolf A, Seltman H, et al. Cyclosporine metabolism and pharmacokinetics following intravenous and oral administration in the dog 20. Transplantation 1986 Mar;41(3):388-391.

28. Cheng X, Maher J, Chen C, Klaassen CD. Tissue distribution and ontogeny of mouse organic anion transporting polypeptides (Oatps). Drug Metab Dispos 2005 Jul;33(7):1062-1073.

29. Peng SX, Rockafellow BA, Skedzielewski TM, Huebert ND, Hageman W. Improved pharmacokinetic and bioavailability support of drug discovery using serial blood sampling in mice. J Pharm Sci 2009 May;98(5):1877-1884.

30. Varma MV, Rotter CJ, Chupka J, Whalen KM, Duignan DB, Feng B, et al. pH-sensitive interaction of HMG-CoA reductase inhibitors (statins) with organic anion transporting polypeptide 2B1. Mol Pharm 2011 Aug 1;8(4):1303-1313.

31. Bergman E, Lundahl A, Fridblom P, Hedeland M, Bondesson U, Knutson L, et al. Enterohepatic disposition of rosuvastatin in pigs and the impact of concomitant dosing with cyclosporine and gemfibrozil. Drug Metab Dispos 2009 Dec;37(12):2349-2358.

32. Yang CH, Glover KP, Han X. Characterization of cellular uptake of perfluorooctanoate via organic anion-transporting polypeptide 1A2, organic anion transporter 4, and urate transporter 1 for their potential roles in mediating human renal reabsorption of perfluorocarboxylates. Toxicol Sci 2010 Oct;117(2):294-302.

33. Schneck DW, Birmingham BK, Zalikowski JA, Mitchell PD, Wang Y, Martin PD, et al. The effect of gemfibrozil on the pharmacokinetics of rosuvastatin. Clin Pharmacol Ther 2004 May;75(5):455-463.

34. Simonson SG, Raza A, Martin PD, Mitchell PD, Jarcho JA, Brown CD, et al. Rosuvastatin pharmacokinetics in heart transplant recipients administered an antirejection regimen including cyclosporine. Clin Pharmacol Ther 2004 Aug;76(2):167-177.

35. Watanabe T, Kusuhara H, Maeda K, Shitara Y, Sugiyama Y. Physiologically based pharmacokinetic modeling to predict transporter-mediated clearance and distribution

of pravastatin in humans. J Pharmacol Exp Ther 2009 Feb;328(2):652-662.

36. Martin PD, Warwick MJ, Dane AL, Hill SJ, Giles PB, Phillips PJ, et al. Metabolism, excretion, and pharmacokinetics of rosuvastatin in healthy adult male volunteers. Clin Ther 2003 Nov;25(11):2822-2835.

37. Nezasa K, Takao A, Kimura K, Takaichi M, Inazawa K, Koike M. Pharmacokinetics and disposition of rosuvastatin, a new 3-hydroxy-3-methylglutaryl coenzyme A reductase inhibitor, in rat. Xenobiotica 2002 Aug;32(8):715-727.

38. Iusuf D, Sparidans RW, van Esch A, Hobbs M, Kenworthy K, van de Steeg E, et al. Organic anion-transporting polypeptides 1a/1b control the hepatic uptake of pravastatin in mice. Mol Pharm 2012 Jul 19.

39. Nezasa K, Higaki K, Takeuchi M, Nakano M, Koike M. Uptake of rosuvastatin by isolated rat hepatocytes: comparison with pravastatin. Xenobiotica 2003 Apr;33(4):379-388.

40. Pasanen MK, Neuvonen PJ, Niemi M. Global analysis of genetic variation in SLCO1B1. Pharmacogenomics 2008 Jan;9(1):19-33.

## *Supplemental data*

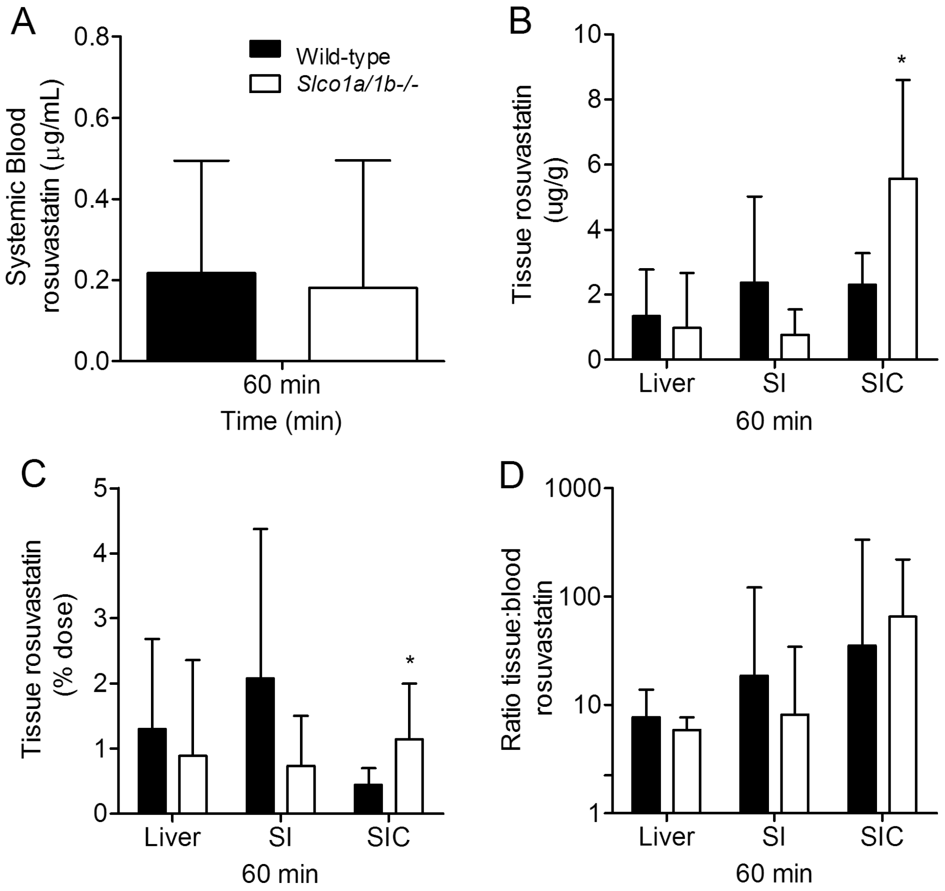

**Supplemental Figure 1.** Role of Oatp1a/1b in the disposition of rosuvastatin in gall bladder-cannulated mice after intravenous administration (5 mg/kg) to wild-type and *Slco1a/1b*(-/-) mice. (A) Rosuvastatin blood concentrations (µg/mL). Liver, small intestinal wall (SI) and content (SIC) in (B) (µg/g) and (C) % of dose. (D) Liver, small intestinal wall, and small intestinal content to blood ratios. Data are presented as mean ± SD (n = 6-7, *, $P < 0.05$; **, $P < 0.01$; ***, $P < 0.001$ when compared with wild-type).

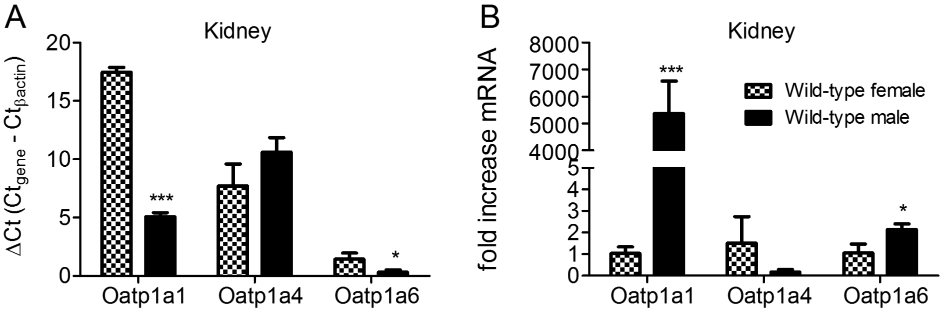

**Supplemental Figure 2.** Kidney Oatp1a expression in male and female wild-type mice. (A) ΔCt values of the RT-PCR analysis. Analysis of the results was done by the comparative Ct method. Quantification of the target cDNAs in all samples was normalized against the endogenous control Gapdh (Cttarget − CtGapdh = ΔCt). Accordingly, the lower the ΔCt value, the higher the expression level. Note that ΔCt values between different genes/primer sets cannot be used to assess relative expression levels between different genes. (B) Fold difference in mRNA expression levels in male wild-type mice relative to values in female wild-type. Data are presented as mean ± S.D (n =3) (*, *P* < 0.05; ***, *P* < 0.001 when compared with female wild-type values).

# *Role of Oatp1a/1b transporters in the pharmacokinetics of anticancer drugs*

# 4

# OATP1A/1B transporters affect irinotecan and SN-38 pharmacokinetics and carboxylesterase expression in knockout and humanized transgenic mice

# 4.1

Dilek Iusuf[1], Marion Ludwig[1], Ahmed Elbatsh[1],
Anita van Esch[1], Evita van de Steeg[1], Els Wagenaar[1],
Martin van der Valk[2], Fan Lin[3], Olaf van Tellingen[3]
and Alfred H. Schinkel[1]

[1]Division of Molecular Oncology,
[2]Department of Animal Pathology,
[3]Department of Clinical Chemistry,
The Netherlands Cancer Institute, Amsterdam, The Netherlands

*Submitted for publication*

# Abstract

Organic anion-transporting polypeptides (OATPs) mediate the hepatic uptake of many drugs, thus co-determining their clearance. Impaired hepatic clearance due to low-activity polymorphisms in human OATP1B1 may increase systemic exposure to SN-38, the active and toxic metabolite of the anticancer pro-drug irinotecan. We investigated the pharmacokinetics and toxicity of irinotecan and SN-38 in Oatp1a/1b-null mice: plasma exposure of irinotecan and SN-38 was increased 2-3 fold after irinotecan dosing (10 mg/kg, i.v.) compared to wild-type mice. Also, liver-to-plasma ratios were significantly reduced, suggesting impaired hepatic uptake of both compounds. After 6 daily doses of irinotecan, Oatp1a/1b-null mice suffered from increased toxicity. However, Oatp1a/1b-null mice had increased levels of carboxylesterase (Ces) enzymes, which caused higher conversion of irinotecan to SN-38 in plasma, potentially complicating pharmacokinetic analyses. Ces inhibitors blocked this increased conversion. Interestingly, liver-specific humanized OATP1B1 and OATP1B3 transgenic mice had normalized hepatic expression of *Ces1* genes. Whereas irinotecan liver-to-plasma ratios in these humanized mice were similar to those in Oatp1a/1b-null mice, SN-38 liver-to-plasma ratios returned to wild-type levels, suggesting that human OATP1B proteins mediate SN-38, but not irinotecan uptake *in vivo*. Upon direct administration of SN-38 (1 mg/kg, i.v.), Oatp1a/1b-null mice had increased SN-38 plasma levels, lower liver concentrations and decreased cumulative biliary excretion of SN-38. Conclusion: Mouse Oatp1a/1b transporters have a role in the plasma clearance of irinotecan and SN-38, while human OATP1B transporters may only affect SN-38 disposition. Oatp1a/1b-null mice have increased expression and activity of Ces1 enzymes, while humanized mice provide a rescue of this phenotype.

# Introduction

Organic anion-transporting polypeptides (human: OATPs; rodents: Oatps; gene names: *SLCO*, *Slco*) are uptake transporters which mediate the cellular uptake of various endogenous and exogenous compounds [1]. Members of the OATP1A/1B subfamilies are of interest for their impact on the pharmacokinetics and hence the therapeutic efficacy of many drugs due to their tissue localization (liver, small intestine, and kidney) and wide substrate specificity. In the liver, human OATP1B1 and OATP1B3 and mouse Oatp1a1, -1a4 and -1b2 are expressed on the basolateral membrane of hepatocytes, where they mediate the hepatic uptake, and therefore the clearance of many (anticancer) drugs [2, 3].

Irinotecan (CPT-11) is an anticancer drug, widely used in the treatment of colorectal, ovarian and lung cancer [4]. Irinotecan's therapeutic index is quite low, mainly due to its complex pharmacokinetics which involves many metabolic enzymes and drug transporters [5]. The pro-drug irinotecan is hydrolyzed to its primary pharmacologically active (cytotoxic) metabolite, SN-38, mostly by carboxylesterase enzymes (CES in humans; Ces in mice), mainly in liver, but also in plasma and small intestine [4]. Uptake into the liver might be mediated by OATP1B transporters, because SN-38 has been described as an OATP1B1 and OATP1B3 substrate *in vitro,* whereas the pro-drug irinotecan did not appear to be a substrate of these transporters *in vitro* [6-8]. In the liver, SN-38 is further metabolized by UGT1A1 to an inactive form, SN-38 glucuronide. Both SN-38 and its glucuronide can be excreted into the bile, mainly by ABCC2 and ABCB1, and to a lesser extent by ABCG2 [5, 9, 10].

Severe unpredictable toxicities, mainly diarrhea and neutropenia, limit irinotecan's therapeutic use. The incidence of toxic effects correlates well with higher systemic exposure to SN-38[10]. Alterations in the activity of metabolizing enzymes and transporters regulating the pharmacokinetics of SN-38 can lead to increased toxicity. Indeed, low-activity polymorphic variants of OATP1B1, which lead to impaired hepatic clearance of irinotecan and/or SN-38, are associated with higher exposure to SN-38 and life-threatening toxicity [11-14]. The risk of toxicity may be even greater for individuals with a complete deficiency of OATP1B1 or OATP1B3 which probably occur at a significant frequency as well as the very rare Rotor syndrome patients, which are deficient in both OATP1B1 and OATP1B3 [15, 16].

Several single (Oatp1b2, Oatp1a1, Oatp1a4) and combined Oatp1a/1b knockout mouse strains are available and these have provided valuable insights into the physiological and pharmacological functions of OATP1A/1B transporters [3]. In addition, liver-specific humanized OATP1A/1B transgenic mice have been recently characterized and they are excellent tools to study the functions of human OATP1A/1B transporters *in vivo* [17]. Here, we aimed to investigate the impact of mouse and human OATP1A/1B transporters on pharmacokinetics and toxicity of irinotecan and SN-38 *in vivo* using Oatp1a/1b knockout mice and liver-specific humanized OATP1B transgenic mice.

# Materials and methods

### *Animals*

Mice were housed in small groups in a temperature-controlled environment with a 12-hour light/ 12-hour dark cycle. They received a standard diet (AM-II; Hope Farms) and acidified water *ad libitum*. All mouse experiments complied with Dutch legislation. Female wild-type, *Slco1a/1b(-/-)* (Oatp1a/1b knockout), *Slco1a/1b(-/-);1B1(tg)* and *Slco1a/1b(-/-);1B3(tg)* (liver-specific OATP1B1 and OATP1B3 humanized transgenic) mice of comparable genetic background (>99% FVB) between 8 and 14 weeks of age were used [17].

### *Chemicals and reagents*

Irinotecan (Irinotecan HCl-trihydrate) was from Hospira Benelux BVBA (Brussels, Belgium). SN-38 was purchased from Sequoia Research Products (Pangbourne, UK). Bis(4-nitrophenyl) phosphate (BNPP) and simvastatin lactone were from Sigma-Aldrich (Steinheim, Germany), isoflurane (Forane) from Abbott Laboratories (Queenborough, Kent, UK) and heparin (5,000 IE/ml) was from Leo Pharma BV (Breda, The Netherlands). Bovine serum albumin (BSA), Fraction V was from Roche (Mannheim, Germany) and drug-free human plasma was obtained from healthy volunteers. Tetra-n-butylammonium bromide (TBABr) was from Merck Schuchardt (Hohenbrunn, Germany). All other reagents were obtained from Sigma-Aldrich (Steinheim, Germany).

### *Plasma and tissue pharmacokinetic experiments*

Irinotecan (20 mg/mL in water-based solution containing NaOH, lactic acid and sorbitol) was diluted with saline (to 2 mg/mL) for administration of 10 mg/kg; 5 μl/g bodyweight were administered intravenously to mice. SN-38 was dissolved in DMSO (1 mg/mL) and 1 μl/g body weight was administered intravenously to mice to achieve a dosage of 1 mg/kg. The experiments were terminated by isoflurane anaesthesia, heparin-blood sampling by cardiac puncture followed by cervical dislocation and tissue collection. Blood samples were centrifuged at 5,200g for 5 min at 4°C and plasma was collected and stored at -30°C until analysis.

### *Drug analysis*

Concentrations of irinotecan and its metabolite SN-38 in plasma, organs (homogenized in appropriate volumes of ice-cold 4% (w/v) BSA) and bile (diluted 10-100-fold with human blank plasma) were determined by HPLC analysis as previously described [18]. Because irinotecan and SN-38 have different molecular weights, we expressed the plasma concentrations in μM.

### *Toxicity studies*

For this experiment, individually housed mice received a daily dose of 30 mg/kg irinotecan intravenously for 6 days. Mice were checked daily for changes in body weight, general appearance and incidence of diarrhea. One day prior to, and 24 hours after the last administration, blood for hematological and drug analysis was isolated from the tail vein. Under isoflurane anaesthesia, the mice were sacrificed by cervical dislocation and several organs (small intestine, stomach, spleen, sternum and extremities) were collected for histological analysis.

### *Hematological analysis*

Hemoglobin level, hematocrit, mean corpuscular volume, red and white blood cells, and platelet counts were analyzed in peripheral blood on a Beckman Coulter analyzer (Florida, US).

### *Histological analysis*

Isolated tissues and organs were handled as described previously and hematoxylin and eosin (H& E) stained sections were analyzed for pathological changes as previously described [19].

### *Ex vivo carboxylesterase activity measurement and inhibition of carboxylesterase activity*

Esterase activity in mouse plasma was measured by monitoring *in vitro* conversion of irinotecan to SN-38 using previously described methods with slight modifications [20]. In short, 50 µl 1 mM irinotecan was mixed with 950 µl 20 mM Tris-HCl buffer (pH 7.5) in a 1.5 ml microcentrifuge tube and incubated at 37°C for 30 min to reach equilibrium between the lactone and carboxylate forms of irinotecan. 540 µl fresh plasma collected from wild-type and *Slco1a/1b(-/-)* mice (n = 3) was mixed with 60 µl of the irinotecan solution (50 µM) (final irinotecan concentration 5 µM) and the mixtures were kept at 37 °C with shaking. At 1, 3, 5, 10, 15, 30, 60, 120 and 240 minutes, 60 µl samples were collected for the determination of irinotecan and SN-38 concentrations. For the inhibition experiment, the non-specific CES inhibitor BNPP [21] (1 mM), the human CES1 and CES2 inhibitor simvastatin (100 µM) [22], BNPP vehicle (0.5% DMSO in water), and simvastatin vehicle (0.5% polysorbate 80 and 0.5% ethanol in water) were preincubated in mouse plasma for 15 min at 37 °C. Reactions were started by adding irinotecan (5 µM) and stopped after 60 min by putting the samples on dry ice. Sample pretreatment and drug analysis were as described above.

### *RNA isolation, cDNA synthesis and RT-PCR*

RNA isolation from mouse liver, kidney, and small intestine and subsequent cDNA synthesis and RT-PCR were performed as described [23]. Specific primers (QIAGEN, Hilden, Germany) were used to detect expression levels of the following mouse esterase genes: *Ces1b, Ces1c, Ces1d, Ces1e, Ces1f, Ces1g, Ces2a, Ces2e, Ces3a, Ces3b, Aadac, Pon1, Pon2, Pon3* and *Bche* [23].

### *Pharmacokinetic and statistical analysis*

Averaged plasma concentrations for each time point were used to calculate the area under the blood concentration versus time curve (AUC) from t = 0 to the last sampling time point by the linear trapezoidal rule; S.E. was calculated by the law of propagation of errors [24].

The two-sided unpaired Student's *t*-test was used throughout the study to assess the statistical significance of differences between two sets of data. Statistical significance of differences between wild-type and *Slco1a/1b(-/-)*, *Slco1a/1b(-/-);1B1(tg)* or *Slco1a/1b(-/-);1B3(tg)* or between *Slco1a/1b(-/-)* mice and *Slco1a/1b(-/-);1B1(tg)* or *Slco1a/1b(-/-);1B3(tg)* mice was assessed by one-way ANOVA followed by Dunett's multiple comparison test. Results are presented as the means ± S.D. Differences were considered to be statistically significant when $P < 0.05$.

## Results

### *Altered disposition of irinotecan and SN-38 in Oatp1a/1b-null mice*

We assessed the role of Oatp1a/1b transporters in the disposition of irinotecan and SN-38 after intravenous administration of 10 mg/kg irinotecan to wild-type and *Slco1a/1b(-/-)* mice. Absence of Oatp1a/1b transporters resulted in significantly increased plasma concentrations of irinotecan and SN-38 at almost all the time points after administration (Figure 1A, B), suggesting a role for Oatp1a/1b transporters in the plasma clearance of irinotecan and SN-38. At 30 min after administration, irinotecan plasma concentrations in *Slco1a/1b(-/-)* mice were 1.9-fold higher than in the wild-type mice (1.89 μM versus 1.01 μM, respectively, Figure 1A), while SN-38 plasma concentrations of *Slco1a/1b(-/-)* mice were 8-fold higher compared with wild-type mice (0.4 μg/ml versus 0.05 μg/ml, respectively, Figure 1B). Overall plasma exposure ($AUC_{(5\text{-}240)}$) of irinotecan was 1.7-fold higher in Oatp1a/1b knockout mice versus wild-type mice (209.8 ± 6.7 versus 120.9 ± 4.4 μM·min, $P < 0.01$), and 2.9-fold higher for SN-38 (50 ± 2.9 versus 12 ± 2 μM·min, $P < 0.001$). The fraction of SN-38 recovered in the plasma represented ~10% of the irinotecan fraction in plasma of wild-type mice, and ~23% in plasma of Oatp1a/1b knockout mice.

Oatp1a/1b uptake transporters control the plasma clearance of many compounds mainly by mediating their liver uptake. There was a slight trend of lower irinotecan and SN-38 liver concentrations in Oatp1a/1b knockout than in wild-type mice, though the differences were mostly not significant (Figure 1C, D). However, liver-to-plasma ratios of both irinotecan and SN-38 were markedly and significantly lower in *Slco1a/1b(-/-)* than in wild-type mice at most time points (Figure 1E, F), suggesting an impaired liver uptake of both compounds in the absence of Oatp1a/1b transporters. We also measured the small intestinal tissue and content concentrations of irinotecan and SN-38 and as the profile of the data was very similar between the two matrices, we present them together (Supplemental Figure 1). Here, we observed a similar pattern as for the liver data, with little differences in absolute drug concentrations and intestinal-to-plasma ratios of both irinotecan and SN-38 lower in Oatp1a/1b knockout mice than in the wild-type. In the kidney, irinotecan concentrations were very similar between the two strains of mice and the kidney-to-plasma ratios of irinotecan significantly decreased in the Oatp1a/1b knockout mice from 30 min onwards, reflecting the higher plasma concentrations in the Oatp1a/1b-null mice (Supplemental Figure 2A, C). Interestingly, SN-38 kidney concentrations were significantly higher in Oatp1a/1b knockout mice than wild-type mice from the first time point on (5 min) (Supplemental Figure 2B). This might be a reflection of the consistently higher SN-38 plasma concentrations in *Slco1a/1b(-/-)* than in wild-type mice (Figure 1B). Indeed, the kidney-to-plasma ratios of SN-38 showed significantly lower values in Oatp1a/1b-null than in wild-type mice, suggesting that relative SN-38 uptake into the kidney was in fact reduced in the knockout mice (Supplemental Figure 2D).

### *Increased systemic toxicity in Oatp1a/1b knockout mice after repeated irinotecan administration*

In patients, low-activity polymorphisms in genes encoding OATP1B1 are associated with increased toxicity due to increased plasma concentrations of SN-38 [5, 25]. We therefore investigated if

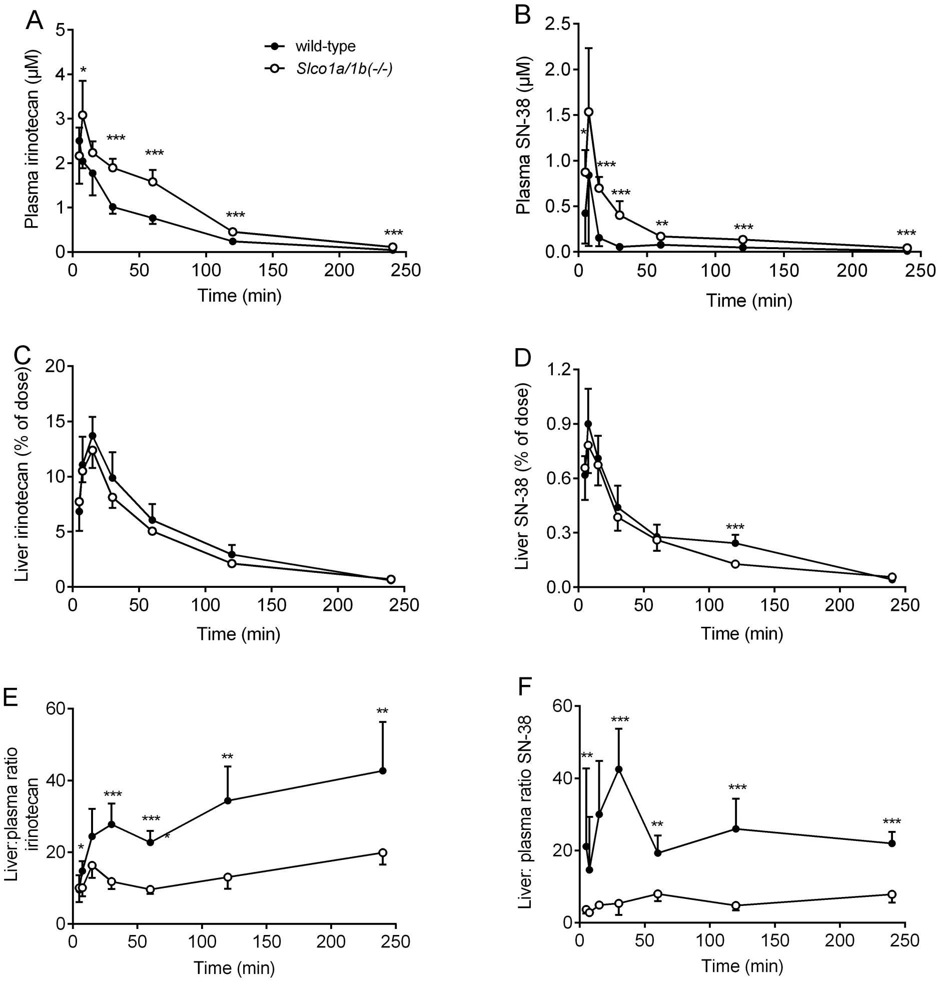

**Figure 1.** Role of Oatp1a/1b uptake transporters in the plasma and liver exposure of irinotecan and SN-38 after intravenous administration of irinotecan (10 mg/kg) to female wild-type and Oatp1a/1b knockout mice. Plasma concentrations of (A) irinotecan and (B) SN-38. Liver concentrations (as % of dose) of (C) irinotecan and (D) SN-38. Liver-to-plasma ratios of (E) irinotecan and (F) SN-38. Data are presented as mean ± S.D. (n = 5-6, *, $P < 0.05$; **, $P < 0.01$; ***, $P < 0.001$ when compared with wild-type).

Oatp1a/1b knockout mice suffer from more toxicity after 6 daily administrations of 30 mg/kg intravenous irinotecan. Up to day 3-4, the loss in body weight was similar between the two strains (~5 %), after which wild-type mice did not lose additional body weight, whereas Oatp1a/1b knockout mice continued to lose significantly more body weight (a cumulative ~10% by the last day) (Figure 2A). Although both strains suffered from neutropenia (lower white blood cells counts) on day 7, this was more pronounced for the Oatp1a/1b-null mice. Wild-type mice had 42% reduced white blood cell counts, but Oatp1a/1b-null mice had 72% reduced white blood cell counts (Figure 2B). These effects were probably a consequence of the increased SN-38 systemic

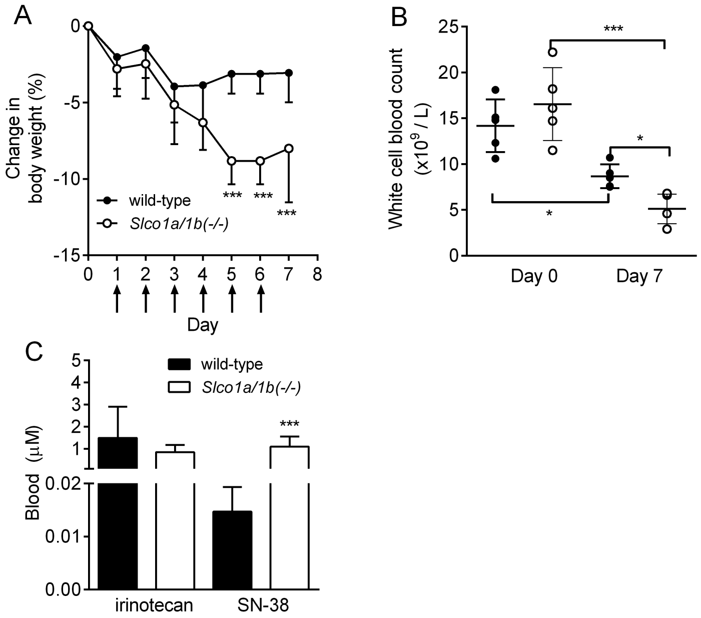

**Figure 2.** Role of Oatp1a/1b uptake transporters in irinotecan-induced toxicity after administration of irinotecan (30 mg/kg i.v. daily) for 6 days to female wild-type and Oatp1a/1b knockout mice. (A) Changes in body weight (as % of difference in comparison with the weight on day 0) measured daily. Arrows below the X-axis indicate irinotecan administrations. (B) White blood cell count on day 0 and day 7 of the experiment. (C) Blood concentrations of irinotecan and SN-38 on day 6 of the experiment (6 hours after the last administration). Data are presented as mean ± S.D. (n = 5-6, *, $P < 0.05$; **, $P < 0.01$; ***, $P < 0.001$ when compared with wild-type).

exposure in Oatp1a/1b-null mice, which had 75-fold higher SN-38 trough blood concentrations at 24 hours after the last administration (0.015 μM in wild-type mice versus 1.10 μM in Oatp1a/1b-null mice, $P < 0.001$) (Figure 2C), whereas differences for irinotecan were not significant.

Accordingly, pathological examination performed 24 hours after the last administration revealed more toxicity in the bone marrow, thymus and small intestine of Oatp1a/1b knockout mice (Figure 3). We compared untreated wild-type mice (Figure 3A, D, G), with treated wild-type (Figure 3B, E, H) and treated Oatp1a/1b knockout mice (Figure 3C, F, I). Tissues of untreated Oatp1a/1b knockout mice were similar to untreated wild-type tissues. When comparing bone marrow (dark blue cells) in sternum sections (Figure 3B versus 3C), it was clear that Oatp1a/1b knockout mice had severe depletion of the bone marrow and dilatation of blood vessels, which is in line with the more severe neutropenia observed (Figure 2B). In normal healthy thymus, the cortex (dark blue cells on the rim) is densely populated with rapidly proliferating cells (Figure 3D). When treated, both wild-type and Oatp1a/1b knockout mice suffered from a depletion of the cortex, but this was more severe in the knockout mice (Figure 3E versus 3F). We found the most striking difference in the small intestine. In the untreated mice the architecture of the small intestine was normal (Figure 3G). In the treated wild-type mice, there is a partial depletion of cells in the villi, which lead to an altered architecture of the small intestine (Figure 3H). In the knockout mice, we observed severe toxicity with many

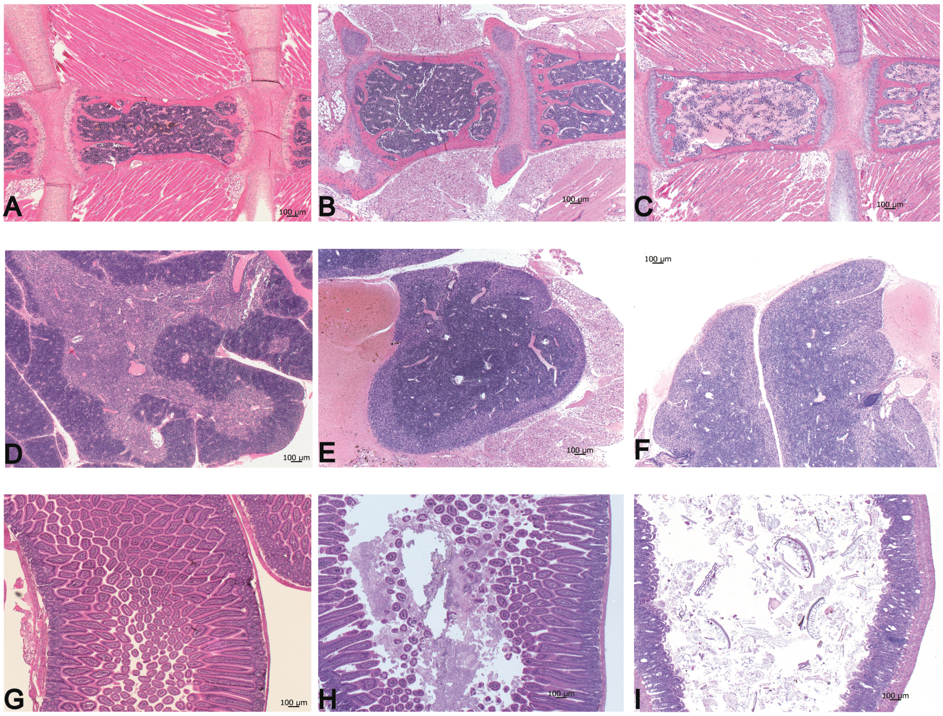

**Figure 3.** Role of Oatp1a/1b uptake transporters in irinotecan/SN-38-induced toxicity after administration of irinotecan (30 mg/kg i.v. daily) for 6 days to female wild-type and Oatp1a/1b knockout mice assessed with microphotographs of H&E sections of tissues. Untreated wild-type mice: (A) the bone marrow with high density of cells (dark blue), (D) thymus with high number of proliferating cells in the cortex (outer rim filled with dark blue cells) and (G) the small intestine with intact villi. Irinotecan-treated wild-type mice: (B) minor depletion of the bone marrow, (E) moderate depletion of the cortex in the thymus and (H) moderate toxicity in the small intestine, with shortened villi. Irinotecan-treated Oatp1a/1b knockout mice: (C) severe depletion of bone marrow, (F) severe depletion of the cortex in the thymus and (I) severe toxicity in the small intestine with very short or absent villi and apoptotic cells. Tissues for the treated mice were isolated at 24 hours after the last administration.

apoptotic cells and drastically shortened or absent villi in the Oatp1a/1b-null mice, together with an increased number of leukocytes (Figure 3I versus H).

### *Increased plasma conversion of irinotecan to SN-38 in Oatp1a/1b knockout mice*

After 6 consecutive administrations of irinotecan, only the SN-38 trough concentrations were increased in the knockout mice, but not the irinotecan concentrations (Figure 2C). We wondered what could explain this higher accumulation of SN-38 in knockout mice. We therefore evaluated the *in vitro* conversion of irinotecan to SN-38 in freshly isolated plasma from wild-type and Oatp1a/1b knockout mice. Surprisingly, we found that this conversion was very slow in wild-type plasma, but highly increased in the Oatp1a/1b knockout plasma (Figure 4A). In plasma from Oatp1a/1b knockout mice, irinotecan was rapidly converted to SN-38, with as early as 10 minutes ~48% of irinotecan converted to SN-38, while in the wild-type mice, this fraction was negligible, only ~0.2%. By 60 minutes nearly all irinotecan was transformed to SN-38 in the knockout mice (88%). In contrast, in wild-type plasma the amount of SN-38 was 125-fold lower (0.7%) (Figure 4A). The conversion of irinotecan to SN-38 can be mediated by plasma (carboxyl)esterases, which are generally much more abundant in mouse plasma than in human plasma [26-28].

### *Several Ces1 genes are upregulated in Oatp1a/1b knockout mice*

Conversion of irinotecan to SN-38 can be mediated by several esterases [29], which are usually synthesized in the liver, but some also in the small intestine and kidney [26, 30]. Therefore, we tested expression levels by RT-PCR of all obvious candidate carboxylesterase, paraoxonase and butyrylcholinesterase genes [31] in the liver, small intestine and kidney of wild-type and Oatp1a/1b knockout, but also of liver-specific humanized OATP1B1 and OATP1B3 transgenic mice (Figure 4C, D, E and Supplemental Table 1-3). The latter can display a rescue of phenotypic changes caused by deletion of the Oatp1a/1b genes [17].

Several members of the Ces1 family were highly upregulated in the livers of Oatp1a/1b knockout relative to wild-type mice: *Ces1b* (10-fold), *Ces1c* (80-fold), *Ces1d* (90-fold) and *Ces1e* (10-fold) (Figure 4C). Expression levels of other esterases, including *Ces2a* and butylcholinesterase (*Bche*) [32], an enzyme present in both human and mouse plasma which is thought to play a role in the conversion of irinotecan to SN-38, were unchanged in Oatp1a/1b knockout or transgenic mice (Supplemental Table 1-3).

The high upregulation of Ces1 genes was surprising because a previous analysis of changes in gene expression of several metabolizing enzymes and influx and efflux drug transporters in Oatp1a/1b knockout mice had revealed very few changes in comparison with wild-type mice, although Ces genes were not directly tested [17]. Also a genome wide RNA microarray screen had not identified significant changes in Ces genes. Interestingly, OATP1B1- and OATP1B3-humanized transgenic mice had strongly reduced mRNA levels of the enzymes that were upregulated in the Oatp1a/1b knockout mice, back to, or even below, the wild-type levels (Figure 4C, Supplemental Table 1). In the small intestine, *Ces1d* was highly upregulated (~2700-fold, albeit from an extremely low baseline expression level) and *Ces1e* ~6-fold, but *Ces1b* and *Ces1c* were unchanged (Figure 4D, Supplemental Table 2). In the humanized mice, the expression of these genes was again roughly back to wild-type levels (Figure 4D). Note that even the highly upregulated *Ces1d* RNA levels in small intestine were still quite low in terms of absolute expression and relative to liver expression, making it unlikely that this would have much functional impact (Supplemental Table 2). In the kidney there was a similar pattern, with primarily *Ces1d*, but not *Ces1b* or *Ces1c*, highly upregulated in the Oatp1a/1b knockout mice and much reduced in the humanized mice (Figure 4E, Supplemental Table 3).

Collectively, these data suggest that one or more of the upregulated Ces1 enzymes is responsible for the conversion of irinotecan to SN-38 in Oatp1a/1b knockout mice.

### *Increased conversion of irinotecan to SN-38 in plasma can be completely inhibited by BNPP and partially by simvastatin*

To further corroborate the involvement of Ces1 enzymes in the increased conversion of irinotecan to SN-38 in plasma of Oatp1a/1b knockout mice, we investigated if this conversion could be inhibited by BNPP, a general (carboxyl-)esterase inhibitor [21], and simvastatin, a human

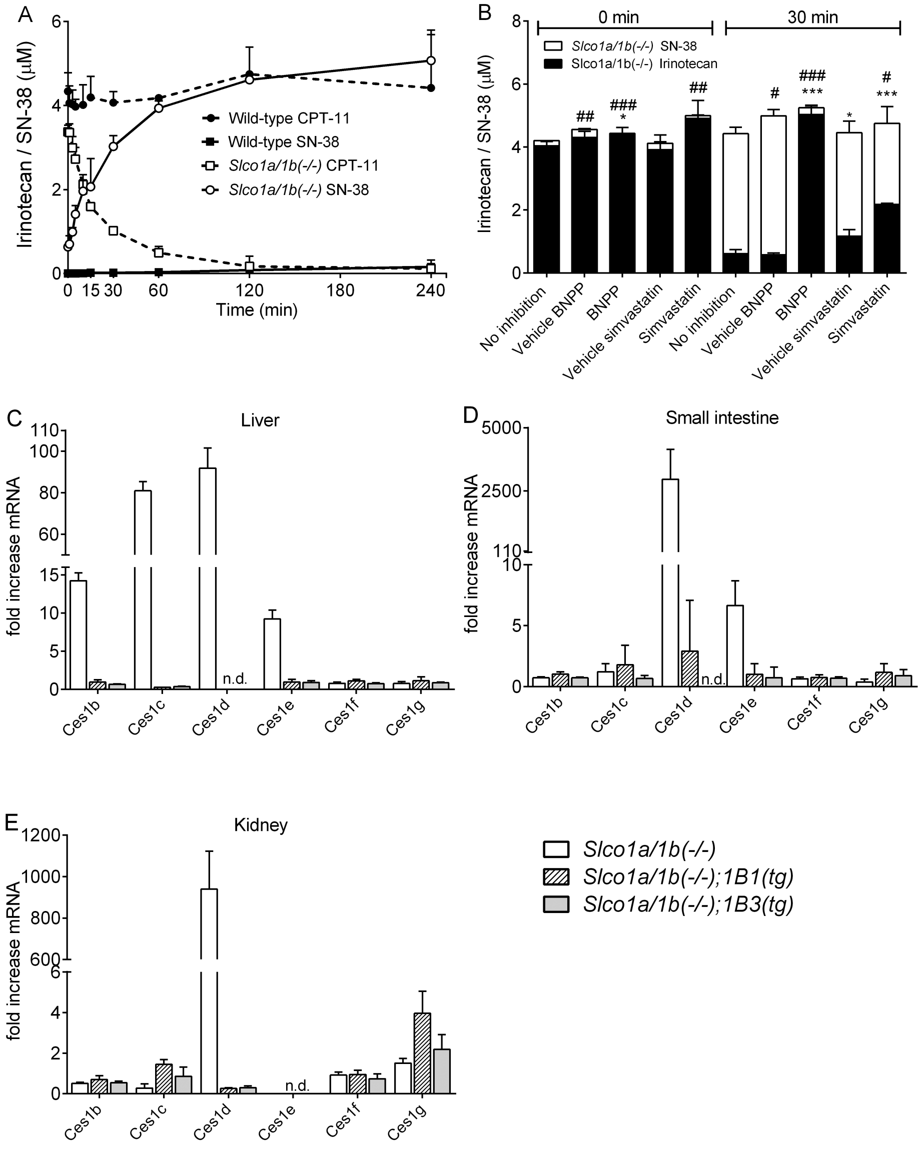

**Figure 4.** Oatp1a/1b knockout mice have higher *in vitro* carboxylesterase activity (A, B) and expression of Ces enzymes (C, D, E). (A) Concentrations of irinotecan (dashed lines) and SN-38 (black lines) over time after addition of irinotecan (5 μM) to freshly isolated wild-type plasma (black symbols) and Oatp1a/1b knockout plasma (white symbols) (B) Cumulative concentrations of irinotecan (black bars) and SN-38 (white bars) in plasma isolated from female Oatp1a/1b knockout mice after addition of irinotecan (5 μM) with or without inhibitors at 0 and 30 minutes. Total bar height indicates the sum of irinotecan and SN-38 concentrations. Data are presented as mean ± S.D (n = 3, *, $P < 0.05$; ***, $P < 0.001$ for irinotecan and #, $P < 0.05$; ##, $P < 0.01$; ###, $P < 0.001$ for SN-38 when compared with no inhibition condition). (C, D, E), *Ces1* family gene mRNA expression measured by RT-PCR. Results are expressed as the fold change in expression of murine *Ces1* genes in female Oatp1a/1b knockout mice and transgenic mice with liver-specific expression of OATP1B1 and OATP1B3 in liver, small intestine and kidney relative to wild-type mice. Data are presented as mean ± S.D. (n=3). n.d.: not detectable.

CES1 and CES2 inhibitor [22]. We incubated irinotecan (5 µM) in Oatp1a/1b knockout plasma for 30 minutes with BNPP (1 mM) or simvastatin (100 µM) and measured the disappearance of irinotecan and formation of SN-38. In wild-type plasma there was hardly any conversion of irinotecan to SN-38 (Figure 4A), and preincubation with inhibitors did not have an additional effect on the formation of SN-38 (data not shown). In contrast, in Oatp1a/1b knockout plasma, after 30 minutes, ~75% of irinotecan was converted to SN-38, and this conversion was almost completely inhibited by BNPP, while simvastatin had a modest inhibitory capacity (1.5-fold) (Figure 4B). Note that the vehicle of simvastatin (water containing 0.5% polysorbate 80 and 0.5% ethanol) also had a minor inhibitory effect (Figure 4B). These inhibition experiments support that one or more of the upregulated carboxylesterase (Ces1) enzymes are responsible for the conversion of irinotecan to SN-38 in Oatp1a/1b knockout mouse plasma.

### *Role of human OATP1B1 and OATP1B3 in disposition of irinotecan and SN-38 after irinotecan administration*

Increased Ces1 activity in plasma of Oatp1a/1b knockout mice obviously complicates pharmacokinetic studies with irinotecan. Humanized transgenic mice, with roughly normal levels of the main Ces enzymes, might be more suitable for studying the impact of OATP1B transporters on the liver uptake of irinotecan and SN-38. Therefore, in an independent experiment, we administered irinotecan (10 mg/kg i.v.) to these mice (and also to wild-type and knockout mice) and evaluated the plasma and liver levels at 15 and 60 minutes (Figure 5).

Plasma levels of irinotecan were significantly higher in the liver-specific OATP1B1 or OATP1B3 humanized mice than in wild-type mice, both at 15 and 60 minutes (Figure 5A). Also liver-to-plasma ratios were significantly decreased in the humanized mice in comparison with wild-type mice, suggesting an impaired liver uptake (Figure 5E). These results show that in the humanized mice, irinotecan could not be cleared as efficiently as in the wild-type mice. This suggests that single human OATP1B1 or OATP1B3 cannot mediate efficient liver uptake of irinotecan *in vivo*. The data also suggest that one or more of the deleted mouse hepatic Oatp1a/1b transporters (Oatp1a1, -1a4 and -1b2) can mediate efficient irinotecan uptake, since replacement of mouse Oatp1a/1b with human OATP1B1 or OATP1B3 resulted in significantly increased plasma levels and decreased liver-to-plasma ratios in comparison with wild-type mice, whereas the *Ces1* expression between these strains was similar.

In contrast, plasma levels of SN-38 were similar between humanized and wild-type mice, and significantly decreased in comparison with the Oatp1a/1b knockout mice (Figure 5B). In view of the normalized *Ces1* expression in the humanized mice, this suggests that human OATP1B1 and OATP1B3 can efficiently clear SN-38 from the plasma, to a similar extent as the Oatp1a/1b transporters in the wild-type mice. Also the liver-to-plasma ratios of SN-38 support this, indicating an equal relative liver uptake in the wild-type and the humanized mice, and an impaired liver uptake in the Oatp1a/1b knockout mice (Figure 5F).

### *Impact of mouse OATPs on SN-38 disposition after direct administration of SN-38*

We next studied the impact of mouse Oatp1a/1b transporters on the disposition of SN-38 after its direct administration in order to bypass the increased formation of SN-38 by upregulated Ces1 enzymes in these mice. Shortly after administration (3 min) of SN-38 (1 mg/kg i.v.),

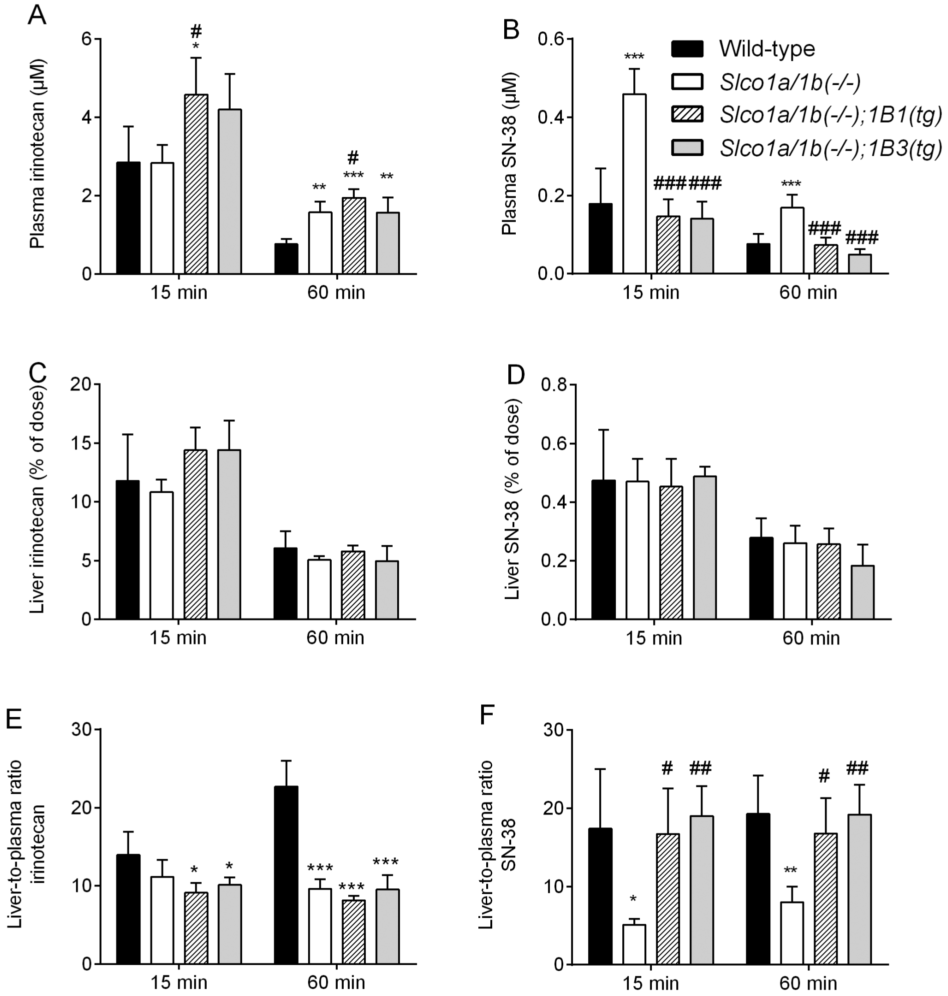

**Figure 5.** Role of human OATP1B1/1B3 uptake transporters in the pharmacokinetics of irinotecan and SN-38 after intravenous administration of irinotecan (10 mg/kg) to female wild-type, Oatp1a/1b knockout and OATP1B1 and OATP1B3 humanized transgenic mice. Plasma concentrations of (A) irinotecan and (B) SN-38. Liver concentrations (as % of dose) of (C) irinotecan and (D) SN-38. Liver-to-plasma ratio of (E) irinotecan and (F) SN-38 at various time points. Data are presented as mean ± SD (n = 4-5, *, $P < 0.05$; **, $P < 0.01$ ; ***, $P < 0.001$ when compared with wild-type; #, $P < 0.05$; ##, $P < 0.01$; ###, $P < 0.001$ when compared with *Slco1a/1b(-/-)*).

Oatp1a/1b knockout mice had modestly, but significantly increased plasma levels of SN-38 (Figure 6A). In the same mice, liver levels were significantly reduced at 5 min after SN-38 dosing (Figure 6B, C). Liver-to-plasma ratios at various time points were also lower in the absence of Oatp1a/1b transporters, suggesting an impaired liver uptake of SN-38 shortly after intravenous dosing (Figure 6D). An impaired early liver uptake of SN-38 was also obvious in an independent experiment, from the reduced cumulative biliary excretion of SN-38 in gall-bladder cannulated mice, which were also dosed with SN-38 (1 mg/kg) (Figure 6E, F). These results further support that mouse hepatic Oatp1a/1b transporters have a role in the disposition of SN-38. However, it should be noted that these experiments were technically challenging due to the extremely poor solubility of SN-38, which necessitated direct i.v. administration in a small volume of DMSO. This may have contributed to the high experimental variation evident in Figure 6 B-F.

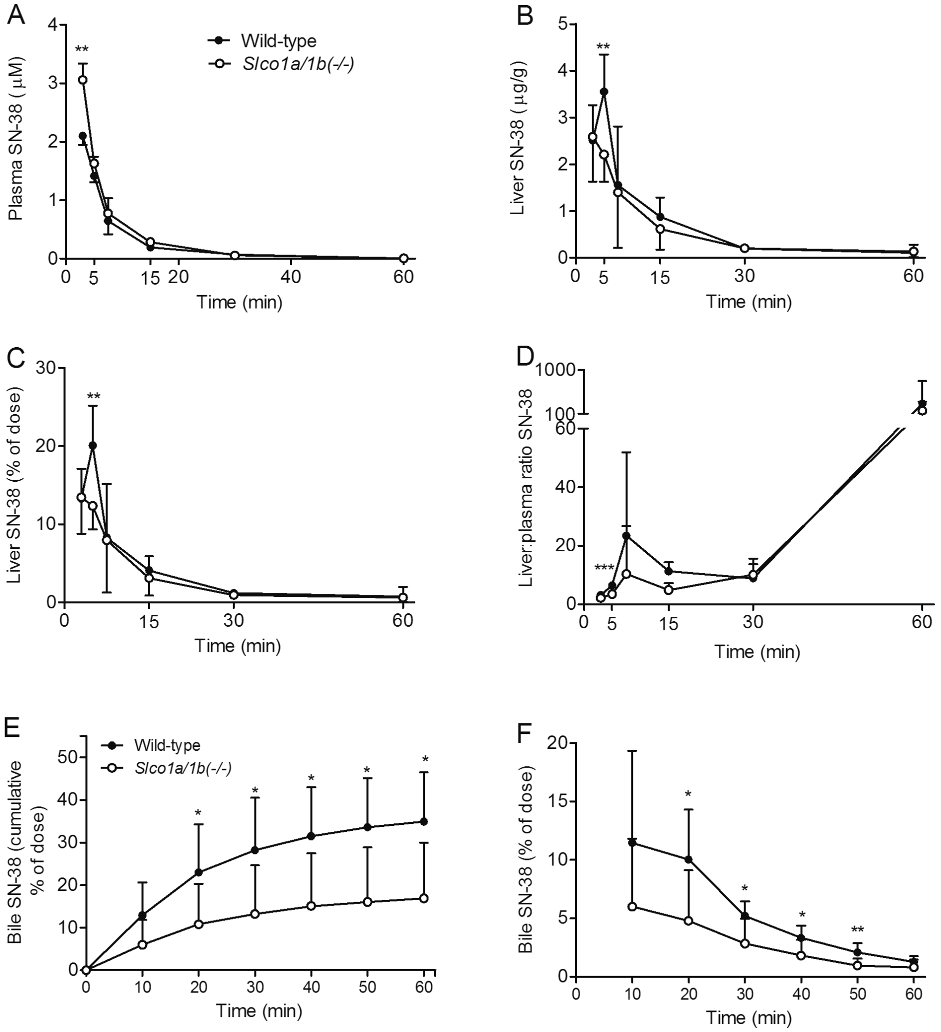

**Figure 6.** Role of Oatp1a/1b uptake transporters in the pharmacokinetics of SN-38 after intravenous administration of SN-38 (1 mg/kg) to female wild-type and Oatp1a/1b knockout mice. (A) Plasma (in µM) and (B) liver concentrations (in µg/g) and (C) (as % of dose) of SN-38 versus time curve. (D) Liver-to-plasma ratio of SN-38 versus time curve. (E) Cumulative biliary excretion of SN-38 (% of dose) and (F) fractional bile output of SN-38 (% of dose) over time. Data are presented as mean ± SD (n = 4-5, *, $P < 0.05$; **, $P < 0.01$ ; ***, $P < 0.001$ when compared with wild-type).

## Discussion

In this study we show that mouse Oatp1a/1b transporters contribute to the plasma clearance of both irinotecan and SN-38. In contrast, human OATPB1 and/or OATP1B3 in humanized transgenic mice do not mediate marked clearance of irinotecan, whereas they do appear to contribute to the hepatic uptake and clearance of SN-38. Unexpectedly, Oatp1a/1b knockout mice displayed highly increased expression and activity of plasma carboxylesterases, with the Ces1c enzyme as the main plasma carboxylesterase (see below) presumably responsible for the increased formation of SN-38 from irinotecan. In addition, we show that Oatp1a/1b knockout mice suffer from increased toxicity after repeated irinotecan administration, correlating with elevated systemic exposure to SN-38.

Low-activity polymorphic variants of *SLCO1B1* (e.g. haplotype *15) have been associated with increased plasma exposure of irinotecan and SN-38 in Asian patients [13]. In another study, carriers of the same polymorphic variant correlated with increased exposure to SN-38, but not irinotecan [11]. Patients with other *SLCO1B1* genotypes associated with low activity (521 T>C and 388 GG) suffered from increased neutropenia and diarrhea, respectively [11]. In addition, there were two isolated cases reported of life-threatening toxicities after irinotecan administration to patients who were carriers of low-activity polymorphic variants of *SLCO1B1* [12, 14]. These data correlate with our own findings in the Oatp1a/1b knockout mice which suffer from increased neutropenia and intestinal toxicity associated with increased plasma exposure to SN-38.

Irinotecan was found not to be transported by human OATP1B1 or OATP1B3 *in vitro* [6-8], which is consistent with the absence of detectable *in vivo* transport that we observed in the OATP1B1- and OATP1B3-humanized mice. On the other hand, our data suggest that mouse Oatp1a/1b transporters do contribute to the plasma clearance and liver uptake of irinotecan. Despite the increased conversion of irinotecan to SN-38 in plasma of the Oatp1a/1b knockout mice, these mice still displayed a clearly increased plasma exposure of irinotecan after intravenous administration, most likely due to impaired liver uptake. This is also evident from the significantly decreased liver-to-plasma ratios of irinotecan (Figure 1). An explanation for this human-mouse difference might be that in mouse liver there are three uptake transporters expressed (Oatp1a1, Oatp1a4 and Oatp1b2), and due to species differences one or more of these could be good irinotecan transporters, in contrast to human OATP1B1 and OATP1B3. Possibly also expression levels of the responsible mouse transporters are relatively high.

Interpretation of data regarding the SN-38 disposition after irinotecan administration was complicated by the increased conversion of irinotecan to SN-38 in plasma of the Oatp1a/1b knockout mice, which might itself contribute to higher plasma levels of SN-38. However, the clearly decreased liver-to-plasma ratios of SN-38 in the knockout mice (Figure 1) strongly supported decreased hepatic uptake. Also after direct administration of SN-38, we could observe an impact of mouse Oatp1a/1b transporters on the plasma clearance and hepatic uptake of SN-38, especially early after intravenous administration. This was also reflected in the decreased biliary output of SN-38 in the absence of Oatp1a/1b transporters. The role of each of the human OATP1B transporters in plasma clearance and liver uptake of SN-38 appeared to be similar to that of the mouse Oatp1a/1b transporters (Figure 5). This would be consistent with previously reported *in vitro* data showing transport of SN-38 by both human transporters [6-8], and it is also in line with the increased irinotecan/SN-38 toxicity observed in patients with low-activity OATP1B1 variants.

The impact of mouse and/or human OATP1A/1B transporters on the irinotecan or SN-38 distribution are mostly evident through altered plasma levels, and liver-to-plasma ratios, without much affecting the liver absolute concentrations (Figures 1 and 5). This is well in line with our previous studies with rosuvastatin and pravastatin in Oatp1a/1b-knockout mice and the findings of a physiologically-based pharmacokinetic model by *Watanabe et al* [33-35]. In short, this model predicts that a reduction in the hepatic uptake will have strong effects on the plasma exposure, and little effect on the liver exposure for drugs that are mostly hepatically cleared and for which there is no substantial alternative clearance route.

Perhaps the most intriguing finding of this study is that Oatp1a/1b knockout mice have highly increased expression of Ces1 enzymes in liver, small intestine and kidney. This correlates with an increased plasma esterase activity leading to far higher formation of SN-38 from irinotecan in plasma. Several Ces1 enzymes were upregulated, of which *Ces1c* and *Ces1d* had the highest fold increase (80-90-fold) in expression in the livers of the Oatp1a/1b knockout mice. This increase in expression correlates well with a ~120-fold increase in the conversion rate of irinotecan to SN-38 (Figure 4A). A recent study reported that, in mouse liver, the absolute mRNA expression levels of *Ces1c* are 1000-fold higher than those of *Ces1d* [31]. Moreover, Ces1d (NCBI Reference Sequence: NP_444430.2) contains an ER retention signal at its C-terminus (EHVEL), which prevents it from being released into the plasma [36]. In contrast, Ces1c lacks this retention signal (NCBI Reference Sequence: NP_031980.2), meaning that it can be secreted into the plasma [36]. In addition, mutant *Ces1c*-deficient mice display a much lower exposure to SN-38 after irinotecan administration, and the *in vitro* conversion rate of irinotecan to SN-38 in plasma isolated from these mice is markedly reduced [37, 38]. Collectively, these results strongly implicate Ces1c as the main plasma carboxylesterase responsible for the increased conversion of irinotecan to SN-38 in the Oatp1a/1b knockout mice. We also demonstrated that BNPP [21], a general CES inhibitor, can almost completely block the conversion of irinotecan to SN-38 in Oatp1a/1b-null plasma. Simvastatin, an inhibitor of human CES1 and CES2 [22], inhibited less than 50% of the conversion activity of mouse Ces1 enzymes. This lower inhibitory capacity might be explained by a difference in affinity for simvastatin between mouse and human Ces enzymes.

It is as yet unclear how Oatp1a/1b deficiency causes Ces1 upregulation. Regulation of Ces1 enzymes is complex and not yet fully elucidated, with many xenobiotics acting as inducers of Ces enzymes, presumably through nuclear receptors [36, 39]. A recent study tested the impact of a few microsomal enzyme inducers on the mouse Ces enzymes, but it did not find a substantial effect on the mRNA expression levels of the Ces1 subfamily [31]. Interestingly, we recently also observed Ces1 upregulation in P-gp- and Cyp3a-deficient mice similar to that in Oatp1a/1b knockout mice [40]. This suggests that when normal detoxification processes of endogenous and/or dietary-derived components are reduced (by knockout of transporters or metabolizing enzymes), Ces1 upregulation can occur. Whatever the underlying mechanism of the upregulation, hepatic expression of human OATP1B1 or OATP1B3 in the humanized Oatp1a/1b-null mice largely normalized this situation. Apparently the detoxification of relevant compounds is sufficiently recovered to normalize expression of the Ces1 enyzmes levels as well. More in depth studies will be required to establish the exact mechanism of Ces1 upregulation in Oatp1a/1b knockout mice.

Although human CES activity in plasma is very low, CES1 and CES2 are abundant in human liver and small intestine, where they can mediate the formation of SN-38, with CES2 enzyme having a higher affinity for irinotecan [26, 30]. There are several polymorphic variants described for both CES1 and CES2 enzymes (reviewed in [41]). However, their impact on irinotecan pharmacokinetics and toxicity has not yet been proven [42-46], with the exception of one study which indicated a possible dose-relationship between several functional variants of CES1 and an elevated exposure to SN-38 and/or SN-38 glucuronide [47]. CES activity might be of importance in tumor cells, where CES expression can increase sensitivity to irinotecan treatment [48], although further studies are necessary to establish their exact contribution.

Obviously, the Ces1 upregulation in the Oatp1a/1b knockout mice, and its subsequent normalization in the humanized OATP1B1 and OATP1B3 mice, should be taken into account when performing pharmacokinetic and toxicological studies in these mouse strains with (pro-)drugs that might be affected by Ces activity. For instance, it may be that the highly increased toxicity of irinotecan treatment that we observed in the Oatp1a/1b knockout mice (Figures 2 and 3) was not only caused by delayed SN-38 clearance, but also in part by increased SN-38 formation. Therefore considerable caution should be exercised when interpreting results obtained with such drugs in these mouse models. Nevertheless, keeping in mind the possible complications brought about by the upregulated Ces1 enzymes for pharmacokinetic studies with irinotecan, we can still conclude that mouse Oatp1a/1b transporters have a role in the plasma clearance of irinotecan and SN-38, while human OATP1B transporters have only an impact on SN-38 disposition.

## Acknowledgements

We thank Dr. Ji-Ying Song for assistance in preparing Figure 3.

## Reference List

1. Hagenbuch B, Meier PJ. Organic anion transporting polypeptides of the OATP/ SLC21 family: phylogenetic classification as OATP/ SLCO superfamily, new nomenclature and molecular/functional properties. Pflugers Arch 2004;447:653-65.
2. Kalliokoski A, Niemi M. Impact of OATP transporters on pharmacokinetics. Br J Pharmacol 2009;158:693-705.
3. Iusuf D, van de Steeg E, Schinkel AH. Functions of OATP1A and 1B transporters in vivo: insights from mouse models. Trends Pharmacol Sci 2012;33:100-8.
4. Mathijssen RH, Loos WJ, Verweij J, Sparreboom A. Pharmacology of topoisomerase I inhibitors irinotecan (CPT-11) and topotecan. Curr Cancer Drug Targets 2002;2:103-23.
5. Innocenti F, Kroetz DL, Schuetz E, et al. Comprehensive pharmacogenetic analysis of irinotecan neutropenia and pharmacokinetics. J Clin Oncol 2009;27:2604-14.
6. Nozawa T, Minami H, Sugiura S, Tsuji A, Tamai I. Role of organic anion transporter OATP1B1 (OATP-C) in hepatic uptake of irinotecan and its active metabolite, 7-ethyl-10-hydroxycamptothecin: in vitro evidence and effect of single nucleotide polymorphisms. Drug Metab Dispos 2005;33:434-9.
7. Oostendorp RL, van de Steeg E, van der Kruijssen CM, et al. Organic anion-

transporting polypeptide 1B1 mediates transport of Gimatecan and BNP1350 and can be inhibited by several classic ATP-binding cassette (ABC) B1 and/or ABCG2 inhibitors. Drug Metab Dispos 2009;37:917-23.

8. Yamaguchi H, Kobayashi M, Okada M, et al. Rapid screening of antineoplastic candidates for the human organic anion transporter OATP1B3 substrates using fluorescent probes. Cancer Lett 2008;260:163-9.
9. Mathijssen RH, van Alphen RJ, Verweij J, et al. Clinical pharmacokinetics and metabolism of irinotecan (CPT-11). Clin Cancer Res 2001;7:2182-94.
10. Smith NF, Figg WD, Sparreboom A. Pharmacogenetics of irinotecan metabolism and transport: an update. Toxicol In Vitro 2006;20:163-75.
11. Han JY, Lim HS, Shin ES, et al. Influence of the organic anion-transporting polypeptide 1B1 (OATP1B1) polymorphisms on irinotecan-pharmacokinetics and clinical outcome of patients with advanced non-small cell lung cancer. Lung Cancer 2008;59:69-75.
12. Takane H, Miyata M, Burioka N, et al. Severe toxicities after irinotecan-based chemotherapy in a patient with lung cancer: a homozygote for the SLCO1B1*15 allele. Ther Drug Monit 2007;29:666-8.
13. Xiang X, Jada SR, Li HH, et al. Pharmacogenetics of SLCO1B1 gene and the impact of *1b and *15 haplotypes on irinotecan disposition in Asian cancer patients. Pharmacogenet Genomics 2006;16:683-91.
14. Takane H, Kawamoto K, Sasaki T, et al. Life-threatening toxicities in a patient with UGT1A1*6/*28 and SLCO1B1*15/*15 genotypes after irinotecan-based chemotherapy. Cancer Chemother Pharmacol 2009;63:1165-9.
15. van de Steeg E, Stranecky V, Hartmannova H, et al. Complete OATP1B1 and OATP1B3 deficiency causes human Rotor syndrome by interrupting conjugated bilirubin reuptake into the liver. J Clin Invest 2012;122:519-28.
16. Iusuf D, van de Steeg E, Schinkel AH. Hepatocyte Hopping of OATP1B Substrates Contributes to Efficient Hepatic Detoxification. Clin Pharmacol Ther 2012;92:559-62.
17. van de Steeg E, van Esch A, Wagenaar E, Kenworthy KE, Schinkel AH. Influence of Human OATP1B1, OATP1B3, and OATP1A2 on the Pharmacokinetics of Methotrexate and Paclitaxel in Humanized Transgenic Mice. Clin Cancer Res 2013;19:821-32.
18. Bardelmeijer HA, Beijnen JH, Brouwer KR, et al. Increased oral bioavailability of paclitaxel by GF120918 in mice through selective modulation of P-glycoprotein. Clin Cancer Res 2000;6:4416-21.
19. van Waterschoot RA, Lagas JS, Wagenaar E, et al. Absence of both cytochrome P450 3A and P-glycoprotein dramatically increases docetaxel oral bioavailability and risk of intestinal toxicity. Cancer Res 2009;69:8996-9002.
20. Guemei AA, Cottrell J, Band R, et al. Human plasma carboxylesterase and butyrylcholinesterase enzyme activity: correlations with SN-38 pharmacokinetics during a prolonged infusion of irinotecan. Cancer Chemother Pharmacol 2001;47:283-90.
21. Heymann E, Krisch K. [Phosphoric acid-bis-(p-nitro-phenylester), a new inhibitor of microsomal carboxylesterases] Phosphorsaure-bis-(p-nitro-phenylester), ein neuer Hemmstoff mikrosomaler Carboxylesterasen. Hoppe Seylers Z Physiol Chem 1967;348:609-19.
22. Fukami T, Takahashi S, Nakagawa N, Maruichi T, Nakajima M, Yokoi T. In vitro evaluation of inhibitory effects of antidiabetic and antihyperlipidemic drugs on human carboxylesterase activities. Drug Metab Dispos 2010;38:2173-8.
23. van Waterschoot RA, van Herwaarden AE, Lagas JS, et al. Midazolam metabolism in cytochrome P450 3A knockout mice can be attributed to up-regulated CYP2C enzymes. Mol Pharmacol 2008;73:1029-36.
24. Iusuf D, Sparidans RW, van Esch A, et al. Organic anion-transporting polypeptides 1a/1b control the hepatic uptake of pravastatin in mice 2. Mol Pharm 2012;9:2497-504.
25. Innocenti F, Vokes EE, Ratain MJ. Irinogenetics: what is the right star? J Clin Oncol 2006;24:2221-4.
26. Holmes RS, Wright MW, Laulederkind SJ, et al. Recommended nomenclature for five mammalian carboxylesterase gene families: human, mouse, and rat genes and proteins. Mamm Genome 2010;21:427-41.
27. Li B, Sedlacek M, Manoharan I, et al. Butyrylcholinesterase, paraoxonase, and albumin esterase, but not carboxylesterase, are present in human plasma. Biochem Pharmacol 2005;70:1673-84.
28. Bahar FG, Ohura K, Ogihara T, Imai T. Species difference of esterase expression and hydrolase activity in plasma. J Pharm Sci 2012;101:3979-88.
29. Shingyoji M, Takiguchi Y, Watanabe-Uruma R, et al. In vitro conversion of irinotecan to SN-38 in human plasma. Cancer Sci 2004;95:537-40.

30. Humerickhouse R, Lohrbach K, Li L, Bosron WF, Dolan ME. Characterization of CPT-11 hydrolysis by human liver carboxylesterase isoforms hCE-1 and hCE-2. Cancer Res 2000;60:1189-92.
31. Zhang Y, Cheng X, Aleksunes L, Klaassen CD. Transcription factor-mediated regulation of carboxylesterase enzymes in livers of mice. Drug Metab Dispos 2012;40:1191-7.
32. Morton CL, Wadkins RM, Danks MK, Potter PM. The anticancer prodrug CPT-11 is a potent inhibitor of acetylcholinesterase but is rapidly catalyzed to SN-38 by butyrylcholinesterase. Cancer Res 1999;59:1458-63.
33. Iusuf D, Sparidans RW, van Esch A, et al. Organic anion-transporting polypeptides 1a/1b control the hepatic uptake of pravastatin in mice. Mol Pharm 2012;9:2497-504.
34. Iusuf D, van Esch A, Hobbs MJ, et al. Murine Oatp1a/1b Uptake Transporters Control Rosuvastatin Systemic Exposure without Affecting Its Apparent Liver Exposure. Mol Pharmacol 2013.
35. Watanabe T, Kusuhara H, Maeda K, Shitara Y, Sugiyama Y. Physiologically based pharmacokinetic modeling to predict transporter-mediated clearance and distribution of pravastatin in humans. J Pharmacol Exp Ther 2009;328:652-62.
36. Hosokawa M, Furihata T, Yaginuma Y, et al. Genomic structure and transcriptional regulation of the rat, mouse, and human carboxylesterase genes. Drug Metab Rev 2007;39:1-15.
37. Morton CL, Wierdl M, Oliver L, et al. Activation of CPT-11 in mice: identification and analysis of a highly effective plasma esterase. Cancer Res 2000;60:4206-10.
38. Morton CL, Iacono L, Hyatt JL, et al. Activation and antitumor activity of CPT-11 in plasma esterase-deficient mice. Cancer Chemother Pharmacol 2005;56:629-36.
39. Satoh T, Hosokawa M. Structure, function and regulation of carboxylesterases. Chem Biol Interact 2006;162:195-211.
40. Lagas JS, Damen CW, van Waterschoot RA, Iusuf D, Beijnen JH, Schinkel AH. P-glycoprotein, multidrug-resistance associated protein 2, cyp3a, and carboxylesterase affect the oral availability and metabolism of vinorelbine. Mol Pharmacol 2012;82:636-44.
41. Sanghani SP, Sanghani PC, Schiel MA, Bosron WF. Human carboxylesterases: an update on CES1, CES2 and CES3. Protein Pept Lett 2009;16:1207-14.
42. Bellott R, Le Morvan V, Charasson V, et al. Functional study of the 830C>G polymorphism of the human carboxylesterase 2 gene. Cancer Chemother Pharmacol 2008;61:481-8.
43. Charasson V, Bellott R, Meynard D, Longy M, Gorry P, Robert J. Pharmacogenetics of human carboxylesterase 2, an enzyme involved in the activation of irinotecan into SN-38. Clin Pharmacol Ther 2004;76:528-35.
44. Kim SR, Nakamura T, Saito Y, et al. Twelve novel single nucleotide polymorphisms in the CES2 gene encoding human carboxylesterase 2 (hCE-2). Drug Metab Pharmacokinet 2003;18:327-32.
45. Kim SR, Sai K, Tanaka-Kagawa T, et al. Haplotypes and a novel defective allele of CES2 found in a Japanese population. Drug Metab Dispos 2007;35:1865-72.
46. Kubo T, Kim SR, Sai K, et al. Functional characterization of three naturally occurring single nucleotide polymorphisms in the CES2 gene encoding carboxylesterase 2 (HCE-2). Drug Metab Dispos 2005;33:1482-7.
47. Sai K, Saito Y, Tatewaki N, et al. Association of carboxylesterase 1A genotypes with irinotecan pharmacokinetics in Japanese cancer patients. Br J Clin Pharmacol 2010;70:222-33.
48. Wu MH, Yan B, Humerickhouse R, Dolan ME. Irinotecan activation by human carboxylesterases in colorectal adenocarcinoma cells. Clin Cancer Res 2002;8:2696-700.

# *Supplemental data*

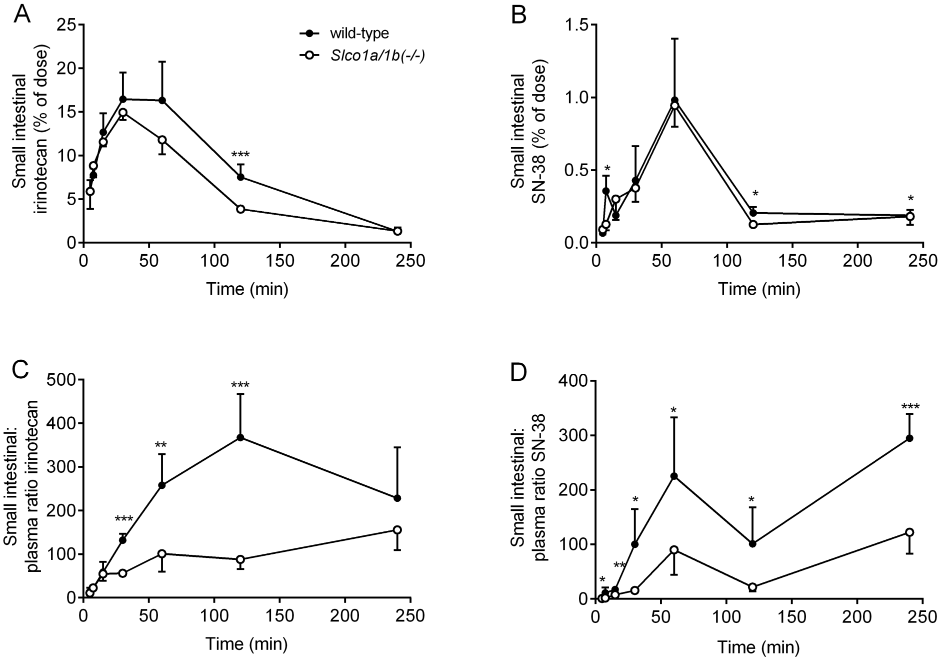

**Supplemental Figure 1.** Role of Oatp1a/1b uptake transporters in small intestinal (tissue plus content) exposure of irinotecan and SN-38 after intravenous administration of irinotecan (10 mg/kg) to female wild-type and Oatp1a/1b knockout mice. Small intestine concentrations (as % of dose) of (A) irinotecan and (B) SN-38. Small intestine-to-plasma ratios of (C) irinotecan and (D) SN-38. Data are presented as mean ± S.D. (n = 5-6, *, *P* < 0.05*;* **, *P* < 0.01; ***, *P* < 0.001 when compared with wild-type).

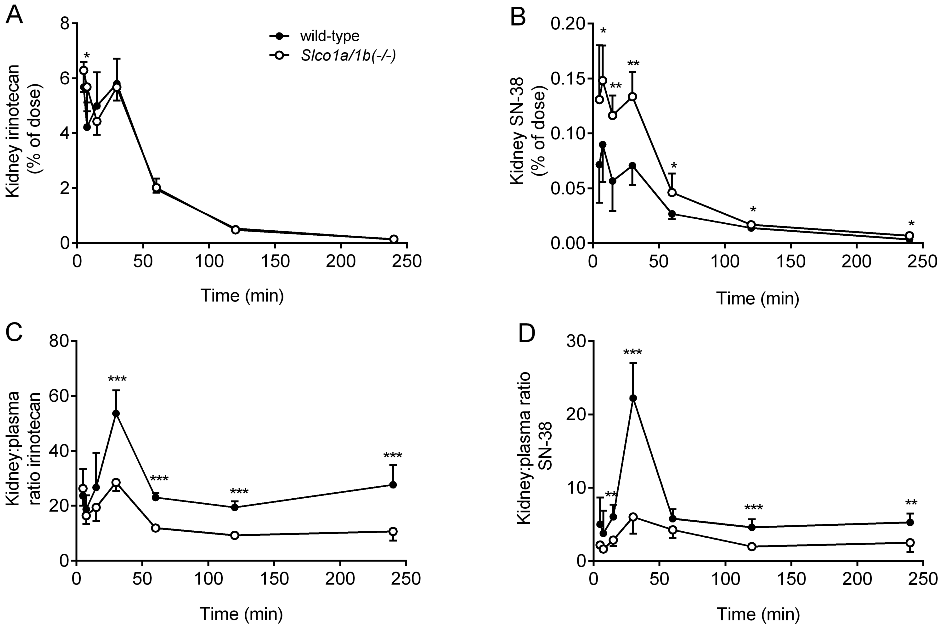

**Supplemental Figure 2.** Role of Oatp1a/1b uptake transporters in kidney exposure of irinotecan and SN-38 after intravenous administration of irinotecan (10 mg/kg) to female wild-type and Oatp1a/1b knockout mice. Kidney concentrations (as % of dose) of (A) irinotecan and (B) SN-38. Kidney-to-plasma ratios of (C) irinotecan and (D) SN-38. Data are presented as mean ± S.D. (n = 5-6, *, $P < 0.05$; **, $P < 0.01$; ***, $P < 0.001$ when compared with wild-type).

**Supplemental Table 1.** Overview of ΔCt values of the RT-PCR analysis of expression of several esterases in liver of female wild-type, Oatp1a/1b knockout (*Slco1a/1b(-/-)*) and OATP1B1/1B3 humanized mice (*Slco1a/1b(-/-);1B1(tg)* and *Slco1a/1b(-/-);1B3(tg)*).

| Gene | Wild-type | *Slco1a/1b(-/-)* | *Slco1a/1b(-/-);1B1(tg)* | *Slco1a/1b(-/-);1B3(tg)* |
|---|---|---|---|---|
| Ces1b | 1.74 ± 0.80 | -1.37 ± 0.11$^{***}$ | 1.86 ± 0.49$^{\#\#\#}$ | 2.37 ± 0.14$^{\#\#\#}$ |
| Ces1c | 3.58 ± 1.84 | -2.76 ± 0.08$^{***}$ | 5.29 ± 0.09$^{\#\#\#}$ | 4.89 ± 0.30$^{\#\#\#}$ |
| Ces1d | 7.69 ± 2.74 | 1.18 ± 0.16$^{***}$ | Not detected | Not detected |
| Ces1e | 6.31 ± 0.62 | 3.11 ± 0.19$^{***}$ | 4.78 ± 0.62$^{*\#}$ | 4.82 ± 0.35$^{*\#\#}$ |
| Ces1f | 1.25 ± 0.47 | 1.60 ± 0.29 | 1.11 ± 0.30 | 1.68 ± 0.21 |
| Ces1g | 1.06 ± 0.22 | 1.49 ± 0.51 | 0.98 ± 0.66 | 1.29 ± 0.17 |
| Bche | -1.46 ± 0.17 | -1.37 ± 0.31 | | |
| Ces2a | 3.26 ± 0.09 | 3.23 ± 0.11 | | |
| Ces2e | 0.96 ± 0.97 | 1.47 ± 0.05 | | |
| Ces3a | -1.50 ± 0.44 | -1.51 ± 0.39 | | |
| Ces3b | -0.72 ± 0.77 | 0.15 ± 0.18 | | |
| Aadac | 1.01 ± 0.14 | 1.53 ± 0.54 | | |
| Pon1 | 0.86 ± 0.33 | 0.48 ± 0.28 | | |
| Pon2 | 3.99 ± 0.26 | 3.94 ± 0.16 | | |
| Pon3 | 2.76 ± 0.20 | 2.72 ±0.25 | | |

(n = 3; each sample was assayed in duplicate). Part of these data is also shown in Figure 5. Analysis of the results was done by the comparative ΔCt method. Quantification of the target cDNAs in all samples was normalized against the endogenous control Gapdh ($Ct_{target}$ – $Ct_{Gapdh}$ = ΔCt). Accordingly, the lower the ΔCt value, the higher the expression level (see also Materials and Methods). (*, *P* < 0.05; ***, *P* < 0.001 when compared with wild-type, $^{\#}$, *P* < 0.05; $^{\#\#}$, *P* < 0.01; $^{\#\#\#}$, *P* < 0.001 when compared with Oatp1a/1b knockout mice).

**Supplemental Table 2.** Overview of ΔCt values of the RT-PCR analysis of expression of several esterases in small intestine of female wild-type, Oatp1a/1b knockout (*Slco1a/1b(-/-)*) and OATP1B1/1B3 humanized mice (*Slco1a/1b(-/-);1B1(tg)* and *Slco1a/1b(-/-);1B3(tg)*).

| Gene | Wild-type | *Slco1a/1b(-/-)* | *Slco1a/1b(-/-);1B1(tg)* | *Slco1a/1b(-/-);1B3(tg)* |
|---|---|---|---|---|
| Ces1b | 8.5 ± 0.17 | 8.9 ± 0.16 | 8.4 ± 0.3 | 8.9 ± 0.12 |
| Ces1c | 12.4 ± 0.54 | 12.3 ± 0.9 | 11.9 ± 1.4 | 13.0 ± 0.6 |
| Ces1d | 22.5 ± 2.9 | 11.1 ± 0.5$^{***}$ | 22.2 ± 2.3$^{\#\#\#}$ | Not detected |
| Ces1e | 11.9 ± 0.2 | 9.3 ± 0.43 | 12.3 ± 1.12$^{\#}$ | 13.3 ± 2.1 |
| Ces1f | 6.4 ± 0.5 | 7.0 ± 0.3 | 6.8 ± 0.5 | 6.9 ± 0.3 |
| Ces1g | 10.0 ± 0.4 | 11.7 ± 1.0 | 9.9 ± 0.8 | 10.4 ± 0.8 |
| Ces2a | 8.4 ± 0.8 | 8.7 ± 1.10 | 8.7 ± 0.4 | 8.4 ± 0.2 |
| Ces2e | 4.3 ± 0.7 | 4.3 ± 0.4 | 4.2 ± 0.1 | 4.3 ± 0.2 |
| Ces3a | 16.9 ± 2.1 | 16.6 ± 3.2 | 13.5 ± 0.6 | 17.1 ± 0.3 |
| Bche | 3.2 ± 3.5 | 1.6 ± 1.04 | 5.3 ± 2.6 | 3.2 ± 3.1 |

(n = 3; each sample was assayed in duplicate). Part of these data is also shown in Figure 5. Analysis of the results was done by the comparative ΔCt method. Quantification of the target cDNAs in all samples was normalized against the endogenous control Gapdh ($Ct_{target}$ – $Ct_{Gapdh}$ = ΔCt). Accordingly, the lower the ΔCt value, the higher the expression level (see also Materials and Methods). (*, *P* < 0.05; ***, *P* < 0.001 when compared with wild-type, $^{\#}$, *P* < 0.05; $^{\#\#\#}$, *P* < 0.001 when compared with Oatp1a/1b knockout mice).

**Supplemental Table 3.** Overview of ΔCt values of the RT-PCR analysis of expression of several esterases in kidney of female wild-type, Oatp1a/1b knockout (*Slco1a/1b(-/-)*) and OATP1B1/1B3 humanized mice (*Slco1a/1b(-/-);1B1(tg)* and *Slco1a/1b(-/-);1B3(tg)*).

| **Gene** | **Wild-type** | ***Slco1a/1b(-/-)*** | ***Slco1a/1b(-/-);1B1(tg)*** | ***Slco1a/1b(-/-);1B3(tg)*** |
|---|---|---|---|---|
| Ces1b | 10.2 ± 0.06 | 11.2 ± 0.14 | 10.7 ± 0.4 | 11.1 ± 0.2 |
| Ces1c | 12.0 ± 0.4 | 14.2 ± 1.3* | 11.5 ± 0.3## | 12.4 ± 0.7 |
| Ces1d | 15.3 ± 3.8 | 5.5 ± 0.3** | 17.3 ± 0.2### | 15.1 ± 3.4### |
| Ces1e | 1.0 ± 0.04 | 0.51 ± 0.05 | 0.7 ± 0.12 | 0.5 ± 0.1 |
| Ces1f | 8.7 ± 0.3 | 8.8 ± 0.2 | 8.8 ± 0.3 | 9.2 ± 0.5 |
| Ces1g | 12.3 ± 1.1 | 11.7 ± 0.2 | 10.4 ± 0.4* | 11.2 ± 0.5 |
| Ces2a | 1.0 ± 0.04 | 0.51 ± 0.05 | 0.7 ± 0.2 | 0.5 ± 0.1 |
| Ces2e | 10.4 ± 0.60 | 10.3 ± 0.3 | 9.8 ± 0.5 | 9.9 ± 0.06 |
| Ces3a | 16.9 ± 2.11 | 16.6 ± 3.2 | 13.5 ± 0.6 | 17.1 ± 0.3 |
| Bche | 6.5 ± 2.0 | 6.9 ± 2.5 | Not detected | Not detected |

(n = 3; each sample was assayed in duplicate). Part of these data is also shown in Figure 5. Analysis of the results was done by the comparative ΔCt method. Quantification of the target cDNAs in all samples was normalized against the endogenous control Gapdh ($Ct_{target} - Ct_{Gapdh} = \Delta Ct$). Accordingly, the lower the ΔCt value, the higher the expression level (see also Materials and Methods). (*, $P < 0.05$; **, $P < 0.01$ ; ***, $P < 0.001$ when compared with wild-type, #, $P < 0.05$; ##, $P < 0.01$ ; ###, $P < 0.001$ when compared with Oatp1a/1b knockout mice).

# 4.2

# *Human OATP1B1, OATP1B3 and OATP1A2 mediate the in vivo uptake of docetaxel*

Dilek Iusuf*[1], Jeroen J.M.A. Hendrikx*[1, 2],
Anita van Esch[1], Evita van de Steeg[1], Els Wagenaar[1],
Jos H. Beijnen[2] and Alfred H. Schinkel[1],

* contributed equally

[1]Division of Molecular Oncology,
The Netherlands Cancer Institute,
[2]Department of Pharmacy & Pharmacology,
Slotervaart Hospital, Amsterdam, the Netherlands

*To be submitted*

## *Abstract*

Organic Anion Transporting Polypeptides (human: OATPs, mouse: Oatps) are uptake transporters which play an important role in drug pharmacokinetics and toxicity. Here, we aimed to study the impact of mouse and human OATP1A/1B transporters on docetaxel intestinal and liver uptake *in vivo* using Oatp1a/1b knockout and liver-specific humanized OATP1B1, OATP1B3 and OATP1A2 transgenic mice. Experiments were conducted with a low polysorbate 80 formulation (2.8%) of docetaxel, as high polysorbate concentrations (8%) inhibited docetaxel plasma clearance after intravenous administration. After i.v. administration (10 mg/kg) Oatp1a/1b knockout mice had a ~3-fold higher plasma AUC, while the liver concentrations remained unchanged in comparison with wild-type mice. Impaired liver uptake was evident from the significantly reduced (~3-fold) liver-to-plasma ratios after i.v. administration. Absence of mouse Oatp1a/1b transporters did not affect the intestinal absorption of docetaxel after oral administration (10 mg/kg), while the systemic exposure of docetaxel was again substantially increased due to impaired liver uptake. Most importantly, liver-specific expression of each of the human OATP1B1, OATP1B3 or OATP1A2 transporters provided a nearly complete rescue of the increased plasma levels of docetaxel in Oatp1a/1b-null mice after i.v. administration (10 mg/kg). Conclusion: One or more of the mouse Oatp1a/1b transporters, and each of the human OATP1A/1B can mediate docetaxel uptake *in vivo*. This might be clinically relevant for OATP1A/1B-mediated tumor uptake of docetaxel and for docetaxel clearance in patients in which the transport activity of OATP1A/1B transporters is reduced due to genetic variation or pharmacological inhibition, leading to potentially increased toxicity.

# Introduction

One of the most widely used chemotherapeutic drugs is docetaxel, a microtubule inhibitor which is approved for the treatment of breast, lung, ovarian, prostate, gastric, and head and neck cancers [1]. An important problem in docetaxel therapy is the inter-patient variability in docetaxel exposure which in turn can lead to unpredictable dose-limiting toxicity (neutropenia, diarrhea) and/or variability in response to treatment [2]. Factors which control plasma exposure to docetaxel include drug-metabolizing enzymes and drug transporters [2]. One of the major clearance mechanisms of docetaxel is metabolism by the Cytochrome P450 3A (CYP3A), a drug-metabolizing enzyme complex expressed both in the intestine and in the liver [3]. Although there are substantial inter-individual differences in expression and activity of CYP3A enzymes, this alone cannot explain entirely the inter-patient variability after intravenously administered docetaxel [1]. Recent studies have pointed to low-activity polymorphic variants of drug transporters involved in the clearance of docetaxel as contributors to the unpredictable systemic exposure of docetaxel [1, 4, 5]. These transporters involve efflux transporters from the ATP-binding cassette (ABC) transporter family (ABCB1 or ABCC2), but also uptake transporters of the Organic Anion Transporting Polypeptide (OATP) family [1, 6].

The OATP superfamily of sodium-independent influx transporters consists of 6 families, of which the OATP1B subfamily are most studied with respect to clinical pharmacogenomics of drugs [7]. It is important to note that between mouse and human Oatps there are no straighforward orthologs, for example humans have one OATP1A transporter (OATP1A2), while in mouse there are at least 4 members known (Oatp1a1, Oatp1a4, Oatp1a5 and Oatp1a6). In contrast, for the OATP1B transporters, humans have 2 members (OATP1B1 and OATP1B3), while in mouse there is only one (Oatp1b2) [8].

Due to their localization in pharmacokinetically relevant tissues (liver, small intestine and kidney) and their capacity to transport many drugs, OATP1A/1B transporters are thought to play a major role in the distribution, pharmacodynamics and toxicity of many drugs [9-11]. In the liver, OATP1B1 and OATP1B3 are highly expressed on the basolateral membrane of hepatocytes where they mediate the hepatic uptake, and therefore clearance of many xenobiotics [8]. OATP1A2 is mainly expressed in other tissues, like brain, kidney, and small intestine while in the liver it is expressed in cholangiocytes and not in hepatocytes. Its role in drug distribution remains to be elucidated [8]. It is thought that in the small intestine human OATP1A2 and/or mouse Oatp1a are expressed on the apical membrane of enterocytes where they might mediate the intestinal uptake of drugs [12]. In addition to their role in the pharmacokinetics of drugs, many OATPs are expressed in breast, gastrointestinal and lung tumors, where they are thought to contribute to the tumor uptake of anticancer drugs [13].

Docetaxel has been described as a substrate of human OATP1B1 and OATP1B3, and rat and mouse Oatp1b2 *in vitro* [14-16]. The impact of the functional alterations in uptake capacity of OATP1B1 and/or OATP1B3 on the docetaxel pharmacokinetics and toxicity (upon intravenous administration) has been studied in several pharmacogenetic studies, but the results are equivocal [4, 6, 14], while the interaction between OATP1A2 and docetaxel has not been reported yet.

In recent years, substantial efforts have been made to obtain an oral formulation for docetaxel [17]. While oral dosing has substantial advantages over intravenous dosing (more patient-friendly, no hospitalization required, lower healthcare costs), it brings the challenge that the drug must pass an additional biological barrier, the intestinal tissue. It might be that mouse Oatp1a or human OATP1A2 uptake transporters have a role in docetaxel intestinal uptake, while metabolizing enzymes and efflux drug transporters might limit its effective absorption [8].

Here, we study the impact of the combined deletion of mouse Oatp1a and Oatp1b genes on the disposition of docetaxel after intravenous and oral administration, using Oatp1a/1b knockout mice [18]. We further focus on the *in vivo* impact of human OATP1B1, OATP1B3 and OATP1A2 on the uptake of docetaxel using humanized transgenic mice with liver-specific expression of OATP1B1, OATP1B3 or OATP1A2 [19, 20].

## Materials and methods

### Animals

Animals were housed in groups as far as possible, in a temperature-controlled environment with a 12-hour light/12-hour dark cycle. They received a standard diet (AM-II; Hope Farms) and acidified water *ad libitum*. All mouse experiments were approved by the Animal Experiments Review Board of the Netherlands Cancer Institute (Amsterdam), complying with Dutch legislation and in accordance with European Directive 86/609/EEC. Male wild-type, *Slco1a/1b(-/-)* (Oatp1a/1b knockout), *Slco1a/1b(-/-);1B1(Tg)* , *Slco1a/1b(-/-);1B3(Tg)* and *Slco1a/1b(-/-);1A2(Tg)* (i.e, liver-specific OATP1B1, OATP1B3 and OATP1A2 humanized transgenic) mice of comparable genetic background (>99% FVB) between 8 and 14 weeks of age were used [19, 21].

### Chemicals and reagents

Docetaxel was obtained from Sequoia Research Products (Oxford, UK). Isoflurane (Forane) was purchased from Abbott Laboratories (Queenborough, Kent, UK) and heparin (5,000 IE/ml) was from Leo Pharma BV (Breda, The Netherlands). Bovine serum albumin (BSA), Fraction V was from Roche (Mannheim, Germany) and drug-free lithium-heparinized human plasma was obtained from Bioreclamation LLC (New York, NY, USA). All other reagents (polysorbate 80, ethanol) were from Sigma-Aldrich (Steinheim, Germany).

### Pharmacokinetic studies

For intravenous studies, solutions containing docetaxel (2 mg/mL) were injected in a volume of 5 μL per g of bodyweight in the tail vein of the mice, in order to achieve a dosage of 10 mg/kg. For solutions with low polysorbate concentrations (2.77% of polysorbate 80 in the final solution), docetaxel was dissolved in a mixture of ethanol:polysorbate 80 (50:50) to a concentration of 36 mg/mL, which was further diluted prior to injection with saline to a concentration of 2 mg/mL docetaxel. For solutions containing high polysorbate concentrations (8.3% in the final solution), docetaxel was dissolved in a mixture of ethanol:polysorbate 80 (50:50) to a concentration of 12 mg/mL, which was further diluted prior to injection with saline to 2 mg/mL docetaxel.

For oral studies, docetaxel (1 mg/mL) was administered in a volume of 10 μL per g of bodyweight by oral gavage to the mice, in order to achieve a dosage of 10 mg/kg. We used the formulation containing low polysorbate 80 concentrations (2.77% in the final solution):

docetaxel was dissolved in a mixture of ethanol:polysorbate 80 (50:50) to a concentration of 18 mg/mL, which was further diluted prior to dosing with saline to 1 mg/mL docetaxel.

Experiments were terminated (at t = 3, 15, 30, 60, 120 and 240 min after i.v. dosing and t = 5, 7.5 and 15 min after oral dosing) by isoflurane anaesthesia, heparin-blood sampling by cardiac puncture followed by cervical dislocation and tissue collection. For the oral studies, portal vein blood samples were taken prior to cardiac puncture. Blood samples were centrifuged at 5,200g for 5 min at 4°C and plasma was collected and stored at -30°C until analysis.

### *Drug analysis*

Concentrations of docetaxel in plasma and livers (homogenized in 3 mL of ice-cold 4% (w/v) BSA) were determined by LC-MS/MS analysis as previously described [22]. D9-labelled docetaxel was used as internal standard for docetaxel. In summary, mouse plasma or tissue homogenate samples of 20 µL were diluted with 180 µL of human plasma. Human plasma was used for dilution of the samples as the concentrations in the undiluted mouse plasma were outside the calibration range and also to mimic the calibration standards which were in human plasma. After dilution of the samples, 25 µL of internal standard working solution was added. Subsequently, the samples were mixed briefly, tertiary-butyl methyl ether was added and the samples were shaken for 10 minutes at 1,250 rpm. The samples were centrifuged at 23,000 g, snap-frozen and the organic layer was collected. After evaporation of the organic layer, the samples were reconstituted with 100 µl of 10 mM ammonium hydroxide pH 5:acetonitrile (1:1, v/v) and an aliquot was injected into the LC-MS/MS system. Calibration standards in human plasma in a range of 0.25-500 ng/mL were used for quantification of docetaxel.

### *Pharmacokinetic and statistical analysis*

Averaged plasma concentrations for each time point were used to calculate the area under the blood concentration versus time curve (AUC) from t = 0 to the last sampling time point by the linear trapezoidal rule; S.E. was calculated by the law of propagation of errors [23].

The two-sided unpaired Student's *t*-test was used throughout the study to assess the statistical significance of differences between two sets of data. Statistical significance of differences between wild-type and *Slco1a/1b(-/-)*, *Slco1a/1b(-/-);1B1(Tg)* or Slco1a/1b(-/-);1A2(Tg) or between *Slco1a/1b(-/-)* mice and *Slco1a/1b(-/-);1B1(Tg)* or *Slco1a/1b(-/-);1B3(Tg)* mice was assessed by one-way ANOVA followed by Dunett's multiple comparison test, taking wild-type or *Slco1a/1b(-/-)* mice as control. Results are presented as the mean ± S.D. Differences were considered to be statistically significant when $P < 0.05$ [19].

## Results

### *Influence of polysorbate 80 concentration on pharmacokinetics of docetaxel*

Docetaxel is hardly soluble in water, and thus the formulation of docetaxel for intravenous administration contains ethanol and polysorbate 80, a detergent used to maintain docetaxel in solution, in concentrations between 0.75-2% [24, 25]. Although polysorbate 80 (or Tween 80) was thought to be pharmacologically inactive, there have been reports showing that it might have an inhibitory effect on the transport activity of OATP uptake transporters [14, 26]. Therefore we started this study by analyzing the effect of polysorbate 80 concentration in the final formulation on the plasma and liver levels of docetaxel after intravenous administration (10 mg/kg). We used two docetaxel formulations: one with high polysorbate 80 concentration (8.3%) and one with a low polysorbate 80 concentration (2.8%) and we administered them to wild-type mice (10 m/kg). At different time points after dosing, we compared the docetaxel plasma and liver levels and liver-to-plasma ratios in these mice (Figure 1). After dosing with the high polysorbate 80 formulation, the plasma levels of docetaxel were modestly, but significantly higher than after dosing with the low polysorbate 80 formulation (Figure 1A), suggesting that polysorbate 80 at high concentrations has a modest *in vivo* inhibitory effect on plasma clearance of docetaxel. The liver concentrations after high polysorbate concentrations were slightly, but not significantly lower than after dosing with low polysorbate 80 formulation (Figure 1B, C). This effect was more obvious in the liver-to-plasma ratios, where low polysorbate 80 formulation lead to higher liver exposure than the high polysorbate 80 formulation (Figure 1D), suggesting that high concentrations of polysorbate

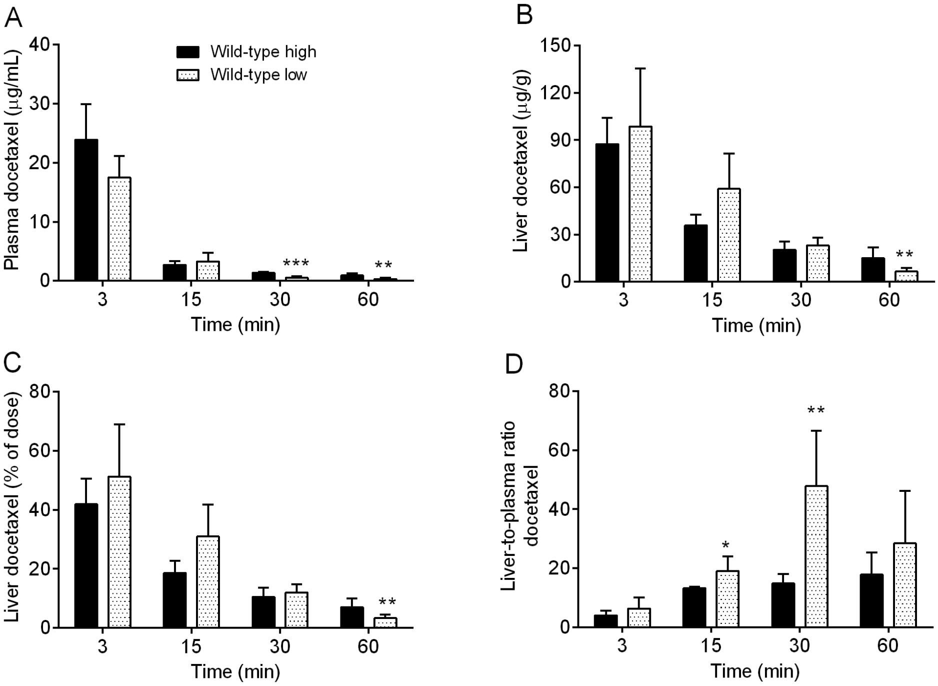

**Figure 1.** Impact of high (black bars) and low polysorbate (white bars) formulation on plasma and liver levels of docetaxel after administration of 10 mg/kg docetaxel i.v. to male wild-type mice. (A) Plasma concentrations of docetaxel, (B, C) docetaxel liver concentrations as µg/g and % of dose, respectively, and (D) liver-to-plasma ratios of docetaxel. Averaged liver-to-systemic plasma ratios were calculated from individual mouse data. Data are presented as mean ± S.D. (n = 5-6, *, $P < 0.05$; **, $P < 0.01$; ***, $P < 0.001$ when compared with wild-type high polysorbate formulation).

80 might inhibit the uptake of docetaxel in the liver. Based on these results, we used the low polysorbate 80 formulation in our subsequent pharmacokinetic studies.

### *Impact of Oatp1a/1b transporters on plasma and liver exposure of docetaxel after intravenous exposure*

Docetaxel was described as a mouse Oatp1b2 substrate *in vitro* and *in vivo* [14]. We here aimed to study the possible additional roles that mouse Oatp1a transporters may have in the plasma and liver exposure of docetaxel. We therefore made use of Oatp1a/1b knockout mice, which lack all Oatp1a and Oatp1b transporters. After intravenous dosing (10 mg/kg), plasma exposure of docetaxel was increased in the Oatp1a/1b knockout mice in comparison with wild-type mice (Figure 2A). The area under the curve (AUC) of the plasma concentrations in Oatp1a/1b-null mice was 2.9-fold increased relative to the wild-type mice (608.7 ± 25.2 versus 211.8 ± 19.8 μg·min/mL, $P < 0.001$), indicating that disposition of docetaxel is impaired in the absence of Oatp1a/1b transporters.

OATP transporters mediate mainly the liver uptake of drugs, thus controlling their clearance and disposition. We therefore measured also the liver concentrations. Similar to previous studies

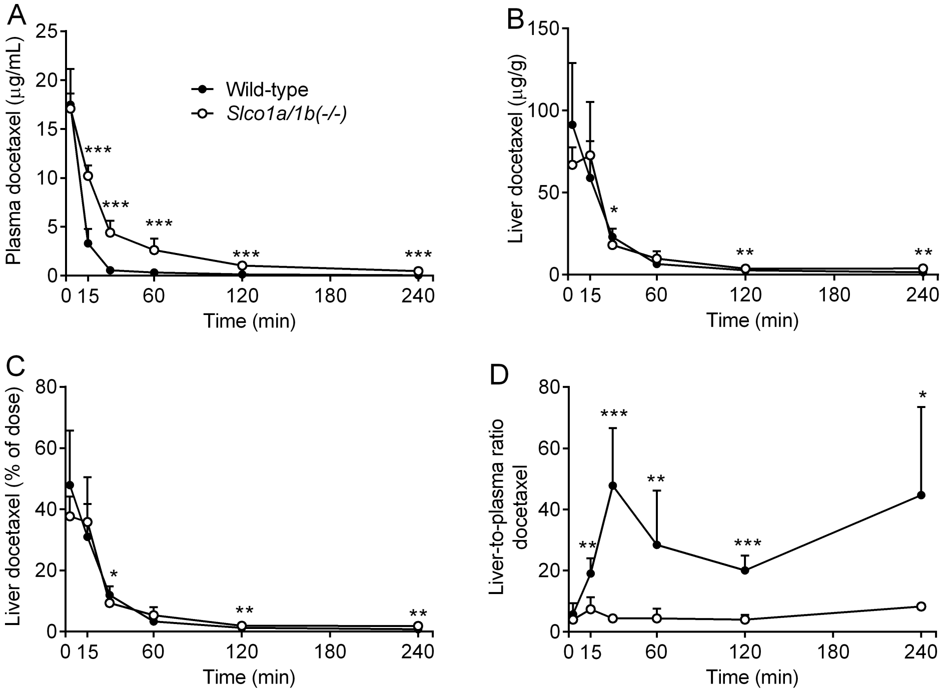

**Figure 2.** Role of Oatp1a/1b uptake transporters in the plasma and liver exposure of docetaxel after intravenous administration of docetaxel (10 mg/kg) to male wild-type and Oatp1a/1b knockout mice. (A) Plasma concentrations of docetaxel, (B, C) docetaxel liver concentrations as μg/g and % of dose, respectively, and (D) liver-to-plasma ratios of docetaxel. Averaged liver-to-systemic plasma ratios were calculated from individual mouse data. Data are presented as mean ± S.D. (n = 5-6, *, $P < 0.05$; **, $P < 0.01$; ***, $P < 0.001$ when compared with wild-type).

with rosuvastatin [27], the liver concentrations were not changed between the two strains of mice (Figure 2B, C), while the liver-to-plasma ratios were significantly reduced at virtually all time points after dosing (Figure 2D), suggesting that liver uptake is impaired in the Oatp1a/1b-null mice.

In contrast to Oatp1b2 which is exclusively expressed in the liver, members of the Oatp1a family are also expressed in the enterocytes [12] where they are thought to mediate the intestinal absorption of drugs. We therefore assessed next the impact of Oatp1a on the intestinal absorption of docetaxel.

### *Oatp1a transporters are not essential in the intestinal absorption of docetaxel*

We compared portal vein concentrations in Oatp1a/1b knockout and wild-type mice, shortly after oral administration (10 mg/kg) of docetaxel, in order to establish if the Oatp1a transporters contributed to the intestinal absorption of docetaxel. However, docetaxel portal vein concentrations were substantially higher at all time points in the Oatp1a/1b knockout mice (Figure 3A). These results suggest that Oatp1a transporters are not essential in the intestinal absorption of docetaxel. The increased portal vein concentrations at all time points after dosing of docetaxel may in part reflect the higher systemic plasma concentrations in the Oatp1a/1b-null mice (Figure 3B). The increased systemic plasma concentrations of docetaxel in these mice were likely to be due to impaired liver uptake in the Oatp1a/1b-null mice, as seen previously (Figure 3D, E and Figure 2). This impaired liver uptake was evident both in the liver-to-systemic plasma and liver-to-portal vein plasma ratios (Figure 3D, E).

### *Human OATP1B, OATP1B3 and OATP1A2 can transport docetaxel in vivo*

In the human liver, OATP1B1 and OATP1B3 are expressed on the basolateral membrane of hepatocytes. Although not straightforward homologues of the mouse Oatp1a/1b proteins, based on amino acid homology and substrate specificity, they are considered to fulfill the same roles as the mouse Oatp1a/1b transporters in the liver [19, 23, 28]. We recently generated and characterized humanized mice with liver-specific expression of OATP1B1, OATP1B3 and OATP1A2 (in an *Slco1a/1b(-/-)* background) [19, 20]. Note that *Slco1a/1b(-/-);1A2(Tg)* do not represent a physiological model for the role of OATP1A2 in hepatic uptake of drugs, as hepatic OATP1A2 in humans is expressed only in cholangiocytes, and not in hepatocytes. Nevertheless, this mouse model has proven useful in studying the *in vivo* transport capacity of OATP1A2, which might be relevant for its activity in other healthy or malignant tissues [19].

We used these models to assess the capacity of the human OATP1A/1B proteins to transport docetaxel *in vivo*. After 10 mg/kg i.v. dosing, the increased docetaxel plasma concentrations in the Oatp1a/1b-null mice were partially or completely brought back to wild-type levels in all the humanized mouse strains (Figure 4A). Only at 30 minutes after dosing, plasma levels in the OATP1B3 humanized mice were as high as in the Oatp1a/1b-null mice, perhaps due to experimental variation (Figure 4A). As also seen in Figure 2B, the liver levels were not significantly changed in the Oatp1a/1b-null mice in comparison with wild-type mice, and accordingly shifts in liver concentration due to the role of OATP1A/1B transporters in rescuing the absence of mouse Oatp1a/1b transporters were modest, albeit significant for OATP1B1 and OATP1B3 at 30 minutes (Figure 4B, C). Liver-to-plasma ratios in the humanized mice (in OATP1A2 mice especially) were also significantly higher than in the knockout

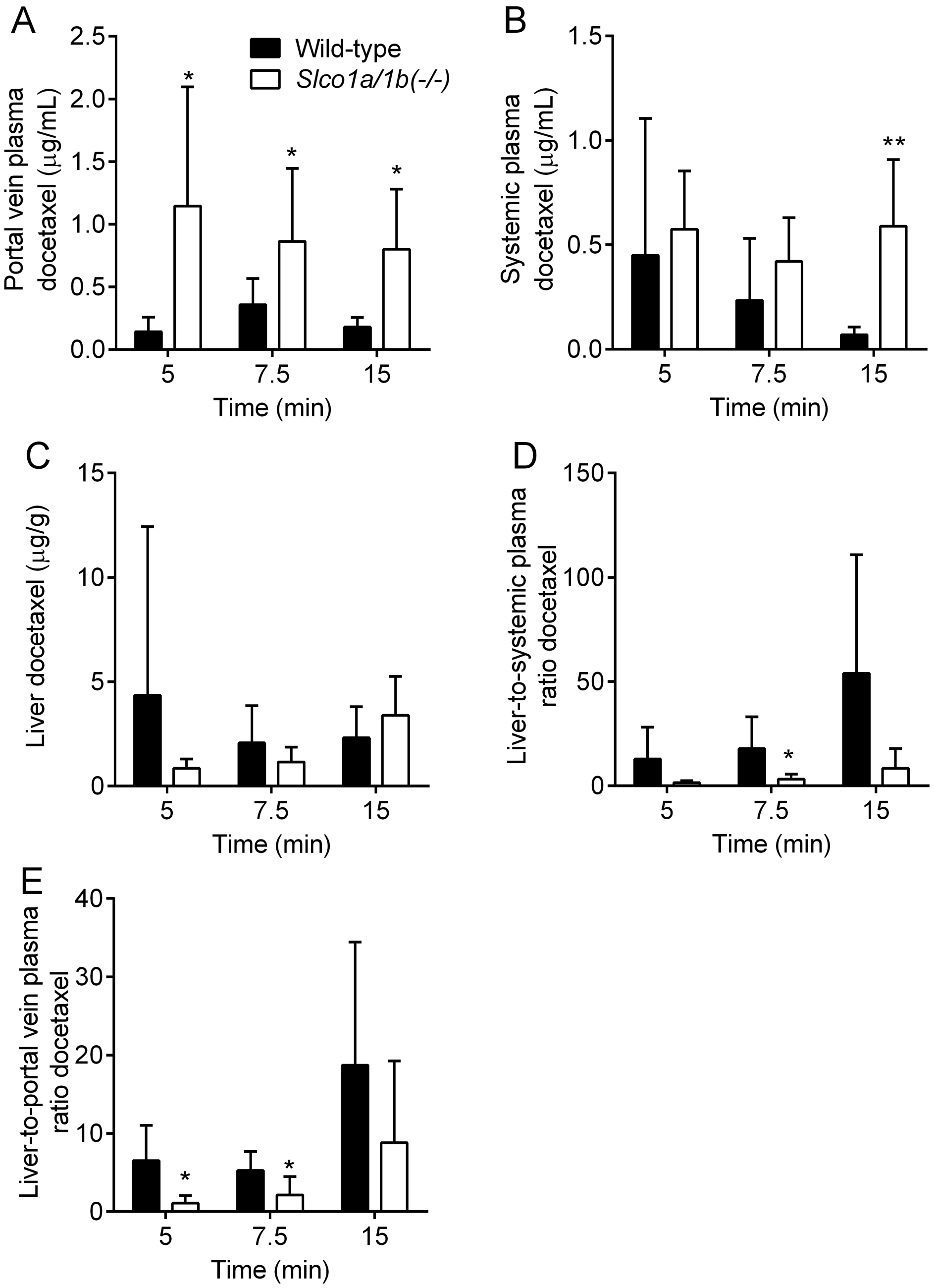

**Figure 3.** Mouse Oatp1a proteins are not essential for the intestinal absorption of docetaxel after oral administration (10 mg/kg) to male wild-type and Oatp1a/1b knockout mice. (A), docetaxel portal vein plasma concentrations and (B) docetaxel systemic plasma concentrations, (C) docetaxel liver levels in μg/g, (D) liver-to-systemic plasma ratios and (E) liver-to-portal vein plasma ratios. Averaged liver-to-systemic plasma (or portal vein plasma) ratios were calculated from individual mouse data. Data are presented as mean ± SD (n = 5-6, *, $P < 0.05$; **, $P < 0.01$ when compared with wild-type).

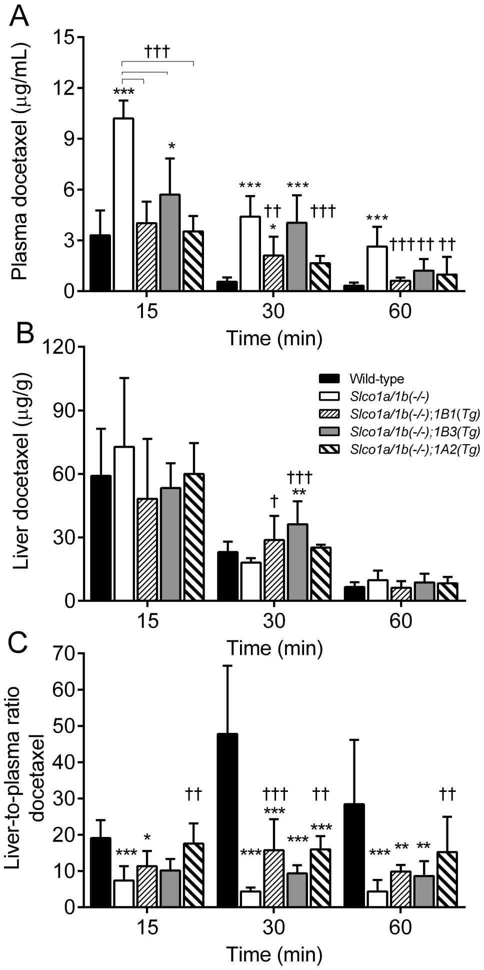

**Figure 4.** Human OATP1B1, OATP1B3 and OATP1A2 transport docetaxel *in vivo* after i.v. administration of docetaxel (10 mg/kg) to male wild-type, Oatp1a/1b knockout and OATP1B1, -1B3, and -1A2 transgenic mice. (A) Plasma concentrations of docetaxel, (B) docetaxel liver concentrations and (C) liver-to-plasma ratios of docetaxel. Averaged liver-to-systemic plasma ratios were calculated from individual mouse data. Data are presented as mean ± S.D. (n = 5-6, *, $P < 0.05$; **, $P < 0.01$; ***, $P < 0.001$ when compared with wild-type, $^{\dagger}$, $P < 0.05$; $^{\dagger\dagger}$, $P < 0.01$ ; $^{\dagger\dagger\dagger}$, $P < 0.001$ when compared with Oatp1a/1b knockout mice).

mice (Figure 4D). However, the liver-to-plasma ratios were not up to levels seen in wild-type mice (Figure 4D). This incomplete rescue is likely an underestimation of the actual OATP1B-mediated liver uptake in humans, as in human liver both OATP1B1 and OATP1B3 function at the same time, likely resulting in additive effects. Nevertheless, these results show that human OATP1B1, OATP1B3 and OATP1A2 can transport docetaxel *in vivo* and that all three transporters can compensate to an extent for the loss of the murine Oatp1a/1b transporters.

## *Discussion*

In the present study we found that mouse Oatp1a/1b transporters have an impact on the plasma clearance of docetaxel, while there is no clear effect on the liver exposure. Impaired liver uptake in the absence of Oatp1a/1b transporters was obvious in the markedly reduced liver-to-plasma ratios. Importantly, liver-specific expression of human OATP1B1, OATP1B3 or OATP1A2 provided extensive rescue of the increased plasma levels of docetaxel in Oatp1a/1b knockout mice. On the liver-to-plasma ratios this rescue was partial. These findings indicate that human OATP1A/1B uptake transporters can mediate the liver uptake of docetaxel *in vivo*, and can thus contribute to docetaxel hepatic clearance, and possibly docetaxel tumor uptake *in vivo*.

To our knowledge, we show here for the first time that OATP1A2 can transport docetaxel *in vivo* and that it can mediate docetaxel liver uptake. Because expression of OATP1A2 in human liver is restricted to cholangiocytes, the epithelial cells of the bile duct, the information provided by our humanized OATP1A2 mice (in which OATP1A2 is expressed in hepatocytes) has only a qualitative meaning. Nevertheless, this information is relevant for the function of OATP1A2 in other tissues like small intestine, kidney and the blood-brain barrier, where it might affect the oral uptake, urinary reabsorption or brain penetration of docetaxel [29-31]. The role of OATP1A2 in small intestine, and thus in the oral biovailibility of docetaxel remains unclear as in our study we observed that mouse Oatp1a transporters are not essential for the intestinal absorption of docetaxel. Nevertheless, when expressed in tumor cells, OATP1A2 can affect the susceptibility of these cells to docetaxel chemotherapy [13].

It has been described previously that human OATP1B1 and OATP1B3 can transport docetaxel *in vitro*, although there is wide variability dependent on the type of cellular uptake system used [1, 14, 15]. Transport activity of OATP1B1 or OATP1B3 can be reduced as a consequence of genetic variation (polymorphic variants) or pharmacological inhibition, leading to decreased liver uptake of docetaxel and thus impaired plasma clearance. There are only two clinical studies that show an association between low-activity polymorphisms in the gene encoding OATP1B3 and altered docetaxel pharmacokinetics [4] or docetaxel-induced neutropenia [32], while others investigating the impact of polymorphic variants of OATP1B1 or OATP1B3 on docetaxel pharmacokinetics and toxicity did not find any associations [1, 6, 14, 33]. Our data suggest that in the case of single polymorphisms affecting only one of the human OATP1B transporters, the remaining OATP1B1 or OATP1B3 can compensate for the loss of function of the other transporter. Accordingly, single polymorphisms in the OATP1B1 or OATP1B3 genes were not clearly associated with altered docetaxel clearance [14]. This is not the case for Rotor syndrome patients, which are deficient in both OATP1B1 and OATP1B3 [20], and might thus be at risk of developing life-threatening toxicity when treated with docetaxel. Also, clinically relevant drug-drug interactions might occur when docetaxel is co-administered with inhibitors of OATP1B transporters (e.g., rifampicin, cyclosporine, statins) or other OATP1B1 substrates (e.g., statins, methotrexate, paclitaxel) which might compete for transport into the liver [34] [35].

OATP1A/1B proteins have been found to be expressed in tumors of almost all the cancer types which are currently treated with docetaxel: colon, gastric, ovarian, breast and lung cancer (reviewed in [13, 36-38]) and OATP1A2 has also been found in the blood-brain barrier of gliomas [39]. Previous studies in our group showed that other anticancer drugs, namely methotrexate and paclitaxel, are also transported *in vivo* by human OATP1A/1B proteins [19]. These data might imply that *in vivo* expression and activity of OATP1A/1B transporters in various tumors might affect the tumor drug uptake, and hence influence their sensitivity to certain anticancer drugs

[36]. Direct studies involving sensitivity to docetaxel in cell lines derived from these tumor types are lacking so far, although there are indications that for paclitaxel and methotrexate, expression and activity of OATP1B1 and/or OATP1B3 transporters can increase sensitivity of tumors cells to these drugs [38, 40]. Moreover, there are several studies trying to correlate the tumor expression levels of OATPs with tumor development and prognosis [41, 42].

In this study we also investigated if Oatp1a mouse transporters expressed on the basolateral membrane of hepatocytes have an additional role to the reported role of mouse Oatp1b2 [14] in mediating the liver uptake, and hence the plasma clearance of docetaxel *in vivo*. However, a direct comparison between our study and the study by *de Graan et al* [14] is not as straightforward as expected, because we observed a 3-fold plasma AUC difference between Oatp1a/1b knockout mice and wild-type mice in our study, while *de Graan et al* noted a 26-fold difference in plasma AUC between Oatp1b2 knockout mice and their wild-type controls [14]. This was mainly due to a much lower plasma AUC in the wild-type mice used in the *de Graan et al* study in comparison with our wild-type mice. This difference could be caused by differences in genetic background, food and housing conditions between the FVB wild-type mice used here and the DBA1/lacJ wild-type mice used by *de Graan et al* [14]. They further observed only a 6.2-fold decrease in the liver-to-plasma AUC ratio, implying that the liver AUC itself was 4-fold increased in the Oatp1b2 knockout strain [14]. The 26.3-fold higher plasma AUC of docetaxel is perhaps surprising for a compound which appears to be modestly transported by various OATPs, including mouse Oatp1b2 *in vitro* [14]. However, possibly Oatp1b2 is very highly expressed in the liver of DBA1/lacJ wild-type mice compared to FVB mice.

There is another discrepancy with our study, in which we observed similar docetaxel liver concentrations in both wild-type and knockout strains. This is in line with the previously reported pharmacokinetic behavior of rosuvastatin [27] where reduced liver uptake (due to the absence of Oatp1a/1b transporters) resulted in marked changes in plasma exposure without affecting the liver concentrations. This pharmacokinetic behavior seems to be common for drugs with a low renal clearance and for which the liver uptake is the rate-limiting step, as appears to be the case for pravastatin, rosuvastatin and docetaxel. This behavior is in line with a physiologically-base pharmacokinetic model by Watanabe *et al* [43-45]. The 4-fold increased liver AUC of docetaxel in DBA1/lacJ Oatp1b2 knockout mice, with presumed reduced liver uptake rates of docetaxel, therefore remains unexplained. Perhaps additional, as yet unidentified other alterations have contributed to the profoundly changed docetaxel pharmacokinetics in these mice, even though a broad microarray screening of detoxifying genes did not yield obvious candidates. The model of Watanabe *et al* would predict an increase in liver AUC primarily as a consequence of diminished canalicular efflux activity. Possibly the activity (though not the expression) of one of the ABC transporters involved in docetaxel biliary excretion (ABCB1 or ABCC2) [45] was compromised in the Oatp1b2 knockout mice. Clearly, more work will be needed to fully understand all the aspects of Oatp1a/1b-mediated hepatic docetaxel clearance.

In line with previous studies [14, 24, 26], we here provide *in vivo* pharmacokinetic evidence that polysorbate 80 in higher concentrations can have an inhibitory effect on plasma clearance of docetaxel, probably by inhibiting Oatp1a/1b-mediated liver uptake. Perhaps new formulations, which have been extensively studied in past years, will provide a better alternative to current polysorbate 80 formulations (reviewed in [46, 47]).

Taken together, our results suggest that human OATP1A/1B uptake transporters can have multiple effects on the docetaxel therapeutic index, on the one hand by controlling its pharmacokinetics and toxicity, but also by possibly mediating its tumor uptake. OATP1A/1B transporters might thus represent a valuable target for improving chemotherapy. Further studies using humanized OATP1A/1B mice may help to better assess the *in vivo* impact of OATP1A/1B transporters on pharmacokinetics, toxicity and therapeutic outcome of anticancer drugs.

## *Reference List*

1. Baker SD, Verweij J, Cusatis GA, et al. Pharmacogenetic pathway analysis of docetaxel elimination. Clin Pharmacol Ther 2009;85:155-63.
2. Baker SD, Sparreboom A, Verweij J. Clinical pharmacokinetics of docetaxel : recent developments. Clin Pharmacokinet 2006;45:235-52.
3. van Herwaarden AE, Wagenaar E, van der Kruijssen CM, et al. Knockout of cytochrome P450 3A yields new mouse models for understanding xenobiotic metabolism. J Clin Invest 2007;117:3583-92.
4. Chew SC, Singh O, Chen X, et al. The effects of CYP3A4, CYP3A5, ABCB1, ABCC2, ABCG2 and SLCO1B3 single nucleotide polymorphisms on the pharmacokinetics and pharmacodynamics of docetaxel in nasopharyngeal carcinoma patients. Cancer Chemother Pharmacol 2011;67:1471-8.
5. Tran A, Jullien V, Alexandre J, et al. Pharmacokinetics and toxicity of docetaxel: role of CYP3A, MDR1, and GST polymorphisms. Clin Pharmacol Ther 2006;79:570-80.
6. Chew SC, Sandanaraj E, Singh O, et al. Influence of SLCO1B3 haplotype-tag SNPs on docetaxel disposition in Chinese nasopharyngeal cancer patients. Br J Clin Pharmacol 2012;73:606-18.
7. Kalliokoski A, Niemi M. Impact of OATP transporters on pharmacokinetics. Br J Pharmacol 2009;158:693-705.
8. Iusuf D, van de Steeg E, Schinkel AH. Functions of OATP1A and 1B transporters in vivo: insights from mouse models. Trends Pharmacol Sci 2012;33:100-8.
9. Hagenbuch B, Meier PJ. Organic anion transporting polypeptides of the OATP/ SLC21 family: phylogenetic classification as OATP/ SLCO superfamily, new nomenclature and molecular/functional properties. Pflugers Arch 2004;447:653-65.
10. Konig J, Seithel A, Gradhand U, Fromm MF. Pharmacogenomics of human OATP transporters. Naunyn Schmiedebergs Arch Pharmacol 2006;372:432-43.
11. Niemi M. Role of OATP transporters in the disposition of drugs. Pharmacogenomics 2007;8:787-802.
12. Klaassen CD, Aleksunes LM. Xenobiotic, bile acid, and cholesterol transporters: function and regulation. Pharmacol Rev 2010;62:1-96.
13. Cutler MJ, Choo EF. Overview of SLC22A and SLCO families of drug uptake transporters in the context of cancer treatments. Curr Drug Metab 2011;12:793-807.
14. de Graan AJ, Lancaster CS, Obaidat A, et al. Influence of polymorphic OATP1B-type carriers on the disposition of docetaxel. Clin Cancer Res 2012;18:4433-40.
15. Smith NF, Acharya MR, Desai N, Figg WD, Sparreboom A. Identification of OATP1B3 as a high-affinity hepatocellular transporter of paclitaxel. Cancer Biol Ther 2005;4:815-8.
16. Yamaguchi H, Kobayashi M, Okada M, et al. Rapid screening of antineoplastic candidates for the human organic anion transporter OATP1B3 substrates using fluorescent probes. Cancer Lett 2008;260:163-9.
17. Moes JJ, Koolen SL, Huitema AD, Schellens JH, Beijnen JH, Nuijen B. Pharmaceutical development and preliminary clinical testing of an oral solid dispersion formulation of docetaxel (ModraDoc001). Int J Pharm 2011;420:244-50.
18. van de Steeg E, van Esch A, Wagenaar E, et al. High impact of Oatp1a/1b transporters on in vivo disposition of the hydrophobic anticancer drug paclitaxel. Clin Cancer Res 2011;17:294-301.
19. van de Steeg E, van Esch A, Wagenaar E, Kenworthy KE, Schinkel AH. Influence of

human OATP1B1, OATP1B3, and OATP1A2 on the pharmacokinetics of methotrexate and paclitaxel in humanized transgenic mice. Clin Cancer Res 2012.

20. van de Steeg E, Stranecky V, Hartmannova H, et al. Complete OATP1B1 and OATP1B3 deficiency causes human Rotor syndrome by interrupting conjugated bilirubin reuptake into the liver. J Clin Invest 2012;122:519-28.
21. van de Steeg E, Wagenaar E, van der Kruijssen CM, et al. Organic anion transporting polypeptide 1a/1b-knockout mice provide insights into hepatic handling of bilirubin, bile acids, and drugs. J Clin Invest 2010;120:2942-52.
22. Kuppens IE, van Maanen MJ, Rosing H, Schellens JH, Beijnen JH. Quantitative analysis of docetaxel in human plasma using liquid chromatography coupled with tandem mass spectrometry. Biomed Chromatogr 2005;19:355-61.
23. Iusuf D, Sparidans RW, van Esch A, et al. Organic anion-transporting polypeptides 1a/1b control the hepatic uptake of pravastatin in mice. Mol Pharm 2012;9:2497-504.
24. Ten Tije AJ, Loos WJ, Verweij J, et al. Disposition of polyoxyethylated excipients in humans: implications for drug safety and formulation approaches. Clin Pharmacol Ther 2003;74:509-10.
25. van Tellingen O, Beijnen JH, Verweij J, Scherrenburg EJ, Nooijen WJ, Sparreboom A. Rapid esterase-sensitive breakdown of polysorbate 80 and its impact on the plasma pharmacokinetics of docetaxel and metabolites in mice. Clin Cancer Res 1999;5:2918-24.
26. Engel A, Oswald S, Siegmund W, Keiser M. Pharmaceutical excipients influence the function of human uptake transporting proteins. Mol Pharm 2012;9:2577-81.
27. Iusuf D, van Esch A, Hobbs MJ, et al. Murine Oatp1a/1b Uptake Transporters Control Rosuvastatin Systemic Exposure without Affecting Its Apparent Liver Exposure. Mol Pharmacol 2013.
28. Iusuf D, van de Steeg E, Schinkel AH. Hepatocyte hopping of OATP1B substrates contributes to efficient hepatic detoxification. Clin Pharmacol Ther 2012;92:559-62.
29. Gao B, Hagenbuch B, Kullak-Ublick GA, Benke D, Aguzzi A, Meier PJ. Organic anion-transporting polypeptides mediate transport of opioid peptides across blood-brain barrier. J Pharmacol Exp Ther 2000;294:73-9.
30. Glaeser H, Bailey DG, Dresser GK, et al. Intestinal drug transporter expression and the impact of grapefruit juice in humans. Clin Pharmacol Ther 2007;81:362-70.
31. Lee W, Glaeser H, Smith LH, et al. Polymorphisms in human organic anion-transporting polypeptide 1A2 (OATP1A2): implications for altered drug disposition and central nervous system drug entry. J Biol Chem 2005;280:9610-7.
32. Kiyotani K, Mushiroda T, Kubo M, Zembutsu H, Sugiyama Y, Nakamura Y. Association of genetic polymorphisms in SLCO1B3 and ABCC2 with docetaxel-induced leukopenia. Cancer Sci 2008;99:967-72.
33. Lewis LD, Miller AA, Owzar K, et al. The relationship of polymorphisms in ABCC2 and SLCO1B3 with docetaxel pharmacokinetics and neutropenia: CALGB 60805 (Alliance). Pharmacogenet Genomics 2013;23:29-33.
34. Karlgren M, Vildhede A, Norinder U, et al. Classification of inhibitors of hepatic organic anion transporting polypeptides (OATPs): influence of protein expression on drug-drug interactions. J Med Chem 2012;55:4740-63.
35. Hagenbuch B, Gui C. Xenobiotic transporters of the human organic anion transporting polypeptides (OATP) family. Xenobiotica 2008;38:778-801.
36. Obaidat A, Roth M, Hagenbuch B. The expression and function of organic anion transporting polypeptides in normal tissues and in cancer. Annu Rev Pharmacol Toxicol 2012;52:135-51.
37. Sissung TM, Reece KM, Spencer S, Figg WD. Contribution of the OATP1B subfamily to cancer biology and treatment. Clin Pharmacol Ther 2012;92:658-60.
38. Svoboda M, Wlcek K, Taferner B, et al. Expression of organic anion-transporting polypeptides 1B1 and 1B3 in ovarian cancer cells: relevance for paclitaxel transport. Biomed Pharmacother 2011;65:417-26.
39. Bronger H, Konig J, Kopplow K, et al. ABCC drug efflux pumps and organic anion uptake transporters in human gliomas and the blood-tumor barrier. Cancer Res 2005;65:11419-28.
40. Abe T, Kakyo M, Tokui T, et al. Identification of a novel gene family encoding human liver-specific organic anion transporter LST-1. J Biol Chem 1999;274:17159-63.
41. Maeda T, Irokawa M, Arakawa H, et al. Uptake transporter organic anion transporting polypeptide 1B3 contributes to the growth of estrogen-dependent breast cancer. J Steroid Biochem Mol Biol 2010;122:180-5.
42. Pressler H, Sissung TM, Venzon D, Price DK, Figg WD. Expression of OATP family members

in hormone-related cancers: potential markers of progression. PLoS One 2011;6:e20372.

43. Watanabe T, Kusuhara H, Sugiyama Y. Application of physiologically based pharmacokinetic modeling and clearance concept to drugs showing transporter-mediated distribution and clearance in humans. J Pharmacokinet Pharmacodyn 2010;37:575-90.
44. Yoon I, Han S, Choi YH, et al. Saturable sinusoidal uptake is rate-determining process in hepatic elimination of docetaxel in rats. Xenobiotica 2012;42:1110-9.
45. Watanabe T, Kusuhara H, Maeda K, Shitara Y, Sugiyama Y. Physiologically based pharmacokinetic modeling to predict transporter-mediated clearance and distribution of pravastatin in humans. J Pharmacol Exp Ther 2009;328:652-62.
46. Engels FK, Mathot RA, Verweij J. Alternative drug formulations of docetaxel: a review. Anticancer Drugs 2007;18:95-103.
47. Hennenfent KL, Govindan R. Novel formulations of taxanes: a review. Old wine in a new bottle? Ann Oncol 2006;17:735-49.

# Role of efflux transporters in the brain accumulation and oral bioavailability of anticancer drugs

# 5

# Introduction: Single and combined roles of P-gp (ABCB1) and ABCG2 (BCRP) efflux transporters in brain disposition and oral bioavailability of anticancer drugs

# 5.1

Dilek Iusuf and Alfred H. Schinkel

Division of Molecular Oncology, The Netherlands Cancer Institute,
Amsterdam, The Netherlands

ATP-binding cassette (ABC) transporters represent a superfamily of transmembrane proteins which are expressed throughout the body, where they efficiently efflux a broad variety of endogenous and exogenous substrates from cells. The best studied members of the ABC transporter family are the multidrug transporters, P-glycoprotein (Pgp, ABCB1, MDR1), Breast Cancer Resistance Protein (BCRP, ABCG2) and MRP1-4 (ABCC1-4) [1]. Because of their localization in pharmacokinetically relevant tissues (liver, small intestine, kidney, brain) and their capacity to transport a wide range of drugs, these transporters are considered major determinants of drug disposition, efficacy and toxicity [2]. They are also often found in cancer cells where they can mediate resistance to anticancer drugs, by limiting the effective concentrations in the tumor cells [1].

In this thesis, we focused on two of the most important members of this family, ABCB1 and ABCG2, which are expressed in the apical membrane of hepatocytes, i.e., the bile canaliculi (in the liver), of enterocytes (in the small and large intestine), and in the kidney in the apical membrane of proximal tubular epithelial cells, where they efflux their substrates into bile, feces and urine, respectively [3]. Their function in the small intestine can have direct clinical consequences for the bioavailability of substrate drugs which are administered orally. In addition to the above-mentioned tissues, ABCB1 and ABCG2 are also expressed at the blood-placenta, blood-testis and blood-brain barriers, where they protect these sanctuary tissues from penetration of harmful compounds [3].

The function of these transporters can be studied among others *in vitro* using stably transfected epithelial kidney cell lines (which grow as monolayers on a filter) overexpressing the ABCB1 or ABCG2 transporters in the apical membrane. By comparing the rate of translocation from apical to basolateral and basolateral to apical, new drug substrates can be identified [1]. Also widely used are the *in vivo* ABC transporter knockout mouse models to study the functions of these transporters in the context of systemic exposure and systemic disposition of drugs [1].

The first pharmacological ABC transporter mouse knockout model described was the *Abcb1a(-/-)* strain. Abcb1a encodes one of the two mouse genes fulfilling the same function as the single human ABCB1 (P-gp) gene [4]. In the mouse, Abcb1a is expressed at the blood-brain barrier and in the small intestine, while Abcb1b is not. Therefore, *Abcb1a(-/-)* knockout mice have been extensively used to elucidate the function of P-gp in brain penetration and oral availability of drugs [4, 5], while Abcb1b knockout mice were hardly used for pharmacological studies. This was also because compound knockout mice lacking both the mouse *Abcb1a* and *Abcb1b* genes, *Abcb1a/1b(-/-)* knockout mice, were soon also available and they proved to be a simpler model to understand the function of P-gp *in vivo* [6, 7]. In chapter 6.2 of this thesis, we used these mice to study the impact of P-gp on the brain disposition of tamoxifen and its metabolites. Absence of P-gp resulted in increased brain accumulation of orally administered tamoxifen and its metabolites without affecting their serum concentrations. Brain accumulation of endoxifen, the 100-fold more active metabolite of tamoxifen, was 10-fold increased in the *Abcb1a/1b(-/-)* mice and we could demonstrate that endoxifen is also a transported substrate of human ABCB1 *in vitro* [8].

ABCG2 (BCRP) is another ABC transporter which is rather similar to P-gp in substrate specificity, tissue distribution and therefore functionality. Single *Abcg2(-/-)* mice have been used to elucidate some of the protective functions of Abcg2 at the blood-brain, blood-testis and blood-fetal barriers [9]. Compound knockout mice, *Abcb1a/1b;Abcg2(-/-)*, were generated in order to distinguish between their separate and overlapping contributions to drug disposition [10]. These mice were especially useful to study the single and combined role of Abcb1 and/or Abcg2 transporters at the blood-barrier. Previous studies have found that brain penetration of topotecan [11] and several tyrosine kinase inhibitors was disproportionally increased in the *Abcb1a/1b;Abcg2(-/-)* knockout mice [12-15] in comparison with either wild-type mice or single *Abcb1a/1b(-/-)* mice or *Abcg2(-/-)* knockout mice, indicating that for many drugs transported by both ABCB1 and ABCG2, loss of either ABCB1 or ABCG2 at the blood-brain barrier can be largely compensated by the activity of the remaining transporter [2].

This concept is illustrated experimentally in chapter 6.3 of this thesis, where we investigated the oral availability and brain accumulation of the novel tyrosine kinase inhibitor and anticancer drug, axitinib. We demonstrated that Abcb1 and Abcg2 have a differential impact on the brain accumulation and oral availability of axitinib. Specifically, at the blood-brain barrier Abcb1 is the main determinant of axitinib brain accumulation and it can completely compensate for the loss of Abcg2, while Abcg2 can only partially take over the function of Abcb1. In contrast, in the intestine, Abcg2 has a strong impact on the oral availability of axitinib, while the role of Abcb1 is negligible [16].

In the two studies on this subject described in this thesis, we used single and combination knockout mice of efflux transporters to study the oral availability and brain penetration of the anticancer drugs tamoxifen and axitinib. These results might have clinical relevance for resistance to treatment with tamoxifen or axitinib of tumors overexpressing P-gp and/or ABCG2, but also for brain tumors positioned behind an intact and functional blood-brain barrier.

## *Reference List*

1. Borst P, Elferink Oude RP. Mammalian ABC transporters in health and disease. Annu Rev Biochem 2002;71:537-92.
2. Lagas JS, Vlaming ML, Schinkel AH. Pharmacokinetic assessment of multiple ATP-binding cassette transporters: the power of combination knockout mice. Mol Interv 2009;9:136-45.
3. Schinkel AH, Jonker JW. Mammalian drug efflux transporters of the ATP binding cassette (ABC) family: an overview. Adv Drug Deliv Rev 2003;55:3-29.
4. Schinkel AH, Smit JJ, van Tellingen O, et al. Disruption of the mouse mdr1a P-glycoprotein gene leads to a deficiency in the blood-brain barrier and to increased sensitivity to drugs. Cell 1994;77:491-502.
5. Schinkel AH, Wagenaar E, van Deemter L, Mol CA, Borst P. Absence of the mdr1a P-Glycoprotein in mice affects tissue distribution and pharmacokinetics of dexamethasone, digoxin, and cyclosporin A. J Clin Invest 1995;96:1698-705.
6. Schinkel AH, Mayer U, Wagenaar E, et al. Normal viability and altered pharmacokinetics in mice lacking mdr1-type (drug-transporting) P-glycoproteins. Proc Natl Acad Sci U S A 1997;94:4028-33.
7. Schinkel AH. Pharmacological insights from P-glycoprotein knockout mice. Int J Clin Pharmacol Ther 1998;36:9-13.
8. Iusuf D, Teunissen SF, Wagenaar E, Rosing H, Beijnen JH, Schinkel AH. P-glycoprotein (ABCB1) transports the primary active tamoxifen metabolites endoxifen and 4-hydroxytamoxifen and restricts their brain penetration. J Pharmacol Exp Ther 2011;337:710-7.
9. Vlaming ML, Lagas JS, Schinkel AH. Physiological and pharmacological roles of ABCG2 (BCRP): recent findings in Abcg2 knockout mice. Adv Drug Deliv Rev 2009;61:14-25.
10. Jonker JW, Freeman J, Bolscher E, et al. Contribution of the ABC transporters Bcrp1 and Mdr1a/1b to the side population phenotype in mammary gland and bone marrow of mice. Stem Cells 2005;23:1059-65.

11. de Vries NA, Zhao J, Kroon E, Buckle T, Beijnen JH, van Tellingen O. P-glycoprotein and breast cancer resistance protein: two dominant transporters working together in limiting the brain penetration of topotecan. Clin Cancer Res 2007;13:6440-9.
12. Kodaira H, Kusuhara H, Ushiki J, Fuse E, Sugiyama Y. Kinetic analysis of the cooperation of P-glycoprotein (P-gp/Abcb1) and breast cancer resistance protein (Bcrp/Abcg2) in limiting the brain and testis penetration of erlotinib, flavopiridol, and mitoxantrone. J Pharmacol Exp Ther 2010;333:788-96.
13. Lagas JS, van Waterschoot RA, van Tilburg VA, et al. Brain accumulation of dasatinib is restricted by P-glycoprotein (ABCB1) and breast cancer resistance protein (ABCG2) and can be enhanced by elacridar treatment. Clin Cancer Res 2009;15:2344-51.
14. Lagas JS, van Waterschoot RA, Sparidans RW, Wagenaar E, Beijnen JH, Schinkel AH. Breast cancer resistance protein and P-glycoprotein limit sorafenib brain accumulation. Mol Cancer Ther 2010;9:319-26.
15. Oostendorp RL, Buckle T, Beijnen JH, van Tellingen O, Schellens JH. The effect of P-gp (Mdr1a/1b), BCRP (Bcrp1) and P-gp/BCRP inhibitors on the in vivo absorption, distribution, metabolism and excretion of imatinib. Invest New Drugs 2009;27:31-40.
16. Poller B, Iusuf D, Sparidans RW, Wagenaar E, Beijnen JH, Schinkel AH. Differential impact of P-glycoprotein (ABCB1) and breast cancer resistance protein (ABCG2) on axitinib brain accumulation and oral plasma pharmacokinetics. Drug Metab Dispos 2011;39:729-35.

# 5.2

# P-glycoprotein (Abcb1) transports the primary active tamoxifen metabolites endoxifen and 4-hydroxytamoxifen and restricts their brain penetration

Dilek Iusuf*[1], Sebastiaan F. Teunissen*[2], Els Wagenaar[1],
Hilde Rosing[2], Jos H. Beijnen[2], and Alfred H. Schinkel[1],

* contributed equally

[1]Division of Molecular Oncology, The Netherlands Cancer Institute,
[2]Department of Pharmacy & Pharmacology,
Slotervaart Hospital, Amsterdam, The Netherlands

*Journal of Pharmacology and Experimental Therapeutics, 2011*

## *Abstract*

P-glycoprotein (P-gp, ABCB1) is a highly efficient drug efflux pump expressed in brain, liver, and small intestine, but also in tumor cells, that affects pharmacokinetics and confers therapy resistance for many anticancer drugs. The aim of this study was to investigate the impact of P-gp on tamoxifen and its primary active metabolites, 4-hydroxytamoxifen, *N*-desmethyltamoxifen, and endoxifen. We used in vitro transport assays and *Abcb1a/1b*(-/-) mice to investigate the impact of P-gp on the oral availability and brain penetration of tamoxifen and its metabolites. Systemic exposure of tamoxifen and its metabolites after oral administration of tamoxifen (50 mg/kg) was not changed in the absence of P-gp. However, brain accumulation of tamoxifen, 4-hydroxytamoxifen, and *N*-desmethyltamoxifen were modestly, but significantly (1.5- to 2-fold), increased. Endoxifen, however, displayed a 9-fold higher brain penetration at 4 h after administration. Endoxifen was transported by P-gp in vitro. Upon direct oral administration of endoxifen (20 mg/kg), systemic exposure was slightly decreased in *Abcb1a/1b*(-/-) mice, but brain accumulation of endoxifen was dramatically increased (up to 23-fold at 4 h after administration). Shortly after high-dose intravenous administration (5 or 20 mg/kg), endoxifen brain accumulation was increased only 2-fold in *Abcb1a/1b*(-/-) mice compared with wild-type mice, suggesting a partial saturation of P-gp at the blood-brain barrier. Endoxifen, the clinically most relevant metabolite of tamoxifen, is a P-gp substrate in vitro and in vivo, where P-gp limits its brain penetration. P-gp might thus be relevant for tamoxifen/endoxifen resistance of P-gp-positive breast cancer and tumors positioned behind a functional blood-brain barrier.

## Introduction

Discovered in the late 1960s, tamoxifen remains the most widely used drug for patients with early-stage breast cancer and estrogen receptor (ER)-positive tumors [1]. Active against all stages of hormone-dependent breast cancer, it was only recently fully realized that tamoxifen owes its efficacy mainly to its active metabolites, 4-hydroxytamoxifen and endoxifen (*N*-desmethyl-4-hydroxytamoxifen). These metabolites exhibit a 100-fold higher binding affinity to the ER and are more effective in suppressing cell proliferation than tamoxifen [2-4]. In humans, the conversion from tamoxifen to endoxifen is predominant, whereas the conversion via 4-hydroxytamoxifen is much lower. *N*-desmethyltamoxifen is another important metabolite in these pathways, exhibiting similar activity to tamoxifen (Supplemental Figure 1). Therefore, circulating concentrations of endoxifen are considerably higher than those of 4-hydroxytamoxifen, pointing to endoxifen as the clinically most relevant metabolite [5-7]. Tamoxifen and its metabolites can occur in two (geometric) isomeric forms, *Z* or *E*, and in general the (*Z*)-isomers are pharmacodynamically active [8]. (*Z*)-tamoxifen is the isomer used in the clinic for its antiestrogenic effects, and, upon metabolism in vivo, the (*Z*)-isomers of the metabolites are predominantly formed, whereas the amount of (*E*)-isomers formed through interconversion is negligible [8].

In addition to its ER-mediated effects against breast cancer cells, tamoxifen is reported to be active against brain metastases of ER-positive breast cancer or glioma. These effects are possibly also mediated via inhibition of the protein kinase C pathway [9;10]. Endoxifen exhibits similar effects as tamoxifen on protein kinase C, but its efficacy against brain cancers has not been tested (Ali et al., 2010). Nevertheless, the accessibility of these compounds to the brain tissue (or tumor) might be functionally impaired by the presence of P-gp (ABCB1, MDR1), an efflux pump that is expressed on the apical membrane of endothelial cells forming the blood-brain barrier, where it efficiently restricts the brain accumulation of a broad range of compounds (reviewed in 12).

Clinically, poor response to tamoxifen treatment can be partially explained by polymorphisms in the gene encoding CYP2D6, the enzyme primarily responsible for the formation of endoxifen, leading to vast interindividual differences in endoxifen circulating concentrations and response to therapy [13; 14]. However, the role of the CYP2D6 genotype alone in predicting tamoxifen-associated outcomes remains controversial. In addition, tamoxifen resistance could perhaps be mediated via P-gp, which has been described to be expressed in the membrane of various breast cancer cells (15). Studies conducted in a small number of breast cancer patients indicate that P-gp (over)expression correlates with a poor response to tamoxifen therapy [16-18].

However, although tamoxifen can interact with P-gp in vitro, it has not been found to be a substrate for transport [19-21]. Regarding the active metabolites, endoxifen and 4-hydroxytamoxifen, knowledge about their transport properties by P-gp (or by the breast cancer resistance protein, BCRP/ABCG2) is lacking. The aim of this study was to investigate the role of P-gp in serum pharmacokinetics and brain accumulation of tamoxifen and its active metabolites in vivo. Furthermore, we focused on the ability of P-gp to transport endoxifen in vitro and the impact of P-gp on serum pharmacokinetics and brain penetration of endoxifen after direct administration of endoxifen in vivo. We were also interested in which factors can lead to the saturation of P-gp at the blood-brain barrier, such as dosage or route of administration.

## Materials and Methods

### Chemicals

Tamoxifen, 4-hydroxytamoxifen, and *N*-desmethyl-4- hydroxytamoxifen (endoxifen) (1:1, *E/Z* mixture) were purchased from Toronto Research Chemicals Inc. (North York, ON, Canada). Zosuquidar (Eli Lilly & Co., Indianapolis, IN) was a generous gift from Dr. Olaf van Tellingen (The Netherlands Cancer Institute, Amsterdam, The Netherlands). $[^{14}C]$Inulin was from GE Healthcare (Chalfont St. Giles, Buckinghamshire, UK). Isoflurane (Forane) was from Abbott Laboratories (Queenborough, Kent, UK). Bovine serum albumin was from Roche Diagnostics (Mannheim, Germany). All other chemicals and reagents were obtained from Sigma-Aldrich (Steinheim, Germany).

### Transport assays

Transport assays in the polarized canine kidney cell line MDCKII and subclones transduced with human ABCB1 [22] were performed as described previously with minor modifications [23]. Experiments were done in the presence or absence of 5 pM zosuquidar, a specific inhibitor of P-gp [24]. When zosuquidar was applied, it was present in both compartments during a 2-h preincubation period and during the transport experiment. After preincubation, the experiment was started (*t* = 0 h) by replacing the medium with fresh Dulbecco's modified Eagle's medium, containing 10% fetal calf serum and 5 pM endoxifen with or without 5 pM zosuquidar. Cells were incubated at 37°C in 5% $CO_2$. Aliquots (100 pl) were taken at 4 and 8 h. Transport was calculated as the fraction of drug recovered in the acceptor compartment versus the fraction added in the donor compartment at the beginning of the experiment. Data are represented as mean ± S.D. (*n* = 3). Transport ratios were calculated by dividing apically directed translocation by basolaterally directed translocation of endoxifen. Tightness of the monolayers was determined in parallel by measuring paracellular $[^{14}C]$inulin leakage (--4 kBq/well) in the same cells seeded and cultured the same way. Inulin leakage had to remain below 1% per hour. At the end of the experiment filters with cell layers were washed twice with ice-cold phosphate-buffered saline, excised, and mixed with 500 pl of ice-cold methanol, followed by mixing for 15 min and centrifugation at 5000 rpm (2100*g*) for 5 min at 4°C. The protein and endoxifen concentrations were determined in the resulting supernatant.

### Animals

All mice were housed and handled according to the institutional guidelines complying with Dutch legislation. Animals used for this study were females of >99% FVB genetic background between 8 and 12 weeks of age. Two strains were used for experiments: wild-type and *Abcb1a/1b*(-/-) mice [25], which lack both functional *Abcb1a* and *Abcb1b* genes, that together fulfill the functions of the single human *ABCB1* gene. Animals were kept in a temperature-controlled environment with a 12-h light/12-h dark cycle and received a standard diet (AM-II; Hope Farms, Woerden, The Netherlands) and acidified water ad libitum.

### *Plasma pharmacokinetics and brain accumulation after oral administration of tamoxifen or endoxifen*

Tamoxifen was dissolved in Tween/ethanol (1:1, v/v) (at 20 mg/ml), 4-fold diluted with 0.9% NaCl (to 5 mg/ml) and administered orally at 50 mg/kg (10 ml/kg mouse). Endoxifen (1:1, *E/Z* mixture) was dissolved in Tween/ ethanol (1:1, v/v) (at 8 mg/ml), 4-fold diluted with 0.9% NaCl (to 2 mg/ml), and administered orally at 20 mg/kg (10 ml/kg). To reduce variation in absorption rates, mice ($n$ = 5 per group) were fasted at least 3 h before tamoxifen or endoxifen was given by gavage into the stomach using a blunt-ended needle. Multiple blood samples (--50 pl) were collected from the tail vein at 0.25, 0.5, 1, or 2 h in 0.75-ml Eppendorf tubes. At 4 h blood was isolated via cardiac puncture under isoflurane anesthesia followed by cervical dislocation. In an independent experiment, 1 h after administration of tamoxifen or endoxifen, blood was isolated via cardiac puncture under isoflurane anesthesia followed by cervical dislocation. Brains were rapidly removed, homogenized on ice in 2 ml of 4% (w/v) bovine serum albumin, and stored at –30°C until analysis. Serum was obtained by centrifugation of the coagulated blood samples (allowed to clot for a minimum of 1 h at room temperature) at 5000 rpm (2100*g*) for 6 min at 4°C.

### *Serum pharmacokinetics and brain accumulation after intravenous administration of endoxifen*

Endoxifen (1:1, *E/Z* mixture) was dissolved in Tween/ethanol (1:1, v/v) (4 or 16 mg/ml), 4-fold diluted with 0.9% NaCl (to 1 or 4 mg/ml) and was administered intravenously at 5 or 20 mg/kg (5 ml/kg) in the tail vein of the mice. Fifteen minutes after administration blood was collected via cardiac puncture under isoflurane anesthesia followed by cervical dislocation. Brain and blood were processed and stored as described above.

### *Drug analysis*

Concentrations of tamoxifen and its metabolites in Dulbecco's modified Eagle's medium, serum, and brain homogenate were analyzed by a validated liquid chromatography-tandem mass spectrometry assay as described previously [26]. (*Z*)- and (*E*)-endoxifen were quantified separately in this assay.

### *RNA isolation, cDNA synthesis, and RT-PCR*

RNA isolation from mouse small intestine and liver and subsequent cDNA analysis and RT-PCR were performed as described previously [27]. Specific primers (QIAGEN GmbH, Hilden, Germany) were used to detect expression levels of the following mouse genes: *Cyp3a11*, *Cyp3a13*, *Cyp3a25*, *Cyp2c38*, *Cyp2c55*, *Cyp2c65*, *Cyp2c66*, *Abcc2*, and *Abcg2*.

### *Pharmacokinetic calculations and statistical analysis*

The AUC was calculated using the trapezoidal rule, without extrapolating to infinity. Brain concentrations of tamoxifen and its metabolites, including endoxifen, were corrected by the amount of drug in the brain vasculature, which corresponded to 1.4% of the serum concentration at the respective time points [28]. Relative brain accumulation (brain-to-serum ratio) was calculated by dividing brain concentrations at $t$ = 0.25, 1 or 4 h by the serum concentrations at the respective time points. To test the statistical significance, we performed a Student's $t$ test, and differences were considered significant when $P < 0.05$. Data are presented as means ± S.D.

# Results

## *Effect of P-gp on serum pharmacokinetics of tamoxifen and its metabolites after oral administration of tamoxifen*

Because tamoxifen is administered orally to patients, we chose to study its serum pharmacokinetics after oral administration at 50 mg/kg to wild-type and *Abcb1a/ 1b*(-/-) mice. In humans, the conversion to endoxifen is predominant over the conversion to 4-hydroxytamoxifen. Our preliminary studies showed that in mice the situation is reversed, with much higher levels of 4-hydroxytamoxifen (Supplemental Figure 1; Figure 1, A versus B and C). Therefore, we chose a relatively high dosage (relative to the regular prescribed human dosage of 20 mg daily dose) to obtain serum levels of tamoxifen and its most clinically relevant metabolite (endoxifen) in mice similar to steady-state serum concentrations in patients [29]. As shown in Figure 1 and Table 1, serum concentrations and AUC(0–4h) for tamoxifen, 4-hydroxytamoxifen, *N*-desmethyltamoxifen, and (*Z*)-endoxifen were not significantly different between the two mouse strains. These results suggest that the absence of P-gp does not significantly affect the oral uptake or elimination of tamoxifen or the formation and elimination of its metabolites.

## *Effect of P-gp on brain accumulation of tamoxifen and its metabolites after oral administration of tamoxifen*

Despite the similar serum levels, brain accumulation of tamoxifen and its metabolites was significantly increased in the absence of P-gp (Figure 2). Tamoxifen showed a modest, but significant, increase (1.6-fold, $P < 0.05$) in brain concentration in the P-gp knockout mice at 4 h after oral administration (Figure 2A). When represented as brain-to-serum ratios the difference between the two strains became significant at 1 h after administration (Table 1). 4-Hydroxytamoxifen and *N*-desmethyltamoxifen exhibited somewhat larger effects, with 2- to 2.3-fold ($P < 0.001$) higher brain levels (represented as absolute concentrations or brainto-serum ratios) in *Abcb1a/ 1b*(-/-) mice at 4 h after administration (Figure 2, B and C; Table 1). The most affected compound was the clinically relevant metabolite, (*Z*)-endoxifen, which showed increases in brain concentrations in the P-gp knockout mice of 6-fold ($P < 0.01$) and 9.4-fold ($P < 0.001$) at 1 and 4 h after tamoxifen administration, respectively. Brain-to-serum ratios gave similar results (Table 1).

For some compounds, it has been reported that P-gp and Abcg2 (Bcrp1) can have additive or even seemingly synergistic effects in restricting drug accumulation into the brain (23). However, pilot experiments including *Abcg2*- and *Abcb1a/1b;Acbg2*-deficient mice failed to indicate any in vivo impact of Abcg2 on serum or brain disposition of tamoxifen and its active metabolites (data not shown). It thus seems highly unlikely that tamoxifen or its metabolites are substantially affected by BCRP/ABCG2, and we therefore did not pursue this further.

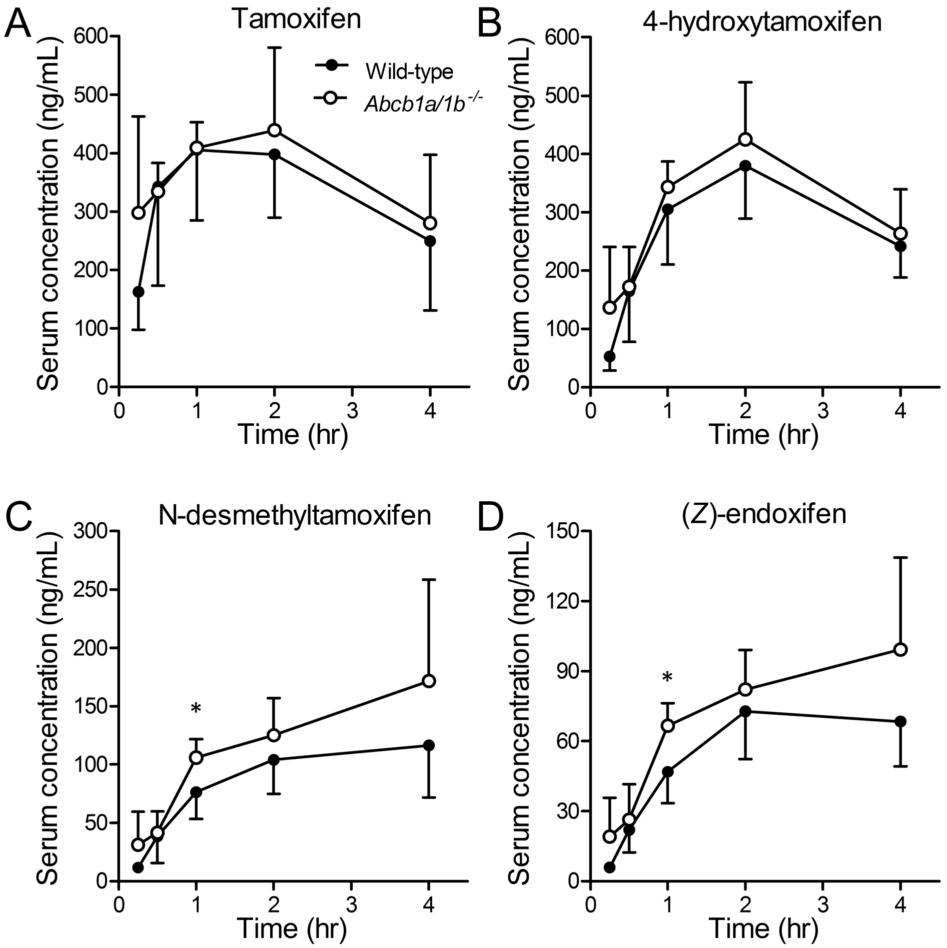

**Figure 1.** Serum concentration versus time curves of tamoxifen (A), 4-hydroxytamoxifen (B), N-desmethyltamoxifen (C), and (Z)-endoxifen (D) after oral administration of 50 mg/kg tamoxifen to female wild-type and P-gp knockout mice [*Abcb1a/1b(-/-)*]. Points, means; bars, S.D. (n = 5). *, $P < 0.05$ compared with wild type. Note differences in y-axis scales.

**Table 1.** Serum $AUC_{(0-4)}$, serum concentrations, and brain-to-serum ratios of tamoxifen and its metabolites in mice at 1 or 4 h after oral administration of 50 mg/kg tamoxifen. Note that the *t* = 1 h data represent an independent experiment from *t* = 4 h.

| | | **Tamoxifen** | | ***N*-Desmethyltamoxifen** | | **4-Hydroxytamoxifen** | | **(*Z*)-Endoxifen** | |
|---|---|---|---|---|---|---|---|---|---|
| **Time** | | **WT** | ***Abcb1a/1b*(-/-)** | **WT** | ***Abcb1a/1b*(-/-)** | **WT** | ***Abcb1a/1b*(-/-)** | **WT** | ***Abcb1a/1b*(-/-)** |
| | $AUC_{(0-4)}$, ng/l · h | 1319 ± 201 | 1445 ± 188 | 347 ± 52 | 462 ± 72 | 1114 ± 133 | 1257 ± 137 | 230 ± 78 | 287 ± 36 |
| 1 h | Serum (ng/ml) | 412 ± 151 | 289 ± 114 | 59.4 ± 26.2 | 34.3 ± 13.3 | 235 ± 66 | 178 ± 52 | 36.1 ± 9.8 | 28.2 ± 6.3 |
| | Brain/serum ratio | 8.1 ± 1.1 | 10.5 ± 1.8* | 6.6 ± 3.2 | 8.3 ± 2.3 | 4.9 ± 1.4 | 7.7 ± 1.5* | 0.6 ± 0.1 | 2.9 ± 1.1* |
| | Fold increase | 1 | 1.3 | 1 | 1.3 | 1 | 1.6 | 1 | 5.0 |
| 4 h | Serum (ng/ml) | 249 ± 119 | 280 ± 117 | 116 ± 45 | 172 ± 87 | 242 ± 53 | 263 ± 76 | 68.5 ± 19.3 | 99.1 ± 39.5 |
| | Brain/serum ratio | 23.4 ± 2.3 | 36.4 ± 7.8** | 8.0 ± 1.3 | 15.8 ± 2.6*** | 9.1 ± 1.7 | 20.7 ± 5.1** | 1.5 ± 0.6 | 9.7 ± 2.6*** |
| | Fold increase | 1 | 1.6 | 1 | 2 | 1 | 2.3 | 1 | 6.4 |

* $P < 0.05$;

** $P < 0.01$;

*** $P < 0.001$ compared with wild type.

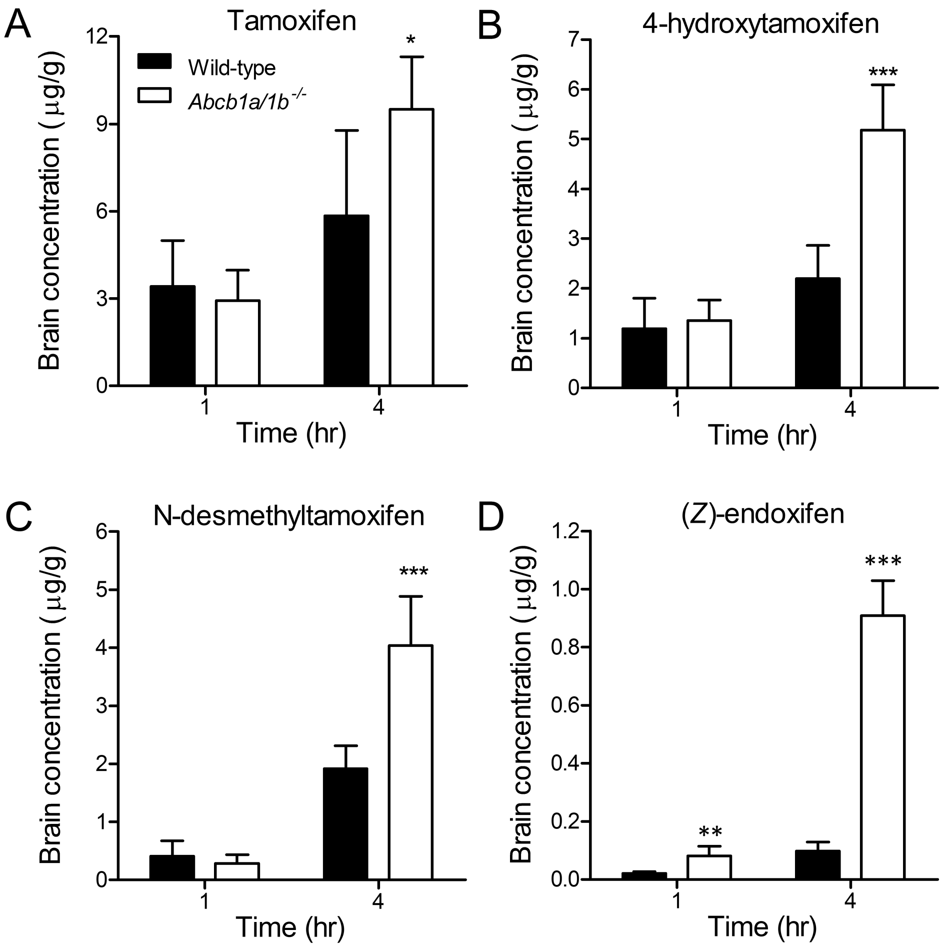

**Figure 2.** Brain concentrations of tamoxifen (A), 4-hydroxytamoxifen (B), *N*-desmethyltamoxifen (C), and (*Z*)-endoxifen (D) at 1 and 4 h after oral administration of 50 mg/kg tamoxifen to female wild-type and P-gp knockout mice [*Abcb1a/1b*(-/-)]. Columns, means; bars, S.D. ($n = 5$). *, $P < 0.05$; **, $P < 0.01$; ***, $P < 0.001$ compared with wild type. Note differences in *y*-axis scales.

### *In vitro transport of endoxifen*

Because we observed a pronounced effect of P-gp on in vivo brain penetration of endoxifen after oral administration of tamoxifen, we investigated endoxifen as an in vitro substrate of ABCB1 by testing its transepithelial transport in polarized monolayers of MDCKII cells stably transduced with ABCB1. Because pure (*Z*)-endoxifen was not available to us, endoxifen was applied as a 1:1 mixture of two isomers, (*Z*)- and (*E*)-endoxifen, which were quantified and represented separately. In parental cells, there was no significant polarized transport of (*Z*)-endoxifen (Figure 3, A and B). In contrast, in the ABCB1- transduced cells there was clear apically directed transport of (*Z*)-endoxifen (Figure 3C), which was completely inhibited in the presence of the P-gp-specific inhibitor zosuquidar (Figure 3D). (*E*)-endoxifen showed virtually identical quantitative results (Supplemental Figure 2), indicating that both isomers are equally good P-gp substrates in vitro and otherwise have similar membrane permeation properties. The intracellular concentration of both isomers in the monolayers of the trans-well assay at the end of the experiment was significantly reduced in the ABCB1-expressing cells compared with the parental cells, from 1.52 ± 0.17 to 0.93 ± 0.1 ng/pg protein (1.6-fold, $P < 0.01$) for (*Z*)-endoxifen and 1.63 ± 0.08 to 0.89 ± 0.09 ng/pg protein (1.8-fold, $P < 0.001$) for (*E*)-endox- ifen. This indicates that P-gp reduces the intracellular accumulation of endoxifen.

### *Effect of P-gp on endoxifen serum pharmacokinetics after oral administration of endoxifen*

Because it has been recognized that the main pharmacodynamically active component of tamoxifen is most likely endoxifen, researchers have considered direct administration of endoxifen, circumventing the complications of interindividually variable conversion of tamoxifen to endoxifen by CYP2D6 (5,b). We therefore administered endoxifen (1:1, *E/Z* mixture) directly at an oral dose of 20 mg/kg to wild-type and *Abcb1a/1b*(-/-) mice. Somewhat unexpectedly, both (*Z*)- and (*E*)-endoxifen serum concentrations and AUC(0–4h) were modestly, but significantly, lower (33–37%) in *Abcb1a/1b* knockout versus wild-type mice (Figure 4A; Supplemental Figure 3A; Supplemental Table 1). Alternative detoxifying mechanisms whose expression is modestly up-regulated in the small intestine (but not in the liver) of *Abcb1a/ 1b*(-/-) mice as judged by RT-PCR, for instance, the metabolizing enzymes Cyp3a11, Cyp3a25, Cyp2c55, and Cyp2c65, might perhaps explain the decreased oral availability (Supplemental Table 2). In addition, slightly increased expression of efflux transporters such as Abcc2 might have an additional role in limiting oral exposure (Supplemental Table 2). It should be noted, though, that very little is known about the impact of these or other detoxifying systems on endoxifen disposition.

### *Effect of P-gp on endoxifen brain accumulation after oral administration of endoxifen*

In contrast to the somewhat decreased serum exposure of (*Z*)-endoxifen in *Abcb1a/1b* knockout mice, brain accumulation of (*Z*)-endoxifen was highly increased in these mice, at both 1 and 4 h ($P < 0.001$) after oral administration of 20 mg/kg of endoxifen (1:1, *E/Z* mixture) (Figure 4, B and C). Fold differences of uncorrected brain concentrations of (*Z*)-endoxifen between knockout and wild-type mice were higher at the later time point (12.8-fold at 4 h and 6-fold at 1 h). When represented as brain-to-serum ratios, the fold differences between the two strains were even higher (23-fold at 4 h and 6.5-fold at 1 h) (Figure 4C; Supplemental Table 1). For (*E*)-endoxifen we observed analogous results, although the (*E*)-endoxifen brain accumulation was overall approximately 2-fold higher in comparison with (*Z*)-endoxifen (Supplemental Figure 3, B and C; Supplemental Table 1). The impact of P-gp on limiting brain accumulation of (*Z*)- or (*E*)-endoxifen was thus even more pronounced after direct administration of endoxifen compared with administration of tamoxifen.

### *Saturation of P-gp-mediated transport after Intravenous administration of endoxifen*

To extend our understanding of the P-gp-mediated transport capacity for endoxifen at the blood-brain barrier, we attempted to saturate it using different (high) intravenous dosages, resulting

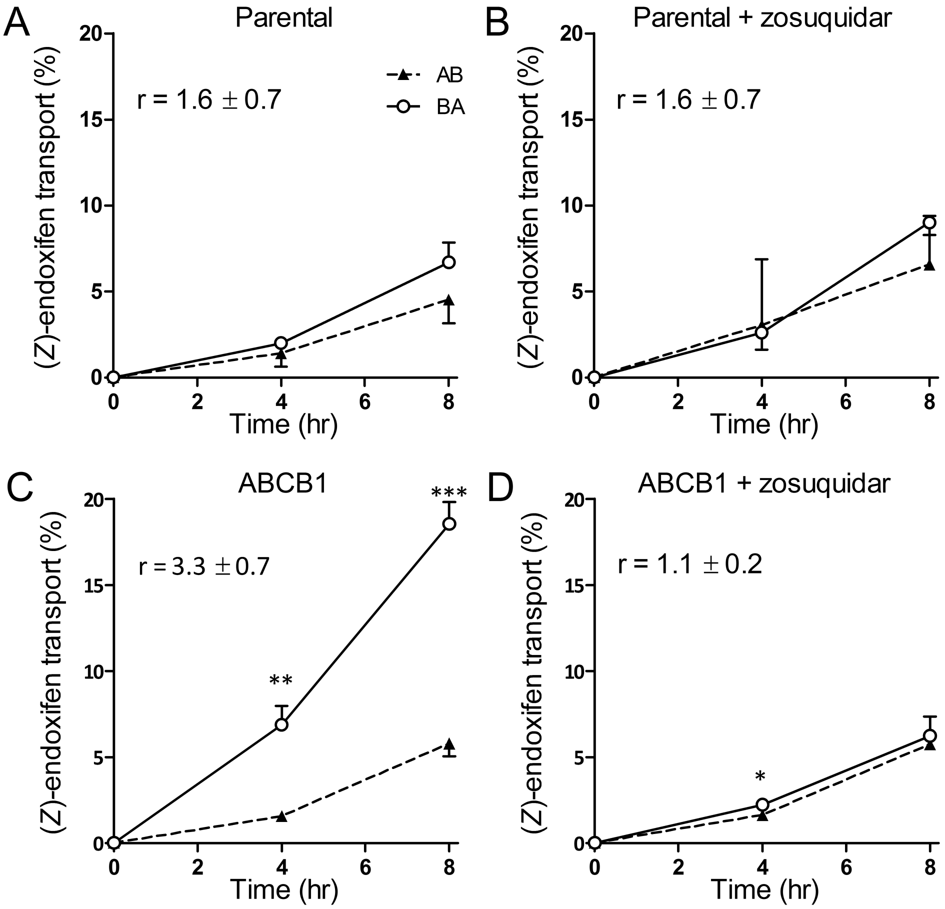

**Figure 3.** Transepithelial transport of (*Z*)-endoxifen was assessed using MDCKII cells, either parental (A and B) or transduced with human ABCB1 (C and D). At $t = 0$ h, endoxifen (5 pM; 1:1, *E/Z* mixture) was applied in one compartment (apical or basolateral), and the amount of drug appearing in the opposite compartment at $t = 4$ and 8 h was plotted as the percentage of the amount of initially applied drug. Zosuquidar (5 pM) was applied to inhibit ABCB1 (D) and/or endogenous canine ABCB1 (B). o, translocation from basolateral to apical compartment (B-to-A); ▲ translocation from apical to basolateral compartment (A-to-B). Points, mean; bars, S.D. ($n = 3$). *, $P < 0.05$; **, $P < 0.01$; ***, $P < 0.001$ comparing B-to-A and A-to-B translocation. $r$ = transport ratio calculated as the quotient of B-to-A and A-to-B directed transport at 8 h.

in high initial serum levels of endoxifen. Fifteen minutes after intravenous administration of either 5 or 20 mg/kg endoxifen (1:1, *E/Z* mixture), serum concentrations of either isomer were similar in both strains (Figure 5A; Supplemental Figure 4A). At the same time point, the impact of P-gp on brain accumulation of endoxifen was still observed, but much reduced in comparison with oral administration. (*Z*)-endoxifen brain concentrations in *Abcb1a/1b* knockout mice were significantly higher (2.8-fold, $P < 0.001$) in comparison with wild-type mice when endoxifen (1:1, *E/Z* mixture) was dosed at 5 mg/kg (Figure 5B). However, when 20 mg/kg was used, the (*Z*)-endoxifen brain concentrations were not significantly different between the two strains

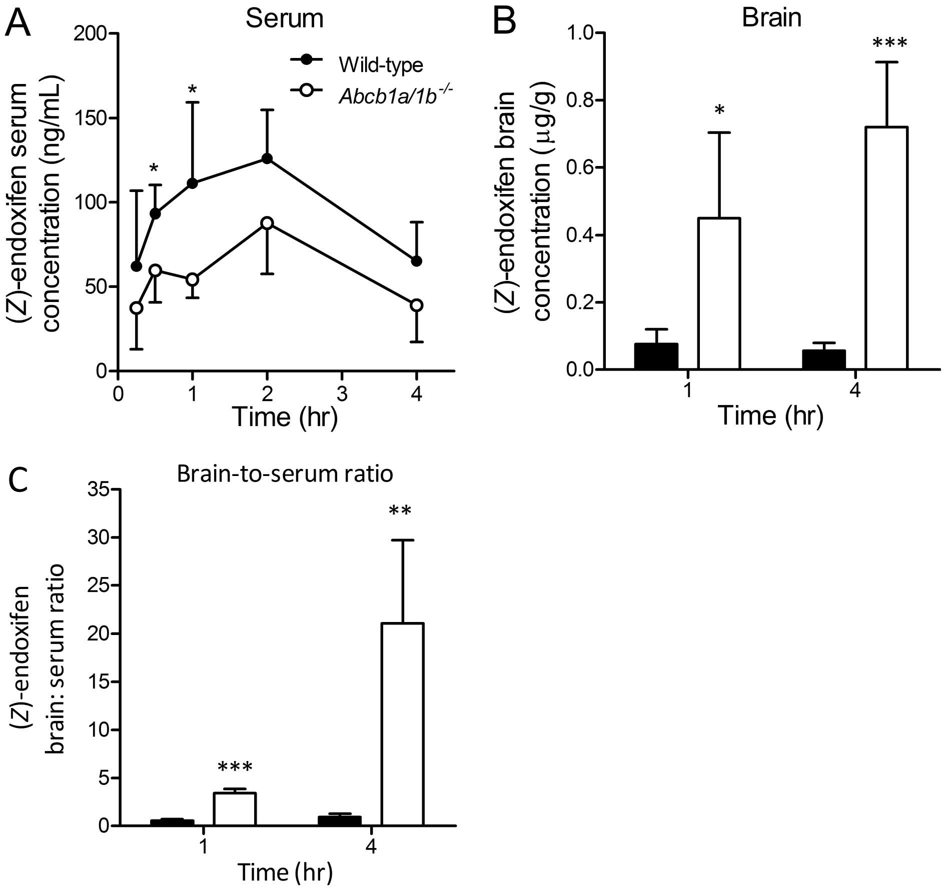

**Figure 4.** Serum and brain levels of (*Z*)-endoxifen after oral administration of 20 mg/kg endoxifen (1:1, *E/Z* mixture) to female wild-type and P-gp knockout mice [*Abcb1a/1b*(-/-)]. Serum concentration versus time curves (A), brain concentrations (B), and brain-to-serum ratios of (*Z*)-endoxifen (C) 1 and 4 h after administration. Points or columns, means; bars, S.D. ($n = 5$). *, $P < 0.05$; **, $P < 0.01$; ***, $P < 0.001$ compared with wild-type mice.

anymore, suggesting a possible near-saturation of the P-gp-mediated transport in the wild-type mice (Figure 5B). That saturation was not complete was evident from the brain-to-serum ratios, which were still significantly increased (-2-fold, $P < 0.05$) in *Abcb1a/1b* knockout versus wild-type mice at both dosages (Figure 5C). Very similar behavior was observed for (*E*)-endoxifen (Supplemental Figure 4, B and C). (*Z*)- and (*E*)-endoxifen serum concentrations 15 min after intravenous administration were still -10-fold higher than peak serum concentrations after oral administration (Figure 5A versus Figure 4A; Supplemental Figure 3A versus Supplemental Figure 4A). These data suggest that when exposed to high (*Z*)- and (*E*)-endoxifen serum concentrations P-gp at the blood-brain barrier can be partially saturated.

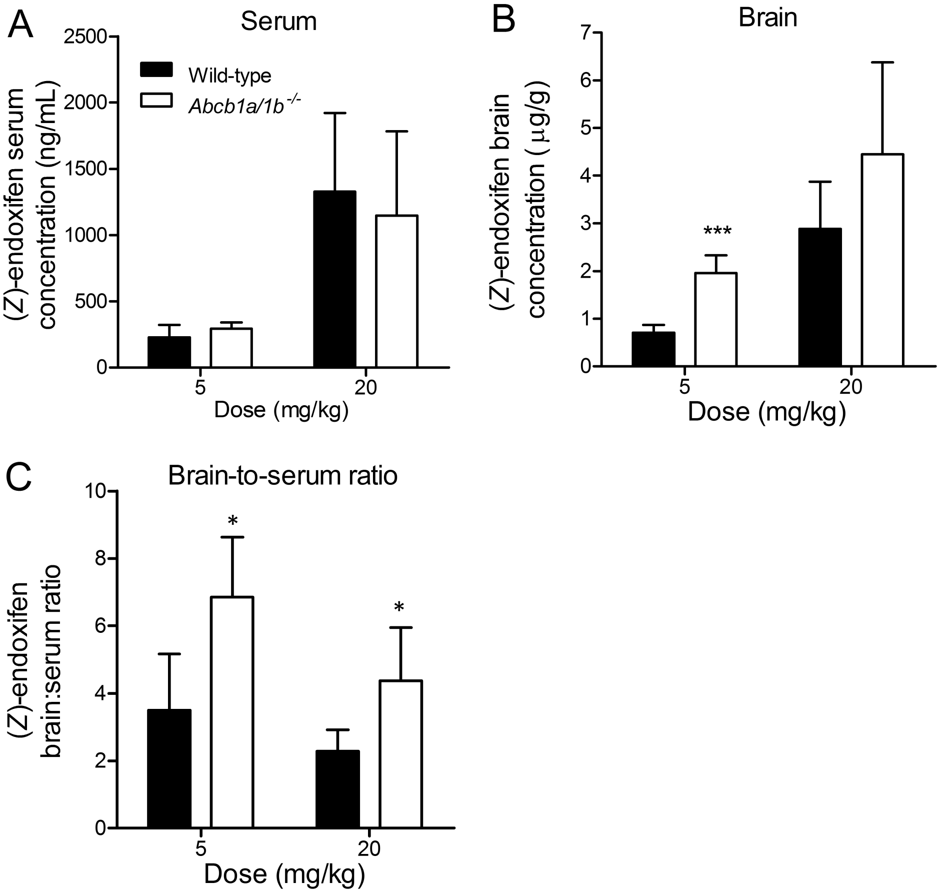

**Figure 5.** Serum concentrations (A), brain concentrations (B), and brain-to-serum ratios of (*Z*)-endoxifen (C) 15 min after intravenous administration of 5 or 20 mg/kg endoxifen (1:1, *E/Z* mixture) to female wild-type and P-gp knockout mice [*Abcb1a/1b*(-/-)]. Columns, means; bars, S.D. ($n = 5$). *, $P < 0.05$; ***, $P < 0.001$ compared with wild type.

## Discussion

P-gp has an important role in protecting tissues and P-gppositive tumor cells from a wide range of compounds. Here, we demonstrate its impact on tamoxifen and its active me-tabolites. Absence of P-gp enhanced the brain accumulation of tamoxifen and its metabolites, but not the serum levels of these compounds. Endoxifen brain accumulation was highly increased in *Abcb1a/1b*(-/-) mice, and in vitro we could demonstrate that both endoxifen isomers are P-gp substrates, and P-gp reduces their cellular accumulation. After direct oral administration of endoxifen (1:1, *E/Z* mixture), differences in brain penetration of both endoxifen isomers between wild-type and *Abcb1a/1b*(-/-) mice were even more pronounced. Finally, P-gp at the blood-brain barrier could be partially saturated after intravenous endoxifen administration when serum concentrations of (*Z*)- and (*E*)-endoxifen and thus the relative exposure of the brain were high.

We observed only a small effect of P-gp on tamoxifen brain accumulation after administration of 50 mg/kg tamoxifen, in line with reports that suggest little, if any, P-gp-mediated transport of tamoxifen [20; 30]. The brain penetration of the main tamoxifen metabolites, 4-hydroxytamoxifen, *N*-desmethyltamoxifen, and endoxifen, is more clearly restricted by P-gp. Our data suggest that 4-hydroxytamoxifen and *N*-desmethyltamoxifen are relatively weak P-gp substrates in vivo, although BekaiiSaab et al. [19] could not demonstrate their P-gp-mediated transport in vitro using Caco-2 cells with modest endogenous levels of P-gp. This apparent discrepancy between in vitro and in vivo data is probably caused by a lower sensitivity of the in vitro assays used in comparison with the blood-brain barrier, a very tight barrier where P-gp activity is very high.

For many years it was thought that 4-hydroxytamoxifen was the main compound responsible for the therapeutic effects of tamoxifen, owing mostly to its 100-fold higher affinity for the estrogen receptor than tamoxifen [2]. With the discovery that endoxifen has a similar activity in its ER interaction as 4-hydroxytamoxifen and exhibits much higher serum levels in patients, the view that endoxifen is the clinically most relevant metabolite is becoming more and more accepted (reviewed in 1). Studies addressing its potential as direct therapeutic agent in breast cancer treatment are emerging [5], and endoxifen's safety, tolerability, and adequate systemic oral bioavailability in human subjects was demonstrated in a recent clinical study [6]. however, little is known about the transport behavior of endoxifen. here, we show that (*Z*)- and (*E*)-endoxifen are transported substrates of P-gp in vitro and in vivo. Zosuquidar, commonly used as a specific inhibitor of P-gp [24], could reverse the ABCB1-mediated transport of endoxifen in vitro. The substantial role of P-gp in limiting brain penetration of (*Z*)- and (*E*)-endoxifen, which is even greater than after administration of tamoxifen, is notable. It is known that only the (*Z*)-isomers of tamoxifen and 4-hydroxytamoxifen exhibit the desired pharmacodynamic properties [8]. Because until recently it was cumbersome to separate the two isomers of endoxifen in large quantities [31], information regarding the biological activity of the (*E*)-isomer is lacking. More in-depth research comparing the pharmacodynamic properties of the two endoxifen isomers may be of interest.

It is worth noting that in wild-type mice 4 h after tamoxifen administration tamoxifen brain concentrations are 60-fold higher than those of endoxifen (Figure 2, A versus D). If the same situation would hold for the human brain, it could be that tamoxifen, in spite of its 100-fold lower affinity for the ER, still contributes nearly as much as endoxifen to the therapeutic effect for tumor cells positioned behind the BBB.

The absence of P-gp did not have an effect on oral bioavailability of tamoxifen or serum concentrations of metabolites after oral administration. In rats, coadministration with dual P-gp and Cyp3a inhibitors resulted in an increased plasma AUC of tamoxifen, effects possibly mediated via Cyp3a inhibition [32; 33]. Upon administration of endoxifen itself in vivo we could directly observe the impact of P-gp on endoxifen oral availability. Serum AUC after oral administration of both endoxifen isomers was somewhat decreased in *Abcb1a/1b*(-/-) mice, an effect that is probably not a direct consequence of the loss of P-gp activity. Possibly up-regulation of alternative detoxifying mechanisms (metabolizing enzymes and efflux transporters) in the small intestine of *Abcb1a/1b*(-/-) mice might explain the decreased oral availability. Data regarding endoxifen metabolism or pharmacokinetics in mice are lacking, so future studies aiming to elucidate the importance of these alternative mechanisms are required.

The absence of P-gp resulted in a strong increase in brain accumulation of endoxifen, but not in serum AUC levels. A substantial difference between the impact of P-gp on brain penetration (high) and oral AUC (low or absent) is often observed for a diversity of P-gp substrate drugs [34]. This difference might be explained by the different physiological properties and functions of the blood-brain barrier and the small intestinal epithellium. The small intestine facilitates the absorption of heterogeneous food-derived nutrients and it is equipped with a substantial and diverse uptake capacity. In contrast, the blood-brain barrier is a highly selective barrier, protecting the brain from harmful compounds, and thus less prone to protein-mediated uptake (and possibly also to passive diffusion) of a wide range of compounds. In addition, the intestinal concentration of oral drugs is usually much higher than plasma concentrations, increasing the likelihood of saturation of P-gp in the intestine. Therefore, the efflux capacity of P-gp in the small intestine can be much more easily overwhelmed by the overall uptake capacity for compounds than in the blood-brain barrier. Finally, P-gp density in the blood-brain barrier might be higher than in the gut. however, these considerations remain hypothetical, and further studies will be required to support them.

The impact of P-gp on the accumulation of tamoxifen's active metabolites, endoxifen, 4-hydroxytamoxifen, and even *N*-desmethyltamoxifen that we observed might have clinical implications for innate or acquired resistance of breast cancers to tamoxifen therapy. It is known that P-gp is expressed in approximately 40% of untreated breast cancers [36]. A meta-analysis study showed that upon exposure to chemotherapeutic drugs (especially those known to be P-gp substrates), P-gp expression increases in breast cancers and this event is associated with lower response rates [35]. In the current study we demonstrated that P-gp has a high impact on brain accumulation of endoxifen and a moderate impact on 4-hydroxytamoxifen. Thus, upon tamoxifen treatment, P-gp (over)expressed in breast cancer cells might also limit the exposure to endoxifen and 4-hydroxytamoxifen, leading to insufficient concentrations of these active metabolites in the tumor cells and poor response to tamoxifen treatment. Accordingly, in the in vitro transport assay we observed significantly lower intracellular concentrations in the cells expressing ABCB1 in comparison with the parental cells. Preliminary clinical evidence supporting this hypothesis is provided by a few clinical studies investigating the effect of P-gp expression in breast tumors on survival after long-term treatment with tamoxifen in a small cohort of patients [18]. P-gp-positive cases had a much lower 3-year overall survival than patients with P-gp-negative tumors. Similar results were obtained in another study in which patients whose tumors did not express P-gp after 3-month treatment with tamoxifen had an 2-fold higher response rate than the patients with P-gppositive tumors [16]. Because tamoxifen was not considered as a substantially transported substrate for P-gp [35], it was previously difficult to explain these findings. The insight that endoxifen is a substantially transported substrate for P-gp can provide a straightforward explanation for these results. Unfortunately, in neither study intratumoral concentrations of endoxifen or 4-hydroxytamoxifen were measured. Extensive studies investigating the P-gp profile before and after treatment, correlating treatment response and overall survival with intratumoral levels of endoxifen and 4-hydroxytamoxifen, are therefore necessary. Nevertheless, collectively, the findings of our study might provide a plausible explanation for poor response or resistance to tamoxifen treatment in breast cancer patients with P-gp-positive tumors.

Possible benefits of applying efficacious in vivo P-gp inhibitors such as elacridar to improve tumor and brain penetration of endoxifen in P-gp-positive breast tumors and ER-dependent tumors positioned behind a functional blood-brain barrier should now also be considered. It is sometimes considered that the BBB in larger brain metastases of breast cancer is often disrupted (e.g., 37), and there would therefore be little therapeutic gain of enhancing BBB penetration of anticancer drugs. However, this view disregards the substantial heterogeneity inside (and between) metastases and their vasculature concerning BBB differentiation characteristics and expression of efflux transporters [38; 39] or the fact that the invasive rims of the tumor are likely to be partially protected by the normal BBB in the surrounding brain tissue. The latter will also apply to small micrometastases in the brain that have not yet recruited their own blood vessel formation [40]. In all such cases P-gp inhibition might potentially improve chemotherapy sensitivity.

## Acknowledgments

We thank Dr. Birk Poller, Anita van Esch, and Ahmed Elbatsh for excellent technical assistance and Seng Chuan Tang, Selvi Durmus, and Dr. Guillaume Filion for critical reading of the article.

## Reference List

1. Hoskins JM, Carey LA, McLeod HL. CYP2D6 and tamoxifen: DNA matters in breast cancer. Nat Rev Cancer 2009;9:576-86.
2. Johnson MD, Zuo H, Lee KH, et al. Pharmacological characterization of 4-hydroxy-N-desmethyl tamoxifen, a novel active metabolite of tamoxifen. Breast Cancer Res Treat 2004;85:151-9.
3. Lim YC, Desta Z, Flockhart DA, Skaar TC. Endoxifen (4-hydroxy-N-desmethyl-tamoxifen) has anti-estrogenic effects in breast cancer cells with potency similar to 4-hydroxy-tamoxifen. Cancer Chemother Pharmacol 2005;55:471-8.
4. Wu X, Hawse JR, Subramaniam M, Goetz MP, Ingle JN, Spelsberg TC. The tamoxifen metabolite, endoxifen, is a potent antiestrogen that targets estrogen receptor alpha for degradation in breast cancer cells. Cancer Res 2009;69:1722-7.
5. Ahmad A, Ali SM, Ahmad MU, Sheikh S, Ahmad I. Orally administered Endoxifen is a new therapeutic agent for breast cancer. Breast Cancer Res Treat 2010;122:579-84.
6. Ahmad A, Shahabuddin S, Sheikh S, et al. Endoxifen, a New Cornerstone of Breast Cancer Therapy: Demonstration of Safety, Tolerability, and Systemic Bioavailability in Healthy Human Subjects. Clin Pharmacol Ther 2010.
7. Stearns V, Rae JM. Pharmacogenetics and breast cancer endocrine therapy: CYP2D6 as a predictive factor for tamoxifen metabolism and drug response? Expert Rev Mol Med 2008;10:e34.
8. Katzenellenbogen BS, Norman MJ, Eckert RL, Peltz SW, Mangel WF. Bioactivities, estrogen receptor interactions, and plasminogen activator-inducing activities of tamoxifen and hydroxy-tamoxifen isomers in MCF-7 human breast cancer cells. Cancer Res 1984;44:112-9.
9. Gupta V, Su YS, Wang W, et al. Enhancement of glioblastoma cell killing by combination treatment with temozolomide and tamoxifen or hypericin. Neurosurg Focus 2006;20:E20.
10. Lien EA, Wester K, Lonning PE, Solheim E, Ueland PM. Distribution of tamoxifen and

metabolites into brain tissue and brain metastases in breast cancer patients. Br J Cancer 1991;63:641-5.

11. Ali SM, Ahmad A, Shahabuddin S, Ahmad MU, Sheikh S, Ahmad I. Endoxifen is a new potent inhibitor of PKC: a potential therapeutic agent for bipolar disorder. Bioorg Med Chem Lett 2010;20:2665-7.
12. Borst P, Elferink Oude RP. Mammalian ABC transporters in health and disease. Annu Rev Biochem 2002;71:537-92.
13. Jin Y, Desta Z, Stearns V, et al. CYP2D6 genotype, antidepressant use, and tamoxifen metabolism during adjuvant breast cancer treatment. J Natl Cancer Inst 2005;97:30-9.
14. Schroth W, Hamann U, Fasching PA, et al. CYP2D6 polymorphisms as predictors of outcome in breast cancer patients treated with tamoxifen: expanded polymorphism coverage improves risk stratification. Clin Cancer Res 2010;16:4468-77.
15. Faneyte IF, Kristel PM, van de Vijver MJ. Determining MDR1/P-glycoprotein expression in breast cancer. Int J Cancer 2001;93:114-22.
16. Keen JC, Miller EP, Bellamy C, Dixon JM, Miller WR. P-glycoprotein and resistance to tamoxifen. Lancet 1994;343:1047-8.
17. Wang CS, LaRue H, Fortin A, Gariepy G, Tetu B. mdr1 mRNA expression by RT-PCR in patients with primary breast cancer submitted to neoadjuvant therapy. Breast Cancer Res Treat 1997;45:63-74.
18. Linn SC, Giaccone G, van Diest PJ, et al. Prognostic relevance of P-glycoprotein expression in breast cancer. Ann Oncol 1995;6:679-85.
19. Bekaii-Saab TS, Perloff MD, Weemhoff JL, Greenblatt DJ, von Moltke LL. Interactions of tamoxifen, N-desmethyltamoxifen and 4-hydroxytamoxifen with P-glycoprotein and CYP3A. Biopharm Drug Dispos 2004;25:283-9.
20. Callaghan R, Higgins CF. Interaction of tamoxifen with the multidrug resistance P-glycoprotein. Br J Cancer 1995;71:294-9.
21. Mutoh K, Tsukahara S, Mitsuhashi J, Katayama K, Sugimoto Y. Estrogen-mediated post transcriptional down-regulation of P-glycoprotein in MDR1-transduced human breast cancer cells. Cancer Sci 2006;97:1198-204.
22. Evers R, Kool M, van Deemter L, et al. Drug export activity of the human canalicular multispecific organic anion transporter in polarized kidney MDCK cells expressing cMOAT (MRP2) cDNA. J Clin Invest 1998;101:1310-9.
23. Lagas JS, van Waterschoot RA, Sparidans RW, Wagenaar E, Beijnen JH, Schinkel AH. Breast cancer resistance protein and P-glycoprotein limit sorafenib brain accumulation. Mol Cancer Ther 2010;9:319-26.
24. Dantzig AH, Shepard RL, Cao J, et al. Reversal of P-glycoprotein-mediated multidrug resistance by a potent cyclopropyldibenzosuberane modulator, LY335979. Cancer Res 1996;56:4171-9.
25. Schinkel AH, Mayer U, Wagenaar E, et al. Normal viability and altered pharmacokinetics in mice lacking mdr1-type (drug-transporting) P-glycoproteins. Proc Natl Acad Sci U S A 1997;94:4028-33.
26. Teunissen SF, Rosing H, Koornstra RH, et al. Development and validation of a quantitative assay for the analysis of tamoxifen with its four main metabolites and the flavonoids daidzein, genistein and glycitein in human serum using liquid chromatography coupled with tandem mass spectrometry. J Chromatogr B Analyt Technol Biomed Life Sci 2009;877:2519-29.
27. van Waterschoot RA, van Herwaarden AE, Lagas JS, et al. Midazolam metabolism in cytochrome P450 3A knockout mice can be attributed to up-regulated CYP2C enzymes. Mol Pharmacol 2008;73:1029-36.
28. Dai H, Marbach P, Lemaire M, Hayes M, Elmquist WF. Distribution of STI-571 to the brain is limited by P-glycoprotein-mediated efflux. J Pharmacol Exp Ther 2003;304:1085-92.
29. Furlanut M, Franceschi L, Pasqual E, et al. Tamoxifen and its main metabolites serum and tissue concentrations in breast cancer women. Ther Drug Monit 2007;29:349-52.
30. Rao US, Fine RL, Scarborough GA. Antiestrogens and steroid hormones: substrates of the human P-glycoprotein. Biochem Pharmacol 1994;48:287-92.
31. Fauq AH, Maharvi GM, Sinha D. A convenient synthesis of (Z)-4-hydroxy-N-desmethyltamoxifen (endoxifen). Bioorg Med Chem Lett 2010;20:3036-8.
32. Piao Y, Shin SC, Choi JS. Effects of oral kaempferol on the pharmacokinetics of tamoxifen and one of its metabolites, 4-hydroxytamoxifen, after oral administration of tamoxifen to rats. Biopharm Drug Dispos 2008;29:245-9.
33. Shin SC, Choi JS, Li X. Enhanced bioavailability of tamoxifen after oral administration of tamoxifen with quercetin in rats. Int J Pharm 2006;313:144-9.
34. Jonker JW, Wagenaar E, van Deemter L, et al. Role of blood-brain barrier P-glycoprotein in limiting brain accumulation and sedative side-effects of asimadoline, a peripherally acting analgaesic drug. Br J Pharmacol 1999;127:43-50.

35. Leonessa F, Clarke R. ATP binding cassette transporters and drug resistance in breast cancer. Endocr Relat Cancer 2003;10:43-73.
36. Clarke R, Leonessa F, Trock B. Multidrug resistance/P-glycoprotein and breast cancer: review and meta-analysis. Semin Oncol 2005;32:S9-15.
37. Yonemori K, Tsuta K, Ono M, et al. Disruption of the blood brain barrier by brain metastases of triple-negative and basal-type breast cancer but not HER2/neu-positive breast cancer. Cancer 2010;116:302-8.
38. Regina A, Demeule M, Laplante A, et al. Multidrug resistance in brain tumors: roles of the blood-brain barrier. Cancer Metastasis Rev 2001;20:13-25.
39. Lockman PR, Mittapalli RK, Taskar KS, et al. Heterogeneous blood-tumor barrier permeability determines drug efficacy in experimental brain metastases of breast cancer. Clin Cancer Res 2010;16:5664-78.
40. Fidler IJ. The role of the organ microenvironment in brain metastasis. Semin Cancer Biol 2010.

# *Supplemental data*

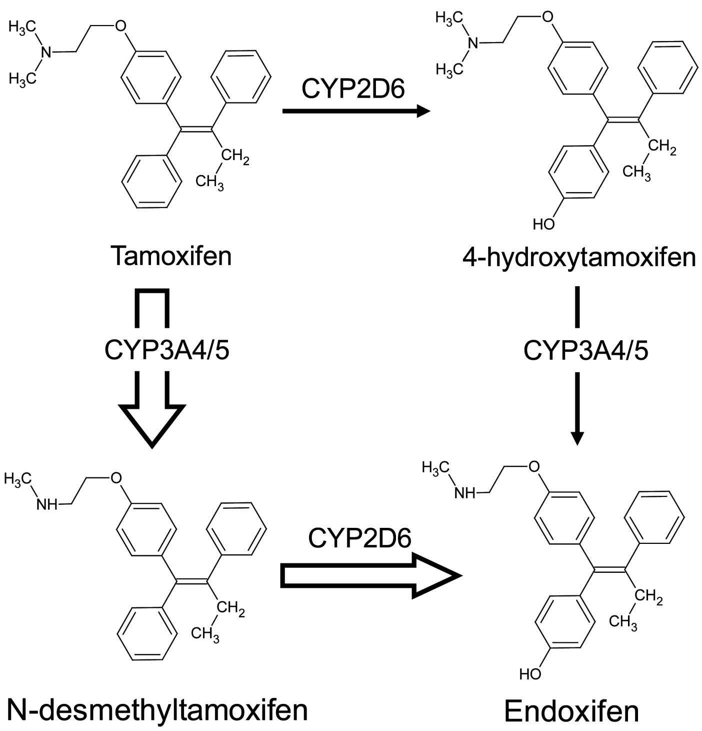
$H_3C$
N
$H_3C$
O
$CH_2$
$CH_3$
Tamoxifen
CYP2D6
HO
4-hydroxytamoxifen
CYP3A4/5
CYP3A4/5
NH
N-desmethyltamoxifen
CYP2D6
Endoxifen

**Supplemental figure 1.** Chemical structures of tamoxifen and its main metabolites. In humans the metabolic pathway towards endoxifen is favored, whereas in mice the pathway through 4-hydroxytamoxifen predominates.

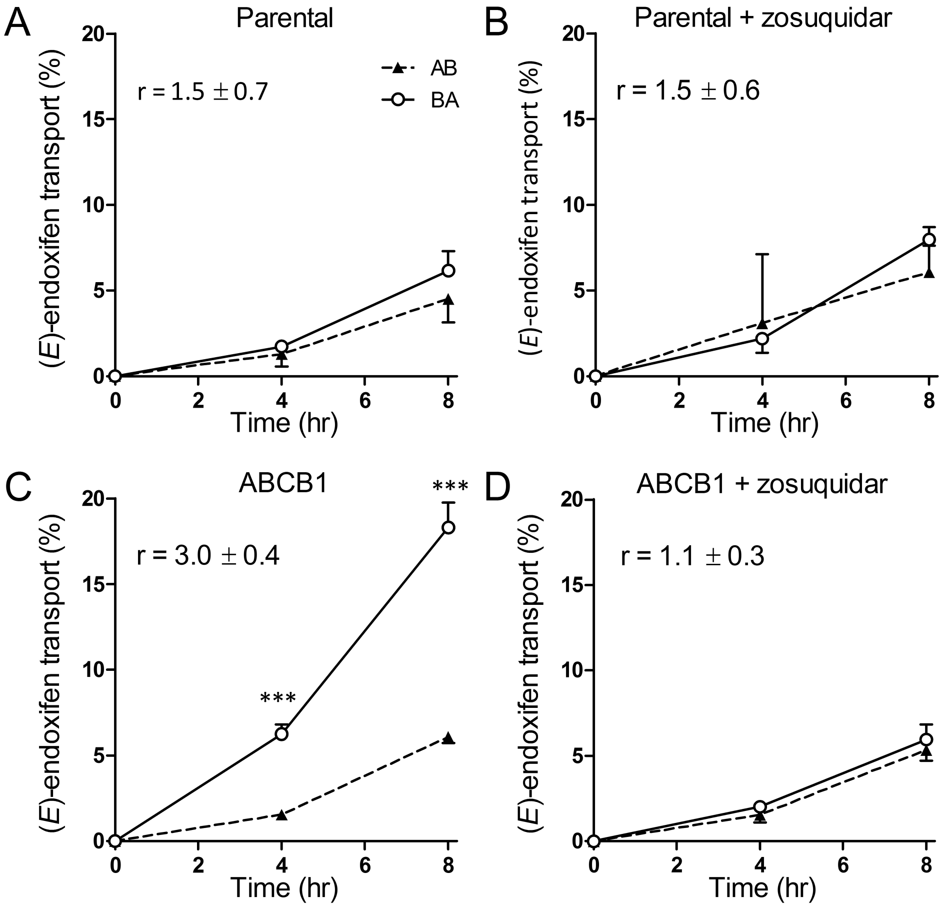

**Supplemental figure 2.** Transepithelial transport of (*E*)-endoxifen was assessed using MDCKII cells, either nontransduced parental (A and B), or transduced with human ABCB1 (C and D). At t = 0 h, endoxifen (5 μmol/L; 1:1, *E/Z* mixture) was applied in one compartment (apical or basolateral), and the amount of drug appearing in the opposite compartment at t = 4 and 8 h was measured by LC-MS/MS and plotted as the percentage of the amount of initially applied drug. Zosuquidar (5 μmol/L) was applied to inhibit ABCB1 (D) and/or endogenous canine ABCB1 (B). o, translocation from basolateral to apical compartment (B-to-A); ▲ translocation from apical to basolateral compartment (A-to-B). Points, mean; bars, SD (n = 3). *, *P* < 0.05, **, *P* < 0.01, ***, *P* < 0.001 when comparing B-to-A versus A-to-B translocation. r = transport ratio calculated as the quotient of B-t-A and A-to-B directed transport at 8 h.

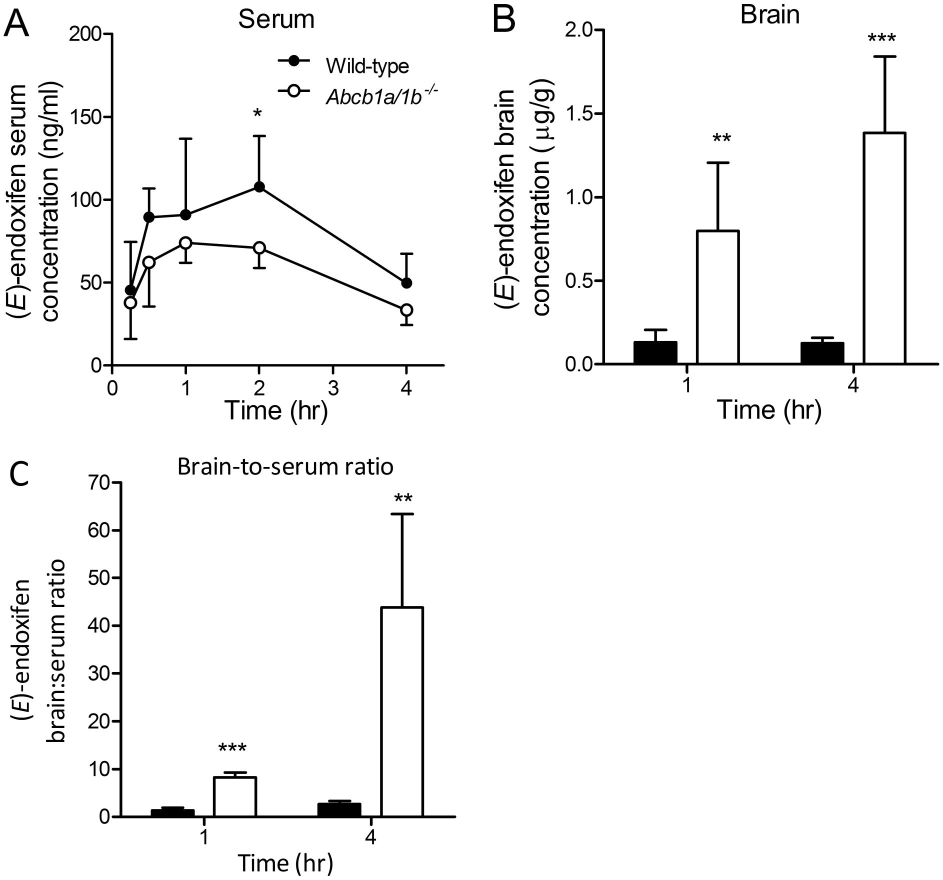

**Supplemental figure 3.** Serum and brain levels of (*E*)-endoxifen after oral administration of 20 mg/kg endoxifen (1:1, *E/Z* mixture) to female wild-type and P-gp knockout mice (*Abcb1a/1b*(-/-)). (A) Serum concentration versus time curves, (B) brain concentrations and (C) brain-to-serum ratios of (*E*)-endoxifen 1 h and 4 h after administration. Points or columns, means; bars, SD (n = 5). *, $P < 0.05$, **, $P < 0.01$, ***, $P < 0.001$ when compared with wild-type mice.

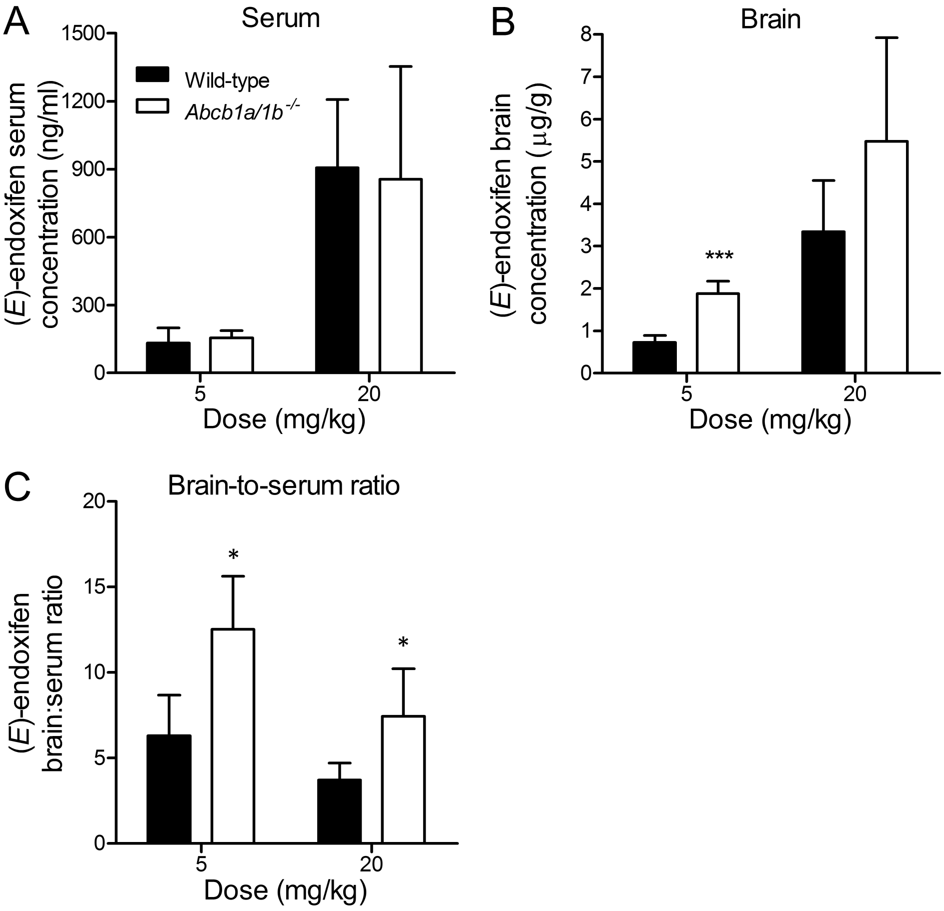

**Supplemental figure 4.** (A) Serum concentrations, (B) brain concentrations and (C) brain-to-serum ratios of (*E*)-endoxifen 15 minutes after intravenous administration of 5 mg/kg or 20 mg/kg endoxifen (1:1, *E/Z* mixture) to female wild-type and P-gp knockout mice (*Abcb1a/1b*(-/-)). Columns, means; bars, SD (n = 5). *, $P < 0.05$, ***, $P < 0.001$ when compared with wild-type.

**Supplemental Table 1.** Serum AUC$_{(0-4)}$, brain concentrations and brain-to-serum ratios of (*Z*/*E*)-endoxifen in mice at 1 h or 4 h after oral administration of 20 mg/kg endoxifen (1:1, *E*/*Z* mixture).

| | | **(*Z*)-endoxifen** | | **(*E*)-endoxifen** | |
|---|---|---|---|---|---|
| | | **WT** | **Abcb1a/1b(-/-)** | **WT** | **Abcb1a/1b(-/-)** |
| | AUC$_{(0-4)}$, ng/L.hr | 388 ± 62 | 243 ± 43* | 325 ± 96 | 217 ± 24* |
| t = 1 h # | Serum (ng/mL) | 137 ± 67 | 130 ± 66 | 92.5 ± 38.6 | 96.5 ± 43.2 |
| | C$_{brain}$ µg/g | 0.08 ± 0.04 | 0.45 ± 0.26* | 0.13 ± 0.08 | 0.80 ± 0.41** |
| | Fold increase | 1 | 6 | 1 | 6 |
| | Brain:serum ratio | 0.53 ± 0.18 | 3.42 ± 0.41*** | 1.35 ± 0.53 | 8.20 ± 1.06*** |
| | Fold increase | 1 | 6.5 | 1 | 6.1 |
| t = 4 h | Serum (ng/mL) | 65.1 ± 23.3 | 39.1 ± 21.9 | 49.8 ± 17.6 | 33.5 ± 9.2 |
| | C$_{brain}$ µg/g | 0.06 ± 0.03 | 0.72 ± 0.19*** | 0.13 ± 0.03 | 1.39 ± 0.46** |
| | Fold increase | 1 | 12.8 | 1 | 10.9 |
| | Brain:serum ratio | 0.91 ± 0.35 | 21 ± 8.7*** | 2.6 ± 0.7 | 43.8 ± 19.6** |
| | Fold increase | 1 | 23 | 1 | 16.6 |

*, $P < 0.05$, **, $P < 0.01$, ***, $P < 0.001$ when compared with wild-type mice. #, note that the t = 1 h data represent an independent experiment from t = 4 h.

**Supplemental table 2.** Overview of ΔCt values of the RT-PCR analysis to investigate the expression of several endogenous metabolizing enzymes and efflux transporters in small intestine and liver of female wild-type and *Abcab1a/1b(-/-)* mice.

| | **Small intestine** | | **Liver** | |
|---|---|---|---|---|
| | **WT** | **Abcb1a/1b(-/-)** | **WT** | **Abcb1a/1b(-/-)** |
| Cyp3a11 | -0.2 ± 0.4 | -1.8 ± 0.2** | -7.2 ± 0.1 | -6.9 ± 0.1 |
| Cyp3a13 | 10.5 ± 0.5 | 9.9 ± 0.1 | 10.5 ± 0.3 | 10.5 ± 0.4 |
| Cyp3a25 | 5.5 ± 0.2 | 4.8 ± 0.4* | 0.5 ± 0.2 | 1.5 ± 0.5* |
| Cyp2c38 | 9.0 ± 0.7 | 8.6 ± 3.5 | -4.3 ± 0.2 | -4.1 ± 0.3 |
| Cyp2c55 | 7.8 ± 0.1 | 6.4 ± 0.2*** | 9.3 ± 0.3 | 9.1 ± 0.8 |
| Cyp2c65 | 3.4 ± 0.2 | 2.0 ± 0.5* | 9.7 ± 2.7 | 16.3 ± 2.2* |
| Cyp2c66 | 5.4 ± 0.8 | 4.4 ± 0.9 | 10.4 ± 0.8 | 13.8 ± 0.9** |
| *Abcc2* (Mrp2) | 0.7 ± 0.8 | -0.2 ± 0.3 | -3.7 ± 0.3 | -3.4 ± 0.1 |
| *Abcg2* (Bcrp1) | 3.1 ± 0.6 | 1.5 ± 0.4* | 1.4 ± 0.5 | 1.7 ± 0.2 |

(n = 3, each sample was analyzed in duplicate). Analysis of results was done by comparative Ct method. Quantification of the target cDNAs in all samples was normalized against the endogenous control β-actin (Ct$_{target}$ – Ct $_{\beta\text{-actin}}$ = ΔCt). Accordingly, the lower the value, the higher the expression level. Data are presented as means ± SD. Each sample was assayed in duplicate.
*, $P < 0.05$, **, $P < 0.01$, ***, $P < 0.001$ when compared with wild-type mice.

# 5.3

# *Differential impact of P-glycoprotein (ABCB1) and breast cancer resistance protein (ABCG2) on axitinib brain accumulation and oral plasma pharmacokinetics*

Birk Poller[1]*, Dilek Iusuf*[1], Rolf W. Sparidans[2], Els Wagenaar[1],
Jos H. Beijnen[2] and Alfred H. Schinkel[1],

* contributed equally

[1]Division of Molecular Oncology,
The Netherlands Cancer Institute, Amsterdam
[2]Department of Pharmaceutical Sciences, Utrecht
University, Utrecht, The Netherlands

*Drug Metabolism and Disposition, 2011*

# ABSTRACT

The second-generation tyrosine kinase inhibitor and anticancer drug axitinib is a potent, orally active inhibitor of the vascular endothelial growth factor receptors 1, 2, and 3. Axitinib has clinical activity against solid tumors such as metastatic renal cell carcinoma and advanced pancreatic cancer. We studied axitinib transport using Madin-Darby canine kidney II cells overexpressing human ABCB1 or ABCG2 or murine Abcg2. Axitinib was a good substrate of ABCB1 and Abcg2, whereas transport activity by ABCG2 was moderate. These transporters may therefore contribute to axitinib resistance in tumor cells. Upon oral administration of axitinib, *Abcg2*(-/-) and *Abcb1a/1b;Abcg2*(-/-) mice displayed 1.7- and 1.8-fold increased axitinib areas under the plasma concentration-time curve from 0 to 4 compared with those of wild-type mice. Plasma concentrations in *Abcb1a/1b*(-/-) mice were not significantly increased. In contrast, relative brain accumulation of axitinib in *Abcb1a/1b*(-/-) and *Abcb1a/1b;Abcg2*(-/-) mice was, respectively, 6.8- and 13.9-fold higher than that in wild-type mice at 1 h and 4.9- and 20.7-fold at 4 h after axitinib administration. In *Abcg2*(-/-) mice, we found no significant differences in brain accumulation compared with those in wild-type mice. Thus, Abcb1 strongly restricts axitinib brain accumulation and completely compensates for the loss of Abcg2 at the blood-brain barrier, whereas Abcg2 can only partially take over Abcb1-mediated axitinib efflux. Hence, Abcg2 has a stronger impact on axitinib oral plasma pharmacokinetics, whereas Abcb1 is the more important transporter at the blood-brain barrier. These findings illustrate that in vitro transport data for ABCB1 and ABCG2 cannot always be simply extrapolated to the prediction of the relative impact of these transporters on oral availability versus brain penetration.

## Introduction

The ATP-binding cassette (ABC) transporters P-glycoprotein (Pgp/ABCB1) and breast cancer resistance protein (BCRP/ABCG2) affect the disposition of a variety of endogenous and exogenous compounds, including many anticancer drugs. Both transporters are expressed at the apical membranes of enterocytes, hepatocytes, and renal tubular epithelial cells, where they potentially limit gastrointestinal absorption or mediate direct intestinal, hepatic, or renal excretion of their substrates. Moreover, ABCB1- and ABCG2-mediated efflux activity in brain endothelial capillary cells of the blood-brain barrier (BBB) is crucial for the protection of the central nervous system from harmful compounds [1, 2]. In addition, ABC transporters are expressed in many tumor types, mediating multidrug resistance against anticancer drugs [3].

Only recently, the combined role of ABCB1 and ABCG2 at the BBB in limiting brain accumulation of shared substrates has been studied in detail using *Abcb1a/1b;Abcg2*(-/-) combination knockout mice. It was found that brain penetration of topotecan and several tyrosine kinase inhibitors (TKIs) including lapatinib, imatinib, dasatinib, sorafenib, gefitinib, and erlotinib was disproportionately increased in *Abcb1a/1b;Abcg2*(-/-) knockout mice compared with that in wild-type (WT) and single *Abcb1a/1b*(-/-) and *Abcg2*(-/-) knockout mice [4-10]. These data suggested that the loss of either ABCB1 or ABCG2 at the BBB can often be largely compensated for by the complementary transporter, which is still present. For most of the above-mentioned drugs, brain penetration was mainly restricted by ABCB1, whereas only for sorafenib was ABCG2 the major factor limiting brain accumulation [8].

Axitinib (*N*-methyl-2-[[3-[(*E*)-2-pyridin-2-ylethenyl]-1*H*-indazol-6-yl] sulfanyl]benzamide, AG013736) is a newly developed oral small-molecule tyrosine kinase inhibitor. It selectively inhibits the vascular endothelial growth factor receptors (VEGFRs)-1, -2, and -3 at picomolar levels and the platelet-derived growth factor receptor 13 at nanomolar levels [11]. In phase II studies axitinib showed efficacy against various tumor types, such as metastatic renal cell carcinoma (RCC) [12, 13], metastatic breast cancer [14], thyroid cancer [15], advanced non–small-cell lung cancer [16], and pancreatic cancer [17]. Phase III studies testing the effect of axitinib in advanced pancreatic cancer and in metastatic RCC and pancreatic carcinoma are ongoing (ClinicalTrials.gov numbers NCT00920816, NCT00678392, and NCT00471146).

Animal studies and early-stage clinical trials have shown beneficial effects of VEGFR-targeting agents including the TKIs cediranib, sorafenib, sunitinib, and dasatinib for the treatment of malignant glioma (summarized in [18]). A crucial characteristic for an anticancer drug in treating brain tumors or brain metastases is its ability to reach all the tumor cells and therefore often its ability to cross the BBB. Many anticancer drugs are subject to ABCB1- and ABCG2-mediated efflux at the BBB, resulting in significantly reduced brain concentrations [2, 19]. Although therapeutic efficacy of axitinib against brain tumors has not yet been assessed, it is relevant to know the impact of ABC transporters on the axitinib brain accumulation with respect to possible future clinical applications.

To our knowledge no data are currently available regarding interactions of axitinib with ABCB1 and ABCG2. Therefore, the aim of this study was to investigate whether axitinib is a substrate of one or both of these transporters and how this would affect oral plasma pharmacokinetics and brain penetration of the drug. To assess the transport of axitinib in vitro we used MDCKII cells overexpressing human ABCB1 and ABCG2 as well as murine Abcg2. We next measured axitinib plasma concentration profiles and brain accumulation in WT, *Abcb1a/1b*(-/-), *Abcg2*(-/-), and *Abcb1a/1b; Abcg2*(-/-) mice upon oral administration.

## Materials and Methods

### Chemicals

Axitinib and elacridar (*N*-(4-[2-(1,2,3,4-tetrahydro-6,7- dimethoxy-2-isoquinolinyl)ethyl]-phenyl)-9,10-dihydro-5-methoxy-9-oxo-4- acridine carboxamide, GF120918) were purchased from Sequoia Research Products (Pangborne, UK). [$^{14}$C]Inulin (5.6 Ci/mol) was from GE Healthcare (Little Chalfont, Buckinghamshire, UK). Zosuquidar (Eli Lilly, Indianapolis, IN) was a kind gift from Dr. O. van Tellingen (The Netherlands Cancer Institute, Amsterdam, The Netherlands). All other chemicals were of analytical grade and were obtained from Sigma-Aldrich (St. Louis, MO) unless indicated otherwise.

### Transport assays

For transepithelial transport assays we used the polarized Madin-Darby canine kidney (MDCKII) cell line and subclones transduced (using retroviral vectors) with human ABCB1, mouse Abcg2 [20, 21], and a newly derived human ABCG2-overexpressing clone, [22]. Transport assays were performed as described previously with minor modifications [7]. Two hours before the experiment was started, cells were washed with phosphate-buffered saline and preincubated with Opti-MEM (Invitrogen, Carlsbad, CA) alone or containing either elacridar (5 AM) or zosuquidar (5 AM). At $t$ = 0 h, the medium in the donor compartment was replaced with Opti-MEM containing axitinib (1 AM) alone or in combination with an inhibitor. Aliquots of 100 Al were taken at 2 and 4 h. The percentage of axitinib appearing in the acceptor compartment relative to the total amount added to the donor compartment at the beginning of the experiment was calculated. All data are means ($n$ = 3) ± S.D. Transport ratios ($r$) were calculated by dividing apically directed by basolaterally directed axitinib translocation. Paracellular [$^{14}$C]inulin leakage (0.09 ACi/well), which had to remain below 1% per hour, was measured in parallel in the same cells seeded and cultured in the same way to assure monolayer integrity. Because axitinib is sensitive to light-induced isomerization [23], adequate precautions were taken throughout all experimental procedures to limit light exposure as much as possible (e.g., reduced lighting during sample handling and collection of samples in amber tubes).

### Animals

All mice were housed and handled according to institutional guidelines complying with Dutch legislation. Animals used for this study were male WT, *Abcb1a/1b*(-/-) [24], *Abcg2*(-/-) [20], and *Abcb1a/1b;Abcg2*(-/-) [25] knockout mice of a >99% FVB genetic background, between 8 and 12 weeks of age. Animals were kept in a temperature-controlled environment with a 12-h light/dark cycle and received a standard diet (AM-II; Hope Farms, Woerden, The Netherlands) and acidified water ad libitum.

### *Plasma pharmacokinetics and brain accumulation of axitinib*

Axitinib was dissolved in polysorbate 80-ethanol (1:1, v/v) (3.3 mg/l) and 3.3-fold diluted with NaCl 0.9% (w/v). Axitinib was administered orally at 10 mg/kg (10 ml/kg). To reduce variation in absorption, mice (*n* = 4–5 per group) were fasted at least 3 h before axitinib was given by gavage into the stomach using a blunt-ended needle. Multiple blood samples (-30 Al) were collected from the tail vein either at 15, 30, and 60 min or at 15, 30, 60, 120, and 240 min using heparinized capillary tubes (Oxford Labware, St. Louis, MO). At the last time points (60 or 240 min), mice were sacrificed by cardiac puncture under isoflurane anesthesia followed by cervical dislocation. Brains were rapidly removed and homogenized on ice in 1 ml of 4% (w/v) bovine serum albumin. Plasma was obtained by centrifugation of blood samples at 5200*g* for 6 min at 4°C. All procedures were performed under limited light exposure of axitinib containing samples.

### *Axitinib analysis*

Axitinib concentrations in Opti-MEM, plasma, and brain homogenate samples were analyzed by a sensitive and specific liquid chromatography-tandem mass spectrometry assay as described previously [23]. Axitinib-containing solutions and samples were protected from light throughout all experimental procedures.

### *Calculation of AUC, relative brain accumulation, and statistical analysis*

The AUC was calculated using the trapezoidal rule, without extrapolating to infinity. One-way analysis of variance (ANOVA) was used for statistical analysis, and data obtained from knockout mice were compared with data from WT mice. Axitinib brain concentrations were corrected by the amount of drug in the brain vasculature, corresponding to 1.4% of the plasma concentration at the last time point [26]. Relative brain accumulation $_{(P\text{brain})}$ was calculated by dividing brain concentrations $_{(\text{Cbrain})}$ at either $t = 1$ h or $t = 4$ h by the area under the plasma concentration-time curve from 0 to 1 h (AUC0–1 h) or 0 to 4 h (AUC0–4 h), respectively. For statistical analysis of brain accumulation data, the individual values were log-transformed to obtain normal distribution, and one-way ANOVA was performed. Differences were considered statistically significant when $P < 0.05$. All data are given as means ± S.D.

## Results and Discussion

We first studied the interaction between axitinib and ABC transporters in vitro by measuring axitinib (1 μM) translocation through polarized monolayers of the MDCKII parental cell line and subclones overexpressing human ABCB1 or ABCG2 or mouse Abcg2. As shown in Figure 1A, we observed moderate apically directed axitinib transport in the parental cell line (transport ratio $r = 1.4$), which was abrogated by treatment with the ABCB1/ABCG2 inhibitor elacridar and the relatively ABCB1-specific inhibitor zosuquidar (Figure 1B). This finding suggests that this background transport was mediated by endogenous canine ABCB1 present in the MDCKII cells [27]. In MDCKII cells transduced with human ABCB1, we observed active apically directed transport with $r = 5.3$ (Figure 1A), which was completely blocked by elacridar, indicating that axitinib is a good substrate of human ABCB1. In subsequent transport experiments using MDCKII cells overexpressing human or mouse ABCG2, zosuquidar was included to block the background transport mediated by endogenous canine ABCB1 (Figure 1B). Whereas axitinib was moderately transported by human ABCG2 (*r* = 1.3), we observed substantial apically directed translocation by the mouse Abcg2 (*r* = 3.4). Axitinib transport by human and mouse ABCG2 was efficiently blocked by elacridar. Axitinib was not significantly transported by human ABCC2 or mouse Abcc2 expressed in MDCKII cells (data not shown). To the best of our knowledge, this is the first report demonstrating active transport of axitinib by ABCB1 and ABCG2/Abcg2.

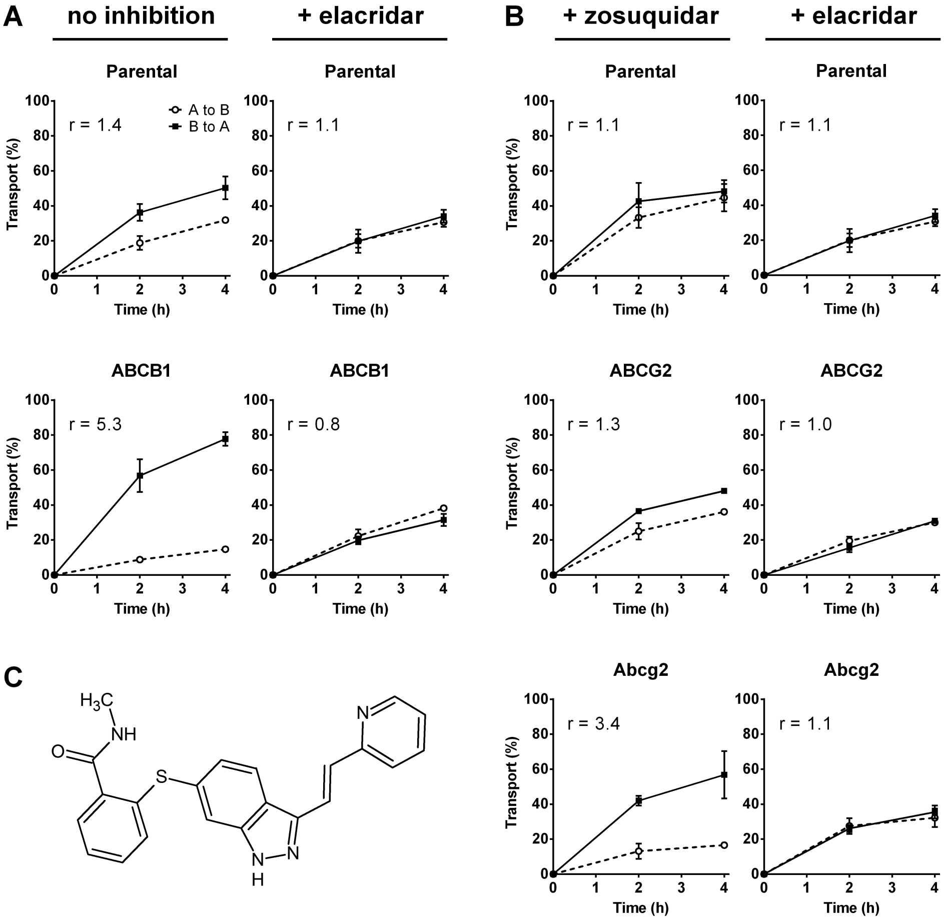

**Figure 1.** Transepithelial transport of 1 μM axitinib through monolayers of MDCKII parental cells and a human ABCB1-transduced subclone (A) or human ABCG2- or mouse Abcg2-transduced subclones (B). Transport was measured in the absence of an inhibitor or in the presence of 5 μM elacridar or 5 μM zosuquidar. Data for parental cells in the presence of elacridar are identical in A and B. ○, translocation from the apical to the basolateral compartment; ■, translocation from the basolateral to the apical compartment. Results are expressed as mean values (*n* = 3) of relative transport (%) ± S.D. The transport ratio (*r*) was calculated as the quotient of apically directed and basolaterally directed transport at 4 h. (C) molecular structure of axitinib.

We subsequently studied the single and combined effects of Abcb1 and Abcg2 on axitinib plasma pharmacokinetics and brain accumulation using WT, *Abcb1a/1b*(-/-), *Abcg2*(-/-), and *Abcb1a/1b; Abcg2*(-/-) mice. Because axitinib is given orally to patients, we administered axitinib orally at a dose of 10 mg/kg. In *Abcg2*(-/-) and *Abcb1a/1b;Abcg2*(-/-) mice we found 1.7- and 1.8-fold, statistically significant increases in AUC0–4 h values compared with those in WT mice (Figure 2; Table 1). In contrast, the AUC0–4 h in *Abcb1a/ 1b*(-/-) mice was not significantly increased (*P* = 0.12). Qualitatively similar results were obtained by measuring the axitinib plasma AUC0–1 h in an independent experiment, with 1.6- and 1.3-fold increased AUC0–1 h in *Abcg2*(-/-) and *Abcb1a/1b;Abcg2*(-/-) mice, but no increase in *Abcb1a/1b*(-/-) mice compared with that in WT mice (Table 1). The virtually identical axitinib plasma concentration-time curves in *Abcg2*(-/-) and *Abcb1a/1b;Abcg2*(-/-) mice as shown in Figure 2 also suggest a substantial impact of Abcg2 on axitinib plasma pharmacokinetics, whereas the effect of Abcb1 on axitinib plasma concentrations appears to be minor or negligible. This finding seems to be at odds with the observed efficient axitinib transport activity by ABCB1 in vitro. However, it is a fairly common observation that many good in vitro ABCB1 substrates show little or no alteration in oral AUC in *Abcb1a/1b*(-/-) mice. For instance, no effect of either Abcb1 or Abcg2 on (oral) plasma concentrations in mice was observed for the shared ABCB1 and ABCG2 substrates sorafenib, gefitinib, and lapatinib [4, 8, 10]. It is possible that the high intestinal luminal concentrations of these drugs obtained after oral administration lead to saturation of the intestinal efflux transporters. In contrast, the oral AUC of dasatinib in mice is somewhat reduced by Abcb1, although not by Abcg2 [7]. The increased axitinib plasma concentrations in *Abcg2*(-/-) and *Abcb1a/1b; Abcg2*(-/-) mice are most likely caused by increased drug absorption from the gastrointestinal tract and/or reduced hepatobiliary excretion when Abcg2 is absent. Although predictions from animal data to the situation in humans can be complicated, the impact of ABCG2 on plasma AUCs might be relevant for potential drug-drug interactions. Because an absolute oral axitinib bioavailability of 58% was

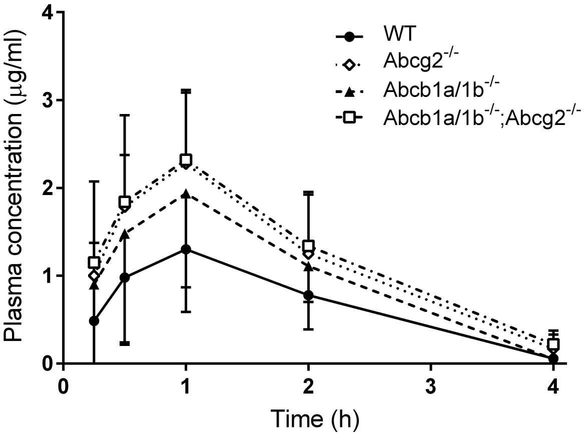

**Figure 2.** Plasma concentration-time curves of axitinib in male WT, *Abcg2*(-/-), *Abcb1a/1b*(-/-), and *Abcb1a/1b;Abcg2*(-/-) mice after oral administration of 10 mg/kg axitinib. Data are given as means ± S.D. (*n* = 5).

reported in patients with cancer [28], our results suggest a potentially increased risk for adverse drug reactions due to higher exposure, when axitinib is given concomitantly with an efficient ABCG2-inhibiting drug such as pantoprazole [9].

We next studied the impact of Abcb1 and Abcg2 on axitinib brain accumulation in different mouse strains. Oral administration of 10 mg/kg axitinib to *Abcg2*(-/-) mice did not result in significantly altered brain concentrations, either at 1 or at 4 h, compared with that in WT animals (Figure 3, A and B; Table 1). In contrast, brain concentrations in *Abcb1a/1b*(-/-) mice showed statistically significant increases by 6.3- and 7.9-fold at 1 and 4 h, respectively, compared with those in WT mice. We further found markedly (and significantly) higher axitinib brain concentrations (20- and 42-fold at 1 and 4 h, respectively) in *Abcb1a/1b;Abcg2*(-/-) mice than in WT mice. Correcting the axitinib brain concentrations for the corresponding plasma AUCs also failed to reveal increased axitinib accumulation in brains of *Abcg2*(-/-) compared with those in WT mice, whereas brain accumulation in *Abcb1a/1b*(-/-) mice at 1 h was 6.8-fold higher than that in WT mice ($P < 0.001$) and 4.9-fold higher at 4 h (Figure 3, C and D; Table 1). In *Abcb1a/1b;Abcg2*(-/-) mice, we found highly significant 14- and 21-fold higher brain accumulation at 1 and 4 h, respectively (Figure 3, C and D; Table 1). In general, axitinib brain concentrations and brain accumulation were roughly 10- and 50-fold lower, respectively, at 4 h than at 1h. This pattern was consistently observed among all mouse strains. These data suggest that in all strains during the 1st h of exposure a more or less steady-state situation in axitinib brain/plasma ratios has been established that is in part determined by Abcb1 and/or Abcg2 activity and that does

**Table 1.** Plasma AUC, brain concentrations, and relative brain accumulation of axitinib in mice at 1 h and 4 h after oral administration at 10 mg/kg.

| | | **Strain** | | | |
|---|---|---|---|---|---|
| | | **WT** | ***Abcg2*(-/-)** | ***Abcb1a/1b*(-/-)** | ***Abcb1a/1b;Abcg2*(-/-)** |
| $t$ = 1 h | $AUC_{(0-1\,h)}$(μg/ml · h) | 1.09 ± 0.58 | 1.76 ± 0.58$^{*}$ | 0.95 ± 0.35 | 1.40 ± 0.53 |
| | $C_{brain}$ (μg/g) | 0.10 ± 0.07 | 0.08 ± 0.03 | 0.64 ± 0.34$^{***,\dagger\dagger\dagger}$ | 1.98 ± 1.26$^{***,\dagger\dagger\dagger,\dagger}$ |
| | Fold increase | 1.0 | 0.8 | 6.3 | 19.6 |
| | $P_{brain}$ ($\times 10^{-3} \cdot h^{-1}$) | 94.8 ± 27.0 | 47.7 ± 12.7$^{*}$ | 643.6 ± 183.2$^{***,\dagger\dagger\dagger}$ | 1315.2 ± 374.9$^{***,\dagger\dagger\dagger,\ddagger\ddagger}$ |
| | Fold increase | 1.0 | 0.5 | 6.8 | 13.9 |
| $t$ = 4 h | $AUC_{(0-4\,h)}$(μg/ml · h) | 2.68 ± 1.36 | 4.67 ± 1.83$^{*}$ | 3.95 ± 1.81 | 4.95 ± 1.96$^{*}$ |
| | $C_{brain}$ (μg/g) | 0.006 ± 0.004 | 0.007 ± 0.003 | 0.047 ± 0.042$^{*,\dagger}$ | 0.25 ± 0.20$^{***,\dagger\dagger\dagger,\ddagger}$ |
| | Fold increase | 1.0 | 1.1 | 7.9 | 42.4 |
| | $P_{brain}$ ($\times 10^{-3} \cdot h^{-1}$) | 2.3 ± 1.0 | 1.5 ± 0.7 | 11.2 ± 10.5$^{*,\dagger\dagger}$ | 47.6 ± 29.6$^{***,\dagger\dagger\dagger,\ddagger\ddagger}$ |
| | Fold increase | 1.0 | 0.7 | 4.9 | 20.7 |

Data are means ($n$ = 4–5) ± S.D. One-way ANOVA was performed for all AUCs and log-transformed brain penetration data obtained for WT and knockout mice. Part of these data are also presented in Figures 2 and 3.

$^{*}$ $P < 0.05$, compared with WT mice.

$^{***}$ $P < 0.001$.

$^{\dagger}$ $P < 0.05$, compared with *Abcg2*(-/-) mice.

$^{\dagger\dagger}$ $P < 0.01$.

$^{\dagger\dagger\dagger}$ $P < 0.001$.

$^{\ddagger}$ $P < 0.05$, compared with *Abcb1a/1b*(-/-) mice.

$^{\ddagger\ddagger}$ $P < 0.01$.

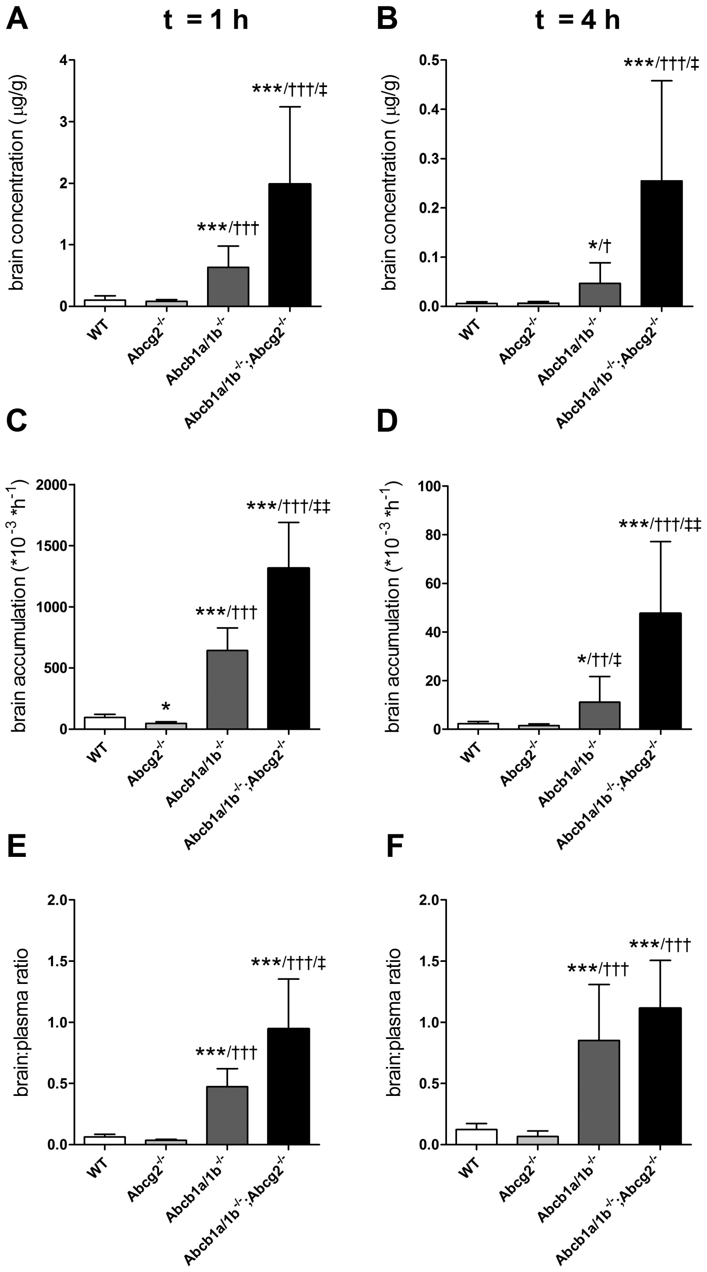

**Figure 3.** Brain concentrations (A and B), relative brain accumulation (C and D), and brain/plasma ratios (E and F) of axitinib in male WT, *Abcg2*(-/-), *Abcb1a/1b*(-/-), and *Abcb1a/1b;Abcg2*(-/-) mice after oral administration of 10 mg/kg axitinib at *t* = 1 h and *t* = 4 h. Relative brain accumulation was calculated by dividing brain concentrations by the axitinib plasma $\text{AUC}^{0-1\,\text{h}}$ and $\text{AUC}^{0-4\,\text{h}}$, respectively. Data are means ± S.D. [*n* = 5, except *n* = 4 for *Abcg2*(-/-) and *Abcb1a/1b;Abcg2*(-/-) at *t* = 1 h]. *, $P < 0.05$; ***, $P < 0.001$, compared with WT mice; $^{\dagger}$, $P < 0.05$; $^{\dagger\dagger}$, $P < 0.01$; $^{\dagger\dagger\dagger}$, $P < 0.001$, compared with *Abcg2*(-/-) mice; $^{\ddagger}$, $P < 0.05$; $^{\ddagger\ddagger}$, $P < 0.01$, compared with *Abcb1a/1b*(-/-) mice, using log-transformed data to normalize the S.D.s between study groups.

not dramatically change between 1 and 4 h, as the plasma levels of axitinib drop. Thus, from 1 h on, the disappearance of axitinib from the brain was only modestly delayed compared with the disappearance from plasma. Brain/plasma ratios, which were quite similar between 1 and 4 h, further supported this observation (Figure 3, E and F). Our results demonstrate that Abcb1 strongly reduces axitinib brain accumulation and can fully compensate for the loss of Abcg2 at the mouse BBB, because axitinib brain levels in *Abcg2*(-/-) mice were virtually identical to those in WT mice. On the other hand, Abcg2 can only partially compensate for the loss of the Abcb1-mediated efflux activity, in view of the increased axitinib brain accumulation in the absence of Abcb1. The 2- to 4-fold further increase in brain accumulation in *Abcb1a/1b;Abcg2*(-/-) mice compared with that in *Abcb1a/ 1b*(-/-) mice demonstrates that Abcg2 can contribute to the BBB for axitinib, but this is only clearly detectable in the absence of Abcb1.

Our brain accumulation data for axitinib are similar to published results in Abcb1 and Abcg2 knockout mice for TKIs such as imatinib, dasatinib, lapatinib, gefitinib, and erlotinib, all shared substrates of both efflux transporters [4, 6, 7, 9, 29]. Abcb1 and Abcg2 limit the brain accumulation of these TKIs in concert, but with Abcb1 providing the major contribution. In contrast, for sorafenib, which is only a very moderate ABCB1 substrate in vitro, Abcg2 was found to be the major determinant for limiting brain accumulation [8, 30]. The disproportionately high brain penetration of the indicated TKIs found in *Abcb1a/1b;Abcg2*(-/-) mice compared with that in mice deficient for only one transporter raised the question of the underlying mechanisms. Various explanations have been proposed, including adaptive increases in the complementary transporter expression in the BBB of single *Abcg2* or *Abcb1a/1b* knockout strains [31] or potential synergistic interactions between ABCB1 and ABCG2 [29]. However, we have found that Abcg2 RNA expression in brain and small intestine of FVB background *Abcb1a/1b* knockout mice was not different from that of WT mice and that Abcb1 RNA expression in brain and small intestine was also not altered in FVB background *Abcg2*(-/-) mice [5, 7, 8, 32]. This makes adaptive changes in transporter expression in the FVB knockout strains used here unlikely. In the course of this study, Kodaira et al. (2010) published a straightforward kinetic analysis of brain penetration data of a wide selection of drugs. These authors concluded that the disproportionately increased drug concentrations in the brains of *Abcb1a/1b;Abcg2*(-/-) mice could be readily explained solely by the additive ABCB1- and ABCG2-mediated net efflux at the BBB, primarily because each in itself is considerably larger than the remaining clearance from the brain in the absence of these transporters. Hence, there is no need to postulate a synergistic interaction between ABCB1 and ABCG2 at the BBB to explain the observed brain accumulation data.

Several drugs targeting VEGFRs demonstrated promising results in early-stage clinical trials or animal experiments (summarized in [18]). However, after an initial response, tumors often quickly became drug-resistant, potentially because of poor tumor cell exposure [33]. Preclinical coadministration of various TKIs such as dasatinib, gefitinib, and sorafenib to WT mice with the dual ABCB1 and ABCG2 inhibitor elacridar has resulted in significantly enhanced brain accumulation to levels similar to those observed in *Abcb1a/1b;Abcg2*(-/-) mice [4, 7, 8]. Furthermore, using the ABCB1- and ABCG2- inhibiting drug gefitinib, enhanced topotecan tumor penetration was demonstrated in mice bearing orthotopic human gliomas [34].

Clinical activity of axitinib was observed in a phase II study in patients with cytokine-refractory metastatic RCC with a response rate of 44.2% [12]. However, in 52% of the initial responders, the disease progressed for unknown reasons. Independent studies analyzing ABCB1 expression in tumors of patients with RCC revealed expression of ABCB1 at different levels in 100% of the tumors analyzed [35, 36]. In addition, ABCB1 was suggested as a prognostic marker for RCC because an association between high ABCB1 expression and poor survival was described [35]. Because the intracellular ATP-binding site of the VEGFR is the molecular target for axitinib [11], high ABCB1 levels in tumor cells might prevent axitinib from crossing the plasma membrane, resulting in insufficient intracellular concentrations and thus resistance to axitinib. Concomitant administration of axitinib with inhibitors of ABCB1 and/or ABCG2 might thus be a promising approach to enhancing axitinib brain and brain tumor cell accumulation or to overcoming ABCB1-mediated drug resistance in RCC therapy.

Of interest, our experiments revealed a major role of Abcb1 in limiting axitinib brain accumulation compared with that of Abcg2, whereas in contrast only Abcg2, and not Abcb1, had a significant (albeit modest) impact on oral axitinib plasma concentrations. A possible explanation for this discrepancy might be different relative expression levels of Abcb1 and Abcg2 in intestinal enterocytes and brain endothelial capillary cells at the BBB. Indeed, several studies suggest higher expression of Abcb1 than Abcg2 in the mouse BBB [31], which might explain why brain penetration data of drugs that are not extremely good Abcg2 substrates (dasatinib, lapatinib, and axitinib) generally show a major role of Abcb1 at the BBB. Regarding (oral) plasma AUCs, effects of ABC transporters are generally small compared with the effects observed at the BBB. This might be caused by higher background permeability for drugs at the intestinal wall, most likely also involving protein-mediated uptake processes, which could considerably reduce or even completely offset the impact of ABC transporter-mediated efflux. This may be the case for TKIs such as sorafenib, gefitinib, and lapatinib, for which neither Abcb1 nor Abcg2 has an impact on plasma kinetics. In contrast, dasatinib oral plasma AUCs are increased in Abcb1-deficient mice, whereas topotecan and axitinib oral AUCs are mainly influenced by Abcg2. The relative efficiency of the uptake processes may differ between individual TKIs and between intestine and BBB, which could also contribute to differential effects of Abcb1 and Abcg2 in intestine and BBB. Differential saturation conditions (intestinal drug concentrations are generally much higher than systemic concentrations upon oral drug administration) for both drug transporters with a specific drug might further play an important role. Our results illustrate that in vitro transport data for ABCB1 and ABCG2 cannot yet be simply extrapolated to the prediction of the relative impact of these transporters on both oral availability and brain penetration, with oral availability in particular being complicated. Therefore, we are still far from fully understanding all factors determining permeation of drugs across the important biological and pharmacological barriers involved

## Acknowledgments

We gratefully acknowledge the technical assistance of Anita van Esch and Ahmed Elbatsh as well as the statistical advice of Dr. Marta Lopez Yurda.

## *Reference List*

1. Schinkel AH, Jonker JW. Mammalian drug efflux transporters of the ATP binding cassette (ABC) family: an overview. Adv Drug Deliv Rev 2003;55:3-29.
2. Vlaming ML, Lagas JS, Schinkel AH. Physiological and pharmacological roles of ABCG2 (BCRP): recent findings in Abcg2 knockout mice. Adv Drug Deliv Rev 2009;61:14-25.
3. Borst P, Elferink Oude RP. Mammalian ABC transporters in health and disease. Annu Rev Biochem 2002;71:537-92.
4. Agarwal S, Sane R, Gallardo JL, Ohlfest JR, Elmquist WF. Distribution of gefitinib to the brain is limited by P-glycoprotein (ABCB1) and breast cancer resistance protein (ABCG2)-mediated active efflux. J Pharmacol Exp Ther 2010;334:147-55.
5. de Vries NA, Zhao J, Kroon E, Buckle T, Beijnen JH, van Tellingen O. P-glycoprotein and breast cancer resistance protein: two dominant transporters working together in limiting the brain penetration of topotecan. Clin Cancer Res 2007;13:6440-9.
6. Kodaira H, Kusuhara H, Ushiki J, Fuse E, Sugiyama Y. Kinetic analysis of the cooperation of P-glycoprotein (P-gp/Abcb1) and breast cancer resistance protein (Bcrp/Abcg2) in limiting the brain and testis penetration of erlotinib, flavopiridol, and mitoxantrone. J Pharmacol Exp Ther 2010;333:788-96.
7. Lagas JS, van Waterschoot RA, van Tilburg VA, et al. Brain accumulation of dasatinib is restricted by P-glycoprotein (ABCB1) and breast cancer resistance protein (ABCG2) and can be enhanced by elacridar treatment. Clin Cancer Res 2009;15:2344-51.
8. Lagas JS, van Waterschoot RA, Sparidans RW, Wagenaar E, Beijnen JH, Schinkel AH. Breast cancer resistance protein and P-glycoprotein limit sorafenib brain accumulation. Mol Cancer Ther 2010;9:319-26.
9. Oostendorp RL, Buckle T, Beijnen JH, van Tellingen O, Schellens JH. The effect of P-gp (Mdr1a/1b), BCRP (Bcrp1) and P-gp/BCRP inhibitors on the in vivo absorption, distribution, metabolism and excretion of imatinib. Invest New Drugs 2009;27:31-40.
10. Polli JW, Humphreys JE, Harmon KA, et al. The role of efflux and uptake transporters in [N-{3-chloro-4-[(3-fluorobenzyl)oxy]phenyl}-6-[5-({[2-(methylsulfonyl)ethyl]amino }methyl)-2-furyl]-4-quinazolinamine (GW572016, lapatinib) disposition and drug interactions. Drug Metab Dispos 2008;36:695-701.
11. Hu-Lowe DD, Zou HY, Grazzini ML, et al. Nonclinical antiangiogenesis and antitumor activities of axitinib (AG-013736), an oral, potent, and selective inhibitor of vascular endothelial growth factor receptor tyrosine kinases 1, 2, 3. Clin Cancer Res 2008;14:7272-83.
12. Rixe O, Bukowski RM, Michaelson MD, et al. Axitinib treatment in patients with cytokine-refractory metastatic renal-cell cancer: a phase II study. Lancet Oncol 2007;8:975-84.
13. Rini BI, Wilding G, Hudes G, et al. Phase II study of axitinib in sorafenib-refractory metastatic renal cell carcinoma. J Clin Oncol 2009;27:4462-8.
14. Rugo HS, Herbst RS, Liu G, et al. Phase I trial of the oral antiangiogenesis agent AG-013736 in patients with advanced solid tumors: pharmacokinetic and clinical results. J Clin Oncol 2005;23:5474-83.
15. Cohen EE, Rosen LS, Vokes EE, et al. Axitinib is an active treatment for all histologic subtypes of advanced thyroid cancer: results from a phase II study. J Clin Oncol 2008;26:4708-13.
16. Schiller JH, Larson T, Ou SH, et al. Efficacy and safety of axitinib in patients with advanced non-small-cell lung cancer: results from a phase II study. J Clin Oncol 2009;27:3836-41.
17. Spano JP, Chodkiewicz C, Maurel J, et al. Efficacy of gemcitabine plus axitinib compared with gemcitabine alone in patients with advanced pancreatic cancer: an open-label randomised phase II study. Lancet 2008;371:2101-8.
18. Rahman R, Smith S, Rahman C, Grundy R. Antiangiogenic therapy and mechanisms of tumor resistance in malignant glioma. J Oncol 2010;2010:251231.
19. Gottesman MM, Fojo T, Bates SE. Multidrug resistance in cancer: role of ATP-dependent transporters. Nat Rev Cancer 2002;2:48-58.
20. Jonker JW, Buitelaar M, Wagenaar E, et al. The breast cancer resistance protein protects against a major chlorophyll-derived dietary phototoxin and protoporphyria. Proc Natl Acad Sci U S A 2002;99:15649-54.
21. Bakos E, Evers R, Szakacs G, et al. Functional multidrug resistance protein (MRP1) lacking the N-terminal transmembrane domain. J Biol Chem 1998;273:32167-75.
22. Poller B, Wagenaar E, Tang SC, Schinkel AH. Double-transduced MDCKII cells to study human P-glycoprotein (ABCB1) and breast cancer resistance protein (ABCG2) interplay in drug transport across the blood-brain barrier. Mol Pharm 2011;8:571-82.

23. Sparidans RW, Iusuf D, Schinkel AH, Schellens JH, Beijnen JH. Liquid chromatography-tandem mass spectrometric assay for the light sensitive tyrosine kinase inhibitor axitinib in human plasma. J Chromatogr B Analyt Technol Biomed Life Sci 2009;877:4090-6.
24. Schinkel AH, Mayer U, Wagenaar E, et al. Normal viability and altered pharmacokinetics in mice lacking mdr1-type (drug-transporting) P-glycoproteins. Proc Natl Acad Sci U S A 1997;94:4028-33.
25. Jonker JW, Freeman J, Bolscher E, et al. Contribution of the ABC transporters Bcrp1 and Mdr1a/1b to the side population phenotype in mammary gland and bone marrow of mice. Stem Cells 2005;23:1059-65.
26. Dai H, Zhang P, Zhao S, Zhang J, Wang B. Regulation of the vascular endothelial growth factor and growth by estrogen and antiestrogens through Efp in Ishikawa endometrial carcinoma cells. Oncol Rep 2009;21:395-401.
27. Goh LB, Spears KJ, Yao D, et al. Endogenous drug transporters in in vitro and in vivo models for the prediction of drug disposition in man. Biochem Pharmacol 2002;64:1569-78.
28. Pithavala YK, Tortorici M, Toh M, et al. Effect of rifampin on the pharmacokinetics of Axitinib (AG-013736) in Japanese and Caucasian healthy volunteers. Cancer Chemother Pharmacol 2010;65:563-70.
29. Polli JW, Olson KL, Chism JP, et al. An unexpected synergist role of P-glycoprotein and breast cancer resistance protein on the central nervous system penetration of the tyrosine kinase inhibitor lapatinib (N-{3-chloro-4-[(3-fluorobenzyl)oxy]phenyl}-6-[5-({[2-(methylsulfonyl)ethyl]amino }methyl)-2-furyl]-4-quinazolinamine; GW572016). Drug Metab Dispos 2009;37:439-42.
30. Agarwal S, Sane R, Ohlfest JR, Elmquist WF. The role of the breast cancer resistance protein (ABCG2) in the distribution of sorafenib to the brain. J Pharmacol Exp Ther 2011;336:223-33.
31. Zhou L, Schmidt K, Nelson FR, Zelesky V, Troutman MD, Feng B. The effect of breast cancer resistance protein and P-glycoprotein on the brain penetration of flavopiridol, imatinib mesylate (Gleevec), prazosin, and 2-methoxy-3-(4-(2-(5-methyl-2-phenyloxazol-4-yl) ethoxy)phenyl)propanoic acid (PF-407288) in mice. Drug Metab Dispos 2009;37:946-55.
32. Jonker JW, Smit JW, Brinkhuis RF, et al. Role of breast cancer resistance protein in the bioavailability and fetal penetration of topotecan. J Natl Cancer Inst 2000;92:1651-6.
33. Tredan O, Galmarini CM, Patel K, Tannock IF. Drug resistance and the solid tumor microenvironment. J Natl Cancer Inst 2007;99:1441-54.
34. Carcaboso AM, Elmeliegy MA, Shen J, et al. Tyrosine kinase inhibitor gefitinib enhances topotecan penetration of gliomas. Cancer Res 2010;70:4499-508.
35. Mignogna C, Staibano S, Altieri V, et al. Prognostic significance of multidrug-resistance protein (MDR-1) in renal clear cell carcinomas: a five year follow-up analysis. BMC Cancer 2006;6:293.
36. Walsh N, Larkin A, Kennedy S, et al. Expression of multidrug resistance markers ABCB1 (MDR-1/P-gp) and ABCC1 (MRP-1) in renal cell carcinoma. BMC Urol 2009;9:6.

# *Conclusions and perspectives* &

In this thesis we studied OATP transporters *in vivo* using several knockout (lacking all mouse Oatp1a and the Oatp1b2 transporters) and humanized transgenic mouse strains with liver-specific expression of human OATP1A2, OATP1B1 or OATP1B3. The concomitant use of these different mouse models is required because mouse and human OATP1A/1B proteins are not straightforward orthologues of each other and their tissue localization and substrate specificity might differ substantially.

We described here three major aspects regarding functions of OATP1A/1B proteins and their clinical implications.

**Firstly, the physiological function of OATP1B transporters**. It is clear now that mouse Oatp1a/1b and human OATP1B proteins have an important role in efficient liver detoxification, amongst others by means of a dynamic process called hepatocyte hopping. This process has been demonstrated experimentally for bilirubin detoxification and aided in elucidating that the mechanistic cause of Rotor syndrome is a complete deficiency in OATP1B1 and OATP1B3. In short, OATP1B uptake transporters together with the efflux transporter ABCC3 form a sinusoidal liver-to-blood shuttling loop, in which bilirubin glucuronide (formed in the liver) is excreted back into the blood, from where it can be again taken up in the downstream hepatocytes by OATP1B proteins, and subsequently excreted into the bile. We believe that this concept might apply to drugs and their conjugates as well, thus allowing for efficient detoxification with profound pharmacological implications. Future studies to test this hypothesis experimentally will be required.

OATP1B transporters also have an important role in maintaining the bile acid homeostasis, by efficient liver uptake of unconjugated bile acids. This is an important role, as bile acids are involved in many physiological processes.  There are additional endogenous substrates (estrogen conjugates, steroid derivates, etc) of OATP1A/1B transporters and future studies may lead to the discovery of additional biological functions of OATP1A/1B proteins.

**Secondly, the pharmacological functions of OATP1A/1B transporters**. The most studied aspect of the OATP1A/1B transporters is their role in controlling the liver uptake, and therefore the hepatic clearance of a wide variety of drugs. Interestingly, the collection of pharmacokinetic studies performed so far indicate that the impact of OATP1A/1B on systemic exposure versus liver exposure depends on the intrinsic pharmacokinetic properties of the drug. More specifically, for drugs with substantial renal clearance (e.g., methotrexate and fexofenadine) absence of OATP1A/1B transporters leads to a marked increase in systemic plasma exposure and qualitatively decreased liver exposure. In contrast, for drugs with almost exclusive hepatic clearance, and almost absent alternative clearance pathways (e.g. pravastatin after bolus administration, rosuvastatin, SN-38 and docetaxel) absence of Oatp1a/1b transporters leads to a marked increase in systemic plasma exposure, without having a clear effect on liver exposure. These findings are supported experimentally by our studies in Oatp1a/1b knockout and concomitantly by a physiologically-based pharmacokinetic model developed by *Watanabe et al* (J Pharmacol Exp Ther. 2009 Feb;328(2):652-62). These findings have pharmacogenomic implications because there are several low-activity polymorphisms of OATP1A/1B transporters described. Also, complete deficiencies of either OATP1B1 or OATP1B3 transporters have been found in addition to the Rotor syndrome patients, which completely lack both OATP1B1 and OATP1B3. All these individuals might be at risk of developing toxicities when treated with OATP1B substrates. Also co-administration of these drugs with OATP1A/1B inhibitors might lead to clinically relevant drug-drug interactions.

Several of the mouse Oatp1a, Oatp2b1 and human OATP1A2 and OATP2B1 transporters are also expressed in the small intestine where it was thought that they contribute to the intestinal uptake of nutrients and/or drugs. Unfortunately, despite our best efforts, we have not been able demonstrate a clear role for mouse Oatp1a in the intestinal uptake of several tested xenobiotics (methotrexate, fexofenadine, docetaxel, pravastatin and rosuvastatin). Perhaps more in depth future studies will aid in elucidating this aspect.

Oatp1a transporters are also expressed in the kidney and in this thesis we provided preliminary experimental evidence that they can mediate the renal reabsorption of rosuvastatin. This finding probably has limited clinical importance as the contribution of renal clearance of rosuvastatin to the total systemic clearance is negligible. Nevertheless, this finding provides the proof-of-concept for future studies with other drugs for which the renal clearance is major determinant of their pharmacokinetics.

**Thirdly, the potential *in* vivo role of OATP1A/1B in tumor uptake and susceptibility to anticancer drugs.** We have shown that several anticancer drugs (methotrexate, paclitaxel, SN-38, docetaxel) can be transported *in vivo* by one or more of the human OATP1A/1B (OATP1A2, OATP1B1 or OATP1B3) transporters. Other studies have detected expression of these transporters in several types of tumors and increased sensitivity to anticancer drugs in cell lines overexpressing these transporters. Taken together, we can speculate that OATP1A/1B transporters might mediate the tumor uptake of these anticancer drugs, and therefore modulate response to chemotherapy. Nevertheless, specific preclinical and clinical studies are still required in order to establish their exact contribution.

It is important to note that Oatp1a/1b knockout mice have increased expression and activity of carboxylesterase (Ces) enzymes, which is normalized in humanized transgenic mice. This should be taken into account when performing pharmacokinetic and toxicological studies in these mouse strains with (pro-)drugs that might be affected by Ces activity. Also, as always, caution should be exerted when extrapolating findings from these preclinical models to humans.

Nevertheless, it is obvious that studies in Oatp1a/1b knockout and transgenic mice have provided important insights into the functions of OATP1A/1B transporters and we expect that they will continue to do so also in the future.

# *Summary* &

In recent years, there has been increasing attention for the drug uptake transporters of the Organic Anion-Transporting Polypeptide (human OATP, mouse Oatp, gene names *SLCO*, *Slco*) superfamily. It became obvious that OATPs, and especially the OATP1A and OATP1B subfamilies, have important physiological and pharmacological functions. Members of the OATP1A/1B subfamilies have received more interest because of their localization in tissues important for detoxification and pharmacokinetics (i.e. liver, small intestine and kidney) and their ability to mediate the cellular uptake of a wide variety of endogenous compounds but also many xenobiotics. Therefore, OATP1A/1B transporters play important roles in the physiological liver detoxification of endogenous compounds, but also in determining tissue distribution, the rate and route of elimination, systemic exposure and oral bioavailability of drugs. In our group we chose to study these transporters using knockout and transgenic mouse models to reveal important physiological and pharmacological functions of mouse and human OATP1A/1B transporters *in vivo*.

**Chapter 1.1** provides an introduction into the tissue localization of mouse and human OATP1A/1B transporters, combined with a description of the existing single and combination knockout mouse models and humanized transgenic mouse models of OATP1A/1B transporters. Further, the crucial physiological role of mouse and human OATP1A/1B proteins in plasma clearance (via efficient liver uptake) of bilirubin and unconjugated bile acids is described. In this chapter we also review the pharmacological importance of OATP1A/1B in the disposition of xenobiotics. In **chapter 1.2** the role of mouse and human OATP1A/1B proteins in efficient liver detoxification by means of hepatocyte hopping is outlined. In this chapter, we review findings from studies using Oatp1a/1b knockout mice and liver-specific OATP1B1 and OATP1B3 humanized transgenic mice, together with data from patients suffering of Rotor syndrome, a rare genetic disorder. Taken together, these findings elucidated that the Rotor syndrome is caused by a complete deficiency of OATP1B1 and OATP1B3 transporters in humans.

In **chapter 2** we established the role of mouse and human OATP1A/1B transporters in the plasma clearance of unconjugated bilirubin after exogenous administration. We showed that mouse Oatp1a/1b transporters play a role, although not essential, in the liver uptake of unconjugated bilirubin and that human OATP1B1 and OATP1A2, but not OATP1B3, can demonstrably transport unconjugated bilirubin *in vivo*. In the same chapter, we also investigated the role of human OATP1A/1B proteins in mediating the liver uptake of unconjugated bile acids. It is known that Oatp1a/1b-null mice have increased plasma levels of unconjugated bile acids, and in this chapter we demonstrated that liver-specific expression of OATP1B1 or OATP1B3 can confer a partial rescue of this phenotype, indicating that human OATP1B1 and OATP1B3 can transport some of the main unconjugated bile acids *in vivo*.

Besides their important physiological functions, OATP1A/1B transporters determine the pharmacokinetics of many drugs.

In **chapter 3**, we investigated the impact of OATP1A/1B proteins on the pharmacokinetics (and toxicity) of two cholesterol-lowering drugs, pravastatin and rosuvastatin. Because of their hydrophilic nature, with little metabolism and mainly hepatic clearance, pravastatin and rosuvastatin are considered prototypical OATP substrates. Hepatic uptake of statins is crucial as the liver represents both the main clearance organ and therapeutic target for these compounds.

In **chapter 3.1** we found that mouse Oatp1a/1b transporters determine the liver uptake of pravastatin, having a marked impact on plasma exposure. This was especially obvious after oral administration, with an up to 30-fold increase in the systemic exposure in Oatp1a/1b-null mice. Interestingly, in the same experiment, the liver exposure was less affected, with only a 2-fold reduction in the absence of Oatp1a/1b transporters. However, after chronic administration (60 days), at steady state exposure, plasma and liver exposure were equally affected by absence of Oatp1a/1b transporters. Therefore, absence of Oatp1a/1b transporters affects the therapeutic index of pravastatin in two ways: through increasing the risk of toxicity by increasing the systemic plasma exposure and through diminishing its therapeutic efficacy by lowering its liver exposure. In **chapter 3.2** we performed similar pharmacokinetic studies with rosuvastatin using Oatp1a/1b-null mice. In contrast to pravastatin, the impact of Oatp1a/1b was only evident in the plasma exposure, without affecting liver exposure. This intriguing observation is most likely due to the compensatory activity of high-capacity, low-affinity alternative liver uptake transporters at higher systemic rosuvastatin levels. Interestingly, we could show that most likely mouse Oatp1a1 in the kidney plays a role in the renal reabsorption of rosuvastatin, although the contribution of renal clearance to the systemic clearance of rosuvastatin is small in wild-type mice. Therefore, in addition to their predominant role in liver uptake, Oatp1a/1b transporters can also have a role in the renal reabsorption of drugs.

In **chapter 4,** we performed pharmacokinetic studies with two anticancer drugs, irinotecan and docetaxel, in both Oatp1a/1b knockout and humanized mice. Irinotecan is a prodrug with a complicated pharmacokinetic behavior, and it needs to be converted by esterases, including carboxylesterase (CES) enzymes to its cytotoxic metabolite, SN-38. In **chapter 4.1** we found that Oatp1a/1b-null mice have increased expression and activity of Ces1 enzymes, while humanized transgenic mice with liver- specific expression of OATP1B1 or OATP1B3 have normalized levels of these enzymes. The mechanism behind this altered expression of Ces1 enyzmes in Oatp1a/1b knockout and transgenic mice is unknown yet. Despite this complication, we could still demonstrate that mouse Oatp1a/1b transporters mediate liver uptake of irinotecan and SN-38, while human OATP1B1 and OATP1B3 transport only SN-38 *in vivo*. Thus, alterations in activity of OATP1B transporters and/or CES enzymes (due to genetic variation or pharmacological inhibition) might lead to unpredictable systemic exposure to irinotecan and/or SN-38, and subsequently increased risks of toxicity.

In **chapter 4.2** we showed that one or more of the mouse Oatp1a/1b transporters mediate the plasma clearance of docetaxel, and in line with previous results for rosuvastatin, do not have a clear effect on the liver exposure. Most importantly, all three human OATP1A/1B transporters (OATP1A2, OATP1B1 and OATP1B3) could mediate the liver uptake of docetaxel *in vivo*. Therefore, activity of OATP1B1 and/or OATP1B3 might be clinically relevant for the hepatic clearance, systemic exposure and therefore toxicity of docetaxel, while OATP1A2 might mediate uptake of docetaxel in tissues like small intestine, brain and kidney. Also of importance, their expression in cancers treated with docetaxel might affect docetaxel tumor uptake and therefore susceptibility to chemotherapy.

Mouse Oatp1a proteins and human OATP1A2 are expressed also in the small intestine, where it is thought that they mediate the intestinal uptake of drugs, thus increasing their oral bioavailability. We investigated this aspect in our studies with pravastatin, rosuvastatin and docetaxel (by measuring portal vein drug concentrations shortly after oral administration) and we found that mouse Oatp1a transporters are not essential in the intestinal uptake of these drugs. One explanation might be provided by the existence of an alternative transporter, Oatp2b1 (OATP2B1) which is highly expressed in the small intestinal as well, and might compensate for the loss of function of Oatp1a transporters.

Taken together, the findings of these four chapters add to our current knowledge of physiological and pharmacological functions of mouse and human OATP1A/1B transporters in handling endogenous substrates and a wide variety of xenobiotics. In addition to their established role in liver uptake of drugs, we could demonstrate that mouse Oatp1a can mediate renal reabsorption of drugs. Also, an important cautionary point is that OATP1A/1B activity can alter expression of Ces enzymes, which should be taken into account for future pharmacokinetic studies with drug substrates of Ces. We believe that Oatp1a/1b knockout and transgenic mice represent valuable *in vivo* tools which can be used in drug development, therapy optimization studies and in predicting outcome to chemotherapy.

In addition to uptake transporters, efflux transporters have a great impact on drug pharmacokinetics, by efficiently mediating the cellular efflux of various drugs. Their expression in tumors might limit the effective intratumoral drug concentrations and thus lead to resistance to chemotherapy. In **chapter 5**, we focus on two of the major efflux transporters, P-gp (ABCB1) and Bcrp (ABCG2) and their single or combined role in the brain disposition of anticancer drugs, tamoxifen and axitinib. In **chapter 5.2** we describe that endoxifen, the 100-fold more active metabolite of tamoxifen, is a P-gp substrate *in vitro* and *in vivo*. High expression of P-gp in breast tumors treated with tamoxifen, might thus lead to insufficient intratumoral endoxifen concentrations and therefore insufficient therapeutic response. In **chapter 5.3**, we found that Brcp has a role in limiting axitinib bioavailability after oral administration, while at the blood-brain barrier, P-gp is the main determinant of axitinib brain penetration. These results might have clinical relevance for brain tumors positioned behind an intact and functional blood-brain barrier.

# *Appendices* &

# *Nederlandstalige samenvatting*

In de afgelopen jaren is er toenemende belangstelling ontstaan voor de geneesmiddelopname transporteurs uit de “Organic Anion-Transporting Polypeptide” superfamilie (OATP in de mens, Oatp in de muis, gennamen *SLCO*, *Slco*). Het is duidelijk geworden dat OATPs, en vooral de OATP1A en OATP1B subfamilies, belangrijke fysiologische en farmacologische functies hebben. Veel aandacht is uitgegaan naar de leden van de OATP1A/1B subfamilies vanwege hun aanwezigheid in weefels die van belang zijn voor detoxificatie en farmacokinetiek (namelijk de lever, dunne darm en nier) en hun vermogen om de cellulaire opname te bewerkstelligen van een grote variëteit aan endogene stoffen en xenobiotica. OATP1A/1B transporteurs spelen dientengevolge een belangrijke rol in de fysiologische detoxificatie van endogene stoffen door de lever, maar ook in het bepalen van de weefselverdeling, de snelheid en route van eliminatie, de systemische beschikbaarheid, en de orale biologische beschikbaarheid van geneesmiddelen. In onze groep hebben we gekozen om deze transporteurs te bestuderen door middel van knockout en transgene muismodellen, teneinde belangrijke *in vivo* fysiologische en farmacologische functies van de muizen- en humane OATP1A/1B transporteurs te doorgronden.

**Hoofdstuk 1.1** is een introductie in de weefselverdeling van de muizen- en humane OATP1A/1B transporteurs, gecombineerd met een beschrijving van de reeds bestaande enkelvoudige en gecombineerde knockout en gehumaniseerde transgene muismodellen voor deze eiwitten. Verder is de essentiële fysiologische rol van muizen- en humane OATP1A/1B eiwitten in de plasmaklaring (middels efficiënte leveropname) van bilirubine en ongeconjugeerde galzuren beschreven. In dit hoofdstuk geven we ook een overzicht van het farmacologische belang van OATP1A/1B in de dispositie van xenobiotica. In **hoofdstuk 1.2** wordt de rol van muizen- en humane OATP1A/1B eiwitten in de efficiënte detoxificatie door de lever middels het proces van hepatocyt-hoppen beschreven. In dit hoofdstuk vatten we bevindingen samen uit studies met Oatp1a/1b knockout en leverspecifieke OATP1B1- en OATP1B3-gehumaniseerde muizen, alsmede gegevens verkregen in patiënten die aan het Rotor syndroom, een zeldzame genetische aandoening, lijden. Samengenomen hebben deze bevindingen uitgewezen dat het Rotor syndroom veroorzaakt wordt door een volledige deficiëntie in de OATP1B1 en OATP1B3 transporteurs in de mens.

In **hoofdstuk 2** hebben we de rol vastgesteld van muizen- en humane OATP1A/1B transporteurs in de plasmaklaring van ongeconjugeerd bilirubine na exogene toediening. We toonden aan dat de muis Oatp1a/1b transporteurs een rol spelen, zij het geen essentiële, in de leveropname van ongeconjugeerd bilirubine en dat OATP1B1 en OATP1A2, maar niet OATP1B3, aantoonbaar ongeconjugeerd bilirubine *in vivo* kunnen transporteren. In hetzelfde hoofdstuk onderzochten we de rol van de humane OATP1A/1B eiwitten in de opname van ongeconjugeerde galzuren in de lever. Het is bekend dat Oatp1a/1b-nul muizen verhoogde plasmaniveaus van ongeconjugeerde galzuren hebben, en in dit hoofdstuk toonden we aan dat leverspecifieke expressie van OATP1B1 of OATP1B3 een gedeeltelijke reversie van dit fenotype kan opleveren, hetgeen aangeeft dat humaan OATP1B1 en OATP1B3 enkele van de belangrijkste ongeconjugeerde galzuren *in vivo* kunnen transporteren.

Naast hun belangrijke fysiologische functies bepalen OATP1A/1B transporteurs ook de farmacokinetiek van een groot aantal geneesmiddelen. In **hoofdstuk 3** onderzochten we de invloed van OATP1A/1B eiwitten op de farmacokinetiek (en toxiciteit) van twee cholesterolverlagende geneesmiddelen, pravastatine en rosuvastatine. Door hun hydrofiele karakter, beperkt metabolisme en primaire klaring via de lever worden deze twee geneesmiddelen gezien als prototypische OATP substraten. De leveropname van statines is essentieel, omdat de lever zowel het belangrijkste klaringsorgaan als het therapeutische doelwitorgaan voor deze stoffen is. In **hoofdstuk 3.1** vonden we dat de muis Oatp1a/1b transporteurs de leveropname van pravastatine bepalen, met een uitgesproken impact op plasmablootstelling. Dit was vooral duidelijk na orale toediening, met een tot 30-voudige toename van de systemische blootstelling in Oatp1a/1b-nul muizen. Opvallend was dat in hetzelfde experiment de leverblootstelling minder aangedaan was, met slechts een 2-voudige afname in de afwezigheid van Oatp1a/1b transporteurs. Echter, bij chronische toediening (60 dagen), met een gestage blootstelling, waren plasma- en leverblootstelling ongeveer even sterk aangedaan door de afwezigheid van Oatp1a/1b transporteurs. Derhalve beïnvloedt de afwezigheid van Oatp1a/1b transporteurs de therapeutische index van pravastatine langs twee wegen: door het risico op toxiciteit te verhogen als gevolg van hogere plasmaniveaus, en door het verlagen van de therapeutische werking door het verlagen van de leverblootstelling. In **hoofdstuk 3.2** voerden we vergelijkbare studies uit met rosuvastatine in Oatp1a/1b-nul muizen. In tegenstelling tot pravastatine was de invloed van Oatp1a/1b alleen merkbaar in de plasmablootstelling, zonder een evident effect op de leverblootstelling. Deze intrigerende waarneming is zeer waarschijnlijk het gevolg van de compensatoire activiteit van alternatieve leveropname systemen met een hoge capaciteit, maar lage affiniteit, die van belang worden bij hogere systemische rosuvastatine niveaus. We konden verder aantonen dat vermoedelijk Oatp1a1 in de nier een rol speelt bij de renale reabsorptie van rosuvastatine, alhoewel de absolute bijdrage van renale klaring aan de systemische klaring van rosuvastatine gering is in wild-type muizen. Naast hun prominente rol in leveropname kunnen Oatp1a/1b transporteurs derhalve ook een rol spelen in de renale reabsorptie van geneesmiddelen.

In **hoofdstuk 4** voerden we farmacokinetische studies uit met twee antikanker geneesmiddelen, irinotecan en docetaxel, in zowel Oatp1a/1b knockout muizen als in OATP1A/1B-gehumaniseerde muizen. Irinotecan is een prodrug met een gecompliceerd farmacokinetisch gedrag, en het moet door esterasen, waaronder carboxylesterase (CES) enzymen omgezet worden tot de cytotoxische metaboliet, SN-38. In **hoofdstuk 4.1** vonden we dat Oatp1a/1b-nul muizen toegenomen expressie en activiteit van Ces1 enzymen hebben, terwijl gehumaniseerde muizen met leverspecifieke expressie van OATP1B1 of OATP1B3 wildtype niveaus van deze enzymen vertoonden. Het mechanisme achter deze veranderde expressie van Ces1 enzymen in Oatp1a/1b knockout en transgene muizen is vooralsnog onbekend. Ondanks deze complicatie konden we toch aantonen dat de muis Oatp1a/1b transporteurs de leveropname van irinotecan en SN-38 bewerkstelligen, terwijl humaan OATP1B1 en OATP1B3 *in vivo* alleen SN-38 transporteren. Veranderingen in de activiteit van OATP1B transporteurs en/of CES enzymen (ten gevolge van genetische variatie of farmacologische remming) kunnen dus leiden tot een onvoorspelbare systemische blootstelling van irinotecan en/of SN-38, en dientengevolge een verhoogd toxiciteitsrisico. In **hoofdstuk 4.2** toonden we aan dat één of meer muis Oatp1a/1b transporteurs de plasmaklaring van docetaxel bewerkstelligen terwijl er, in overeenstemming met eerdere resultaten voor rosuvastatine, geen duidelijk effect op de leverblootstelling was. De belangrijkste bevinding was dat alle drie de humane

OATP1A/1B transporteurs (OATP1A2, OATP1B1 en OATP1B3) de *in vivo* leveropname van docetaxel konden bewerkstelligen. De activiteit van OATP1B1 en/of OATP1B3 kan dus klinisch relevant zijn voor de leverklaring en systemische blootstelling, en derhalve de toxiciteit van docetaxel, terwijl OATP1A2 de opname van docetaxel in weefsels zoals dunne darm, hersen en nier zou kunnen bewerkstelligen. Ook van belang is dat hun expressie in kankers de tumoropname van docetaxel zou kunnen beïnvloeden, en derhalve de gevoeligheid voor deze chemotherapie.

Muis Oatp1a eiwitten en humaan OATP1A2 komen tot expressie in de dunne darm, en men denkt dat ze aldaar de darmopname van geneesmiddelen kunnen bewerkstelligen, en zo de orale biologische beschikbaarheid ervan kunnen verhogen. We onderzochten dit aspect in onze studies met pravastatine, rosuvastatine en docetaxel (door de geneesmiddel concentratie in de poortader kort na orale toediening van het geneesmiddel te testen), en we vonden dat de muis Oatp1a/1b transporteurs niet essentieel zijn voor de darmopname van deze geneesmiddelen. Een mogelijke verklaring hiervoor zou het bestaan van een alternatieve transporteur, Oatp2b1 (OATP2B1 in de mens) kunnen zijn, welke eveneens hoog tot expressie komt in de dunne darm, en aldus zou kunnen compenseren voor het verlies van de Oatp1a transporteur functies.

Samen genomen dragen de bevindingen uit deze vier hoofdstukken bij aan onze huidige kennis over de fysiologische en farmacologische functies van de muizen en humane OATP1A/1B transporteurs in het verwerken van endogene substraten en een ruime variëteit aan xenobiotica. Naast hun eerder vastgestelde rol in de leveropname van geneesmiddelen konden we aantonen dat muis Oatp1a kan bijdragen aan de renale reabsorptie van geneesmiddelen. Een belangrijk punt dat aanleiding geeft tot voorzichtigheid is de bevinding dat OATP1A/1B activiteit de expressie van Ces enzymen in muizen kan veranderen. Dit dient meegenomen te worden in toekomstige farmacokinetische studies met geneesmiddelen die substraat van Ces enzymen zijn. Wij denken dat Oatp1a/1b knockout en transgene muizen waardevolle *in vivo* gereedschappen zijn die gebruikt kunnen worden bij de ontwikkeling van geneesmiddelen, bij studies om therapieën te optimaliseren, en bij het beter voorspellen van de uitkomst van chemotherapie.

Naast de opname transporteurs hebben ook efflux transporteurs een grote invloed op geneesmiddel farmacokinetiek, door de efficiënte cellulaire uitstroom van verschillende geneesmiddelen te bewerkstelligen. Hun expressie in tumoren kan de effectieve intratumorale geneesmiddelconcentratie beperken, en dus tot resistentie tegen chemotherapie leiden. In **hoofdstuk 5** concentreren we ons op twee belangrijke efflux transporteurs, P-gp (ABCB1) en Bcrp (ABCG2), en hun enkelvoudige of gecombineerde rol in de hersendispositie van de antikanker geneesmiddelen tamoxifen en axitinib. In **hoofdstuk 5.2** beschrijven we dat endoxifen, de 100-voudig actievere metaboliet van tamoxifen, een P-gp substraat is *in vivo* en *in vitro*. Hoge expressie van P-gp in borsttumoren behandeld met tamoxifen zou dus kunnen leiden tot onvoldoende intratumorale endoxifen concentraties, en dus onvoldoende therapeutische respons. In **hoofdstuk 5.3** vonden we dat Bcrp een rol heeft in het beperken van axitinib biologische beschikbaarheid na orale toediening, terwijl in de bloed-hersen barrière P-gp de belangrijkste determinant is voor de axitinib hersenpenetratie. Deze resultaten zijn mogelijk klinisch relevant voor hersentumoren die zich functioneel achter de bloed-hersen barrière bevinden.

# Rezumat

Succesul terapeutic al unui medicament depinde de ușurința cu care respectivul medicament ajunge la organele si celulele țintă din organism. Pentru că majoritatea țintelor terapeutice se află intracelular, este esențial ca medicamentul să poată pătrunde în celulă. Toate celulele sunt dotate cu sisteme de transport transmembranar care mediază influxul sau efluxul medicamentelor și astfel influențează sensibilitatea celulelor pentru medicamentul respectiv. Aceste proteine de transport transmembranar determină în mare măsură farmacocinetica unui medicament, adică drumul parcurs de medicament în organism plecând de la absorbția, continuând cu distribuția și eliminarea acestuia. Atunci când aceste procese sunt perturbate pot apărea efecte secundare sau efectul terapeutic este diminuat.

În această teză de doctorat am studiat proteinele de transmembrane de influx, OATP și de eflux, ABC. Am utilizat diverse modele genetice (șoricei de laborator manipulați genetic), investigând funcția de transport a proteinelor murine Oatp1a/1b, Abcb1, Abcg2 și a proteinelor umane OATP1A2, OATP1B1 și OATP1B3. Am studiat în detaliu mecanismele prin care aceste proteine de transport influențează farmacocinetica unor medicamente anticanceroase sau a statinelor (medicamente anticolesterol utilizate pe scară largă), măsurând absorbția, concentrația în diverse organe, în urină sau în fecale, precum și efectele secundare ale acestor medicamente.

Concluziile studiilor prezentate în această teză furnizează informații noi relevante pentru funcțiile farmacologice și toxicologice ale acestor proteine de transport. Aceste descoperiri au importanță clinică pentru pacienții care suferă de mutații genetice ale acestor proteine de transport. Ca urmare a acestor mutații activitatea de transport este diminuată, având drept consecință acumularea medicamentelor în organism și posibila apariție a efectelor secundare. În pacienții fără mutații genetice co-administrarea unor medicamente care inhibă funcția proteinelor de transport poate avea consecințe similare.

# *Curriculum Vitae*

Dilek Iusuf was born on May 22nd, 1981 in Constanta (Romania). After obtaining her highschool diploma in 2000, she began her studies in Pharmacy, at the University of Pharmacy and Medicine "Iuliu Hatieganu", Cluj-Napoca (Romania). During her bachelor studies, she did a 4 month-internship at the Department of Clinical Pharmacology, at the General Hospital in Valencia (Spain), as part of the EU exchange program Erasmus. In September 2005, she obtained her Bachelor degree in Pharmacy. In 2006, Dilek joined the Topmaster program "Medical and Pharmaceutical Drug Innovation" at the University of Groningen (The Netherlands). During this 2-year master program, she performed one internship project in the laboratory of Prof. Dr. R.H. Henning and one in the laboratory of Dr. B. J. Kroesen. After obtaining her MSc diploma (*cum laude*), Dilek started her doctoral research in the laboratory of Dr. Alfred H. Schinkel at the Netherlands Cancer Institute in Amsterdam (The Netherlands), where she combined *in vivo* and *in vitro* techniques to study the physiological and pharmacological functions of uptake transporters, OATPs, and efflux transporters (ABC transporters). This project was conducted in collaboration with the research lab of Prof. Dr. J.H. Beijnen (Slotervaart Hospital, Amsterdam, The Netherlands).

# *List of publications*

1. **OATP1A/1B transporters affect irinotecan and SN-38 pharmacokinetics and carboxylesterase expression in knockout and humanized transgenic mice**
   Dilek Iusuf, Marion Ludwig, Ahmed Elbatsh, Anita van Esch, Evita van de Steeg, Els Wagenaar, Martin van der Valk, Fan Lin, Olaf van Tellingen and Alfred H. Schinkel
   *Submitted for publication*
2. **Human OATP1B1, OATP1B3 and OATP1A2 mediate the in vivo uptake of docetaxel**
   Dilek Iusuf*, Jeroen J.M.A. Hendrikx*, Anita van Esch, Evita van de Steeg, Els Wagenaar, Jos H. Beijnen and Alfred H. Schinkel. * contributed equally
   *To be submitted*
3. **Mouse and human OATP1A/1B transporters mediate plasma clearance of unconjugated bilirubin and bile acids**
   Dilek Iusuf, Anita van Esch , Dirk R. de Waart, Els Wagenaar , Evita van de Steeg , Ronald P.J. Oude Elferink and Alfred H. Schinkel
   *To be submitted*
4. **Abcc4 together with Abcb1 and Abcg2 form a robust co-operative drug efflux system that restricts the brain entry of camptothecin analogs.**
   Lin F, Marchetti S, Pluim D, Iusuf D, Mazzanti R, Schellens JH, Beijnen JH, van Tellingen O.
   *Clin Cancer Res. 2013 Mar 5*
5. **Murine Oatp1a/1b uptake transporters control rosuvastatin systemic exposure without affecting its apparent liver exposure**
   Iusuf D, van Esch A, Hobbs MJ, Taylor MA, Kenworthy KE, van de Steeg E, Wagenaar E, Schinkel AH.
   *Mol Pharmacol. 2013 Feb 19*
6. **Hepatocyte hopping of OATP1B substrates contributes to efficient hepatic detoxification**
   Iusuf D, van de Steeg E, Schinkel AH.
   *Clin Pharmacol Ther. 2012 Nov*
7. **Organic anion-transporting polypeptides 1a/1b control the hepatic uptake of pravastatin in mice**
   Iusuf D, Sparidans RW, van Esch A, Hobbs M, Kenworthy KE, van de Steeg E, Wagenaar E, Beijnen JH, Schinkel AH.
   *Mol Pharm. 2012 Sep 4*
8. **P-glycoprotein, multidrug-resistance associated protein 2, Cyp3a, and carboxylesterase affect the oral availability and metabolism of vinorelbine**
   Lagas JS, Damen CW, van Waterschoot RA, Iusuf D, Beijnen JH, Schinkel AH.
   *Mol Pharmacol. 2012 Oct*

9. **Functions of OATP1A and 1B transporters in vivo: insights from mouse models**
   Iusuf D*, van de Steeg E*, Schinkel AH. * contributed equally
   *Trends Pharmacol Sci. 2012 Feb*

10. **P-glycoprotein (ABCB1) transports the primary active tamoxifen metabolites endoxifen and 4-hydroxytamoxifen and restricts their brain penetration**
    Iusuf D*, Teunissen SF*, Wagenaar E, Rosing H, Beijnen JH, Schinkel AH. * contributed equally
    *J Pharmacol Exp Ther. 2011 Jun*

11. **Differential impact of P-glycoprotein (ABCB1) and breast cancer resistance protein (ABCG2) on axitinib brain accumulation and oral plasma pharmacokinetics**
    Poller B*, Iusuf D*, Sparidans RW, Wagenaar E, Beijnen JH, Schinkel AH. * contributed equally
    *Drug Metab Dispos. 2011 May*

12. **Liquid chromatography-tandem mass spectrometric assay for pravastatin and two isomeric metabolites in mouse plasma and tissue homogenates**
    Sparidans RW, Iusuf D, Schinkel AH, Schellens JH, Beijnen JH.
    *J Chromatogr B Analyt Technol Biomed Life Sci. 2010 Oct 15*

13. **Liquid chromatography-tandem mass spectrometric assay for the light sensitive tyrosine kinase inhibitor axitinib in human plasma**
    Sparidans RW, Iusuf D, Schinkel AH, Schellens JH, Beijnen JH.
    *J Chromatogr B Analyt Technol Biomed Life Sci. 2009 Dec 15*

14. **Bradykinin protects against oxidative stress-induced endothelial cell senescence**
    Oeseburg H, Iusuf D, van der Harst P, van Gilst WH, Henning RH, Roks AJ.
    *Hypertension. 2009 Feb*

15. **Angiotensin-(1-7):pharmacological properties and pharmacotherapeutic perspectives**
    Iusuf D, Henning RH, van Gilst WH, Roks AJ.
    *Eur J Pharmacol.2008 May 13*

# Acknowledgements

Yuhuu! I have completed my thesis! I am really happy to have achieved this milestone, and now I get to look back at the wonderful time I had in the NKI. In the last five years, I grew a lot both personally and professionally, I learned so many things and I have experienced a lot. But most importantly I met and worked with a lot of great people who I would like to thank now.

First of all, I would like to thank my co-promotor and supervisor. **Alfred**, your style of letting your PhD students work as independently as possible, but also offering them lots of support, fitted me perfectly. It was great that I had the freedom to plan my work, but at the same time I knew that I could always ask your opinion and advice, which I did so many times. I learned many things from you: integrity, precision and to be less impulsive. Moreover, your kindness, correctness and respect for your students and co-workers impress me deeply. I really enjoyed our discussions about everything: from science to politics, history and in the last period also about babies :). Thank you for your support and trust!

Further I would like to thank my promotor, **Jos**. I really admire your enthusiasm and energy you have for each PhD student (although you had so many already!). Every time I got an email from you, I felt more positive about my work. Your passion and dedication for your work is inspirational. Also, I would like to thank the members of my reading committee for their time and evaluation of my work.

What I liked most in my research is that I got the chance to collaborate with many people from different departments and institutes. Dear **Olaf**, you are the one who introduced me to the world of HPLC and even if (by coincidence!) something got broken down while I was using it, you kept on trusting me and offered me unconditional advice and support. I wish you lots of success in your research! **Bas**, thanks for all your help and lively discussions about our tamoxifen study. It was fun to collaborate with you and despite being initially scooped, we still got a good publication out of it. Best of luck in your carreer! Dear **Rolf**, I do not dare to count back the amount of samples I sent you for measuring. We had a very successful collaboration which resulted in four published articles, two of them presented in this thesis. Thank you for your efficiency, promptness and hard-work and I wish you all the best in the future. Dear **Kathryn** and **Mike**, although we have never met face to face, I feel like I know you a little bit. Thank you for agreeing to provide analytical support for the rosuvastatin study. **Mike**, thank you for the pharmacokinetic modelling of the statin data and for teaching me (over the phone!) how to perform a portal vein puncture. Dear **Rudi**, we both work in Amsterdam, but we only have communicated via e-mail. Nevertheless, our collaboration was successful and hopefully will lead to a good publication. Thank you so much for your support and sorry if I asked too often "when will you have the results?". **Birk**, you had a great idea to come to Amsterdam to do a post-doc in Alfred's group. Not only you did you teach me how to perform transwell experiments and co-authored a chapter of my thesis, but you also became a good friend. Thanks for your tips about good series and music, and all the job offers at Novartis ;). I am happy that we keep in touch and hope to see you soon! **Jeroen**, I hope that I am half as efficient as you are. Thank you for your collaboration with the docetaxel study, hopefully we will have it published soon. I am sure that you will finish your PhD with flying colors!

Of course there also some projects which did not deliver publishable results, but still a lot of effort was put into them. Therefore I would like to thank **Hilde Rosing**, for never saying "no" to yet another collaboration with the Schinkel group. Also **Nynke Jager**, thanks for your help with the endoxifen project.

My dear pharanimfs, **Charlotte** and **Arantxa**, thanks for agreeing to stand next to me on this special day! **Charlotte**, we shared so many things in the last years! Just to name a few: office, running, secrets, recipes, gossip, holidays, laughter, tears, French expressions, chocolate.... Thank you for your unlimited generousity, I will miss you a lot when you go back to France. **Arantxa**, guapa! Nos hicimos muy buenas amigas en un momento difícil de nuestras vidas, y que bien lo pasamos! Contigo al lado, con tu actitud positiva, tus ganas de reírte y pasártelo bien, la vida es más fácil! Gracias por escucharme, tus consejos y tu ayuda durante 2 mudanzas! Que te vaya estupendo en Barcelona, aquí te echamos mucho de menos!

In the last five years, the Schinkel group went through a radical change in its composition. But some people were there throughout my whole PhD, like **Anita** and **Els. Anita**, you helped me so much when I was struggling with several projects and too many experiments. Thanks to your efficiency and talent for certain techniques we made a lot of progress and we managed to finalize a lot of projects. It was a pleasure to work with you, thanks for helping me with most of the experiments described in this thesis, but also with practicing Dutch in the animal facility! I wish you and your family lots of health and happiness! **Els**, you are the glue that keeps us together. And not only with your fantastic work on making new cell lines, new knockout and transgenic mice and keeping everything organized, but also with your social skills. Thank you for spoiling us (with chocolate, fruit and stroopwafels), entertaining us with your funny stories and sarcastic comments and making us behave in the lab. And now my old Schinkel colleagues: I really appreciate that you made me feel welcomed. I learned useful things from all of you and I am really glad that we still keep in touch. **Evita**, you were great in teaching me all there was about Oatps, gall bladder cannulations and how to play practical jokes on our colleagues. All the best in your career and with your family! **Robert**, you were a lot of fun to be around, but also you gave me good scientific advice. Enjoy your new adventure in Basel with your family! **Marijn**, you were the first one who took me to the animal facility, thanks for all your advice. Best of luck in the future! **Jurjen**, thanks for all your practical tips and for starting the Ces investigation in our lab. Good luck with your next career step! And now my PhD buddies, **Selvi** and **Seng**, thanks for sharing so many good times in and outside the office. **Seng**, I knew that I could always count on you to help me with all sorts of stuff, thank you for that. You are incredibly hard-working, dedicated and generous. Good luck in finding a job and lots of happiness in the future! **Selvi**, you are such a good colleague: always willing to help and to ensure a nice atmosphere in the office! I really admire your way of being direct and sweet at the same time and that you are never afraid to ask questions. Lots of success in your next (Oatp) projects and finishing your thesis! And to our guests from Asia: **Ning** (or Panda): it was lots of fun to have you around, thank you for your kindness and your friendship. **Kazuya**, your insight about the pravastatin data saved the project, and broadened our knowledge about Oatps. Also thanks for inviting us to karaoke night when we were in Tokyo!

I was lucky to have the chance to supervise two very good and hard-working students, **Marion** and **Ahmed**, who, in hindsight, worked on a very difficult and complex project. Nevertheless, you did great and hopefully our work together will be published soon. **Marion**, you were very organized and had a good overview of the project and literature. I think these traits come in handy during your PhD also, good luck in completing it! **Ahmed**, I think you got to know everybody at the NKI only a few months and probably that is why you came back to do your PhD here. I admire your willingness and determination to take on difficult project lines like the paclitaxel pilot studies or setting up a method for the SN-38 glucuronide. I wish you lots of success in your PhD!

I spent a lot of my time performing experiments and listening to nice Dutch music in the animal facility on G3. I am very grateful to **Marissa**, **Yvonne**, **Adrie**, **Klaas**, **Jeroen**, **Sido**, **Jolanda** and **Jurriaan** for taking such good care of our mice. Het was echt leuk met jullie te werken, bedankt voor alles! **Ton**, bedankt voor jouw hulp de met galblaas cannulatie! **Bjorn** and **Tania**, thank you for relocating my mice to the RNC! **Maaike**, you were so nice and always willing to help with my DEC applications. **Marco**, **Roel**, **Phillip** and **Carla** thank you for your support regarding the DEC approvals.

Many people throughout the NKI provided so much support in my studies. Bedankt **Desiree** en **Theo** voor jullie steun tijdens mijn experimenten in de RNC! **Lin**, we shared a lot of worries about the HPLC, irinotecan and Ces upregulation, but also lots of fun in Texel and during Chinese dinners. I wish you and your family all the best in your new life in Singapore! **Levi**, thanks to your organizational skills, it was much easier to use the HPLC or the homogenizer. **Ji-Ying**, I really enjoyed our talks about mountains and holidays. Thank you for your enthusiasm and efficiency in evaluating all those slides I gave you! **Martin**, thank you for waiting to retire until I was almost done with my PhD. Joke aside, it was very nice to work with you and I am grateful for all your input to my research.

The Schinkel group moved to P2in order to be closer to the Borst group, and with good reason. I got to know very nice people which made coffee breaks, lab-outings and Christmas dinners very enjoyable. **Piet**, you are truly a living legend. Your charisma, sharp mind and dedication to science will remain vivid in my memories of the NKI. **Henri**, you always greeted me with a smile and some funny comments. Thanks for keeping the NKI together, for your support and all the gossip. **Tom**, thanks to you the division is so well organized. Sorry if I sent too many packages with samples, thank you for all your help! **Janneke** and **Ariena**, I really enjoyed our trip to Prague, thanks for your friendship. **Koen** and **Robert**, I really appreciate our discussions about drug transporter studies, HPLC or radioactive samples, but also making fun of each other during social events. **Sven**, **Wendy**, **Asli**, **Nikola**, **Sunny**, **Ewa**, **Guotai**, **Paul-Andre**, **Sabrina**, **Marco**, **Serge and Marcel** thanks for all the nice times on P2 and/or H5. **Liesbeth**, bedankt voor de nederlandse les!

Speaking about P2, it was a shock to see it disappear. **Marta**, gracias por las charlas y por tu ayuda con la estadística! **Jelle**, ik zou ook zo relax als jij willen zijn! **Hein**, thank you for your scientific input as member of my PhD committe and for the funny speeches at Christmas dinners! Also, members of the **Wessels**, **Linn**, **Jonkers** and **te Riele** groups, you made P2 a lovely place to work! Moving to H5 was postponed so many times, but in the end it did happen. There we got to share the tissue culture with the **Jacobs** group, and it made culturing less lonely, as at least one of you is always there. **Sedef**, thanks for ordering the Nesspresso pads, they also contributed to this thesis. **Joanna**, **Patricia**, **Judith**, **Niels** and the rest of the **Peeper** group: it was nice to share a department with you!

But NKI is not only work, it is also about borrels, summer parties and being social. **Roel**, we can laugh so much about simple things! You are such a good friend, thank you for always being there for me! **Pablo**, he disfrutado mucho de nuestras conversaciones en el animalario y últimamente del intercambio de opiniones sobre niños! Fun and party people like **Francesca**, **Rogier**, **Bert**, **Rik**, **Dalila**, **Marieke van K**., **Bastiaan**, **Cesare**, **Marcello**, **Jens**, **Ewald**, **Andy**, **Veronica**, **Xanthippi**, **Marieke P**., **Metamia**, **Linda** and many others thank you for the great times! And living for some years in the NKI ghetto, I could enjoy Sinterklaas parties, international dinners, lunches and parties within 5 minutes from my home. Thank you **Guillaume**, for your friendship and provocative ideas. **Maria**, **Vicky**, **Charlotte S**. and **Petra**, I really enjoyed spending time with you!

And when it was time for me to leave the ghetto, I found some wonderful and extremely generous friends in the Pijp. **Izhar**, thanks for the diving lessons and the support during a difficult period in my life. **Maaike**, my pregnancy buddy, thanks for all your advice in these first months as a mother! I wish you both lots of health, happiness and I hope that our kids will become good friends!

Believe or not, there is life outside the NKI and I got some wonderful people to share it with. **Martuky**, con tu energia vital y ideas locas, uno no se aburre nunca. Gracias por ser una amiga estupenda! **Reichel**, espero que te quedes mucho tiempo en Amsterdam! Dragă **Roxana**, mi-a fost greu când ai plecat din Amsterdam, dar acum îmi dau seama că nu contează distanța, noi rămânem la fel de apropiate! **Mirela** și **Edi,** mă bucur foarte mult că am devenit prieteni mai apropiați, sunteți foarte faini! **Tom (Tieman)**, you did a great job to introduce me to the Dutch culture, lifestyle and politics. Thanks for keeping in touch! **Pieter** en **Linda**, jullie zijn mijn allereerste nederlandse vrienden! Bedankt voor al jullie steun, fietsen, meubels, concerten, feesten en cadeautjes! Nu gaan we, als ouders, naar de volgende fase van onze levens.

Dragi prieteni din facultate, iată că sunt aproape doctor! **Măriuța** dragă, tu ești un factor constant în viața mea, o inepuizabilă sursă de dragoste, sfaturi și încurajări pentru care îți multumesc din suflet. **Rareș** scumpule, sunt tare fericită ca am păstrat legătura atât de strâns în toții anii aceștia. **Ede**, **Andreea**, **Ade**, **Dadi**, **Iulia**, **Cristina, Lorand** mi-e dor de voi! **Luminița B**(oruzi sau ătrânu) îți mulțumesc pentru cuvintele calde și urările de bine!

**Jaume**, compartimos muchos años de mi doctorado y de nuestras vidas. Te agradezco muchísimo todo tu apoyo, consejos, y los dibujos divertidos tipo "cuando Dilek dejó de trabajar con ratones..". Siempre tendrás un lugar especial en mi corazón, y espero que en un futuro podamos tener más contacto. Te deseo mucha felicidad en el futuro! También quiero agradecer a **Mari**, **Pedro**, **Raquel**, **Jaime** y **Amparo** por todo que hicisteis por mí en estos años!

Special thanks to my family in the US: **Rahmi** and **Altay** thanks for making me feel at home with you! **Marjorie**, my role model, it makes me sad that you are no longer here, but it makes me happy to think that you would have been so proud of me!

Ook bedankt aan mijn nederlandse familie: **Jurriën**, **Jeanette**, **Elske** en **Sander**. Jullie hebben mij echt snel thuis laten voelen en ik kijk er naar uit om samen met jullie Max op te zien groeien.

**Paizertizi**, sawbol pentru toate fursecurile, cuvintele calde și alintăturile de-a lungul anilor. Mulțumesc deasemena unchilor, mătușilor, verilor și verișoarelor de acasă.

Dragul meu **Oznurabi**, ești un frate minunat! Îți mulțumesc pentru că ai avut întotdeauna grijă de mine, ai încercat să mă protejezi, să mă sfătuiești numai de bine și să mă înconjori de multă, multă iubire. Ești atât de bun, darnic și sufletist și sunt foarte mândră că ești abi-ul meu. Chiar dacă nu reușim să vorbim pe skype, avem o legătură foarte specială care sper să nu dispară niciodată. **Cristina**, mă bucur că faci parte din familia noastră și îți mulțumesc pentru tot ceea ce ai făcut pentru mine. **Daria**, nepoțica mea dragă, pentru mine ești cea mai deosebită fetiță din lume: atât de deșteaptă, simpatică, curajoasă, și mai ales atât de iubitoare! O să-l iubești așa de mult și pe verișorul tău Max Aydin? **Babai**, chiar dacă comunicarea directă nu e punctul tău forte, indirect am simțit întotdeaunca cât de mult mă iubești și cât de mândru ești de mine. Faptul că am moștenit mintea ta analitică și practică mi-a fost de mare folos în doctorat. Sawbol! Draga mea **Neni,** tu ești fanul meu Nr. 1. Din clasa întâi și până acum ai fost alături de mine, făcându-ți griji și încurajându-mă. Am trăit împreună toate lucrările, tezele, meditațiile, examenele de admitere, din sesiuni, de licență și stressul unui Topmaster. Iar acum în timpul doctoratului, mi-ai ținut pumnii pentru fiecare articol trimis pentru publicare și te-ai bucurat pentru toate reușitele mele. De aceea, îți dedic cu mare dragoste această teză de doctorat!

Lieve **Jorma**, dankzij jou heb ik mijzelf veel beter leren kennen. Met jou ben ik sterker, minder control-freak, positiever en gelukkiger. Ik vind het ontzettend speciaal dat wij zo veel hebben mee gemaakt in het laatste jaar, en geweldig dat wij samen nergens bang voor zijn. Ik kijk uit naar ons leven samen, het wordt een prachtig avontuur! Și în cele din urmă ajungem la cel mai tânăr cititor al acestei teze, Max Aydin. Dragul meu puișor, îți mulțumesc că mai ai și dormit câteodată și astfel am putut să îmi termin teza. Deși ești cu noi numai de câteva luni, nu îmi pot imagina viața fără tine și te iubesc atât de mult!